

Proliferating NG2-glia and their functional importance in the healthy and injured brain



**Dissertation der Graduate School of Systemic
Neurosciences der Ludwig-Maximilians-Universität
München**

Submitted by
Sarah Schneider

08.10.2015

Performed at the Institute of Physiology at the
Ludwig-Maximilians Universität München
Head: Prof. Dr. Magdalena Götz

**Proliferating NG2-glia and their
functional importance in the healthy and
injured brain**

Dissertation with the aim of achieving a PhD at the
Graduate School of Systemic Neurosciences
Ludwig-Maximilians Universität München

Submitted by
Sarah Schneider
2015

Date of submission: 08.10.2015

Supervisor: Dr. Leda Dimou

2nd reviewer: Prof. Dr. Martin Kerschensteiner

3rd external reviewer: Prof. Dr. Patrick Küry

Date of oral defense: 03.02.2016

„Manchmal hat man eine sehr lange Straße vor sich. Man denkt, die ist so schrecklich lang; das kann man niemals schaffen, denkt man [...] Und dann fängt man an, sich zu beeilen. Und man eilt sich immer mehr. Jedes Mal, wenn man aufblickt, sieht man, dass es gar nicht weniger wird, was noch vor einem liegt. Und man strengt sich noch mehr an, man kriegt es mit der Angst, und zum Schluss ist man ganz außer Puste und kann nicht mehr. Und die Straße liegt immer noch vor einem. So darf man es nicht machen. [...] Man darf nie an die ganze Straße auf einmal denken. Man muss nur an den nächsten Schritt denken, an den nächsten Atemzug, an den nächsten Besenstrich. Und immer wieder nur an den nächsten. [...] Auf einmal merkt man, dass man Schritt für Schritt die ganze Straße gemacht hat.“

(Beppo der Straßenkehrer, aus *Momo*,
Michael Ende

I SUMMARY

NG2-glia - also known as oligodendrocyte progenitor cells - constitute a fraction of around 5% of the adult cells in the rodent brain. NG2-glia are the only proliferating cells in the adult brain parenchyma and are additionally able to generate mature and myelinating oligodendrocytes throughout lifetime. Despite their high number and substantial characterization, their functional role both in the intact and injured adult brain remains unclear. To address this question, this thesis exploited the conditional genetic deletion of the *Esco2* protein in the inducible *Sox10iCreER^{T2}xCAG-eGFPxEsco2^{fl/fl}* mouse line to specifically trigger apoptosis in dividing NG2-glia during M-phase. Using this mouse line, it could be shown in this work that deletion of the *Esco2* protein in NG2-glia in the adult brain induced progressive cell death in the dividing recombined cells. This process is compensated by enhanced proliferation of the non-recombined subpopulation, so that no change in the overall NG2-glia numbers could be observed. Specifically in the white matter of the cerebral cortex, the continuous loss of NG2-glia resulted in a decreased number of newly generated oligodendrocytes that was followed by structural as well as functional changes in the nodes of Ranvier. As a consequence, a deceleration in the nerve conduction velocity of myelinated WM fibers could be measured. These animals – in contrast to control littermates – developed progressive motor deficits both in general as well as in the fine-coordinated movements.

As NG2-glia after acute brain injury strongly react to this insult by increasing their proliferation rate more than 15-fold, the function of these proliferating NG2-glia was also analyzed by ablating them after an acute stab wound lesion using the above mentioned genetic model. The fast ablation of proliferating recombined NG2-glia resulted in a transient but significant diminishment of the overall NG2-glia population in close proximity to the lesion site. As a consequence of this cell number reduction, the wound closure capacity was significantly delayed. Furthermore, the transient reduction of these cells resulted in a severely disturbed reaction of both the microglial and astrocyte population.

Taken together, the findings obtained in this work strongly suggest that proliferating NG2-glia and newly generated oligodendrocytes in the adult brain are: (I) crucial for the maintenance of myelin-associated structures and the underlying physiological function in the healthy mouse, as well as (II) for proper tissue repair and the injury-related glial reaction in the pathological brain.

II ZUSAMMENFASSUNG

NG2-glia – auch bekannt als Oligodendrozyten-Vorläuferzellen – bilden mit etwa 5% eine Hauptfraktion der Zellen im erwachsenen Gehirn von Nagetieren und sind dort die einzigen sich teilenden Zellen außerhalb der neurogenen Nischen. Zudem sind sie während des ganzen Lebens fähig, reife und myelinisierende Oligodendrozyten zu bilden. Trotz ihres hohen Vorkommens sowie ihrer umfangreichen Charakterisierung ist ihre eigentliche Funktion sowohl im intakten als auch im verletzten erwachsenen Gehirn größtenteils unbekannt. Um dieses Feld näher zu untersuchen, wurde in der vorliegenden Arbeit die genetische Entfernung des Esco2-Proteins in der induzierbaren Sox10iCreER^{T2}xCAG-eGFPxEsco2^{fl/fl}-Mauslinie verwendet, um spezifisch den apoptotischen Zelltod während der M-Phase in proliferierenden NG2-glia auszulösen. Mit dieser Mauslinie konnte gezeigt werden, dass der Verlust des Esco2-Proteins in NG2-Glia im erwachsenen Gehirn einen fortschreitenden Zelltod in sich teilenden, rekombinierten Zellen auslöst, der von nicht rekombinierten Zellen durch eine erhöhte Teilungsrate kompensiert wird. Besonders in der weißen Substanz führte der kontinuierliche Verlust von NG2-glia zu einer reduzierten Anzahl an neu gebildeten Oligodendrozyten. Dieser Beobachtung folgten weiterhin sowohl strukturelle als auch funktionale Veränderungen in den Ranvierschen Schnürringen. Diese Veränderungen führten wiederum zu einer Verlangsamung in der Geschwindigkeit der Nervenleitung. Im Gegensatz zu den Kontrolltieren entwickelten diese Mäuse zunehmende motorische Störungen - sowohl in den generellen als auch im feinmotorischen Bewegungsablauf.

NG2-glia erhöhen ihre Proliferationsrate nach einer Verletzung mehr als 15-fach und reagieren auch anderweitig sehr stark auf pathologische Einflüsse. Daher wurde in dieser Arbeit mit dem gleichen Mechanismus zusätzlich die Funktion von proliferierenden NG2-Glia nach akuter Gehirnverletzung untersucht. Der schnelle Zelltod der rekombinierten NG2-Glia führte in diesem Fall zu einer erheblichen, vorübergehenden Reduktion der NG2-Glia-Population in unmittelbarer Umgebung der Verletzung. Als Konsequenz dieses Zellverlustes resultierte eine Verspätung im Wundverschluss. Zusätzlich führte der vorübergehende Zellverlust ebenso zu einer stark veränderten Reaktion der Mikroglia- als auch der Astroglia-Populationen.

Zusammenfassend suggerieren diese Ergebnisse, dass sich im physiologischen Maße teilende NG2-Glia sowie eine korrekte Anzahl neu gebildeter Oligodendroglia einen beträchtlichen Einfluss auf die Erhaltung der Ranvierschen Schnürringe, auf deren grundlegende physiologische Funktionen im gesunden Gehirn sowie auf eine angemessene Reparatur und die damit verbundene allgemeine Gliazellen-Reaktion im verletzten Gehirn haben.

III TABLE OF CONTENTS

| | | |
|---------|---------------------------------------------------------------------------------------------------------------|-----|
| I | Summary..... | I |
| II | Zusammenfassung | II |
| III | Table of contents | III |
| 1 | Introduction | 1 |
| 1.1 | Glial cells in the adult mammalian brain..... | 1 |
| 1.2 | Origin and persistence of the oligodendrocyte lineage | 2 |
| 1.3 | NG2-glia – the fourth glial cell population | 5 |
| 1.3.1 | NG2-glia form a tight homeostatic network..... | 7 |
| 1.3.2 | NG2-glia are proliferative, self-renewing and keep producing mature oligodendrocytes throughout lifetime..... | 7 |
| 1.3.3 | Neuron-NG2-glia synapses and activity-dependent reaction of NG2-glia..... | 8 |
| 1.3.4 | Regional and cell-intrinsic heterogeneity of NG2-glia | 10 |
| 1.3.5 | Ablation attempts of NG2-glia | 12 |
| 1.4 | Myelin | 13 |
| 1.4.1 | Function and composition of myelin | 13 |
| 1.4.2 | The process and kinetics of myelin formation..... | 14 |
| 1.4.3 | Oligodendrocyte and myelin plasticity during adulthood..... | 15 |
| 1.5 | Traumatic brain injury | 17 |
| 1.5.1 | Models of traumatic brain injury..... | 18 |
| 1.5.2 | Tissue reaction and following scar formation after brain injury | 18 |
| 1.5.3 | Separate reaction of major glial cell types..... | 20 |
| 1.5.3.1 | Reaction of microglia and macrophages to brain injury | 21 |
| 1.5.3.2 | Reaction of NG2-glia to brain injury | 22 |
| 1.5.3.3 | Reaction of astrocytes to brain injury..... | 24 |
| 1.6 | Tamoxifen-inducible transgenic mouse models..... | 26 |
| 1.7 | The cell cycle regulator Esco2 | 28 |
| 2 | Aim of the Study..... | 30 |
| 3 | Results..... | 31 |
| 3.1 | NG2-glia ablation in the healthy brain..... | 31 |

| | | |
|-------|-----------------------------------------------------------------------------------------------------------------|----|
| 3.1.1 | Esco2 deletion causes slow but progressive loss of proliferative recombined NG2-glia | 31 |
| 3.1.2 | NG2-glia ablation decreases oligodendrogenesis..... | 37 |
| 3.1.3 | NG2-glia ablated mice show disruptions in the nodes of Ranvier | 39 |
| 3.1.4 | NG2-glia ablated mice develop long-term motor dysfunctions | 42 |
| 3.1.5 | The NG2CreER ^{t2} xcag-egfpxEsco2 ^{fl/fl} control mouse line | 46 |
| 3.1.6 | Behavioral phenotype is not derived from the peripheral nervous system ... | 50 |
| 3.1.7 | NG2-glia ablated mice develop a decelerating nerve conduction velocity..... | 51 |
| 3.2 | NG2-glia ablation in the injured brain | 53 |
| 3.2.1 | Esco2 deletion causes fast loss of proliferative recombined NG2-glia in close proximity to the lesion site..... | 54 |
| 3.2.2 | NG2-glia ablation delays wound closure..... | 58 |
| 3.2.3 | Closure of the Blood-Brain-Barrier | 59 |
| 3.2.4 | Reduced injury response of other glial cell populations | 60 |
| 4 | Discussion and future perspectives | 63 |
| 4.1 | Ablation of NG2-glia in the healthy brain..... | 63 |
| 4.1.1 | NG2-glia network is maintained at the expense of oligodendrogenesis..... | 63 |
| 4.1.2 | Oligodendrocyte lineage equilibrium is required to maintain nodes of Ranvier in the white matter..... | 68 |
| 4.1.3 | Nodes of Ranvier are important to maintain physiological motor functions .. | 72 |
| 4.1.4 | NG2-glia functions are lost despite network Maintenance..... | 76 |
| 4.2 | Injury | 78 |
| 4.2.1 | Ablation of recombined NG2-glia induces a deficit in cell numbers in the lesion site..... | 78 |
| 4.2.2 | Increase in NG2-glia numbers in the lesion core is essential for wound closure | 81 |
| 4.2.3 | Wound healing is the result of a NG2-glia orchestrated cell-to-cell signaling cascade | 83 |
| 4.3 | Translational approaches and clinical implications | 86 |
| 5 | Materials | 88 |

| | | |
|---------|------------------------------------------------------------------|----|
| 5.1 | Chemicals | 88 |
| 5.2 | Drugs | 89 |
| 5.3 | Consumables | 89 |
| 5.4 | Software..... | 90 |
| 5.5 | Technical equipment | 90 |
| 5.6 | Buffers and solutions..... | 91 |
| 5.6.1 | Buffers for DNA extraction and genotyping | 91 |
| 5.6.2 | Buffers for animal tissue preparation | 92 |
| 5.6.3 | Buffers for immunohistochemistry | 92 |
| 5.6.4 | Buffers for In situ cell death detection | 93 |
| 5.6.5 | Buffers for cresylviolet staining | 93 |
| 5.6.6 | Buffers for Sudan Black staining..... | 94 |
| 5.6.7 | Buffers for electron microscopy | 94 |
| 5.6.8 | Solutions for drug and die applications | 95 |
| 6 | Methods..... | 96 |
| 6.1 | Animals | 96 |
| 6.1.1 | Mouse lines..... | 96 |
| 6.1.1.1 | Sox10iCreER ^{T2} xCAG-eGFPxEsco2 ^{fl/fl} | 96 |
| 6.1.1.2 | NG2CreER ^{T2} xCAG-eGFPxEsco ^{fl/fl} | 96 |
| 6.1.2 | Genotyping | 96 |
| 6.1.2.1 | DNA isolation | 96 |
| 6.1.2.2 | PCR | 97 |
| 6.1.3 | Tamoxifen administration | 98 |
| 6.1.4 | BrdU administration..... | 98 |
| 6.1.5 | Behavioral assessment | 98 |
| 6.1.5.1 | Grid walk | 98 |
| 6.1.5.2 | Beam crossing..... | 99 |
| 6.1.5.3 | Horizontal ladder | 99 |
| 6.1.5.4 | Open field | 99 |

| | | |
|---------|----------------------------------------------------------------------|-----|
| 6.1.5.5 | Novel object recognition test | 99 |
| 6.1.6 | Anesthesia | 99 |
| 6.1.6.1 | Ketamine/Rompune | 99 |
| 6.1.6.2 | MMF | 100 |
| 6.1.7 | Model of stab wound injury..... | 100 |
| 6.1.8 | Transcardial perfusion | 100 |
| 6.2 | immunohistochemistry..... | 101 |
| 6.2.1 | Tissue collection and sectioning | 101 |
| 6.2.1.1 | Brains | 101 |
| 6.2.1.2 | Sciatic nerves | 101 |
| 6.2.1.3 | Skeletal Muscles | 101 |
| 6.2.2 | Immunohistochemical stainings..... | 101 |
| 6.2.3 | Quantifications and statistical analysis | 102 |
| 6.3 | TUNEL staining | 103 |
| 6.4 | Cresylviolet staining..... | 103 |
| 6.5 | Myelin visualization | 103 |
| 6.5.1 | Sudan Black Staining | 103 |
| 6.5.2 | Electron Microscopy..... | 104 |
| 6.5.2.1 | Tissue preparation | 104 |
| 6.5.2.2 | Ultratome sectioning..... | 104 |
| 6.5.2.3 | Contrasting | 104 |
| 6.5.2.4 | Picture acquisition and analysis of myelin abberations..... | 104 |
| 6.6 | BBB closure analysis..... | 105 |
| 6.7 | Determination of the lesion size | 105 |
| 7 | References | 106 |
| 8 | Acknowledgements | 135 |
| 9 | Appendix..... | 137 |
| 9.1 | Supplementary tables | 137 |
| 9.1.1 | Supplementary tables for NG2-glia ablation in the healthy brain..... | 137 |

| | | |
|-------|-----------------------------------------------------------------------|-----|
| 9.1.2 | Supplementary tables for NG2-glia ablation in the injured brain | 139 |
| 9.2 | Abbreviations..... | 142 |
| 9.3 | List of figures..... | 144 |
| 9.4 | List of tables | 145 |
| 9.5 | Curriculum Vitae | 147 |
| 9.6 | List of publications | 149 |

1 INTRODUCTION

1.1 GLIAL CELLS IN THE ADULT MAMMALIAN BRAIN

Beside neurons, glial cells constitute a major fraction of the total brain mass ranging from 33% up to 66% within different mammalian species. The mouse brain only consists of 35% glial cells and is therefore located near the lower border, whereas the human brain with 50% glial cells is situated towards the upper border of this range (Herculano-Houzel 2014; Azevedo et al. 2009). Glial cells have already been identified in the 19th century by many famous neuroscientists. At that time they were suggested to function as the so-called 'Nervenkitz' (German for *nerve glue*); meaning that their inherent function was meant to provide a foundation for the neurons in the brain. However, with the progression of time, scientists started to ask questions about possible and additional functions of these cells. Although these questions have already been asked decades ago, many of them remain unanswered until today (Somjen 1988). At least, it became increasingly clear that glial cells are more than just brain glue; nowadays, they attract a lot of scientific interest.

Traditionally glial cells in the adult mammalian central nervous system (CNS) can be subdivided into three major groups according to their inherent functions as illustrated in Figure 1: microglia, astrocytes and oligodendrocytes, with the latter two forming together the macroglia (reviewed in Barres 2008; He and Sun 2007).

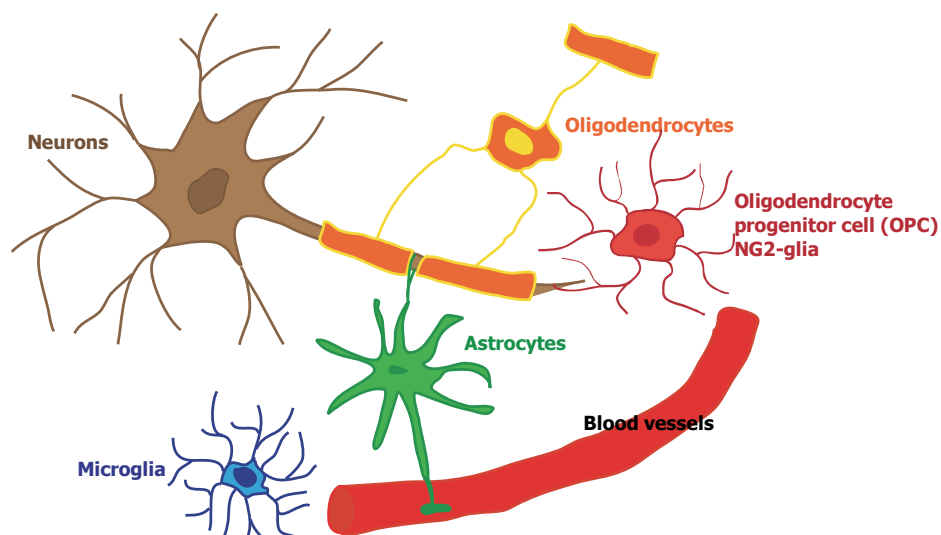


Figure 1: Cell types in the adult central nervous system (CNS). Microglia (blue) are the immune-surveilling cells in the CNS, although they developmentally derive from another origin. Astrocytes (green) extend their endfeet to blood vessels and to neuronal nodes of Ranvier located at myelinated axons. Oligodendrocytes (orange) form myelin sheaths that enwrap neuronal axons (brown) allowing saltatory nerve conduction and hence increase the conduction velocity and information processing. Oligodendrocyte progenitor cells (OPCs) – also named NG2-glia (red) – are a fourth glial cell population in the adult CNS with a possible yet unknown function (besides being the progenitors for mature oligodendrocytes) which only came into the focus in the last decades.

In a simplified view microglia – that are developmentally not glial cells but migrate into the brain from the mesoderm at neonatal stages – are the immunocompetent and phagocytosing cells of the brain parenchyma (Kim and Vellis 2005; Santambrogio et al. 2001; Kettenmann et al. 2011). They are not only constantly sensing their environment with their highly motile filopodia during healthy conditions, but also react rapidly as a response to changes in the environment and to extrinsic insults (Nimmerjahn et al. 2005). Macroglial astrocytes constitute the major fraction of glial cells in the brain. They have many different pivotal functions, also depending on their location in the brain. The most prominent astrocytic functions are: the maintenance of the fluid and ion concentration homeostasis, their functional and modulatory role in the tripartite synapse (presynaptic membrane, postsynaptic membrane and glial cell), as well as their contribution to the formation of the blood-brain-barrier (BBB) (Halassa et al. 2009; Kimelberg 2010; Kimelberg and Nedergaard 2010). The third glial cell population – the oligodendrocytes – produces myelin sheaths that enwrap neuronal axons and therefore both allow and increase the nerve impulse conduction (Baumann and Pham-Dinh 2001). In the late 1980's another cell type was identified that can be distinguished in the brain by the expression of the proteoglycan neuron-glia antigen 2 (NG2) (French-Constant and Raff 1986; Stallcup and Beasley 1987). This discovery was the starting point of a further macroglial cell population – the nowadays so called NG2-glia – the cell type this thesis is focused on and that is described in more detail below.

1.2 ORIGIN AND PERSISTENCE OF THE OLIGODENDROCYTE LINEAGE

Progenitors of the oligodendrocyte lineage (oligodendrocyte progenitor cells, OPCs), located in the developing spinal cord and brain stem, start to develop at embryonic day 12.5 (E12.5) in the ventral progenitor zone together with motor neurons from a common source of precursor motoneuron (pMN) progenitor cells that express the oligodendrocyte transcription factor 2 (Olig2) (Lu et al. 2002; Takebayashi et al. 2002). A second source of these progenitor cells in the neural tube starts to emerge at E15.5 from more dorsal regions. However, the latter ones are generally outnumbered and suppressed by their ventrally-derived counterparts (Calver et al. 1998; Vallstedt et al. 2005; Cai et al. 2005; Richardson et al. 2006).

Like in the spinal cord, OPCs in the forebrain pass through different stages and derive from multiple sources, starting from ventral to more dorsal regions, as depicted in Figure 2. The first wave of precursors that express and can therefore be identified by the transcription factor Nkx2.1 starts to emerge at E12.5 from the medial ganglionic eminence (MGE) and the anterior entopeduncular area (AEP). Subsequently these cells migrate into other parts of the developing brain.

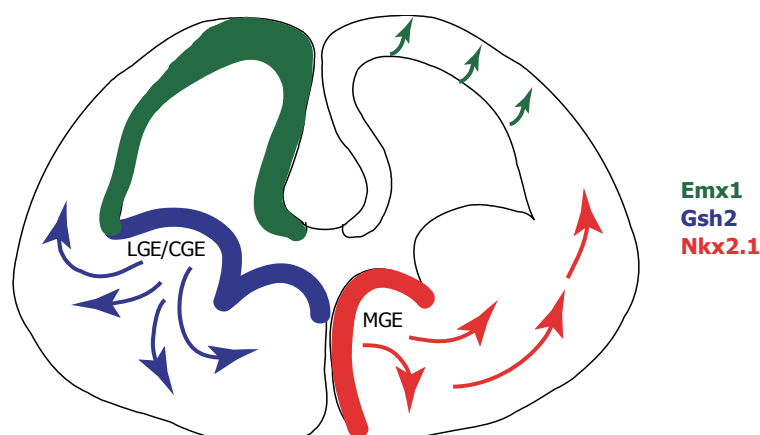


Figure 2: Waves of oligodendrocyte progenitor cells (OPCs) in the developing brain. The first wave of OPCs that are expressing $Nkx2.1^+$ (red) emerge at E12.5 from the medial ganglionic eminence (MGE). At E15.5 a second wave of $Gsh2$ -expressing progenitors (blue) starts to populate the brain from the medial and the caudal ganglionic eminence (LGE/CGE). At P0 a third wave of $Emx1$ -expressing OPCs (green) derive directly from the cortex. During postnatal stages, $Nkx2.1$ -expressing OPCs disappear, whereas those from the second and third wave persist into adulthood (adapted from Kessaris et al. 2006).

Most interestingly, $Nkx2.1^+$ OPCs are eliminated during the further development and do not persist into adulthood (Kessaris et al. 2006). A second wave of precursors starts to develop at E15.5 from the lateral and caudal ganglionic eminence (LGE and CGE). Unlike cells of the first wave, they can be identified by the expression of $Gsh2$. These cells migrate from their place of origin into the whole brain and although many of these cells are also eliminated, some persist into adulthood. A third wave of $Emx1^+$ precursor cells can be found right after birth at the first postnatal day zero (P0) deriving directly from the cortex (Kessaris et al. 2006; Richardson et al. 2006). Like the $Gsh2^+$ precursor population, $Emx1^+$ precursors migrate within the brain, both populations together form the oligodendrocyte progenitor pool in the brain at postnatal stages. So far, no clear evidence was found indicating any functional differences between the cells deriving from the different origins. The fact that the ventrally and dorsally-derived progenitors have very similar electrophysiological properties suggests a high degree of redundancy (Tripathi et al. 2011). Genetic ablation studies of both populations showed that the cells are fully replaced by progenitors of the other origin, however, detailed functional analysis of the different populations, including the influence of the same environment in which they are located has not been performed (Kessaris et al. 2006; Ventura and Goldman 2006; Mitew et al. 2014). After populating the brain, the majority of the OPCs start to differentiate into mature and myelinating oligodendrocytes; both differentiation and myelination is peaking in the second postnatal week (Sturrock 1980; Greenwood 2003). Although oligodendrogenesis and myelination decline thereafter, OPCs are still persistent in the adult brain in high numbers (Pringle et al. 1992).

As OPCs differentiate into oligodendrocytes along the oligodendrocyte lineage, they do not only undergo morphological and functional changes (e.g. myelination), but also express different markers, as depicted in Figure 3. Some transcription factors (Olig2 and sex determining region Y-related high mobility group box protein, Sox10) are commonly expressed during all differentiation stages, hence using Olig2 and Sox10 as markers, cells of the oligodendrocyte lineage can be distinguished from other cell types in the brain (Kuhlbrodt et al. 1998; Takebayashi et al. 2002). OPCs additionally express characteristic surface markers like the platelet-derived growth factor receptor α (PDGFR α) and NG2, that is encoded by the chondroitin sulfate protein 4 gene (*cspg4*) (Nishiyama et al. 1997; Dawson 2003). When these cells differentiate further into mature and myelinating oligodendrocytes, they stop to express the precursor markers and become postmitotic. It is proposed that they subsequently differentiate via a stage of premyelinating oligodendrocytes. In this phase they are thought to acquire a more complex morphology with additional ramified processes. Boda et al. (2011) suggested this stage to be distinguishable by the expression of the G-protein coupled receptor 17 (GPR17). A very recent study from our lab in which the GPR17⁺ cell population was genetically labelled, however disproved this marker to be specific for this stage (Viganò and Schneider et al. in press).

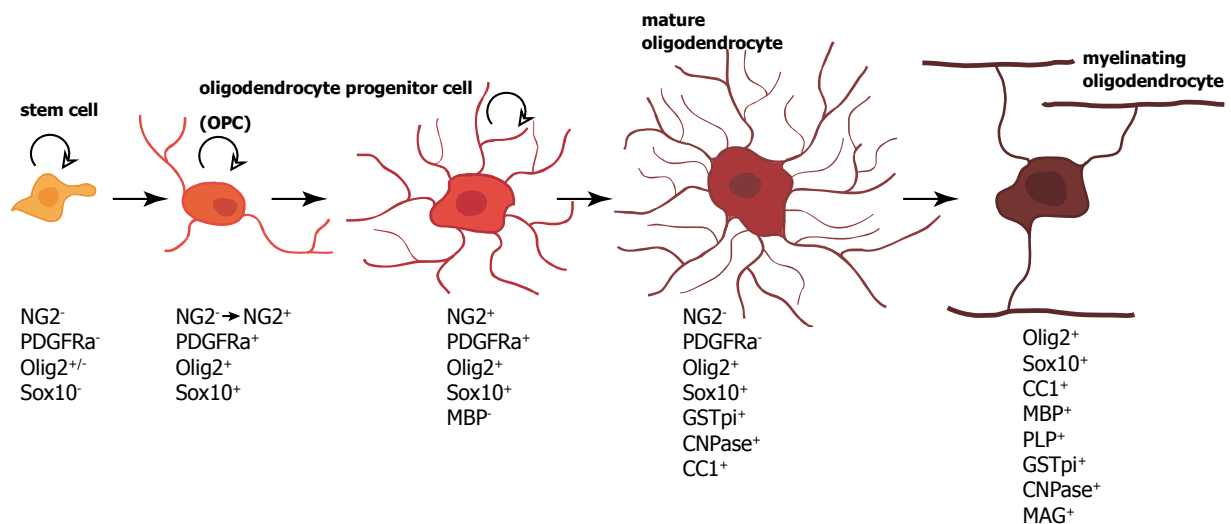


Figure 3: Oligodendrocyte lineage during differentiation. As soon as lineage-specific stem cells differentiate, they start to express progenitor markers like NG2 and PDGFR α . These oligodendrocyte progenitor cells (OPCs) still have the capacity to proliferate (indicated with a loop arrow). Alongside the differentiation they lose their precursor markers and also their ability to proliferate. Mature oligodendrocytes express markers like adenomatous polyposis coli (APC or CC1), 2', 3'-cyclic nucleotide 3'-phosphodiesterase (CNPase) or the Glutathione S-transferase π (GST π). Myelinating oligodendrocytes additionally express typically myelin-associated markers like the proteolipid protein (PLP), the myelin associated glycoprotein (MAG) and the myelin basic protein (MBP). The transcription factors OLIG2 and Sox10 are expressed throughout the lineage (modified after Nishiyama et al. 2009).

Along with their differentiation and maturation, oligodendrocytes start to express proteins like adenomatous polyposis coli (APC, better known as CC1), 2', 3'-cyclic nucleotide 3'-phosphodiesterase (CNPase) or the Glutathione S-transferase π (GST π). In the final step of differentiation when the oligodendrocytes start to myelinate axons, they express markers that are typically located in the myelin sheaths: the myelin basic protein (MBP) and its isoforms, proteolipid protein (PLP) as well as the myelin associated glycoprotein (MAG) (Pfeiffer et al. 1993; Baumann and Pham-Dinh 2001; Nishiyama et al. 2009; Fulton et al. 2010). As the differentiation of OPCs to fully mature oligodendrocytes is a continuous process, there might be intermediate stages where specific markers could overlap.

1.3 NG2-GLIA – THE FOURTH GLIAL CELL POPULATION

OPCs are progenitors that produce mature and myelinating oligodendrocytes during development, but although most of oligodendrocyte and myelin production occurs during the first postnatal weeks (Sturrock 1980; Greenwood 2003), these cells are persistent in the adult brain where they make up 5-8% of the rodent's adult CNS (Pringle et al. 1992; Dawson 2003). Due to their specific cellular characteristics, OPCs have been drawing a lot of attention by neuroscientists. The fact that they are not only progenitors of the oligodendrocyte lineage, but also comprise additional physiological functions cannot be argued any more. OPCs can already be found in lower vertebrates which do not have myelinated axons (Banerjee et al. 2006; Banerjee and Bhat 2008), supporting the idea of the functional importance of these cells as a separate cell type. The idea that they comprise a fourth glial cell population in the CNS is more and more established within the research community. Due to the novelty of this specific field, not only their function is extensively discussed, but also a number of different denominations is associated with them. In the beginning, this cell type was named *O-2A progenitors*, due to the fact that it was identified to be *in vitro* the precursor of oligodendrocytes and type 2 astrocytes (Raff et al. 1983). However, after type 2 astrocytes could not be detected *in vivo*, as they turned out to be a cell culture artefact, this term was replaced by the current expression: OPCs. *Polydendrocytes* is another common term for OPCs, used to emphasize the fact that they are different from other glial cell types, including oligodendrocytes, and to refer to their specific morphology (Nishiyama et al. 2002). NG2-expressing cells that form synapses together with neurons and contact the nodes of Ranvier have been referred to as *synantocytes* (Butt et al. 2002). Other names like *NG2⁺ cells*, or simply *NG2 cells* are also commonly used, as they are characterized by the expression of the proteoglycan NG2. In order to separate them from their embryonic counterparts which majorly create mature and myelinating

oligodendrocytes and to stress the fact that they represent a distinct glial cell population, the term *NG2-glia* is used throughout this thesis.

The proliferative character and abundance of NG2-glia in both the developmental and the adult CNS created the idea that they are not only lineage-committed progenitors, but also multipotent stem cells that can be exploited for tissue repair after injury. After scientists showed that postnatal, optic nerve-originated NG2-glia are multipotent and able to give rise to neurons, astrocytes and oligodendrocytes *in vitro* (Kondo and Raff 2000), scientific interest noticeably increased. In order to clarify the multipotency of NG2-glia *in vivo*, a high number of fate mapping analyses with recombinant mouse lines have been used allowing specific labelling of NG2-glia to determine their cellular fate.

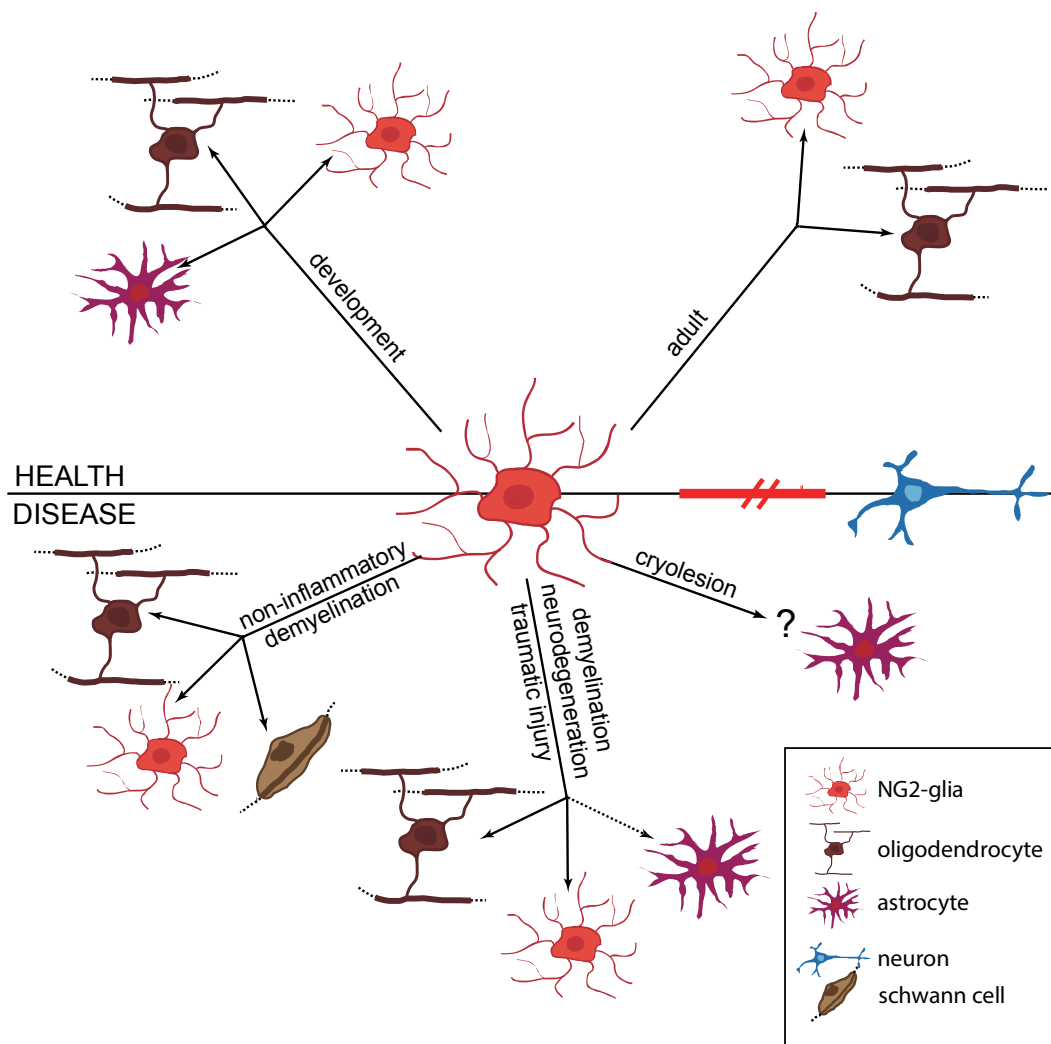


Figure 4: Lineage specificity of NG2-glia in health and disease. In the healthy brain (upper part) NG2-glia give mainly rise to NG2-glia, oligodendrocytes and some astrocytes during development. However, upon some specific pathological conditions (like e.g. non-inflammatory and inflammatory demyelination, neurodegeneration or traumatic injury), NG2-glia were shown to generate astrocytes as well as myelinating Schwann cells. Lineage plasticity into neurons is however still controversially discussed (adapted from Dimou and Gallo 2015).

Although some of the studies demonstrated controversial results, it is now generally accepted that during health NG2-glia give rise to oligodendrocyte lineage cells as well as to a low number of astrocytes during development (Guo et al. 2009; Zhu et al. 2011; Huang et al. 2014b), while they remain committed to their own lineage in the adult brain (Dimou et al. 2008; Rivers et al. 2008; Kang et al. 2010; Simon et al. 2012). In contrast, during disease the lineage-commitment in the adult brain changes: upon different pathological insults (e.g. non-inflammatory and inflammatory demyelination, neurodegeneration and traumatic injury), NG2-glia can be reactivated to give rise to astrocytes or Schwann cells (Figure 4, Alonso 2005; Cassiani-Ingoni et al. 2006; Magnus et al. 2007; Zhao et al. 2009; Tripathi et al. 2010; Komitova et al. 2011). The fate switch of NG2-glia into neurons that was observed *in vitro* could on the contrary not be verified *in vivo* yet, indicating that these cells do not carry a full multipotent potential in comparison with neural stem cells (Richardson et al. 2011; Dimou and Götz 2014; Dimou and Gallo 2015).

1.3.1 NG2-GLIA FORM A TIGHT HOMEOSTATIC NETWORK

It has been shown that NG2-glia are evenly distributed throughout the whole brain (Nishiyama et al. 1999). They feature a stellate morphology with a very elaborate tree of processes evenly distributed around their central cell body. Utilizing a three dimensional (3D) reconstruction method, a total surface area of around 2000 μm^2 was calculated for one single cell (Kukley et al. 2007). A recent study showed that NG2-glia processes are very motile and that even their whole cell body moves in the adult cortex in a non-directed manner, wherefore the net movement is hardly detectable (Hughes et al. 2013). Within this movement, they sense their environment using filopodia, with each cell keeping its own territory through self-repulsion of its filopodia from adjacent cells. As soon as one cell is lost, either through cell death or differentiation, neighboring cells are able to detect the emerged gap in the homeostatic network and fill it up (Hughes et al. 2013). Besides this intercellular network, NG2-glia (and the other cells of the oligodendrocyte lineage) form multiple heterologous networks and connections with astrocytes as well as with neurons that are mediated by connexins (Parenti et al. 2010; May et al. 2013). Additionally, they were shown to extend some of their processes into the nodes of Ranvier, suggesting interaction with neuronal axons (Butt et al. 1999; Wigley et al. 2007; Wigley and Butt 2009).

1.3.2 NG2-GLIA ARE PROLIFERATIVE, SELF-RENEWING AND KEEP PRODUCING MATURE OLIGODENDROCYTES THROUGHOUT LIFETIME

The most significant cellular property of NG2-glia is that they are the only cells being able to proliferate under physiological conditions in the adult brain parenchyma outside the neurogenic niches. Simon et al. (2011) showed that some of the NG2-glia can enter the cell cycle at least

twice, meaning that they are not only proliferative, but also self-renewing. A recent study using the *Star Trek* clonal analysis method demonstrated that even in the adult brain, one single NG2-glia can generate up to 400 progenies (García-Marqués et al. 2014). Although there is an age-dependent decline, proliferation of NG2-glia never stops throughout lifetime (Gensert and Greenwood 1997; Dimou et al. 2008; Psachoulia et al. 2009; Simon et al. 2011; Young et al. 2013). Experiments using 5'-bromo-desoxyuridine (BrdU) and 5'-ethynyl-2'-deoxyuridine (EdU) labelling to follow cells that have proliferated, showed that almost all NG2-glia (80-98%, depending on the type of analysis) in the cortical gray matter (GM) and white matter (WM) do proliferate. Due to a comparatively long G₁ resting phase, the average cell cycle length of NG2-glia in the cortical GM accounts to 37 days in three months old mice (Simon et al. 2011). Region-dependent analysis showed that WM-derived NG2-glia cycle much faster. Notably, the cell cycle length of different WM tracts can also vary significantly from approximately ten days in the corpus callosum up to 20 days in the optic nerve. The cell cycle length also increases during aging (Kang et al. 2010; Young et al. 2013).

NG2-glia do not only differentiate during development, but they also keep producing mature and myelinating oligodendrocytes throughout lifetime (Dimou et al. 2008; Simon et al. 2011; Young et al. 2013). BrdU label retaining experiments demonstrated that around 50% of BrdU incorporating NG2-glia have differentiated into mature oligodendrocytes during a time window of three months in young adult mice (Simon et al. 2011). Another study showed that 30% of all mature oligodendrocytes in the adult corpus callosum emerge after the age of eight weeks in rodents (Rivers et al. 2008). Comparable to proliferation, differentiation of NG2-glia is region-dependent: the proportion of differentiated cells is much higher in WM tracts compared with GM in the adult brain. In line with proliferation properties, differentiation has been shown to decline with age (Dimou et al. 2008; Young et al. 2013). However, the functional role of this adult oligodendrogenesis that will be discussed elsewhere in this discussion (chapter 1.4.3) remains highly debated.

1.3.3 NEURON-NG2-GLIA SYNAPSES AND ACTIVITY-DEPENDENT REACTION OF NG2-GLIA

As already mentioned above, NG2-glia in the adult brain highly interconnect with neurons (Wigley et al. 2007). Bergles and colleagues first demonstrated that hippocampal NG2-glia are not only connected, but also actively receive synaptic input from neurons. These synapses can be both glutamatergic, mediated by α -amino-3-hydroxy-5-methyl-4-isoxazolepropionic acid (AMPA) or N-methyl-D-aspartic acid (NMDA) receptors, as well as 'GABAergic' via gamma-aminobutyric acid (GABA_A) receptors (Bergles et al. 2000; Lin and Bergles 2002, 2004). Although GABA_A signaling is usually considered as inhibitory, this does not seem to be the case with NG2-glia where the glutamatergic and the GABAergic signals evoke an identical reaction

(Passlick et al. 2013). Subsequent studies identified a high number of additional neurotransmitter receptors *in vitro*: nicotinic and muscarinic acetylcholine, dopamine, cannabinoid, glycine and purinergic receptors, however their functionality *in vivo* has not been verified so far (Sun and Dietrich 2013). It became clear that neuron-NG2-glia synapses are not exclusively found on NG2-glia in the hippocampus, but throughout the CNS in both GM and WM tracts (Káradóttir et al. 2005; Mangin and Gallo 2011; in Sun and Dietrich 2013; Dimou and Gallo 2015). Most of these synapses are at least physically maintained during proliferation and are only being retracted during differentiation (Kukley et al. 2008; Ge et al. 2009; Kukley et al. 2010; Fröhlich et al. 2011). A very recent study from Sahel et al. (2015) however suggested for the first time that NG2-glia do not receive synaptic input during the process of proliferation, but that the connection has to be re-established afterwards.

The neuron-NG2-glia synapses work via a classical vesicular release that is indistinguishable from the mechanism in neurons (Paukert and Bergles 2006; Maldonado et al. 2011). Although at least some NG2-glia express voltage-gated ion channels – both potassium (K^+) and sodium (Na^{2+}) channels – it is not clear whether NG2-glia are able to integrate and remit the electrical signal they receive from neurons (Steinhauser et al. 1994; De Biase et al. 2010; Kukley et al. 2010; Sun and Dietrich 2013). Káradóttir et al. (2008) suggested that upon synaptic vesicular release some NG2-glia in the rat WM are able to fire axon potentials independently by opening voltage-gated Na^{2+} channels, however, this functionality could not be verified in mice (De Biase et al. 2010; Clarke et al. 2012).

The synaptic transmission results in a local intracellular increase in calcium (Ca^{2+}) in the processes of NG2-glia that could be important as a second messenger inducing functional changes (Bergles et al. 2000; Ge et al. 2006; Tanaka et al. 2009; Haberlandt et al. 2011; Sun and Dietrich 2013). Whether the observed Ca^{2+} elevation is caused by entry through ionotropic receptors or by release of intracellular Ca^{2+} storage is still being discussed (Sun and Dietrich 2013). Another trigger to increase NG2-glial intracellular Ca^{2+} is the neuronal and astrocytic release of adenosine triphosphate (ATP) into the synaptic space that furthermore acts via metabotropic P2Y1 and ionotropic P2X7 receptors on NG2-glia (Hamilton et al. 2010; Butt et al. 2014).

NG2-glia show a strong neural activity-dependent behavior with regard to proliferation, migration, differentiation and myelination both under physiological conditions as well as after injury that might be mediated via these described synapses between NG2-glia and neurons (Simon et al. 2011; Wake et al. 2011; Boscia et al. 2012; Mangin et al. 2012; Hill and Nishiyama 2014; Gibson et al. 2014). On the other hand, it is becoming increasingly evident that neuronal activity is not only influencing NG2-glia, but that NG2-glia are also a potent modulator of the neuronal network themselves. Sakry et al. (2014) demonstrated that the proteoglycan NG2

expressed on NG2-glia can be shed from the cell and has then an effect on the NMDA-dependent long-term potentiation (LTP) in pyramidal neurons as well as on their AMPA receptor composition. The same group recently reported that NG2-glia express the neuro-modulatory proteins prostaglandin D2 synthase (PTGDS) and neuronal pentraxin 2 (Nptx2/Narp). These findings suggest that NG2-glia have a higher influence on the neuronal network than previously expected (Sakry et al. 2015).

1.3.4 REGIONAL AND CELL-INTRINSIC HETEROGENEITY OF NG2-GLIA

Since NG2-glia in the adult CNS are homogeneously distributed and so far no further markers for specific subpopulations could be detected, they have been considered to be a homogeneous population. Nevertheless, they show a high variability with regard to their cell cycle length and differentiation properties throughout different brain regions, giving a body of evidence that a certain heterogeneity exists. A recent gene expression profile study where NG2-glia were isolated from adult humans suggests the existence of three different subpopulations of NG2-glia (Leong et al. 2014). However, the authors neither distinguished between GM or WM tracts, nor between cells that are in a different cell cycle status or in various differentiation stages. To further address the question of possible variability between cells of different origin, Viganò et al. (2013) transplanted NG2-glia from the cortical GM into the WM and vice versa. The authors demonstrated that the WM is in general a more supportive environment for differentiation, with cell-intrinsic factors being evenly important for regulating the cell fate of NG2-glia.

Electrophysiological analysis revealed WM-derived NG2-glia to exhibit a different resting membrane potential than GM-derived cells. This is achieved through differential expression of voltage gated potassium (Kv1) and inward rectifying Kir channels as well as through a different ability to elicit immature action potentials (Chittajallu et al. 2004). However, no differences in cell-intrinsic signaling pathways between WM-derived and GM-derived NG2-glia were detected so far (Hill and Nishiyama 2014). In a study using organotypic slice culture explants from postnatal mice, the authors demonstrated that WM-derived NG2-glia show a significantly stronger response to PDGF-AA compared with their GM-derived counterparts (Hill et al. 2013), although PDGFR α expression and the intracellular transduction pathway of these two populations is not detectably different (Pringle et al. 1992; Nishiyama et al. 1996; Hill et al. 2013). This finding suggests PDGF to be an extrinsic factor differentially regulating the proliferation of NG2-glia. Within these differing microenvironments, the extracellular matrix as well as paracrine signaling molecules from other cells could play an important role as well (Hill et al. 2013; Hill and Nishiyama 2014). Figure 5 is summarizing the heterogeneity of GM- and WM-derived NG2-glia, as far as it is known to date.

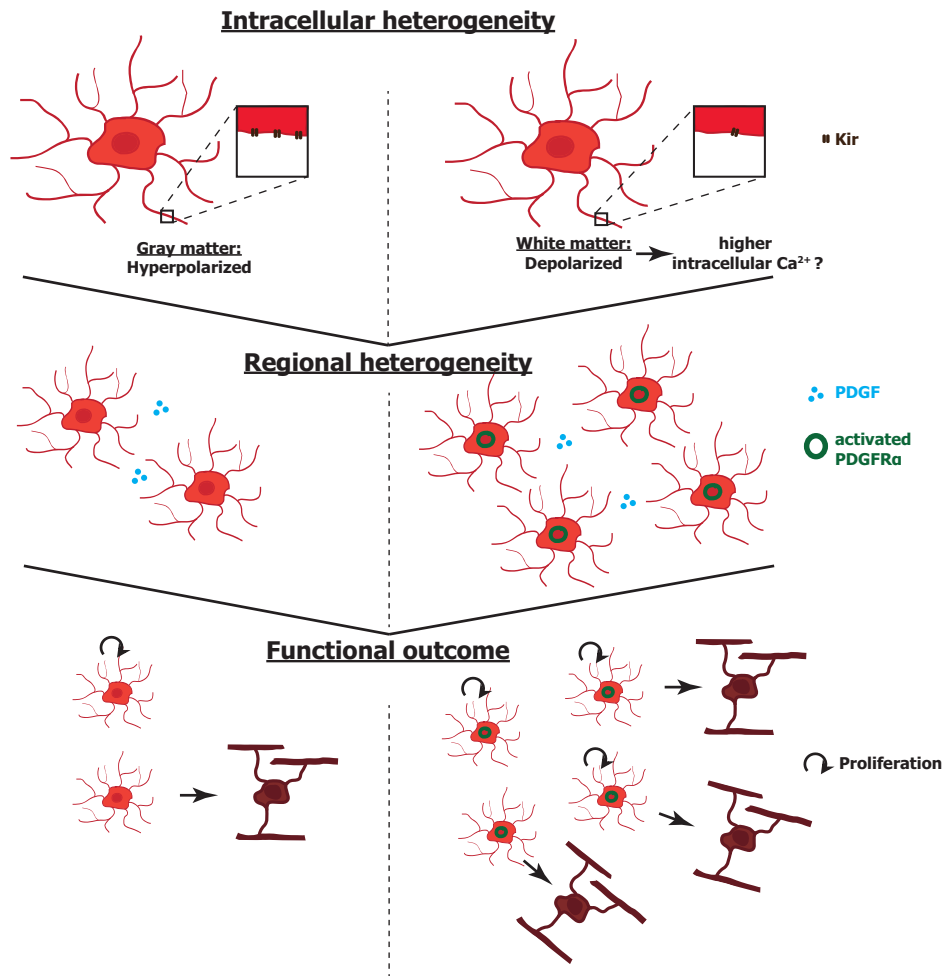


Figure 5: Heterogeneity of NG2-glia between gray and white matter. Top: White matter-derived NG2-glia (right) are reported to be less electrically polarized compared with those originating from gray matter (left), due to their different expression of Kir channels. Middle: Despite the expression of comparable amounts of PDGFR α on the cell surfaces and the availability of PDGF in the environment, WM-derived NG2-glia are increasingly activated due to different receptor activation mechanisms. Bottom: The intracellular and regional heterogeneity result in a variability in proliferation and differentiation rates between WM and GM-derived NG2-glia (modified after Hill and Nishiyama 2014).

Besides the regional heterogeneity, in the last years many studies aimed to assess the topic of intracellular heterogeneity within the same cortical region as well as the cellular factors driving NG2-glia to proliferate or to differentiate. At least in the telencephalon, a subpopulation of NG2-glia was found to uniquely express the transcription factor mammalian achaete scute homolog 1 (Mash1), indicating some intra-regional heterogeneity. However, the factor's functional role within this subpopulation has not been ascertained yet (Parras et al. 2007).

One proposed possibility that could be the driving force for an intraregional heterogeneity could be a different cellular origin. Indeed, it was demonstrated that in the adult corpus callosum there is a continuous addition of new NG2-glia deriving from progenitors in the subventricular zone (Menn et al. 2006; Ortega et al. 2013). Hence, as the NG2-glia population in the corpus callosum could derive from different origins, the cells could have variable cellular

characteristics and functions. Although this hypothesis attracted a great scientific interest, neither a specific marker for these two distinct populations from different origins could be found, nor could it completely be verified until now. One protein and possible candidate that is only expressed by a subset of NG2-glia in all regions throughout the brain is the G-protein-coupled receptor 17 (GPR17) (Boda et al. 2011). Recent studies from our lab assessed the GPR17-expression heterogeneity using the novel GPR17iCreER^{T2} mouse line: especially in the GM, a specific subpopulation expressing GPR17 seems to serve as a reserve pool of NG2-glia that under physiological conditions differentiate slower compared to those not expressing the receptor. After lesion, this subpopulation reacts with an increase in differentiation, indicating that it represents a reservoir for brain repair. Cellular mechanistic pathways driving this heterogeneity have not been identified so far (Viganò and Schneider et al. in press).

As the interest in heterogeneous subpopulations of NG2-glia is just evolving, there is a high demand for finding new markers that could possibly identify them. RNA-sequencing techniques for transcriptome analysis of single cells have recently been established and conducted in order to analyze the transcriptome of variably matured cells within the oligodendrocyte lineage (Zhang et al. 2014). Using this technique for multiple regions or sub-regions could be a promising approach for disclosing the root of intracellular NG2-glia heterogeneity in the CNS.

1.3.5 ABLATION ATTEMPTS OF NG2-GLIA

Although only little is known about their elusive physiological functions, NG2-glia attracted the attention of many scientists in the last decades, leading to the identification and thorough description of many of their cellular characteristics. In order to address this point, many studies tried to analyze the CNS in the absence of NG2-glia by ablating them with irradiation, chemical agents like arabinofuranosyl cytidine (AraC) or diphtheria toxin (DT) and immunotoxins (Chari and Blakemore 2002; Chari et al. 2003; Irvine and Blakemore 2007; Robins et al. 2013; Leoni et al. 2014; Birey and Aguirre 2015). Most of these studies targeted the proliferative capacity of NG2-glia for the ablation approach, as they are vulnerable to agents that interfere with DNA synthesis (e.g. AraC) or to irradiation. Independent from the used method, NG2-glia could be ablated in the region of interest only for a short time period within those studies. Remaining NG2-glia from the same or neighboring regions quickly repopulated the ablated areas by increasing their rate of proliferation. The repopulation capacity is maintained throughout lifetime, although the proliferation rate and the thereof resulting speed of repopulation is declining with age (Chari et al. 2003). As these approaches unspecifically depleted all proliferating cells including microglia and astrocytes, a serious conclusion cannot be drawn for the function of one specific cell type. Although no significant conclusions about the

physiological functions of NG2-glia in the adult could be drawn with these studies, the maintenance of the homeostatic network seems to play a key role in this context.

1.4 MYELIN

1.4.1 FUNCTION AND COMPOSITION OF MYELIN

Myelin - originally referred to as the 'fatty marrow' - is an electrical insulator allowing faster velocity through saltatory conduction in axons that is required for higher organisms to achieve a better temporal resolution. It took several decades to understand that myelin is indeed a motile membrane produced by living cells (Virchow 1854; Geren and Raskind 1953; Rosenbluth 1999). With the invention of electron microscopy (EM), it could be disclosed that myelin is formed by compacted plasma membrane extensions that are wrapped multiple times around the axons. Although it was thought to be a very simple structure, a recent proteomic analysis demonstrated that myelin is – besides its basic fatty component cholesterol – composed of 342 different proteins. The major myelin associated proteins like proteolipid protein (PLP) and myelin basic protein (MBP) amount to only 17% and 8%, respectively (Jahn et al. 2009). In the same study, the authors showed that many of these proteins are important for the cytoskeleton, vesicular trafficking, cell adhesion and catalytic activities. The multilamellar wrappings around the axons that form the compact myelin and represent the internodes are interrupted by the myelin free nodes of Ranvier alongside the axons. In these structures, a lot of ion channels accumulate directly on the axon to generate action potentials, being the basis for saltatory nerve conduction (Nave 2010). Moreover, the node of Ranvier is a complex functional unit. It is subdivided into the node, the paranode being the axon-glia contact zone and separating the periaxonal space from the outside, as well as the juxtaparanode where many potassium channels are located (Salzer et al. 2008). As the myelin sheaths are strongly insulating the axons from their environment, it became clear that myelin is not only needed for faster nerve conduction, but also for long-term integrity of the tissue. Furthermore it is important for the survival of axons: myelin abnormalities are leading to thinner axon diameters, general axonal malformations like axonal swellings, as well as to long-term axonal degeneration (Griffiths et al. 1998; Edgar et al. 2009; Brady et al. 1999). The signals that are important for the interaction between the axon and the established myelin sheath are not well defined yet. Myelin associated glycoprotein (MAG) seems to play an important role, as mice that completely lack the MAG, do not show any perturbation in myelin but in axon diameters (Yin et al. 1998) as well as in exosome-mediated transport from oligodendrocytes to axons (Frühbeis et al. 2013). In proteolipid protein (Plp1)-null mice completely lacking the PLP protein, myelin formation and the physical development of the body occurs normally. During adulthood, however, these mice undergo neurodegeneration, indicating that this axon-glia

interdependence is not only based on myelin ensheathment but also that glia may give other support to axons (Griffiths et al. 1998). Indeed, some studies suggested that oligodendrocytes that are capable of anaerobic glycolysis, provide lactate to axons mediated via the monocarboxylate transporter 1 (MCT1) in case that other energy sources are limited (Fünfschilling et al. 2012; Lee et al. 2012b). These new insights in the oligodendrocyte-neuron interactions yield a deeper understanding of myelin diseases like multiple sclerosis (MS) or leukodystrophies that lead to long-term Wallerian degeneration (Nave 2010; Bercury and Macklin 2015).

1.4.2 THE PROCESS AND KINETICS OF MYELIN FORMATION

In different brain regions, a vast number of axons remains unmyelinated even in the adult (Sturrock 1980). Hence, there has been a long discussion about how oligodendrocytes are deciding on which axon to myelinate and which to leave unmyelinated. It was recently shown that both a neuronal activity-dependent as well as a neuronal activity-independent mode of myelination exists. The activity-dependent mode could be induced by neuronal action potentials and the thereby implemented synaptic vesicular release of glutamate or GABA (Lundgaard et al. 2013; Mensch et al. 2015). The activity-independent mode on the other hand is based on the axon calibers, confirmed by another study showing that oligodendrocytes in culture are able to myelinate nanofibers but just with a certain caliber (Lee et al. 2012a). The number of myelin sheaths on a single axon, expressed in the g-ratio (ratio of the inner axonal diameter to the total outer diameter), was shown to be individually regulated by the axon caliber itself. The same oligodendrocyte is able to myelinate both large as well as small diameters properly (Almeida et al. 2011). However, the sheath length on a myelinated axon was shown to be regulated by the oligodendrocyte itself (Bechler et al. 2015).

The molecular axonal signaling pathways involved in the process of myelin encasement are not fully understood. Axonal neuregulin-1/ErbB signaling was shown to regulate myelination in the PNS (Nave and Salzer 2006), these factors could however not be verified to play the same role in CNS myelination, wherefore it was suggested that oligodendrocytes developed an alternative mechanism for axonal interactions compared with Schwann cells (Brinkmann et al. 2008).

Besides the search for factors regulating myelination, there was a long debate about how the myelin sheath is wrapped around the axon during the myelination process. Over the years several mechanisms for this process have been suggested. The most accepted ones that have long been accepted in the field are: (I) the so called 'rolled up carpet' model where the initial wrap is elongating and moving underneath itself to form multiple layers that was adapted from the model for PNS myelination (Geren and Schmitt 1954), and (II) an initial wrap that is moving

around the axons in spirals. After a sufficient amount of wraps have been formed, the myelin is flattening and moving laterally to finally form the sheaths (Robertis et al. 1958; Bauer et al. 2009; Bercury and Macklin 2015). As imaging techniques have become better over time, these models were refined, suggesting the 'liquid croissant' model of myelination where myelin is 'poured out' in a triangular shape and concurrently moving sideways (Sobottka et al. 2011). In this model, new myelin wraps are proposed to be added on top of the former ones. By using a combination of different high resolution imaging techniques, it was demonstrated that the originally proposed 'rolled up carpet' model is indeed the appropriate one. Myelin is extending as an inner tongue underneath existing sheaths and moving laterally along the axons, where the paranodal loops are then formed (Snaidero et al. 2014; Snaidero and Simons 2014). A recent study from Kerman et al. (2015) exploiting the oligodendrocytes' capacity to myelinate *in vitro* now additionally unraveled the early mechanisms of the myelin initiation. The authors demonstrated that the oligodendrocyte process surveys the axons before it anchors and that after the anchoring the unanchored part of the oligodendrocyte process starts to wrap the axon. Together with the late stage mechanisms from older studies they suggested the 'SARAPE' mechanism: survey, anchor, wrap and expand.

Regarding the kinetics of myelination, live-imaging in a transgenic zebrafish model showed that it is a very fast and dynamic process. Individual oligodendrocytes produce stable myelin sheaths within a time window of only five hours (Czopka et al. 2013). Whether this time window also applies to rodents and other mammalian species still needs to be investigated.

1.4.3 OLIGODENDROCYTE AND MYELIN PLASTICITY DURING ADULthood

The dynamics of adult oligodendrogenesis in a few brain regions are well characterized, however we are just at the beginning of understanding the functional role of these adult-born oligodendrocytes. Recent studies demonstrated that under physiological conditions myelin is continuously generated and remodeled in the adult CNS, even without any injury, explaining the high amount of newly generated oligodendrocytes (Young et al. 2013; Yeung et al. 2014). It is not clear whether the newly generated oligodendrocytes and the resulting myelin are required to replace already existing oligodendrocytes and myelin sheaths, or if it is added into already existing structures. Several arguments support the case of de-novo myelination: (I) already years ago different studies demonstrated that both the number of oligodendrocytes and myelinated fibers in the adult rodent brain are accumulating over time and do not seem to be replaced by others (McCarthy and Leblond 1988; Yates and Juraska 2007). (II) As about two thirds of the callosal axons remain unmyelinated in the adult mouse, de-novo myelination of previously unmyelinated fibers is possible (Sturrock 1980). (III) Tomassy et al. (2014) reported also in the GM about an uneven distribution of myelin thickness along the axonal

length and that axons can be only partially myelinated, allowing additional space for de-novo myelination. Additionally, for other brain areas – and hence supporting the myelin remodeling thesis – newly generated myelin can also be found in highly myelinated WM tracts, e.g. in the optic nerve where ~98% of the axons are myelinated (Honjin et al. 1977; Young et al. 2013). The authors showed that in this area pre-existing myelin is remodeled by inserting new myelin sheaths into the node of Ranvier (Young et al. 2013). The fact that during aging internodes are increasing in numbers while their length is decreasing, supports this later finding (Lasiene et al. 2009). Summarizing these data, de-novo myelination and myelin remodeling are most likely happening concurrently in the CNS. The question about the underlying physiological function of this remodeling, however, remains at least partially unanswered.

With the myelination of previously unmyelinated fiber tracts or partially myelinated axons, new neuronal circuits, e.g. after learning a new skill, could be established and strengthened in the brain. This hypothesis was not only based on rodents, but also human functional magnetic resonance imaging (fMRI) studies indeed demonstrated long-term myelin remodeling in WM tracts of the brain after motor training, juggling, playing the piano and learning a second language (Bengtsson et al. 2005; Scholz et al. 2009; Schlegel et al. 2012; Sampaio-Baptista et al. 2013). The structural changes are reported to be visible within hours after training by measuring the fractional anisotropy (FA) of water in WM tracts, suggesting a very high remodeling rate of myelin (Pierpaoli and Basser 1996; Yamasaki et al. 2005; Hayashida et al. 2006). However, to which extent these observations in the FA represent myelin remodeling or other changes, has still to be clarified (Pierpaoli and Basser 1996; Yamasaki et al. 2005; Hayashida et al. 2006; Zatorre et al. 2012). Along the same line, Gibson et al. (2014) reported that artificial stimulation of neurons by optogenetics results in higher myelin production of adjacent oligodendrocytes and improved motor performance in mice. Using a transgenic mouse line that blocks the generation of new oligodendrocytes and therefore myelin, another study suggested that myelin remodeling is not only beneficial, but even required for learning new complex motor skills (McKenzie et al. 2014; Bercury and Macklin 2015, Figure 6).

Besides the involvement of myelin remodeling in motor skills, white matter and myelin volumes including intracortical myelin are thought to also be correlated to cognitive functions, as the volume of white matter tracts drastically decreases during aging and other cognitive impairments (Lebel et al. 2012; Sala et al. 2012; Haroutunian et al. 2014). As this decline is going hand in hand with a reduced oligodendrogenesis and myelin production, myelin remodeling could be a physiological mechanism for maintaining cognitive functions. Thus, keeping up NG2-glia proliferation and differentiation into old age could be a useful tool for medical applications in the treatment of cognitive impairment (Richardson et al. 2011; Bercury and Macklin 2015).

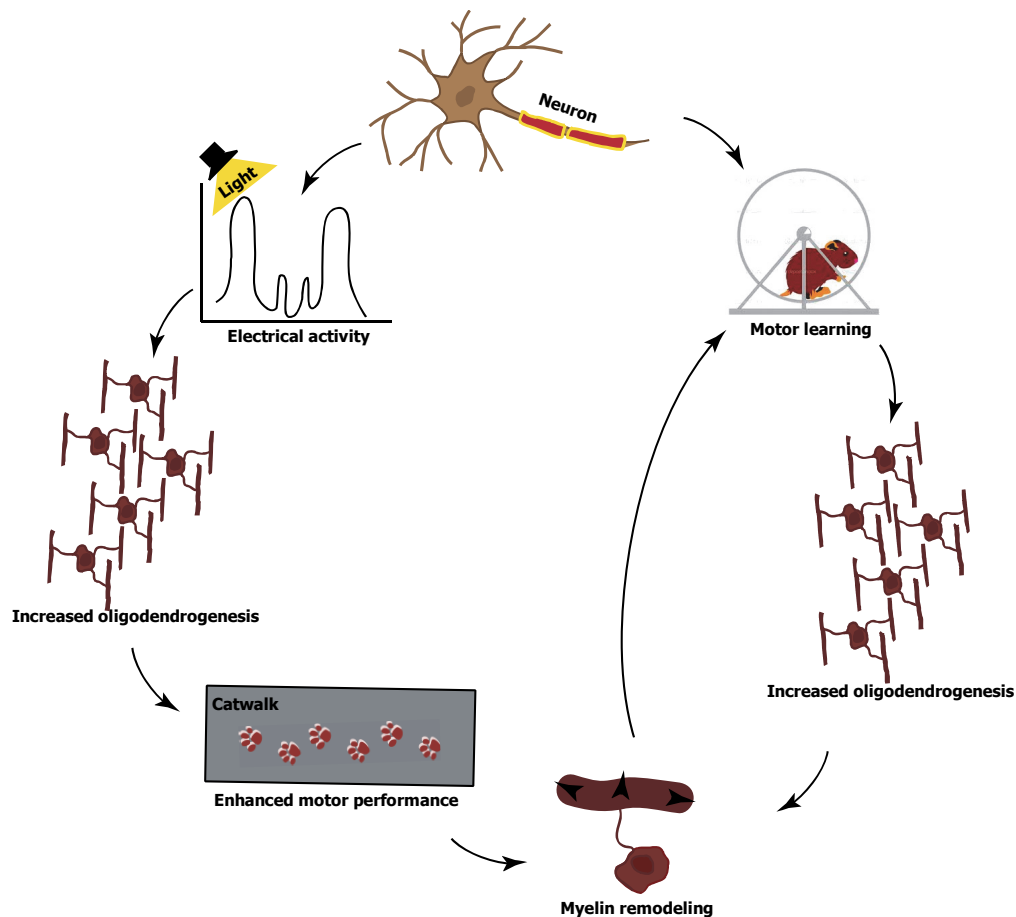


Figure 6: Neuronal activity and motor learning influences myelin plasticity. Optogenetic-induced activation in neurons increases adult oligodendrogenesis that results in enhanced motor performance on the catwalk in mice that is itself correlated with myelin plasticity (left side). Motor learning on a complex wheel was shown to require oligodendrogenesis and myelin plasticity (adapted from Bercury and Macklin 2015).

1.5 TRAUMATIC BRAIN INJURY

According to the Brain Association of America, traumatic, also classified as acquired brain injury is defined as: 'Alteration of the brain function, or other evidence of brain pathology, caused by an external force, which is not hereditary, congenital, degenerative or induced by birth trauma.' As this is a very broad definition, traumatic brain injuries (TBI) include a big variety of insults that can either be focused on the site of the primary insult or diffused with damages at more remote sides from the origin of the injury. Brain injuries can furthermore be closed (most of the time resulting from a crash), meaning that both the skull and the underlying dura mater remain intact, or open with an object penetrating these physical barriers. Besides the original insult, a secondary injury caused by the opening of the blood-brain-barrier (BBB), inflammation and other biochemical processes worsen the outcome of the original insult (Park et al. 2008; Maas et al. 2008; O'Connor et al. 2011). TBI is a major cause of death and disability all over the world, especially in children and young adults (Clark and Kochanek 2001). Hence, a deep understanding of brain-intrinsic mechanisms following TBI that cause severe

deficits is important to foster repair and improvement for affected patients. In order to address this issue, scientists developed a number of animal models to mimic and systemically study TBI.

1.5.1 MODELS OF TRAUMATIC BRAIN INJURY

TBI is a multifaceted injury that cannot be mimicked in a single model, and hence a lot of different injury models are required to observe the full spectrum of TBI. As deformations of the brain tissue are commonly found, many different models to mimic this insult exist: (I) the controlled cortical impact (CCI) model, where mechanical energy from a pneumatic cylinder is applied directly to the dura mater, (II) the weight drop model, where a weight is dropped either on the dura mater or the cranium in a controlled manner and (III) the vacuum deformation model, where the exposed brain is rapidly deformed by a vacuum pulse applied through the meninges (O'Connor et al. 2011).

Besides the typical deformation models, a variety of models to mimic different brain injuries exist, but although not emphasized specifically, deformation of the brain tissue as a consequence of tissue reaction and swelling is included in those models as well. Applying cryolesions is another commonly used method to produce long lasting, inflammatory brain damage with an eventual opening of the BBB depending on the severity of the lesion. To achieve this, a steel rod that was cooled in liquid nitrogen is directly applied to the dura mater (Sun et al. 2000). A relatively new method to induce and study a rather small lesion in which cells are locally destroyed is to apply a high energy laser pulse to the tissue that is sometimes referred to as focal laser lesion. This method is often used in combination with bi-photon *in vivo* live imaging techniques. The advantage thereof is the controllability of both size and location of the lesion (Nimmerjahn et al. 2005; Hughes et al. 2013). Open brain injuries are often mimicked by a stab wound injury (SWI): after a craniotomy above the region of interest, the brain tissue is deeply cut with a knife, resulting in the opening of the BBB, inflammation and local tissue damage causing a reaction of different cell types like the resident glial cells as well as infiltrating cells from the periphery. This injury can easily be controlled in size as well as in location (Buffo et al. 2005; Bardehle et al. 2013).

1.5.2 TISSUE REACTION AND FOLLOWING SCAR FORMATION AFTER BRAIN INJURY

The immediate reaction of the CNS tissue resulting in scar formation are the hallmarks of TBI in the mammalian brain that can persist for weeks or even months. However, the tissue reaction in the CNS is highly variable between injuries with an intact or an open BBB, as in the latter ones infiltrating peripheral immune cells and other factors play an additional role, mostly leading to increased cellular reactions. (Dimou and Götz 2014). Moreover, a lot of studies addressing this point have been performed in the spinal cord of rodents, and yet it is not clear

whether the findings from there can directly be translated to brain injuries or if other mechanisms also apply in the brain.

Following brain injury with an open BBB, three different stages of tissue reaction can be distinguished (Figure 7): (I) cell death and inflammation, (II) tissue replacement and (III) tissue remodeling (Burda and Sofroniew 2014). The first stage starts already within seconds after the injury and includes rapid cell death, blood coagulation, and the release of signaling molecules for attracting inflammatory cells to clear out the debris (Pineau and Lacroix 2009). Although immediate inflammatory signals are crucial to initiate these responses, a sensitive regulation between pro- and anti-inflammatory signals is required, as excessive inflammation can also be detrimental for tissue repair (Sofroniew 2015). This first stage is also accompanied by the deposition of additional extracellular matrix proteins (e.g. fibrinogen, collagen), and the immediate reaction of brain intrinsic microglia and NG2-glia (Nimmerjahn et al. 2005; Hughes et al. 2013; Burda and Sofroniew 2014; von Streitberg and Schneider et al. submitted;).

In the second stage where the BBB is still leaky, a massive proliferation and migration of cells - including endothelial lineage, fibroblast-like and glial cells - can be observed to regenerate and repopulate the damaged tissue. Astrocytes start to elongate around the lesion to corral the lesion core and the inflammatory response from the healthy tissue (Wanner et al. 2013). Recent studies demonstrated that within the corralled lesion core a high number of reactive microglia and NG2-glia can be found trapping dystrophic axons (Cregg et al. 2014).

In the tissue remodeling stage, the astrocytic scar is tightened and forms a sticky physical barrier while the cells in the peri-lesion already start to go back to normal. This is generally a chronic stage with gradual, continuous changes in the lesion core and its surroundings (Silver and Miller 2004). The glial scar has been shown to be beneficial shortly after injury by hampering the spreading of the lesion and by closure of the BBB, in the long-term, however, it is detrimental to complete tissue regeneration. Secreted molecules like proteoglycans, semaphorins as well as phosphatase and tensin homolog (PTEN) accumulate in the lesion core and seem to block the regrowth of neurons. Therefore, the lesion core cannot be functionally recovered (Silver and Miller 2004; Zukor et al. 2013; Dimou and Götz 2014; Burda and Sofroniew 2014). Indeed, mouse models with limited scar formation showed to allow the integration and long-time survival of neurons in the lesion core (Magavi et al. 2000; Chen et al. 2004).

From a historical point of view, the glial scar was thought to be exclusively formed by astrocytes and contributing to closing the lesion (Wanner et al. 2013). However, as high-resolution techniques evolved during the last decades, it became possible to study glial scar formation in more detail. Many studies elucidated the glial scar to be a complex and highly regulated composition of various cell types (reviewed in Cregg et al. 2014).

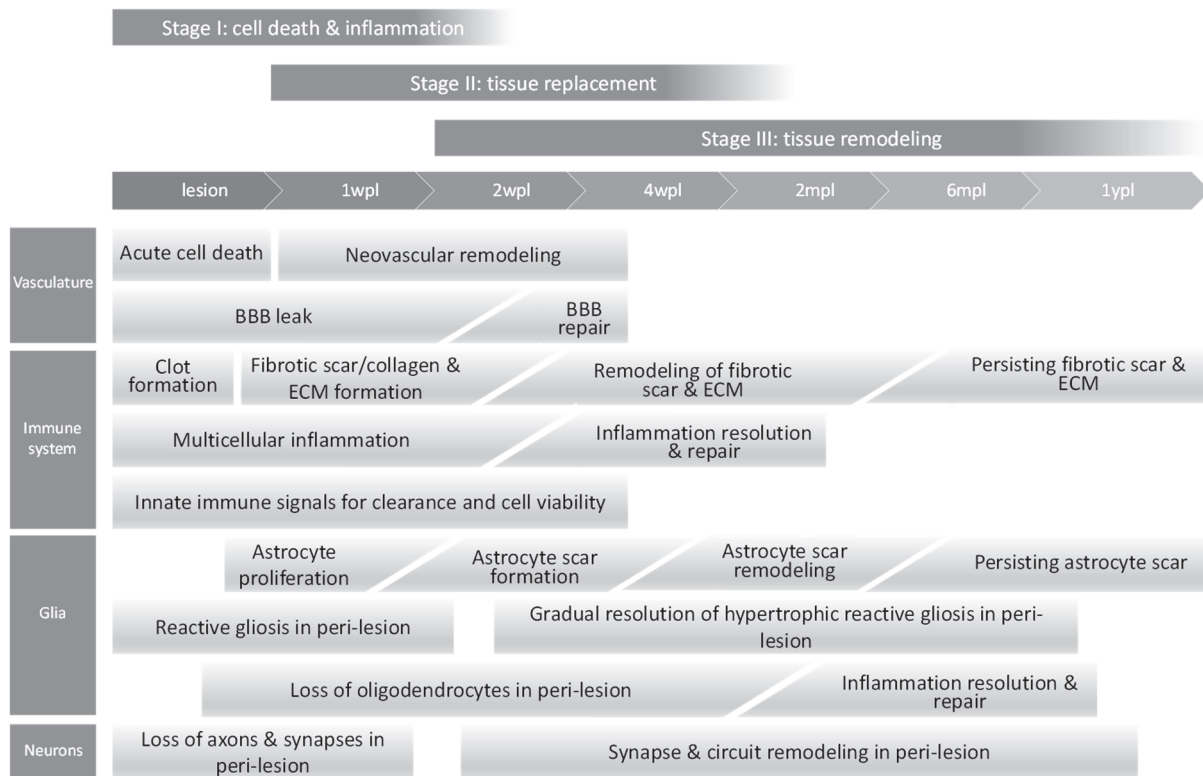


Figure 7: Stages and time line of different cellular responses after acute brain injury. After a focal lesion at least in rodents, three stages of scar formation can be observed: (I) cell death and inflammation, (II) tissue replacement and (III) tissue remodeling. During these stages multiple cellular responses over a long time frame are happening, including the vasculature, the immune system, glial cells as well as neurons. BBB: blood-brain-barrier, ECM: extracellular matrix, wpl: weeks post lesion, mpl: months post lesion, ypl: years post lesion (adapted from Burda and Sofroniew 2014).

Besides astrocytes, the glial scar contains high numbers of functional glial cells, fibromeningeal cells, endothelial cells, pericytes and a dense collagenous matrix that all have an important contribution to the functional tissue remodeling of the scar (Sofroniew and Vinters 2010; Cregg et al. 2014).

1.5.3 SEPARATE REACTION OF MAJOR GLIAL CELL TYPES

In this chapter the individual reaction of microglia, NG2-glia and astrocytes toward acute brain injury will be discussed. Microglia immediately respond and strongly proliferate very shortly after the injury. NG2-glia start to proliferate and respond after. The last glial cell type that is reacting to injury are astrocytes having their proliferative peak even later with the number of proliferating astrocytes being rather low compared with microglia and NG2-glia (Buffo et al. 2005; Simon et al. 2011; Robel et al. 2011b; Bardehle et al. 2013). This exemplary time course is strongly dependent on the type of lesion and on the cortical brain area it occurred in. In general, bigger lesions elicit a stronger reaction of glial cells (at least as shown for astrocytes and NG2-glia) compared to smaller lesions (Bardehle et al. 2013; von Streitberg and Schneider et al. submitted). In addition, stab wound injuries that are touching the WM, induce a stronger

reaction than those locally restricted to the GM (Mattugini and Götz unpublished observations). Most of the numerous studies that tried to unravel the detailed mechanisms and functions of glial cell reaction after injury only looked at the glial populations in a very isolated way. As these cell types already functionally interact in the intact brain, there is evidence that they also communicate with each other after injury and that their individual reactions are dependent on each other. However, as this is an emerging field, there are only few studies so far addressing this point. Wu et al. (2010b) suggested that the tissue inhibitor of metalloproteinase 1 (TIMP 1) amongst others plays an important role in the signaling between microglia and NG2-glia. Another study could show that this very same factor is also influencing astrocyte reaction after injury (Welser-Alves et al. 2011) and macrophage-derived osteopontin was shown to be important for activating astrocytes (Gliem et al. 2015).

1.5.3.1 REACTION OF MICROGLIA AND MACROPHAGES TO BRAIN INJURY

Microglia, the tissue-surveilling cells of the immune-privileged CNS, are the environmental sensor to injury and react after any kind of injury with a fast and long-lasting immune reaction (Silver et al. 2014; Zhou et al. 2014). Activated microglia retract their ramified processes to become amoeboid-shaped and are actively phagocytosing to clear the tissue from debris, damaged cells or even microbes. Hence, activated microglia are often denoted as macrophages (Kettenmann et al. 2011). Moreover resident microglia increase their cell numbers by proliferation in close proximity to the lesion site, chemo-tactically polarize and migrate towards the lesion site and were even shown to contribute to scar formation (Davalos et al. 2005; Dibaj et al. 2010). Activated macrophages can be distinguished from their surveilling counterparts by the up-regulation of the ionized calcium binding adaptor 1 (Iba1), leucocyte common antigen, LCA (CD45) and macrosialin (CD68) amongst others (Kettenmann et al. 2011). Starting from around 2dpl, monocytes from the blood are recruited into the lesion site via pro-inflammatory signals mainly derived from astrocytes (Pineau et al. 2010). They locally differentiate into macrophages afterwards. As these infiltrating bone marrow-derived macrophages (BMDMs) share the same developmental origin, no reliable markers could be identified until recently to distinguish these two populations. Additionally, they cannot be discriminated by their morphology from resident microglia, hence the term 'macrophages' referring to the time after lesion, is commonly used for both the resident macrophages as well as the BMDMs (Silver et al. 2014). Several studies already addressed the differences between resident and bone marrow-derived macrophages, and suggested that low CX3CR1 chemokine receptor 1 and high macrophage 1 antigen expressing BMDMs (CX3CR1^{low}/Mac-2^{high}) predominantly migrate into the lesion core, while the CX3CR1^{high}/Mac-2^{low} resident macrophages predominantly stay in the peri-lesion (Zhou et al. 2014). Therefore, macrophages

in the peri-lesion seem to block the tissue damage (Hines et al. 2009), whereas the BMDMs are devoted to clear the cell debris in the lesion core (David and Kroner 2011). Another recent study could show that macrophages support the short-term clearance of cell debris, while BMDMs are important for the less efficient long-term phagocytosis; they are moreover responsible for the protracted axonal dieback (Greenhalgh and David 2014; Evans et al. 2014). Along the same line of ambiguity, it cannot clearly be determined if the inflammatory effect of macrophages and their released cytokines are beneficial or detrimental to tissue repair after TBI (Hohlfeld et al. 2007; Kerschensteiner et al. 2009). The idea of two different types of macrophages is becoming increasingly accepted: classified into the traditionally activated M1 and the alternatively activated M2 macrophages. M1 macrophages – that are colloquially called the ‘bad’ macrophages – secrete high levels of pro-inflammatory factors, e.g. interleukine 6 (IL-6) and interferone gamma (INF- γ), as well as proteolytic enzymes, like metalloproteinases that are degrading the ECM and other proteins. Moreover the secretion of the inducible nitric oxide synthase (iNOS) directly induces neuronal death and secondary tissue damage (Kigerl et al. 2009; Zhou et al. 2014). M2 macrophages on the other hand secrete anti-inflammatory factors (e.g. IL-4, IL-10) to support neuroprotection, tissue regeneration and even the differentiation of neural stem cells and re-myelination in the injury core (Varnum and Ikezu 2012; Zhou et al. 2014). Whether M2 macrophages are derived from a fate switch of M1 macrophages to resolve the inflammation, or from an alternative subgroup of immature cells, and when this occurs, is still being controversially discussed (Varnum and Ikezu 2012; Weisser et al. 2013). Many studies, including a clinical trial in phase 2, tried to exploit M2-primed macrophages for a better clinical outcome after injury. However, especially the phase 2 study was not successful, as the efficacy could not be established and the adverse effects were too high (Lammertse et al. 2012). The limits for this application could be that not enough is known about the internal and external cues inducing this fate switch and about the maintenance of M2 macrophages (reviewed in Silver et al. 2014). For this reason, some scientists already start to retract the simple idea about this ‘good’ and ‘bad’ microglia populations.

1.5.3.2 REACTION OF NG2-GLIA TO BRAIN INJURY

NG2-glia are another cell type reacting within a quite short time window to different kinds of brain insults: within three days following the injury, they significantly increase their proliferation rate resulting in an increase in cell numbers in the proximity of the lesion site (Tan et al. 2005; Buffo et al. 2005; Simon et al. 2011). Moreover, NG2-glia are becoming hypertrophic what is accompanied by morphological changes including a shortening and a thickening of their processes as well as the up-regulation of NG2 (Levine 1994). Post mortem analysis as well as recent *in vivo* imaging studies demonstrated that these cells polarize and

even migrate towards and into the lesion core, suggesting that they are involved in the wound closure and also in the formation of the glial scar (Levine et al. 2001; Hughes et al. 2013; von Streitberg and Schneider et al. submitted).

NG2-glia do not only have a cellular function, they can also provide signals to the surrounding matrix and other cells. As the proteoglycan NG2 is a transmembrane spanning protein, its extracellular domain can be cleaved in the extracellular space by proteases that are present in the lesion (Nishiyama et al. 2009; Trotter et al. 2010). The functions of this shed NG2 are not fully understood yet. It could be active in cell-to-cell signaling and activation of other cells, as the proteoglycan is involved in cell migration (Karram et al. 2005; Binamé et al. 2013). Several studies demonstrated that NG2 – or better said the chondroitin sulfate proteoglycan – is inhibiting neuronal regrowth inside the lesion (Levine et al. 2001; Tan et al. 2005; Galtrey and Fawcett 2007). *In vivo* injections of chondroitinases indeed improve axonal regeneration after injury (Bradbury et al. 2002). Other studies, however, contradictorily demonstrated that the unshed NG2 proteoglycan is supportive to axonal survival (Busch et al. 2010), and that even the shed proteoglycan enhances axonal regrowth for some neurons at least after spinal cord injury (Castro et al. 2005). These data suggest that NG2 could be both supportive and repulsive to neuronal regrowth, depending on the type of neurons or the type of lesion as well as on the area (reviewed in Karram et al. 2005).

While bi-photon *in vivo* imaging is giving new ways to follow individual NG2-glia for longer time periods after the lesion in order to answer the questions of migration, it also enabled scientists to observe the heterogeneity of the cell population. The reaction of NG2-glia close to the lesion site is highly heterogeneous (Figure 8): some NG2-glia migrate, some proliferate, some become hypertrophic and others remain stable; a combination of these reactions can also be observed (von Streitberg and Schneider et al. submitted).

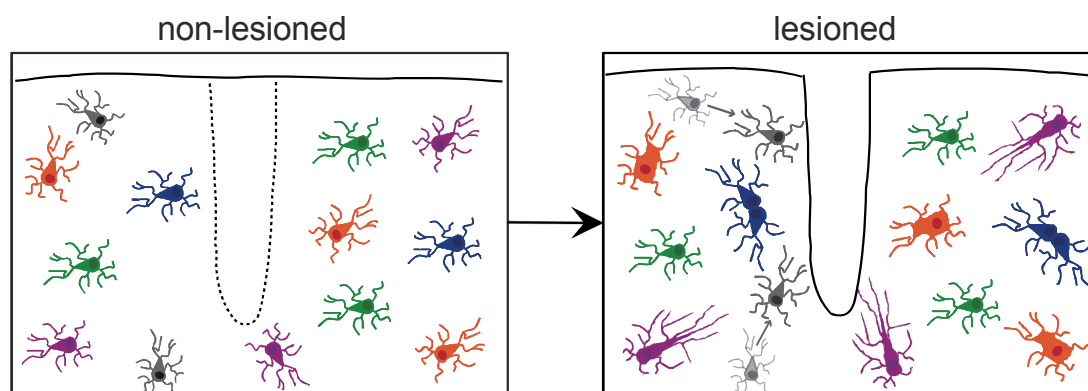


Figure 8: Heterogeneous reaction of NG2-glia after cortical stab wound injury. In the non-lesioned condition, NG2-glia are homogeneously distributed in the cortical GM. Upon injury, some NG2-glia start to migrate (gray) towards the lesion, some become hypertrophic (orange), some proliferate (blue), some polarize toward the lesion (purple) and some few cells remain stable (green). Whether these heterogeneous reactions are due to intrinsic or external cue differences is still unknown (adapted from Dimou and Götz 2014).

However, to which extent these cellular differences occur and whether intrinsic or local external cues are involved still needs to be clarified.

NG2-glia reaction is also highly dependent on the lesion paradigm. Although they react in a comparable manner to viral injections, demyelinating and other inflammatory diseases (Levine et al. 1998; Levine et al. 2001; Zawadzka et al. 2010), they do not become reactive in lesions where the BBB remains closed, although a reaction of both microglia and astrocytes can be observed. Indeed, other studies suggest that platelets, macrophages and other inflammation-associated cytokines derived from the blood are needed to elicit a reaction in NG2-glia (Rhodes et al. 2006; Wang and He 2009; Sirko et al. 2013; Dimou and Götz 2014).

1.5.3.3 REACTION OF ASTROCYTES TO BRAIN INJURY

Astrocytes are showing a heterogeneous reaction to any kind of damage to the CNS and the process of combined astrocyte reactions is commonly termed astrogliosis. As this term has been used unequally by different scientists, a common definition was suggested (Sofroniew and Vinters 2010). In order to term some astrocyte reaction as astrogliosis, the reaction needs to include: (I) a spectrum of changes occurring to all kinds of insults, (II) a variation in the reaction according to the severity of the insult, (III) a context-specific reaction induced by signaling molecules, (IV) the alteration of physiological astrocyte function and most recently, (V) the identification of gradations in different diseases (Sofroniew 2009; Sofroniew and Vinters 2010). The initiation of astrogliosis occurs by pro-inflammatory cytokines like the transforming growth factor α (TGF α) or IL-6, that are released from the injured environment or other cells (Pekny and Pekna 2014).

Although astrogliosis is subdivided into different grades of severity – depending on the type of insult – the hallmarks thereof are the up-regulation of intermediate filaments like the glial fibrillary acidic protein (GFAP), nestin and vimentin, as well as the hypertrophy of both the cell body and the processes. (Wilhelmsson et al. 2006; Sofroniew and Vinters 2010). When astrocytes in the healthy tissue and even after a mild injury become hypertrophic, they occupy separate distinct and non-overlapping domains (Bushong et al. 2002; Wilhelmsson et al. 2006). However, this feature is abrogated after severe injury and scar formation (Sofroniew 2009). In addition to their increase in size, astrocytes that are quiescent in a healthy situation also increase in number due to proliferation in close proximity to the lesion site (Buffo et al. 2005; Robel et al. 2011b). However, this increase in number was now shown to be much lower as previously thought. Most likely, the GFAP upregulation and the hypertrophy was misinterpreted as an increase in numbers, although it is apparently mostly an increase in cell size. Compared with the other glial cell types, less astrocytes re-enter the cell cycle, proliferation starts later, and the proliferating cells are found in great numbers amongst the juxtavascular astrocytes

that contact the blood-vessels not only with their endfeet but with the whole cell soma (Bardehle et al. 2013). As *in vitro* scratch wound models demonstrated, astrocytes were previously thought to migrate into the lesion core to close the lesion (Robel et al. 2011a). However, a recent *in vivo* study proved that their processes polarize toward the lesion, while the cell body remains stable (Bardehle et al. 2013).

From a historical point of view, the astrocytic glial scar and the therein included molecules like chondroitin sulfate proteoglycans or ephrins was seen as a detrimental border for the long-term axonal regrowth and functional improvement after TBI for more than 100 years (Ramón y Cajal, Santiago 1928). Indeed, GFAP/vimentin double knockout mice, in which the dense astrocytic scar formation is limited, exhibit an initially negative but on the long-term better neuroregenerative potential after injury (Wilhelmsson et al. 2004). Recent findings on the other hand using different loss-of-function approaches give evidence that astrocytes have a protective role for the tissue surrounding the lesioned area and that they are an important player in the regulation of CNS inflammation (Sofroniew 2015). Rothstein et al. (1996) demonstrated that astrocytes take up free, diffusing glutamate from the lesion to protect neurons from degeneration. As astrocytes are additionally a key player in the BBB-formation, their proper function is also required for the BBB-closure after injury (Sofroniew and Vinters 2010).

Besides their cellular properties, astrocytes tightly regulate CNS inflammation by secretion of several both anti-inflammatory, e.g. sonic hedgehog (SHH), IL-6 and retinoic acid, as well as pro-inflammatory signals, e.g. the chemokine (C-C motif) ligand 2 (CCL2), the tumor necrosis factor α (TNF α) and the vascular endothelial growth factor (VEGF). Hence, an excessive astrocyte reaction can also lead to a detrimental outcome due to an excessive inflammation (reviewed in Sofroniew 2015).

Table 1: Positive and negative effects of reactive astrogliosis (modified after Pekny and Pekna 2014).

| Positive effects | Negative effects |
|-----------------------------------------------------------------------------------------|------------------------------------------------------------------------------------|
| Physical barrier formation to restrict inflammation | Block of axonal regrowth |
| Restriction of injury size | Limitation of regenerative response & functional recovery after spinal cord injury |
| Blood-brain barrier repair | Limitation of synaptic regeneration |
| Limitation of neuronal loss by uptake of glutamate & release of neuroprotective factors | Negative influence on integration of transplanted neurons/stem cells |
| Protection from long-term neurodegeneration | |
| Reduction of synaptic loss | |

Taken together, a well-balanced astrocyte reaction after TBI requires a complex regulation by intrinsic and extrinsic signals and is furthermore of high importance for the regulation of tissue reaction itself (Pekny and Pekna 2014; Sofroniew 2015).

Besides their general reaction following brain injury, mature parenchymal astrocytes acquire properties that make them similar to adult neural stem cells (NSCs) in the subventricular zone (SVZ) and radial glia during development, from which they developmentally originate, although they only give rise to neurons *in vitro* but not *in vivo* (Robel et al. 2011b; Sirko et al. 2013). These properties are e.g. the upregulation of GFAP, vimentin, tenascin C (TNC) as well as the ability to proliferate. Whether these cells acquire their stem cell potential via de-differentiation from mature astrocytes, or if these neural stem cell-like cells are indeed stem cells migrating into the lesion site from neurogenic niches, is still not fully understood (Lang et al. 2004; Brill et al. 2009). Although these properties and the included mechanisms are only partially understood, they are very attractive to be utilized for endogenous neuronal repair after TBI (Robel et al. 2011b).

1.6 TAMOXIFEN-INDUCIBLE TRANSGENIC MOUSE MODELS

Transgenic inducible mouse lines are a tool to target, visualize and manipulate a specific cell type of interest at a defined stage in the lifetime of a mouse. Although several mechanisms to achieve that goal have been developed, most of the mouse lines employ the CreER/LoxP technology (reviewed in Bockamp et al. 2002). In this system, the cyclization recombination (Cre) site-specific DNA recombinase of the bacteriophage P1 is fused with a modified estrogen receptor (ER) binding domain that has a high affinity to the artificial estrogen tamoxifen (TAM) and the 4-hydroxy-tamoxifen (OHT) derivative, but not to mouse endogenous estrogens. This fusion protein can be placed into the mouse genome under the control of a specific promoter of interest, therefore only cells that are actively expressing the gene of the targeted promoter of interest do translate the CreER fusion protein. By choosing the promoter of interest, the specificity of the targeted cell type can be controlled to a high extent. As the modified ER follows the localization of the endogenous ones without ligand binding, it remains in the cytoplasm and also keeps the Cre recombinase there (Jaisser 2000). Upon TAM induction, the CreER fusion protein is translocated into the nucleus where the Cre recombinase is becoming active. However, the recombination does not occur randomly, but at specific locus of crossover phage (LoxP) sites that have been inserted into the mouse genome. This can be used to specifically delete or activate – by removing a stop cassette – the gene of interest (Sauer 2002), dependent on the localization of the LoxP sites. So-called reporter lines carry a reporter, e.g. the green fluorescent protein (GFP), or β -galactosidase (lacZ), with an upstream stop

cassette that is flanked by LoxP sites. As this system modifies the genome, the induced changes are stable and the reporter remains active until the death of the cells independent from further activity of the promoter, making this system highly favorable for fate-mapping analysis. The advantages hereof compared with constitutively active reporter, or knock-out lines is the increased controllability of the tamoxifen dose (and recombination) as well as the timing of the induction, e.g. when comparing mice at embryonic, postnatal and adult stages, or after injury.

Three types of CreER mouse lines exist: (I) knock-in, (II) transgenic, and (III) bacterial/phage artificial chromosome (BAC/PAC)-transgenic mouse lines. In the knock-in line, the CreER is placed downstream the endogenous promoter, replacing at least parts of the endogenous gene. Although these mice are generally bred heterozygous to maintain the endogenous gene expression, the partial loss can already influence cellular or even behavioral characteristics and can result in a phenotype, as e.g. observed in mice with a heterogeneous paired box 6 (Pax6) mutation (Baulmann et al. 2002). However, using these knock-in lines homozygous serves as a good tool to knock out any gene of interest and to analyze its function. In transgenic and BAC/PAC transgenic mouse lines, the CreER fusion protein is randomly inserted into the genome together with the endogenous promoter sequence and its corresponding regulatory elements, therefore maintaining the endogenous expression levels of the targeted gene.

Table 2: Tamoxifen-inducible mouse lines to target NG2-glia.

| Name | Type | Efficiency | Targeted cell types | Reference |
|----------------------------|---------------|------------|------------------------------------------------------------------------|--------------------------------------|
| GPR17iCreER ^{T2} | BAC-transgene | high | Subsets of NG2-glia expressing GPR17 | Viganò and Schneider et al. in press |
| NG2CreER ^{T2*} | Knock-in | medium | NG2-glia, few neurons | Huang et al. 2014b |
| NG2CreER TM | BAC-transgene | low | NG2-glia, mature oligodendrocytes | Zhu et al. 2008 |
| Olig2::CreER TM | Knock-in | low | Total oligodendrocyte lineage, few astrocytes, few neurons | Dimou et al. 2008 |
| PDGFRαCreER ^{T2} | PAC-transgene | high | NG2-glia, mature oligodendrocytes, few neurons | Rivers et al. 2008 |
| PDGFRαCreER TM | BAC-transgene | medium | NG2-glia, few neurons, few pericytes | Kang et al. 2010 |
| Plp1CreER ^T | transgene | low | NG2-glia, mature and myelinating oligodendrocytes, astrocytes, neurons | Doerflinger et al. 2003 |
| Sox10iCreER ^{T2*} | BAC-transgene | high | Total oligodendrocyte lineage | Simon et al. 2012 |

*These mouse lines were used within the presented work.

Compared to conventional transgenes, the BAC/PAC plasmid is bigger, being of advantage, as the promotor region of a gene can be very big and small vectors can only carry parts of it. Moreover, BACs/PACs were shown to insert into the genome multiple times, resulting in a higher recombination efficiency (Chandler et al. 2007).

A second modulatory factor that can influence the outcome of a transgenic mouse is the use of different estrogen receptors. Some mouse lines carry a modified mouse ER (ERTM), whereas others use the later on developed human ER^T or its improved ER^{T2} version (Metzger et al. 1995; Indra et al. 1999; Vasioukhin et al. 1999). Apart from modulating the estrogen receptor, Shimshek et al. (2002) developed a novel improved form of the Cre recombinase (iCre) that allows a more stable and efficient recombination also improving the outcome.

Although NG2-glia only came into the focus in the last decades, already several mouse lines exist using the above described systems to target and analyze these cells. Table 2 gives a summary of the existing inducible mouse lines for NG2-glia. Within the work presented in this thesis, both the Sox10iCreER^{T2} as well as the NG2CreER^{T2} line were used.

1.7 THE CELL CYCLE REGULATOR **Esco2**

Mitosis is a complicated cellular process that requires a high number of control mechanisms in order to be completed accurately. Especially during S-phase, dividing cells have to ensure that the sister chromatids are symmetrically passed to the two daughter cells in the telophase. Before the separation, the chromatids need to be actively held together. This so called cohesion is mainly mediated by the cohesin: a protein complex consisting of four major subunits as well as many different additional regulatory proteins. The formation of the cohesion machinery that is necessary to provide proper sister chromatid separation can be divided into four major stages: (I) loading, in which the non-cohesive cohesin binds to chromatin, (II) establishment, where cohesin becomes cohesive, (III) maintenance, to keep the chromatids together, and (IV) dissolution, where the chromatids are finally separated. Each of these stages require individual regulatory proteins. The acetyl-transferase establishment of cohesion 1 homologue 2 (Esco2) is one of the most important regulatory proteins in the second stage (reviewed in Onn et al. 2008). This protein was originally discovered in *Saccharomyces cerevisiae* (Eco1), where it is essential for cell viability, but it was also found to be highly conserved in other mammalian as well as non-mammalian species (Uhlmann and Nasmyth 1998; Onn et al. 2008). At least in humans and rodents the Esco2 gene is located on the short arm of chromosome eight. Mammalian genomes encode two orthologues: Esco2 and Esco1 that are variable in their N-termini. Esco1 has been suggested to be partially redundant, but cannot completely replace the function of Esco2 (Hou and Zou 2005; Whelan et al. 2012b;

Rahman et al. 2015). Loss-of function studies demonstrated that Esco2 is only required for the establishment of the cohesion, but dispensable for the loading as well as the maintenance (Unal et al. 2007). Esco2 mutations in humans are associated with the Roberts syndrome in which patients suffer from mild to severe congenital disorders and their chromatogram shows a typical form of 'railroad-track' chromosomes (Vega et al. 2005).

Hence Esco2 is an efficient regulator for proper cohesion and therefore the whole cell cycle. The loss of the gene function was exploited to systemically drive proliferating cells in culture into apoptosis as it causes severe chromatid defects (Whelan et al. 2012a). The same group demonstrated a very efficient use of the Esco2 loss-of-function using an *Emx1CrexEsco2^{fl/fl}* mouse line recombining in cortical neuronal progenitors, in which the knockout mice in postnatal stages completely lack the cortex and half of the hippocampus as cortical neurogenesis does not take place (Whelan et al. 2012b; Hammerschmidt et al. 2015).

2 AIM OF THE STUDY

The cellular characteristics of NG2-glia in the adult brain are well characterized, however still very much remains unknown about their physiological functions in the homeostatic brain network as well as after traumatic brain injury.

Thus, the main objective of my PhD thesis was to address the physiological function of NG2-glia both under physiological conditions as well as after brain injury. Therefore I used a novel approach to deplete proliferating NG2-glia in the adult mouse brain. The depletion was achieved with the tamoxifen-inducible Sox10iCreER^{T2}xCAG-eGFPxEsc^{o2}^{fl/fl} mouse line, in which targeted proliferating NG2-glia are driven into apoptosis during M-phase and are therefore depleted as soon as they try to finish their cell cycle.

Using this novel tool that induces a reduction in the pool of proliferating NG2-glia, I tried to disclose the following more specific questions:

- Does the lack of proliferating NG2-glia alter the tightly regulated homeostatic network?
- Does the depletion influence other cell types in the brain?
- Does the intervention in the physiological lineage progression elicit changes in the cell distribution within the oligodendrocyte lineage?
- Does the depletion of NG2-glia influence the behavioral phenotype in living mice?

Moreover, I used the cortical stab wound injury model in the Sox10iCreER^{T2}xCAG-eGFPxEsc^{o2}^{fl/fl} mouse line to specifically answer those questions:

- Does the fast depletion of individual NG2-glia affect the total NG2-glia population and its reaction upon brain injury?
- Does the lack of NG2-glia in the injury site modify the reaction of other cell types after brain lesion?
- Does the lack of NG2-glia influence the wound healing capacity of the brain?

3 RESULTS

This chapter summarizes the results that were obtained from the genetic ablation of proliferating NG2-glia using the Sox10iCreER^{T2}xCAG-eGFPxEsc^o2^{fl/fl} mouse line. The first part addresses the inducible NG2-glia ablation, its long-term cellular as well as functional consequences for the mice under physiological conditions. In the second part, this mouse line was used to analyze the cellular function and consequences of the ablation of proliferating NG2-glia after acute traumatic brain injury.

3.1 NG2-GLIA ABLATION IN THE HEALTHY BRAIN

3.1.1 ESCO2 DELETION CAUSES SLOW BUT PROGRESSIVE LOSS OF PROLIFERATIVE RECOMBINED NG2-GLIA

To ablate proliferating NG2-glia in the adult brain we used the inducible Sox10iCreER^{T2}xCAG-eGFPxEsc^o2^{fl/fl} mouse line. In all cells with an active Sox10 promoter, tamoxifen induction resulted in a permanent expression of the green fluorescent protein (GFP) as well as in a deletion of the acetyl transferase Esc^o2 (Figure 9-A), whose permanent loss is detrimental for the assembly of the cohesion apparatus during mitosis.

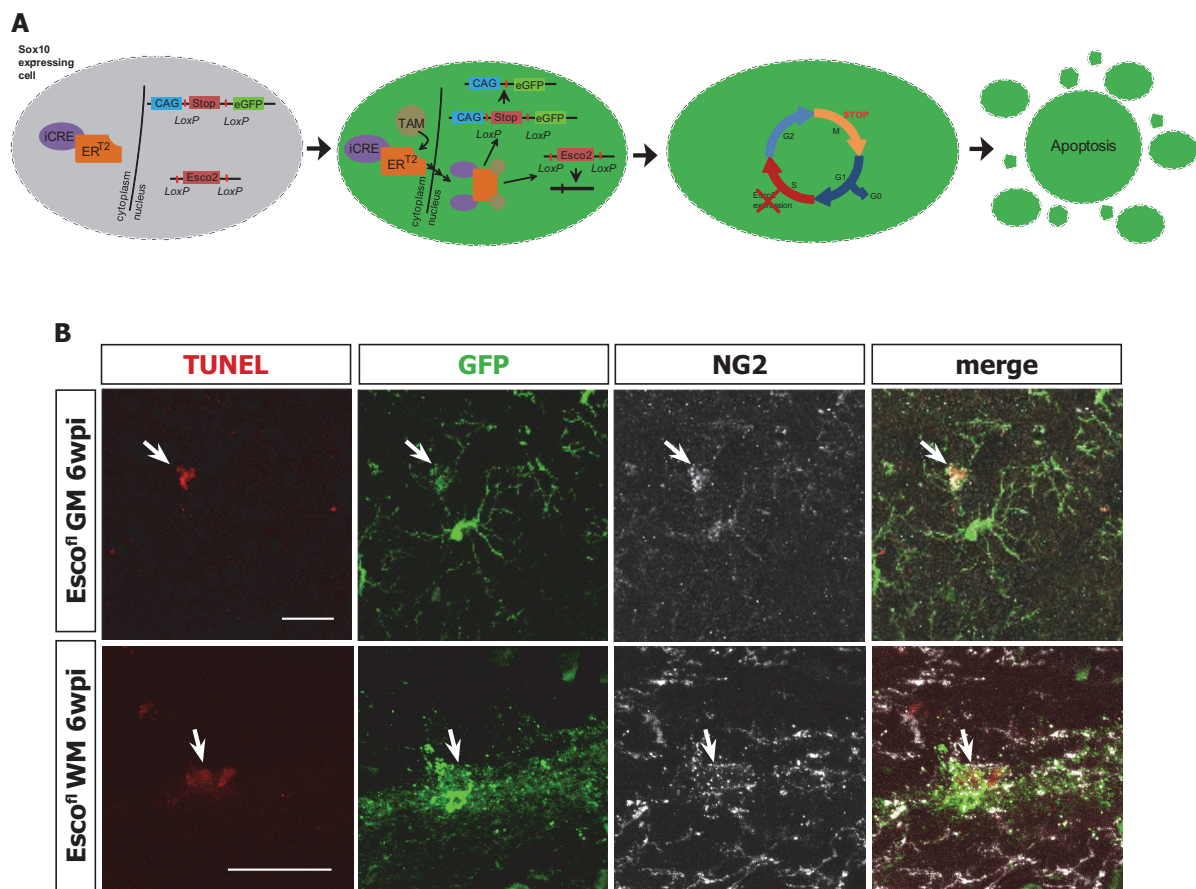


Figure 9: Genetic ablation of proliferating NG2-glia in the adult brain. (A) Schematic drawing of the inducible Sox10iCreER^{T2}xCAG-eGFPxEsc^o2^{fl/fl} mouse model. (B) Examples of apoptotically dying TUNEL⁺/GFP⁺/NG2⁺ cells in the cortical GM (upper panel) and WM (lower panel) at 6wpi. Scale bars represent 25µm.

Consequently, cycling cells that were lacking the Esco2 protein in this mouse model were not able to complete their cycle and were thus driven into apoptosis by cell cycle checkpoints during M-phase. The Sox10 promoter that was used as a driver for this mouse line is active throughout the oligodendrocyte lineage, therefore also mature and myelinating oligodendrocytes were recombined. However, as mature cells are postmitotic and further functions of Esco2 in postmitotic cells are not known, no obvious effects of the Esco2 depletion were expected. Hence, this mouse model represents a novel tool that specifically allows the ablation of cycling NG2-glia in the adult brain.

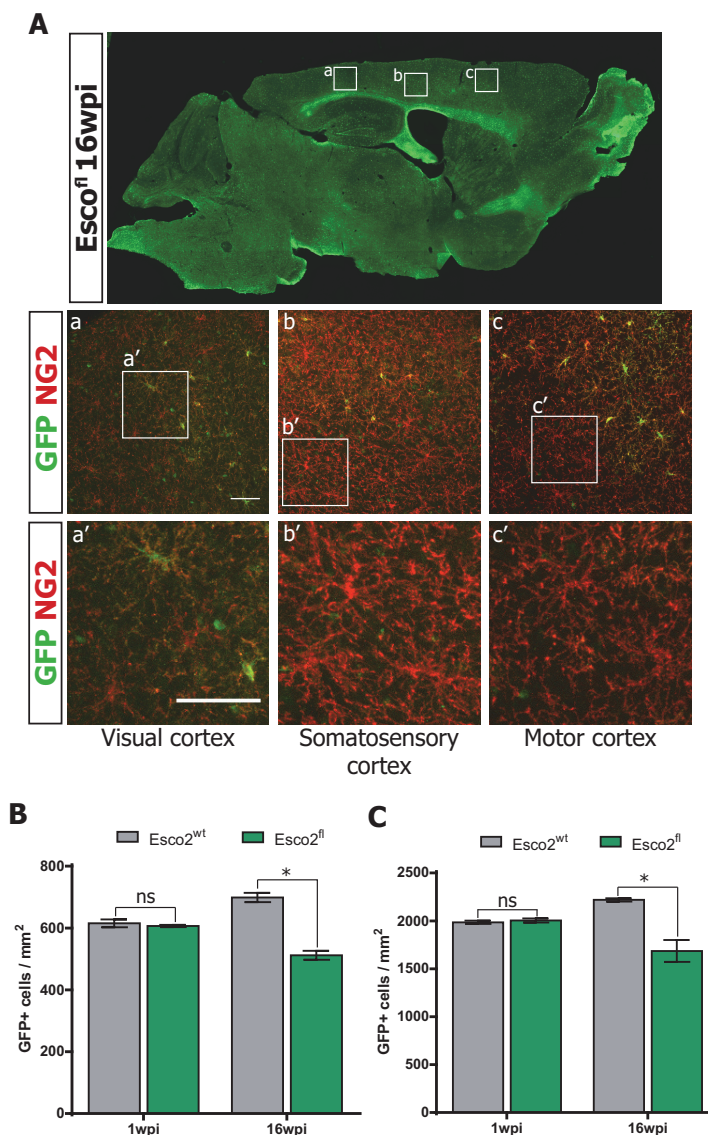


Figure 10: NG2-glia ablation in different cerebral areas. (A) GFP staining in a sagittal section of an Esco2^{fl} mouse at 16wpi. Blow-ups show NG2⁺ (red) and NG2⁺/GFP⁺ (yellow) NG2-glia in the visual (a, a'), somatosensory (b, b') and motor cortex (c, c'). (B) Quantification of GFP⁺ cells in the GM of the whole cerebral cortex. (C) Quantification of GFP⁺ cells in the WM underlying the whole cerebral cortex. Scale bars represent 50µm. Number of animals: n=3 for each bar. Data are presented as mean±sem. Statistical analysis: One-way ANOVA, ^{ns}p>0.05, *p<0.05.

To analyze the loss of NG2-glia in the adult brain, we induced adult mice at the age of eight to ten weeks and investigated coronal brain sections for dying cells by terminal deoxynucleotidyl transferase dUTP nick end labeling (TUNEL) staining at six weeks post induction (wpi). TUNEL⁺/NG2⁺/GFP⁺ cells could be found both in the GM and the WM throughout the cerebral cortex of *Esco2^{fl}* mice, meaning that recombined NG2-glia in our mouse model were indeed diminished by apoptotic cell death (Figure 9-B).

In order to see if the loss of recombined cells occurred evenly distributed or preferentially in distinct areas of the cortical WM, sagittal sections to better compare different cortical areas within one section were immunohistochemically analyzed at 16wpi (Figure 10-A). These data revealed that despite the same recombination rate, the loss of recombined (GFP⁺/NG2⁺) NG2-glia was higher in the GM of the somatosensory cortex compared with the GM of the visual and motor cortex, indicating that the proliferation rate and therefore the death of NG2-glia did not occur equally in different cortical areas. However, it cannot be ruled out that in some cortical areas the loss of *Esco2* was more easily compensated, and hence more cells could escape and still be able to proliferate. For the WM on the other hand, no region-specific differences between rostral and caudal areas could be observed (data not shown).

To determine the dimension of the loss of recombined cells, the total number of GFP⁺ cells (including NG2-glia as well as mature and myelinating oligodendrocytes) was analyzed at 1wpi and 16wpi both in the GM and the WM of the cerebral cortex as an average of all cortical areas (Figure 10-B and C). At 1wpi, the total number of GFP⁺ cells was observed to be similar in *Esco2^{wt}* and *Esco2^{fl}* mice, both in the GM as well as in the WM. However, while the cell number during the 16 weeks of analysis in the *Esco2^{wt}* group significantly increased in both cortical areas – most likely due to the expansion of the proliferative NG2-glia pool – it even decreased in the *Esco2^{fl}* (Table 8 in supplementary tables).

To investigate whether the above described reduction in the GFP⁺ cell pool specifically derived from the ablation of recombined NG2-glia and to address the time course of their death, immunohistochemical analysis in coronal sections of the GM and the WM of the cerebral cortex was performed at 1wpi, 6wpi, 11wpi and 16wpi after tamoxifen induction (Figure 11-B). Initially, the recombination rate at 1wpi reached $76.03 \pm 0.46\%$ of the total NG2-glia in *Esco2^{wt}* and $74.67 \pm 0.57\%$ in *Esco2^{fl}* animals in the GM (Figure 11-C, Table 9 and Table 10 in supplementary tables). For the WM, the recombination rate was even significantly higher with $85.2 \pm 2.3\%$ of all NG2-glia in the *Esco2^{wt}* and $83.3 \pm 3.1\%$ of all NG2-glia in the *Esco2^{fl}* mice (Figure 11-D, Table 9 and Table 10 in supplementary tables). As recombined NG2-glia were apoptotically lost after proliferation in *Esco2^{fl}* mice, a progressive decrease in the absolute number of NG2⁺GFP⁺ cells could be observed, both in the GM as well as in the WM. As expected, the loss of these cells was much more prominent in the WM compared with the GM

(Table 9 in supplementary tables), due to the shorter cell cycle length of NG2-glia in the WM. In contrast, in the wildtype control group the total number of recombined NG2-glia remained almost stable in the GM and decreased – although significant – only little in the WM. Notably, the absolute number of cells in the NG2-glia population (GFP⁺ and GFP⁻) in *Esco2*^{fl} mice was never reduced over the whole analysis time compared with the *Esco2*^{wt} group, neither in the GM nor in the WM of the cerebral cortex (Figure 11, Table 10 in supplementary tables). To test whether the stability of the total NG2-glia numbers derived from a compensatory proliferation of non-recombined NG2-glia, Ki67 staining to label actively proliferating cells was performed at 11wpi in coronal sections of the GM and the WM (Figure 12).

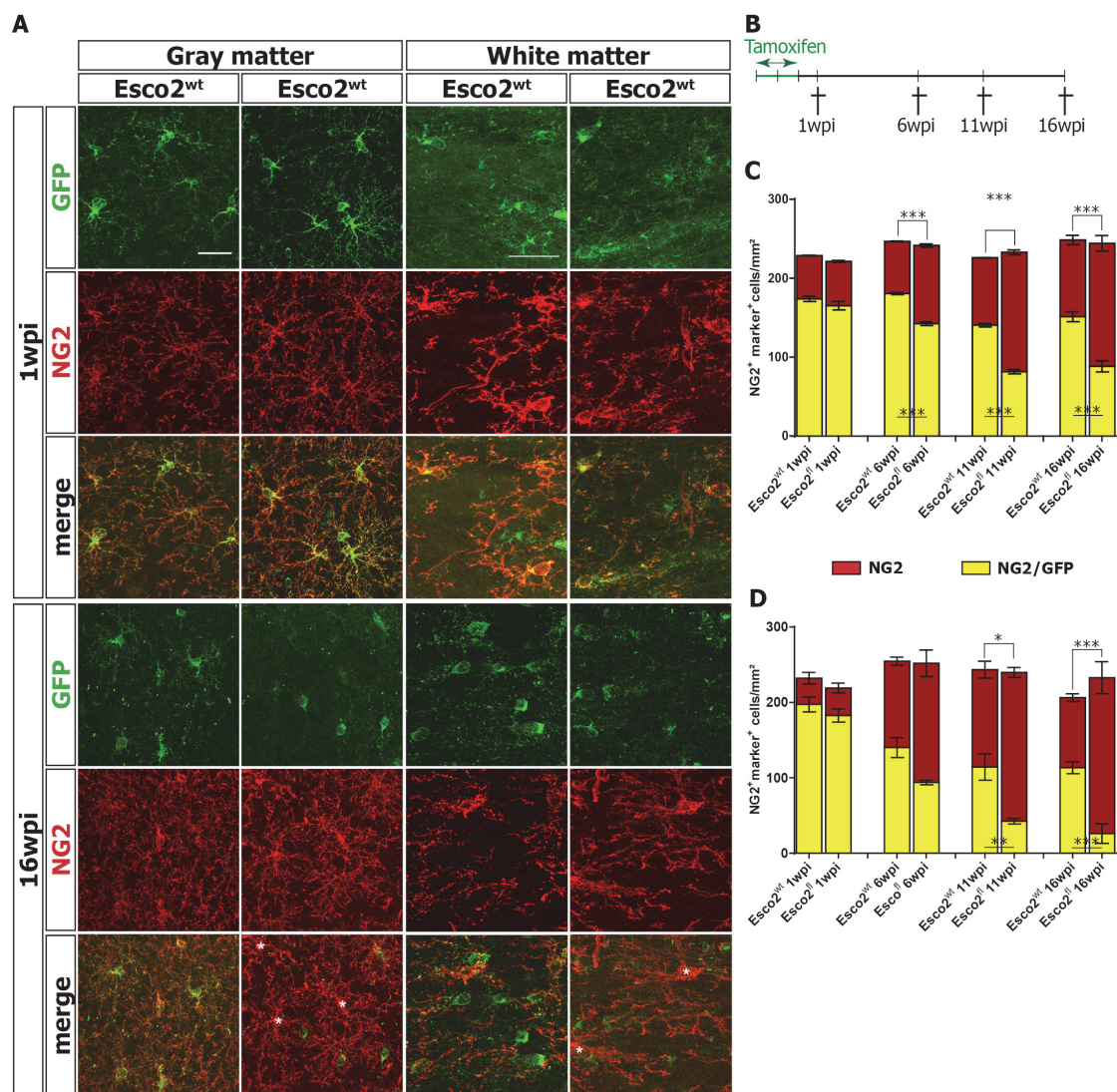


Figure 11: Long term analysis of recombined NG2-glia. (A) Images of recombined and non-recombined NG2-glia in the cortical gray and white matter at 1wpi and 16wpi. Non-recombined NG2-glia are indicated with an asterisk. (B) Scheme of the experimental procedure. (C) Absolute numbers/mm² of recombined (yellow) and non-recombined (red) NG2-glia in the cortical GM at different timepoints after induction. (D) Absolute numbers/mm² of recombined (yellow) and non-recombined (red) NG2-glia in the cortical WM at different timepoints after induction. Scale bars represent 25µm. Data are presented as mean±sem. Number of animals: n=3 for each bar (n=4 for *Esco2*^{fl} GM 11wpi). Statistical analysis: One-way ANOVA, *p<0.05, **p<0.001, ***p<0.0001.

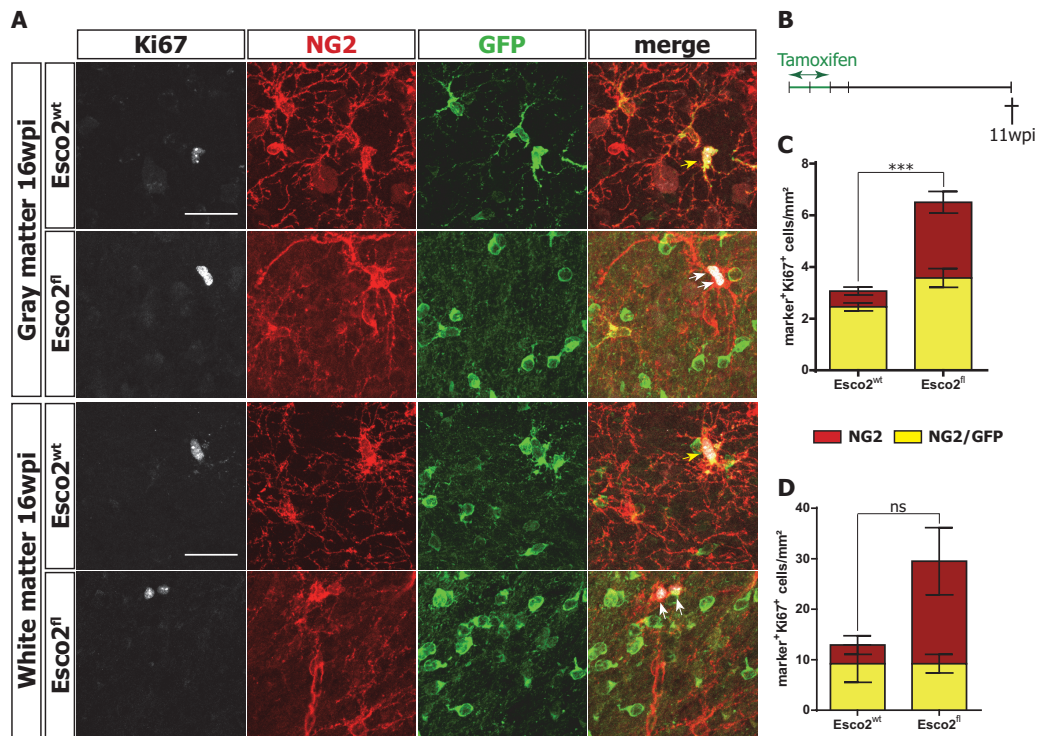


Figure 12: Proliferating NG2-glia in the cortical GM and WM. (A) Proliferating (Ki67⁺) recombined (yellow arrows) and non-recombined (white arrows) NG2-glia in the cortical GM and WM. (B) Scheme of experimental procedure. Absolute numbers/mm² of recombined (yellow) and non-recombined (red) Ki67⁺ NG2-glia in the cortical (C) GM and (D) WM at 11 weeks after induction. Scale bars represent 25μm. Data are presented as mean±sem. Number of animals: n=3 for each bar. Statistical analysis: unpaired students t-test, ^{ns}p>0.05, ***p<0.0001.

Indeed, we found that the number of the non-recombined, actively cycling NG2⁺/Ki67⁺/GFP⁺ cells was significantly higher in Esco2^{fl} (2.9±1.1 cells/mm² in the GM and 20.3±6.7 cells/mm² in the WM) than in Esco2^{wt} animals (0.6±0.2 cells/mm² in the GM, 3.7±1.8 cells/mm² in the WM), demonstrating a compensatory increase in the proliferation of non-recombined NG2-glia.

In order to analyze whether the progressive apoptotic loss and subsequent change in the proliferative behavior of NG2-glia induced any changes or even activation in other major brain cell populations, microglia/macrophages, astrocytes as well as neurons were immunohistochemically analyzed in coronal sections of the cerebral GM at 16wpi (Figure 13). As the apoptotic loss of NG2-glia occurred progressively and was widely distributed in the used mouse model, we did not observe a significant infiltration of blood-derived (CD45⁺/Iba1⁺) macrophages (data not shown) that would display a strong sign of inflammation. Furthermore Iba1/CD45-activated microglia were not significantly augmented in the Esco2^{fl} mice (2.7±0.5 cells/mm²) compared with the wildtype controls (8.6±2.4 cells/mm²), although the number of actively cycling microglia (Iba1⁺/Ki67⁺) was increased in the Esco2^{fl} (0.2±0.2 cells/mm²), compared with the Esco2^{wt} mice (1.7±0.2 cells/mm², Figure 13-A and B). However, the proliferation rate was still low and therefore the absolute cell number of microglia in the cortex was not affected (data not shown), meaning that the overall cell population did not change.

Analysis of the astrocyte population showed that some of the cells upregulated GFAP in the GM, that is usually only expressed by activated protoplasmic astrocytes in *Esco2^{fl}* mice (91.5 ± 3.2 cells/mm²), but only little under physiological conditions in control animals (13.3 ± 1.5 cells/mm²). Actively cycling, reactive astrocytes (GFAP⁺/Ki67⁺) on the other hand were not present (data not shown), meaning that the *Esco2^{fl}* mice did not develop a full astrogliosis, as the hallmark thereof is both activation and proliferation of astrocytes. Additionally, neuronal cresylviolet staining did not reveal any observable modifications in the neuronal population that could have been induced by the cumulative changes in the NG2-glia population (Figure 13-C).

In summary, successful Sox10-promoter-driven ablation of proliferating NG2-glia was achieved both in the GM as well as in the WM of the cerebral cortex. The progressive loss of proliferating recombined NG2-glia resulted in an increased proliferation of non-recombined cells, without inducing any changes in numbers and morphology of GM neuronal cell bodies. Only minor changes in cell numbers or reaction of the other major glial cell populations in the GM were observed.

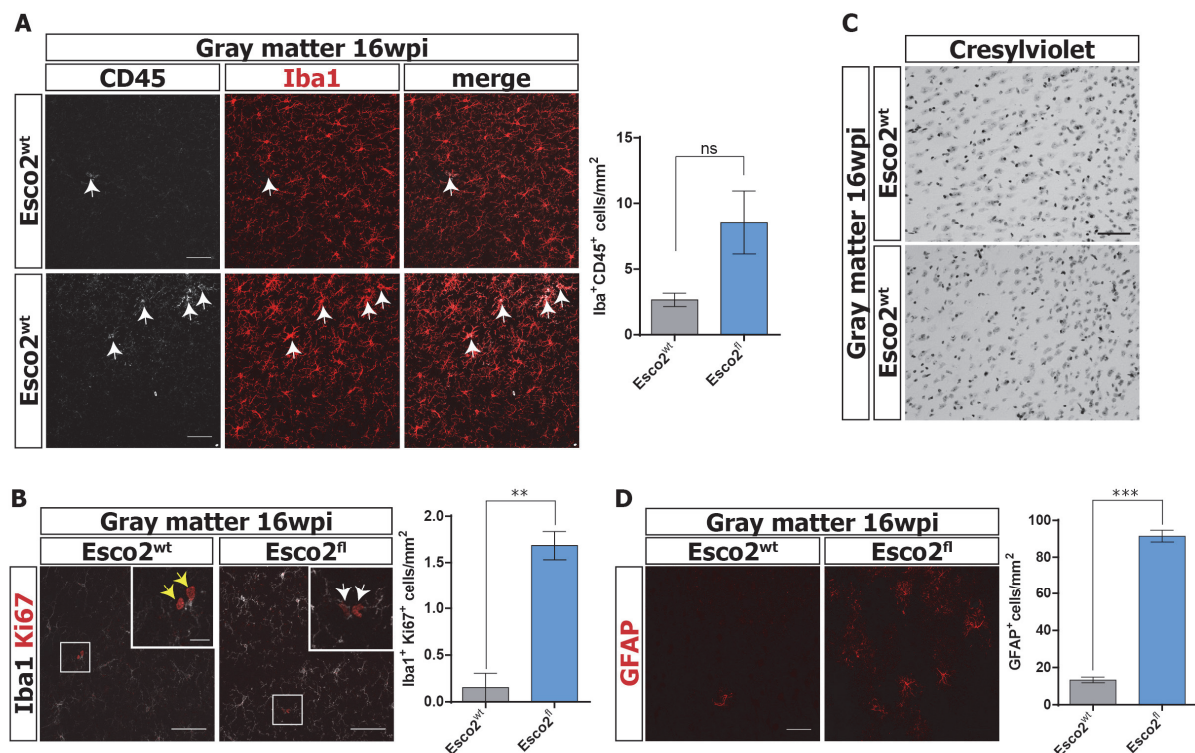


Figure 13: Reaction of other cell types in the cortical gray matter at 16wpi. (A) Examples and absolute numbers/mm² of CD45/Iba1-activated microglia (white arrows) in the cortical gray matter. (B) Proliferating (Ki67⁺, white arrows) and non-proliferating Iba1⁺ microglia/mm² in the cortical gray matter. Yellow arrows indicate Ki67⁺Iba1⁺ proliferating cells. (C) Cortical neuronal cell bodies stained with cresylviolet. (D) Examples and absolute numbers/mm² of GFAP-reactive astrocytes in the cerebral gray matter. Scale bars represent 50μm, 25μm in inlays in D. Data are presented as mean±sem. Number of animals: n=3 for each bar. Statistical analysis: unpaired student's t-test, ^{ns}p>0.05, **p<0.001, ***p<0.0001.

3.1.2 NG2-GLIA ABLATION DECREASES OLIGODENDROGENESIS

The NG2-glia network displays a tightly regulated system in which the homeostasis between proliferation and differentiation is strongly controlled. In order to analyze whether the altered proliferation characteristics of NG2-glia in the above described mouse model also affected their differentiation properties, we analyzed the oligodendrocyte turnover in coronal sections of adult animals. After tamoxifen induction the animals received the thymidine analog 5-Bromo-2'-deoxyuridine (BrdU) for two weeks via the drinking water. BrdU is integrated into the newly synthesized DNA strand of dividing cells and can be identified by directing an antibody against it. After a nine week retaining period (11wpi in total) animals were sacrificed (Figure 14-B). During this retaining period, the mice received normal drinking water, however, BrdU has permanently been integrated into the DNA strand and therefore retained in the originally proliferating cells, allowing the determination of the fate of those cells. As CC1⁺ oligodendrocytes are postmitotic, potential BrdU⁺/CC1⁺ cells were originally proliferating NG2-glia that incorporated BrdU, and subsequently differentiated into mature oligodendrocytes during the retaining period. Newly generated oligodendrocytes could therefore be identified by BrdU/CC1 double labeling at the end of the retaining period.

In the GM, no obvious differences in the absolute number of newly generated oligodendrocytes could be found between the Esco2^{fl} and control animals (64.6±3.3 cells/mm² in the Esco2^{wt} and 53.5±2.9 cells/mm² in the Esco2^{fl} mice, Figure 14-C). Only the amount of CC1⁺BrdU⁺GFP⁺ triple positive, newly generated oligodendrocytes was reduced (14.7±1.6 cells/mm²) compared with the wildtype group (32.5±2.6 cells/mm²), demonstrating that the differentiation capacity of recombined NG2-glia was decreased, as these cells were either depleted or forced to proliferate in the Esco2^{fl} mice. However, this fraction was slightly compensated by the increased differentiation of non-recombined (CC1⁺/BrdU⁺/GFP⁻) cells (32.1±1.6 cells/mm² in the Esco2^{wt} and 38.8±2.1 cells/mm² in the Esco2^{fl} mice). Regarding the percentage of total BrdU cells in the cortical GM (Figure 14-D), the fraction of newly generated oligodendrocytes in total (CC1⁺/BrdU⁺/GFP⁺ and CC1⁺/BrdU⁺/GFP⁻) was significantly lower in the Esco2^{fl} mice (29.4±1.1%) than in the wildtype controls (47.6±3.5%). Moreover, NG2-glia in the Esco2^{fl} mice increased their proliferation at the expense of differentiation (57.9±1.1%), as their fraction within the BrdU (NG2⁺BrdU⁺) pool was highly increased compared with the controls (42.9±2.6%, Figure 14-E).

In the WM on the other hand, the total number of newly generated oligodendrocytes that were BrdU⁺/CC1⁺-labelled was significantly lower in Esco2^{fl} animals (49.6±12.9 cells/mm²), compared with their Esco2^{wt} littermate controls (153.6±4.1 cells/mm², Figure 14-D).

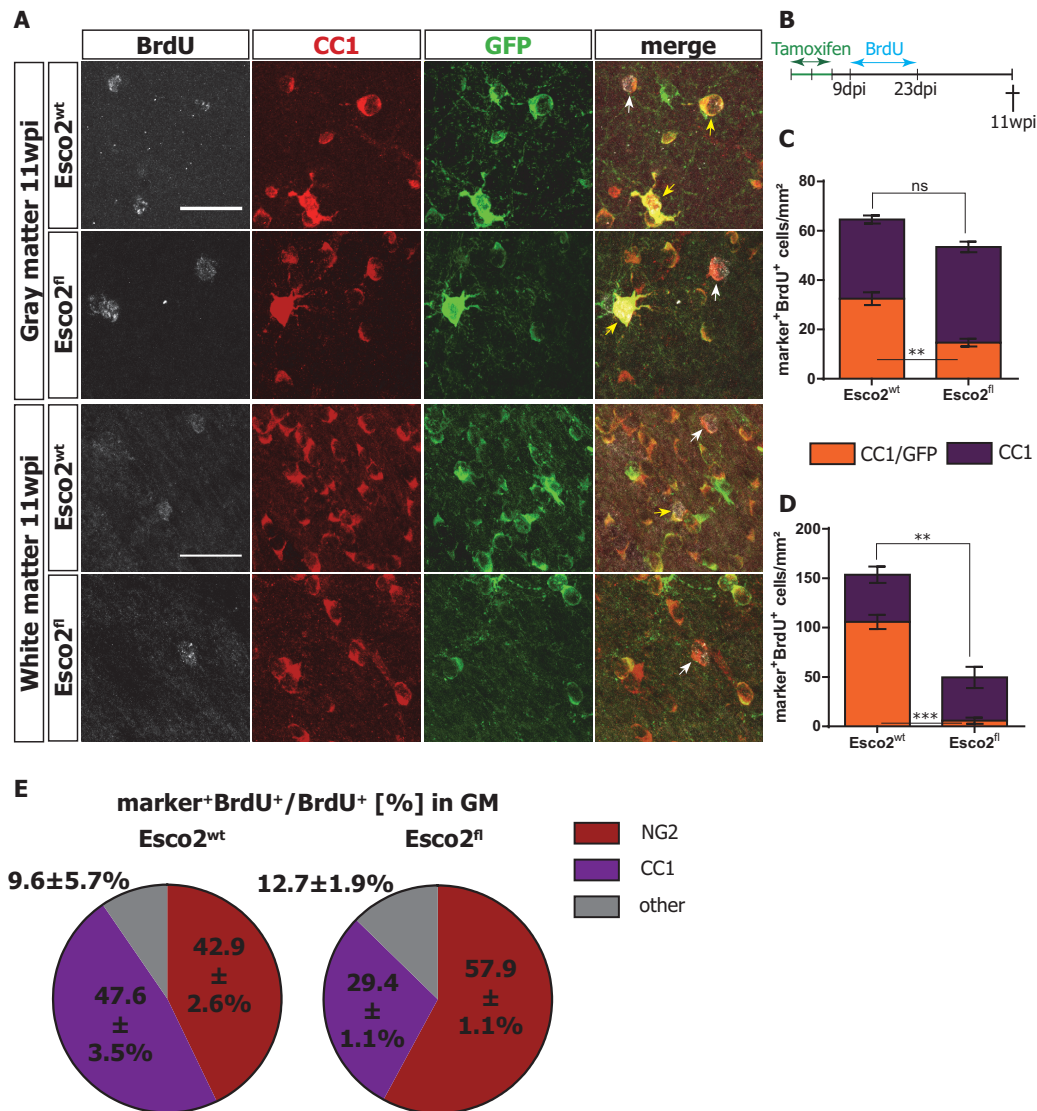


Figure 14: Newly generated oligodendrocytes in the cortical GM and WM. (A) Recombined (yellow arrows) and non-recombined (white arrows) newly generated oligodendrocytes (BrdU⁺/CC1⁺) in the cortical GM and WM at 11wpi. (B) Scheme of the experimental procedure. Absolute numbers/mm² of recombined (orange) and non-recombined (purple) BrdU⁺ oligodendrocytes in the cortical (C) GM and (D) WM at 11wpi. (E) Percentage distribution of different cell types amongst the total BrdU population in Esco2^{wt} and Esco2^{fl} mice at 11wpi. Scale bars represent 25µm. Data are presented as mean±sem. Number of animals: n=3 for each bar or pie. Statistical analysis: unpaired student's t-test, ^{ns}p>0.05, **p<0.001, ***p<0.0001.

The major reduction in the Esco2^{fl} mice could again be observed in the CC1⁺/BrdU⁺/GFP⁺ recombined cell fraction (105.8±7.2 cells/mm² in the Esco2^{wt} and 5.8±3.2 cells/mm² in the Esco2^{fl} mice), whereas the non-recombined cells contributing to the newly generated oligodendrocytes CC1⁺/BrdU⁺/GFP⁻ were similar in both groups (47.7±8.3 cells/mm² in the Esco2^{wt} and 43.8±10.8 cells/mm² in the Esco2^{fl} mice). Analysis of WM tracts in the cerebellum yielded similar results (data not shown), where newly generated oligodendrocytes of 116.2±8.3 cells/mm² in the Esco2^{wt}, but only 30.4±9.9 cells/mm² in the Esco2^{fl} mice, were found. Also here, the reduction of the total number of oligodendrocytes was mainly derived from the loss of the recombined (GFP⁺) cell fraction.

In summary, this experiment revealed that the increased proliferation and the death of NG2-glia resulted in a decreased differentiation into mature oligodendrocytes; predominantly in WM tracts of the cortex.

3.1.3 NG2-GLIA ABLATED MICE SHOW DISRUPTIONS IN THE NODES OF RANVIER

As the proliferation and differentiation capacities of NG2-glia in the cortical GM are known to be much lower compared with those in the WM, the progressive ablation of NG2-glia did not result in significant cellular changes in the cortical GM but only in the WM. Therefore, all further analysis was carried out in the cortical WM, where significant changes in proliferation as well as in differentiation properties of NG2-glia were identified in the *Esco2^{fl}* mice. In recent years, many studies demonstrated – against the old dogma of solely postnatal myelin production – that new oligodendrocytes and consequently new myelin sheaths are produced throughout the whole lifespan. Therefore we hypothesized that the lack of adult oligodendrogenesis in our mouse model could affect the myelin turnover and subsequently lead to disruptions in the global myelin structure. Consequently, a global Sudan black myelin staining as well as an ultrastructural analysis was performed in the cortical WM of our animal model at 16wpi and 12wpi, respectively.

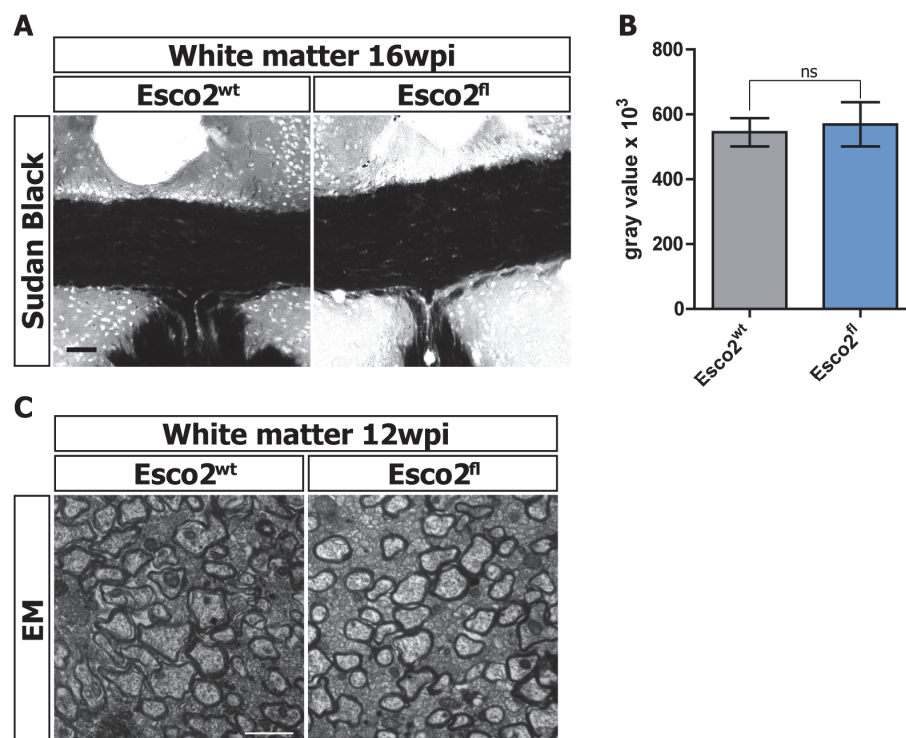


Figure 15: Myelin analysis in the white matter. (A) Sudan black staining in the white matter in *Esco2^{wt}* and *Esco2^{fl}* mice at 16wpi. (B) Gray value intensity measurement of myelin staining in *Esco2^{wt}* and *Esco2^{fl}* mice at 16wpi. (C) Ultrastructural analysis (electron microscopy) of sagittal sections in the white matter in *Esco2^{wt}* and *Esco2^{fl}* animals at 12wpi. Scale bars represent 50 μ m (A) and 1250nm (B). Data are presented as mean \pm sem. Number of animals: n=3 for the *Esco2^{wt}* and n=4 for the *Esco2^{fl}*. Statistical analysis: unpaired student's t-test, ^{ns}p>0.05.

Compared with the wildtype controls, the global myelination was not different in the *Esco2^{fl}* mice: the Sudan black gray value intensity analysis in coronal WM sections did not reveal any differences between the two groups ($544.7 \pm 43.4 \times 10^3$ for the *Esco2^{wt}*, $569.3 \pm 68.4 \times 10^3$ for the *Esco2^{fl}*, Figure 15-B), meaning that no obvious demyelinated areas were present that would appear white in the staining (and give a high gray value in the analysis, Figure 15-A).

To additionally investigate the myelin integrity of single axons in the WM, electron microscopy was performed in sagittal sections at 12wpi. In accordance with the myelin staining, *Esco2^{fl}* mice did not show severe signs of demyelination (Figure 15-C). The number of myelinated axons did not seem to be different and the myelin sheaths around the axons also appeared normally wrapped and compacted. We found some myelin aberrations in the *Esco2^{fl}* mice (multiply myelinated axons, myelin protrusions), but they were not significantly higher compared with the rarely appearing aberrations in the *Esco2^{wt}* mice (data not shown).

Although the analysis of the global myelination did not yield any disturbances in the *Esco2^{fl}* mice neither at 12wpi nor at 16wpi, we wanted to investigate the integrity of the nodal regions in these mice as the nodes of Ranvier are a highly structured functional entity of the myelin (Figure 16-F). Each of these compartments carry specific functional components and their structural loss is often accompanied by a loss of its specific function, e.g. the propagation of the axon potential, what can also be observed in different diseases (Arancibia-Carcamo and Attwell 2014). The immunohistochemical analysis of the myelin-associated structures at 16wpi on the other hand revealed that both in the nodes and paranodes of the *Esco2*-depleted animals, significant structural changes were present. Measuring the paranode length with an immunohistochemical CASPR staining in coronal sections demonstrated that the paranodes were significantly longer in the *Esco2^{fl}* animals compared with the controls (average length of $2.28 \pm 0.14 \mu\text{m}$ in the *Esco2^{wt}* vs. $3.10 \pm 0.06 \mu\text{m}$ in the *Esco2^{fl}* mice). Also the non-myelin nodes whose lengths were determined by measuring the distance between two adjacent paranodal CASPR stainings were affected (Figure 16-B and C): an elongation of approximately 50% of the nodes in the *Esco2*-depleted animals was observed (average length of $0.77 \pm 0.01 \mu\text{m}$ in the *Esco2^{wt}* vs. $1.18 \pm 0.02 \mu\text{m}$ in the *Esco2^{fl}* mice).

In order to determine how many of the nodes and paranodes in the *Esco2^{fl}* mice were affected by the elongation, a frequency distribution of different length intervals of these structures was performed (Figure 16-D and E). For both the nodes and the paranodes, a length interval of $0.4 \mu\text{m}$ was chosen, ranging from $0 \mu\text{m}$ to $2.8 \mu\text{m}$ in the nodes and from $1.2 \mu\text{m}$ to $6.0 \mu\text{m}$ in the paranodes. This analysis revealed that not all of the structures were elongated, but only some of those concentrated in the middle of the chosen range, while the extremely short and long structures appeared as often as in the *Esco2^{wt}* control animals.

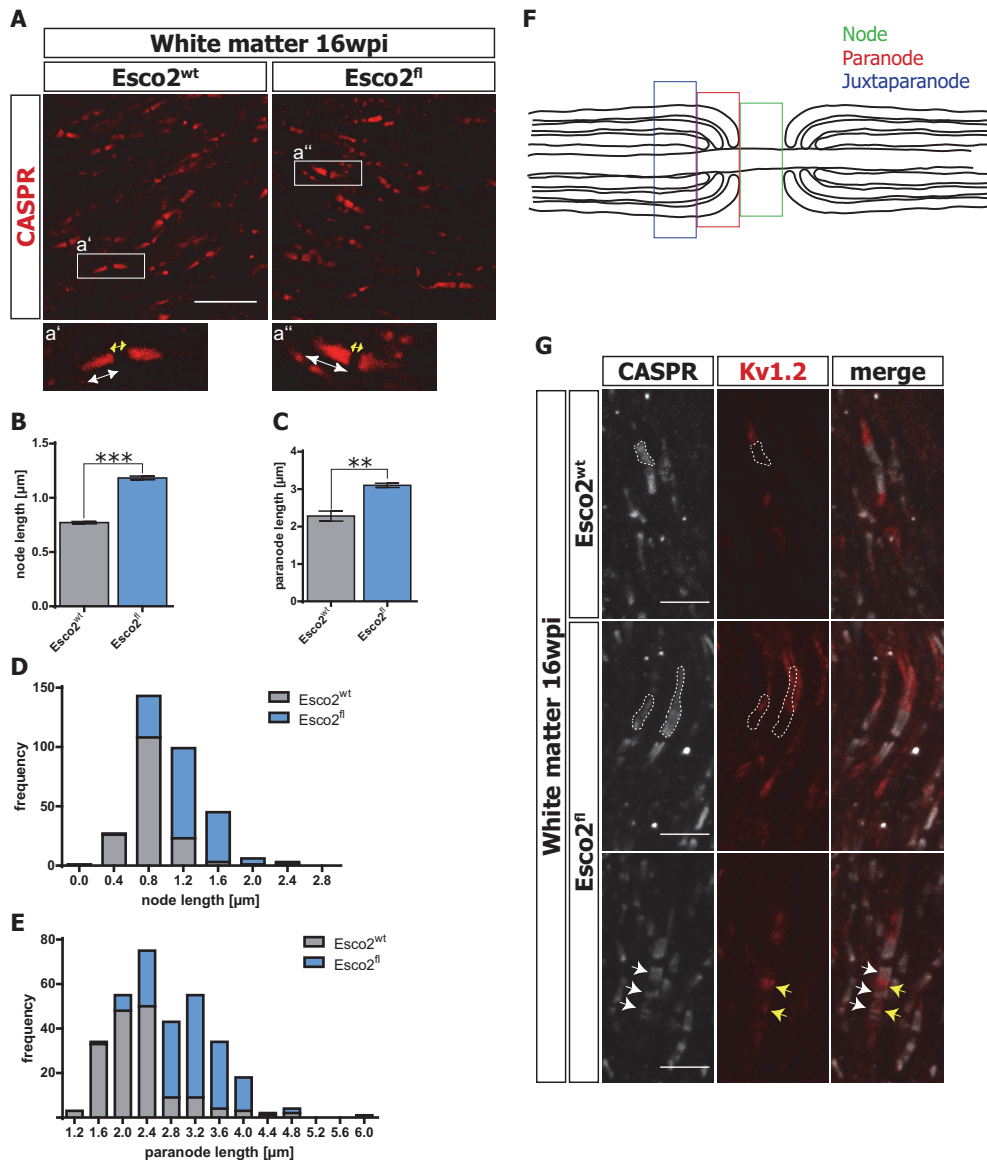


Figure 16: Nodes of Ranvier at 16wpi in the cortical white matter. (A) Paranodal CASPR staining in *Esco2*^{wt} and *Esco2*^{fl} animals. Quantification of average length of the (B) nodes and (C) paranodes in *Esco2*^{wt} and *Esco2*^{fl} animals. Frequency distribution of length intervals of the (D) nodes and (E) paranodes in *Esco2*^{wt} and *Esco2*^{fl} animals. (F) Schematic drawing of the node of Ranvier in the CNS. (G) Paranodal (CASPR) and juxtaparanodal (Kv1.2) staining in *Esco2*^{wt} and *Esco2*^{fl} animals. Dashed lines frame the paranodal CASPR staining (upper and mid panel), that is adjacent to Kv1.2 staining in the *Esco2*^{wt} but overlapping in the *Esco2*^{fl} animals. White arrows (lower panel) indicate discontinuous CASPR staining with Kv1.2 staining (yellow arrows) in between. Scale bars represent 10 μ m (A) and 5 μ m (G). Data are presented as mean \pm sem. Number of animals: n=3 for each bar. Number of nodes and paranodes: n=54 for each animal. Statistical analysis: unpaired student's t-test, **p < 0.001, ***p < 0.0001.

In the nodes, an increase in the frequency of lengths between 0.8 μ m-1.6 μ m and in the paranodes, an increase in the frequency of lengths between 2.0 μ m and 4.0 μ m could be observed in the *Esco2*^{fl} mice.

To identify the onset of the destabilization in the nodes of Ranvier in the *Esco2*^{fl} mice, we performed the immunohistochemical CASPR analysis already at 11wpi (data not shown). However, at this earlier timepoint no changes in the nodal and paranodal structures were

detected, demonstrating that the disturbances only start at late stages, when already a high number of recombined NG2glia have been ablated.

Disintegration of one component of the node of Ranvier is usually accompanied by the disintegration of other physiologically important components like the ion channels, as it occurs in different myelin pathologies (Arancibia-Carcamo and Attwell 2014). For this reason, the integral localization of the potassium channel Kv1.2 was immunohistochemically analyzed in the *Esco2^{fl}* mice that, under physiological conditions is located at the juxtaparanode without overlapping with the paranode (Wang et al. 1993b). At 16wpi we found paranodes with overlapping CASPR and Kv1.2 stainings in the *Esco2^{fl}* animals (Figure 16-G mid), as well as discontinuous CASPR stainings with some clustered Kv1.2 channels in between (Figure 16-G bottom), meaning that the juxtaparanodal Kv1.2 channels were spreading in the paranode and indicating that the juxtaparanodal integrity is also affected in these mice.

In conclusion, some of the nodes of Ranvier in the cortical WM of the NG2-glia ablated mice – the same area where a reduced oligodendrogenesis was observed – showed a disintegration of their highly structured compartmentalization.

3.1.4 NG2-GLIA ABLATED MICE DEVELOP LONG-TERM MOTOR DYSFUNCTIONS

Proper structural organization of the nodes of Ranvier and subsequently an appropriate conduction velocity for propagating the axon potential alongside the axon are important factors to fulfil a normal physiology in the body, enable movements and motor coordination. In order to analyze whether the disintegration of the paranodal structures led to a phenotype in the motoric performance in our animal model, we carried out repetitive long-term behavioral tests (Figure 17). Animals were trained for two weeks and received three doses of tamoxifen during this time. After the training period, motor assessment was carried out on a weekly basis until the animals were perfused 29 weeks later (29wpi). The following standardized behavioral tests to assess motor functions were performed: I) a beam crossing test for coordination and balance, II) a grid walk test which accounts for a fine limb motor coordination, III) a rotarod test for cerebellar coordination and balance, IV) a horizontal irregular ladder test that is specific for corticospinal defects, as well as V) an open field test for general activity evaluation. The corticospinal-specific test was performed as a control experiment, to rule out that the NG2-glia ablation not only affected the brain, but possibly also the spinal cord, where NG2-glia are less proliferative. In addition, a novel object recognition (NOR) test to evaluate the short-term memory of the *Esco2^{fl}* mice was performed.

In the beam crossing experiment, a progressive motor deficiency could be observed in the *Esco2^{fl}* mice.

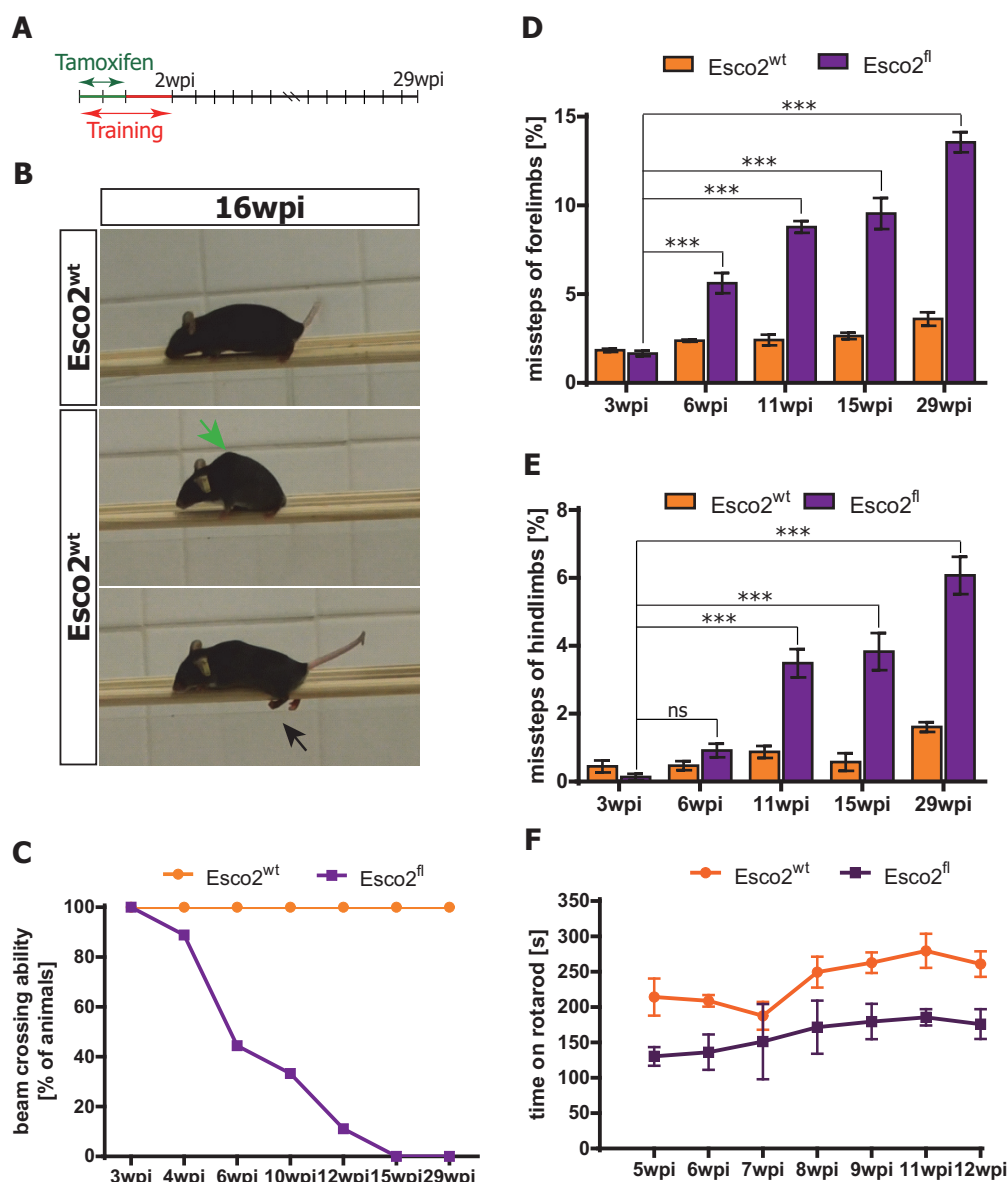


Figure 17: Beam crossing, grid walk and rotarod behavioral experiment. (A) Scheme of the experimental procedure. (B) Examples of Esco2^{wt} and Esco2^{fl} mice during the beam crossing experiment at 16wpi. Green arrow indicates a kyphosis (mid panel), black arrow the clamped hindlimbs (lower panel) in the Esco2^{fl} mice. (C) Beam crossing performance of Esco2^{wt} (orange) and Esco2^{fl} (purple) animals at different timepoints after the training period. (D) Percentage of forelimb grid walk performance of Esco2^{wt} (orange) and Esco2^{fl} (purple) animals at different timepoints after the training period. (E) Percentage of hindlimb grid walk performance of Esco2^{wt} (orange) and Esco2^{fl} (purple) animals at different timepoints after the training period. (F) Time spent successfully on accelerating rotarod paradigm of Esco2^{wt} (orange) and Esco2^{fl} (purple) animals at different timepoints after the training period. Number of animals: Beam crossing: n=9 for Esco2^{fl} 2, 4, 6, 12wpi, n=8 for Esco2^{fl} 14wpi, n=7 for Esco2^{wt} 2, 4, 6wpi, n=6 for Esco2^{wt} 10 and 12wpi and Esco2^{fl} 29wpi, n=5 for Esco2^{wt} 14wpi, n=3 for Esco2^{wt} 29wpi. Forelimb and hindlimb grid walk analysis: n=9 for Esco2^{fl} 3, 6, 11wpi, n=8 for Esco2^{fl} 15wpi, n=7 for Esco2^{wt} 3, 6, 11wpi, n=6 for Esco2^{fl} 29wpi and Esco2^{wt} 15wpi, n=4 for Esco2^{wt} 29wpi. Rotarod: n=3 for each timepoint. Data are presented as mean±sem. Statistical analysis: repeated measures ANOVA, ^{ns}p>0.05, ***p<0.0001.

These motoric disturbances increased over time and reached several stages: at the beginning of the experiment, 100% of the Esco2^{fl} mice crossed the beam normally, at 10wpi only 30% of the mice were able to cross the beam and the others were only able to hold themselves for

several seconds. By the end of the experiment, all of the mice were incapable to even sit on the beam. Finally, all *Esco2^{fl}* animals lost their ability to cross the wooden beam within 14wpi, whereas 100% of the control littermates maintained their ability to do so (Figure 17-C). Additionally to the decreased coordination performance, we observed postural abnormalities in our mice while crossing the beam that was shown to be typical in de- or dysmyelinating diseases (Lappe-Siefke et al. 2003; Kassmann et al. 2007): a kyphosis, (Figure 17-B mid) as well as clamping of hind limbs around the beam (Figure 17-B bottom).

Also in the grid walk experiment testing for fine limb coordination, a progressive misstep rate of the forelimbs in the *Esco2^{fl}* animals was observed until the end of the experiment at 29wpi (Figure 17-D, Table 11 in supplementary tables). Both the *Esco2^{wt}* and the *Esco2^{fl}* mice started with a low misstep rate shortly after the training period at 3wpi ($1.8 \pm 0.1\%$ for the *Esco2^{wt}* and $1.7 \pm 0.2\%$ for the *Esco2^{fl}* mice). In the *Esco2^{wt}* animals the misstep rate did not increased significantly during the course of the experiment, whereas the fine-tuned motor functions of *Esco2^{fl}* animals progressively declined over time. Additionally, we observed progressively increasing postural abnormalities in this experimental paradigm: the misstep rate of the mice did not only increase, they also became slower and more instable in their movements during the motor tasks. The increasing misstep rate in the *Esco2^{fl}* mice was also observed at the hindlimbs, but the effects were generally less severe compared with the forelimbs and also started later (Figure 17-E). In accordance with the forelimbs, also at the hindlimbs the *Esco2^{wt}* control mice only showed a tendency to increase the misstep rate during the whole experiment. On the accelerating rotarod, *Esco2^{fl}* mice showed a deteriorating ability to walk and balance themselves throughout the experiment compared to the littermate controls, although not significant (Figure 17-F, Table 13 in supplementary tables).

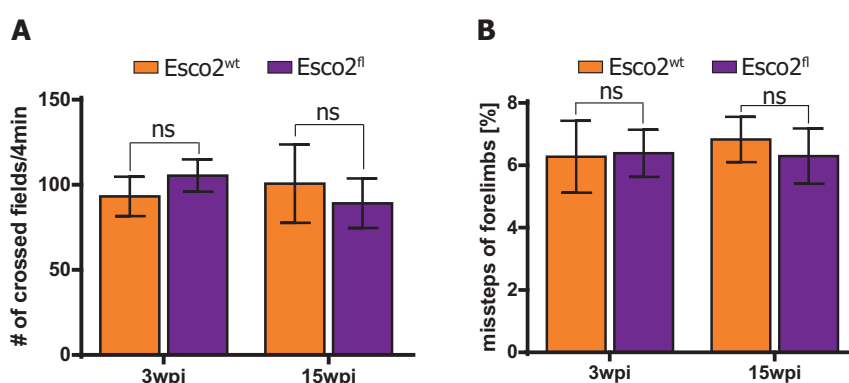


Figure 18: Open field and horizontal ladder behavioral experiment. (A) Open field performance of *Esco2^{wt}* (orange) and *Esco2^{fl}* (purple) animals at different timepoints after the training period. (B) Forelimb horizontal ladder performance of *Esco2^{wt}* (orange) and *Esco2^{fl}* (purple) animals at different timepoints after the training period. Data are presented as mean±sem. Number of animals: open field: n=7 for *Esco2^{wt}* w3, n=6 for *Esco2^{wt}* w15, n=5 for *Esco2^{fl}* w3, n=4 for *Esco2^{fl}* w15; ladder: n=7 for *Esco2^{wt}* w3, n=6 for *Esco2^{wt}* w15, n=8 for *Esco2^{fl}* w3, n=8 for *Esco2^{fl}* w15. Statistical analysis: repeated measures ANOVA, ^{ns}p>0.05.

As this experiment was only performed starting at 5wpi onwards when the *Esco2^{fl}* mice already suffered from behavioral deficits in other paradigms, the two groups were already different during the first measurement.

In contrast, the general activity of the *Esco2^{fl}* animals in the open field – tested by counting the number of crossed fields within a period of four minutes during free movement in an open field arena – neither significantly changed over time in the *Esco2^{fl}* mice (3wpi: 105.4 ± 9.5 fields/4min, 15wpi: 89.1 ± 14.6 fields/4min), nor was it different compared with the *Esco2^{wt}* mice (3wpi: 93.2 ± 11.6 fields/4min, 15wpi: 100.8 ± 23.0 fields/4min, Figure 18-A). The ability of *Esco2^{fl}* mice to perform the corticospinal-specific horizontal ladder task with different step sizes did also not change between 3wpi and 15wpi (3wpi: $6.4 \pm 0.8\%$, 15wpi: $6.3 \pm 0.9\%$) and was comparable to age-matched littermate controls (3wpi: $6.3 \pm 1.2\%$, 15wpi: $6.8 \pm 0.7\%$, Figure 18-B).

In order to assess whether the *Esco2^{fl}* mice did not only develop deficits in motoric tasks, but also in establishing a short-term memory at long timepoints after induction, a novel object recognition (NOR) test was performed (Figure 19). This test was shown to be specific to short- and long-term memory formation located in the perirhinal cortex (Murray and Richmond 2001; Balderas et al. 2015). During the acquisition time with the presence of two similar objects, both *Esco2^{wt}* and *Esco2^{fl}* mice did not favor any of the objects, and explored them in a comparable fashion.

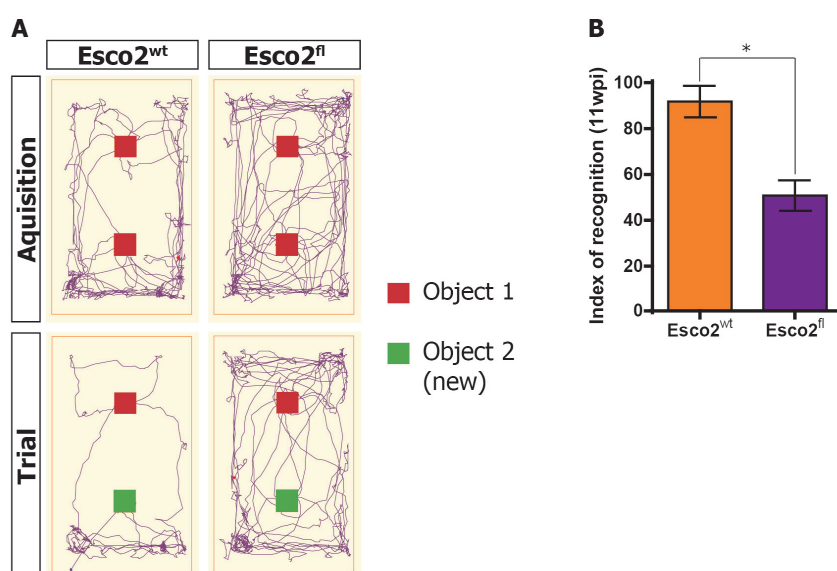


Figure 19: Novel object recognition (NOR) experiment at 11wpi. (A) Examples of tracking plots from an *Esco2^{wt}* and an *Esco2^{fl}* mouse during the acquisition (upper panel) with two identical objects (red square) and the trial phase where one new object (green square) was placed in the open field arena. (B) Index of recognition (percentage of interaction with the new object) in *Esco2^{wt}* and an *Esco2^{fl}* mice at around 2 months after induction. Data are presented as mean \pm sem. Number of animals: $n=3$ for each bar. Statistical analysis: unpaired student's t-test, * $p < 0.05$.

In the trial phase that was performed 30min after the acquisition phase, one object was replaced by a new and obviously different object (Figure 19-A). While the *Esco2*^{wt} mice preferentially targeted the new and unknown object (index of recognition: $91.8 \pm 6.9\%$), the *Esco2*^{fl} mice explored both the old and the new object similarly (index of recognition: $50.8 \pm 6.6\%$, Figure 19-B), indicating that the *Esco2*^{fl} mice did not remember the old object and hence were not able to establish a short-term memory.

Summarizing the findings of the described behavioral assessment, *Esco2*^{fl} mice develop – in contrast to littermate controls – progressively worsening motoric dysfunctions, including disorders in the fine movement coordination (grid walk), general movement coordination (grid walk, beam crossing) as well as in body balance (rotarod, beam crossing). Moreover, they are unable to establish a short-term memory that can specifically be located to the perirhinal cortex.

3.1.5 THE NG2CreER^{T2}XCAG-EGFPX*Esco2*^{FL/FL} CONTROL MOUSE LINE

As the *Sox10* transcription is expressed in all cells of the oligodendrocyte lineage we wanted to rule out that the deletion of *Esco2* in the genetic mouse model also affected mature oligodendrocytes or their derived functions. To prove that the above described phenotype solely derives from the ablation of NG2-glia, the inducible NG2CreER^{T2}XCAG-eGFPX*Esco2*^{fl/fl} line served as a control. As the NG2-promoter is only active in NG2-glia, the *Esco2* deletion was only induced in the cells of interest and not in mature oligodendrocytes or any other cells within the oligodendrocyte lineage.

Analyzing this mouse line by immunohistochemistry in coronal sections at 1wpi (Figure 20), we found a similar recombination of NG2-glia in the cortical GM ($40.5 \pm 2.1\%$ for NG2-*Esco2*^{wt} vs. $46.8 \pm 1.7\%$ for NG2-*Esco2*^{fl} mice) as well as in the cortical WM ($49.2 \pm 2\%$ for NG2-*Esco2*^{wt} vs. $45.5 \pm 4.8\%$ for NG2-*Esco2*^{fl} mice, Table 14 and Table 15 in supplementary tables). We did not find GFP-reporter expression in mature oligodendrocytes (CC1⁺/GFP⁺, data not shown) in this mouse line in comparison with the *Sox10*iCreER^{T2}XCAG-eGFPX*Esco2*^{fl/fl} line shortly after recombination (see chapter 3.1.1). Furthermore the recombination within the total NG2-glia population was much lower (around 80% in the *Sox10*-*Esco2* and around 40% in the NG2-*Esco2* mouse line for both the *Esco2*^{wt} and the *Esco2*^{fl} mice). One year after the initial induction (1 year post induction, ypi), the recombined fraction of NG2-glia in the NG2-*Esco2*^{fl} mice significantly decreased to $22. \pm 2.7\%$ in the GM and to $10.1 \pm 2.9\%$ in the WM (Table 14 and Table 15 in supplementary tables). During this long analysis period, some of the recombined NG2-glia differentiated into mature oligodendrocytes (CC1⁺/GFP⁺).

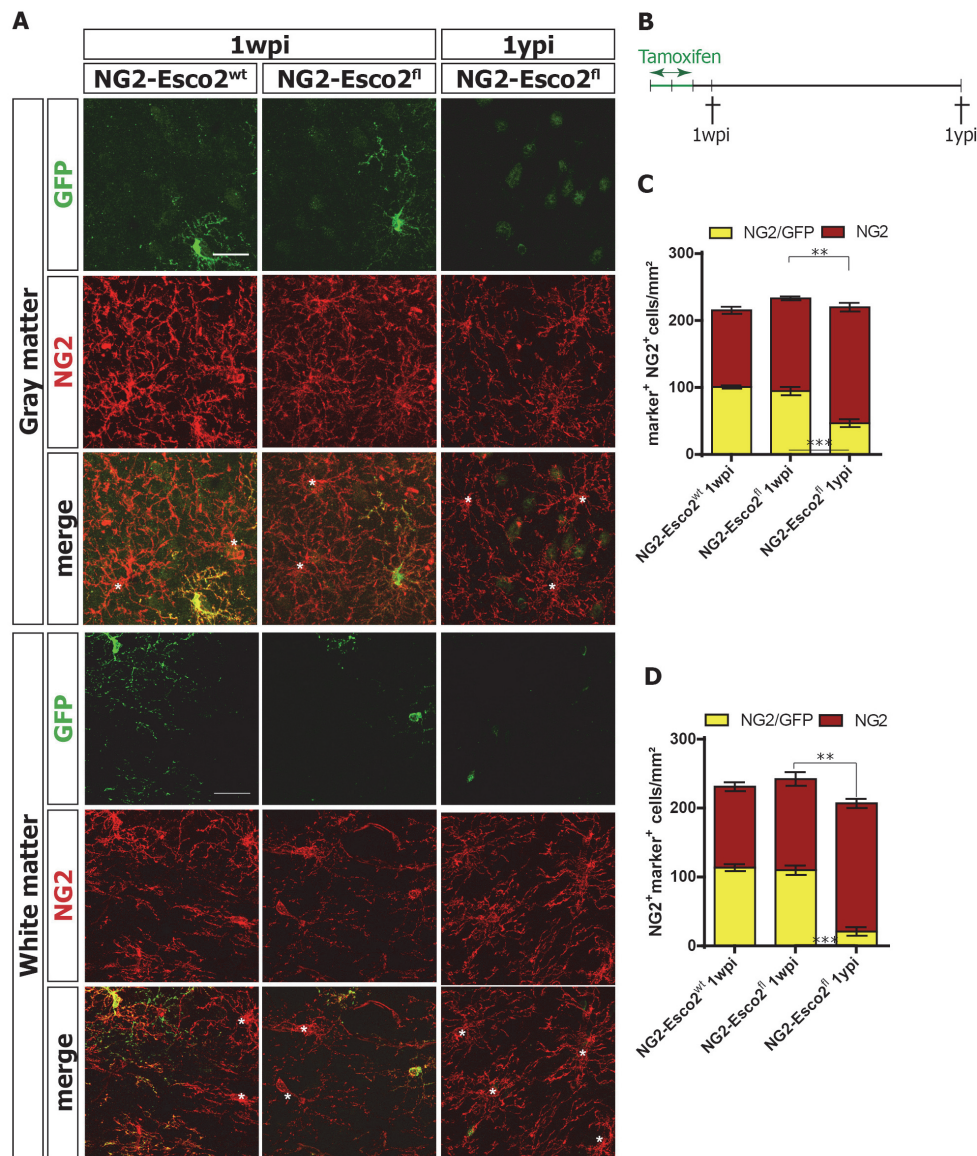


Figure 20: Long-term analysis of recombined NG2-glia in NG2CreERT² mice. (A) Recombined and non-recombined NG2-glia in the cortical gray and white matter at 1wpi and 1ypi. Non-recombined NG2-glia are indicated with an asterisk. (B) Scheme of experimental procedure. (C) Absolute numbers of recombined (yellow) and non-recombined (red) NG2-glia in the cortical GM at 1wpi and 1ypi in NG2-Esco2^{wt} and NG2-Esco2^{fl} mice. (D) Absolute numbers of recombined (yellow) and non-recombined (red) NG2-glia in the cortical GM at 1wpi and 1ypi in NG2-Esco2^{wt} and NG2-Esco2^{fl} mice. Scale bars represent 25μm. Data are presented as mean±sem. Number of animals: n=3 for Esco2^{wt} and Esco2^{fl} 1wpi, n=4 for Esco2^{fl} 1ypi. Statistical analysis: One-way ANOVA, *p<0.05, **p<0.001, ***p<0.0001.

However, the total number of GFP⁺ cells did not increase as expected because of the proliferative behavior of the NG2-glia population, but even slightly decreased over time (data not shown). To analyze whether these mice develop a similar phenotype due to a similar loss of recombined proliferating NG2-glia and its subsequent differentiation defects, we performed the same behavioral experiments that were used for the Sox10iCreERT²xCAG-eGFPxEsco2^{fl/fl} line (Figure 21-A).

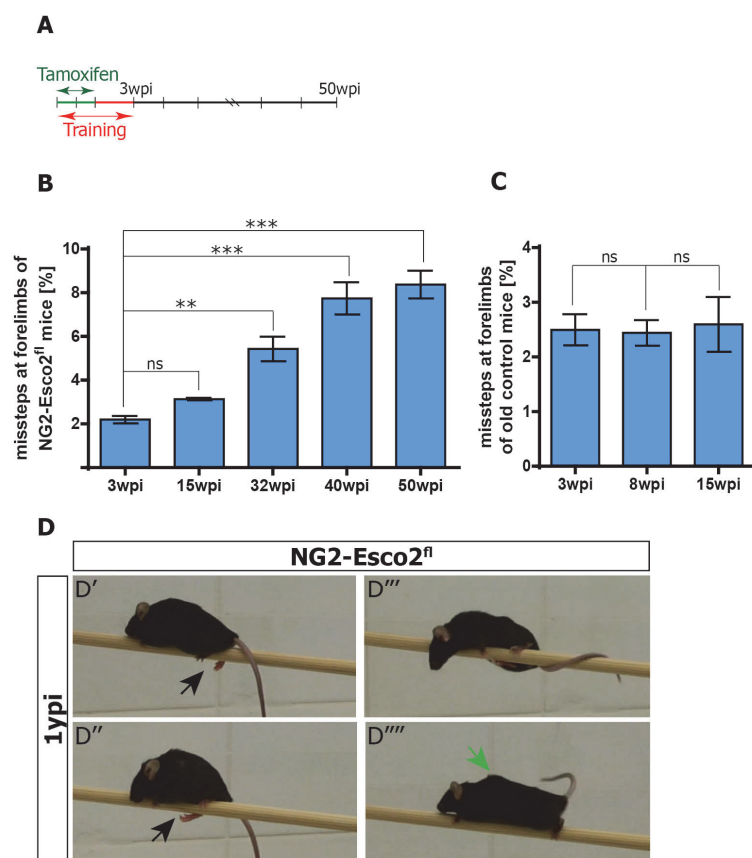


Figure 21: Motor behavior assessment of NG2CreER^{T2}xCAG-eGFPxEsco2^{fl} mice. (A) Scheme of experimental procedure. (B) Percentage of forelimb missteps during grid walk of NG2-Esco2^{fl} animals at different timepoints after the training period. (C) Percentage of forelimb missteps during grid walk of age-matched control animals (45 weeks of age) at different timepoints after the training period. (D) Examples of NG2-Esco2^{fl} mice during beam crossing. Arrowheads indicate clamping of the hind limbs (D', D''), additional stabilization with the tail (D''') and kyphosis (D'''). Data are presented as mean±sem. Number of animals: n=4 for each bar. Statistical analysis: repeated measures ANOVA, ^{ns}p>0.05, **p<0.001, ***p<0.0001.

The grid walk experiment revealed that also the NG2-Esco2^{fl} mice developed a progressive forelimb misstep rate over time (Figure 21-B, Table 16 in supplementary tables), although it occurred later and less severe compared with the Sox10-Esco2^{fl} mice. Therefore this control experiment gave further evidence that the motor phenotype was a result of the NG2-glia ablation rather than of malfunctioning oligodendrocytes. Interestingly, the misstep rate of the NG2-Esco2^{fl} mice reached a plateau starting at 40wpi and no further increase could be observed until 50wpi. As no control littermates of the NG2CreER^{T2}xCAG-eGFPxEsco2^{fl/fl} line were available, the control experiments were carried out with mice of a similar breeding background (NG2CreER^{T2}xCAG-eGFP mouse line). To rule out that the increase in misstep rate was solely caused by the effect of aging, the grid walk experiment was performed at the starting age of 45 weeks in those mice what corresponded to the age of the NG2-Esco2^{fl} mice at the end of the experiment. The forelimb grid walk performance of those age-matched control animals did not increase between 3wpi and 15wpi (Figure 21-C, Table 17 in supplementary tables), proving that the motor phenotype was not an age-correlated effect. In

addition to the grid walk experiment, the NG2-Esco2^{fl} mice were analyzed for their beam crossing performance during the whole period. Although only 75% the mice (three out of four) failed to cross the wooden beam by the end of the experiment at 50wpi, all of them developed similar postural abnormalities that were already observed in the Sox10-Esco2^{fl} mice (Figure 21-D). During the motor performance tests, they clamped their hindlimbs around the beam (D' and D''), sometimes additionally twisted their tail around the beam (D''') or showed the typical kyphosis (D''').

As the experiment proved, the NG2-Esco2^{fl} mice developed a motor phenotype comparable to the Sox10-Esco2^{fl} mice, however the effects were lower and appeared later in this mouse line. The difference could be explained by the significantly lower recombination rate of NG2-glia in the NG2CreER^{T2}xCAG-eGFPxEsco2^{fl/fl} line. To correlate the observed phenotype with subcellular changes in the cortical WM, both the average lengths of the paranodes and nodes of these mice were immunohistochemically measured in coronal sections at 1ypi for the NG2-Esco2^{fl} mice as well as for the age matched control animals that were used for the behavioral experiments (Figure 22). Indeed, the NG2-Esco2^{fl} mice showed a significantly longer average node length ($1.14 \pm 0.03 \mu\text{m}$) compared with aged-matched controls ($0.81 \pm 0.02 \mu\text{m}$). Moreover, the paranodes of these mice were similarly elongated ($2.40 \pm 0.06 \mu\text{m}$ in the control and $3.16 \pm 0.03 \mu\text{m}$ in the NG2-Esco2^{fl} mice).

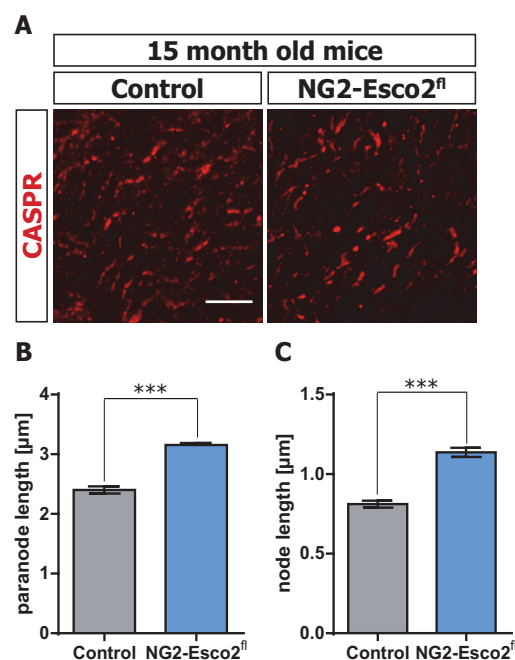


Figure 22: Nodes of Ranvier in the NG2CreER^{T2}xCAG-eGFPxEsco2^{fl} mice. (A) Paranodal CASPR staining in the cortical WM of 15mo old recombined control and NG2-Esco2^{fl} mice. Quantification of average length of the (B) paranodes and the (C) nodes in control and NG2-Esco2^{fl} animals at the age of 15 months. Data are presented as mean±sem. Number of animals: n=4 for each bar. Number of nodes: n=58 for each animal. Statistical analysis: unpaired student's t-test, ***p<0.0001.

In summary, *Esco2*⁻ and the resulting NG2-glia-ablation could also be achieved using the NG2 promoter in the NG2CreERT²xCAG-eGFP mouse line, but as the recombination rate in this mouse line was much lower, the ablation effects were less severe. However, these mice also developed a motor phenotype as well as nodal disturbances, although both observations appeared milder and at later timepoints after the induction.

3.1.6 BEHAVIORAL PHENOTYPE IS NOT DERIVED FROM THE PERIPHERAL NERVOUS SYSTEM

Sox10 is a promoter that is not only active in all cells within the oligodendrocyte lineage in the adult brain, but also in several cells of other tissues including the Schwann cells in the peripheral nervous system (PNS) and in neuromuscular junctions. Given the described reduction in motor skills, it was mandatory to exclude the possibility that this phenotype was intensified or even induced by the ablation of recombined cells in the PNS. Therefore, Schwann cells in the sciatic nerves as well as in muscle spindles and neuromuscular junctions of multiple skeletal muscles were analyzed in the *Esco2*^{fl} mice. Although we found a high number of recombined cells within the Schwann cell population in the sciatic nerve at 5dpi (data not shown), the number of these cells was not changed in the *Esco2*-ablated animals at 16wpi compared with the *Esco2*^{wt} mice (88.7±0.4% for the *Esco2*^{wt} and 88.9±1.1% for the *Esco2*^{fl}, see Figure 23-A and B). However, as Schwann cells in the adult mouse were shown to be postmitotic under physiological conditions (Cheng and Zochodne 2002), a cell death of recombined Schwann cells in the *Esco2*^{fl} mice was not expected. Analyzing the total number of DAPI⁺ in sciatic nerves (data not shown), we did not find any differences in the *Esco2*^{fl} (1926±23.6 cells/mm²) compared with the *Esco2*^{wt} animals (1889±6.5 cells/mm²), indicating that also other cell types were not affected in the sciatic nerve. This leads to the assumption that the genetic deletion of *Esco2* in postmitotic peripheral Schwann cells did neither induce cell death in this population, nor did it affect the cellular composition of peripheral nerves.

In order to determine if the myelin structure in the periphery shows some abnormalities in their nodal organisation as it could be observed in the corpus callosum, we additionally analyzed teased fibers of sciatic nerves, measured the internode length and analysed the organization of the nodal structures by means of immunohistochemical CASPR staining. Again, this analysis did neither reveal any difference in the average internode length between the NG2-depleted animals and their controls (143.7±2.1µm for the *Esco2*^{wt} and 142.9±2.1µm for the *Esco2*^{fl} mice), nor in the structural organization of the node of Ranvier (Figure 23-C and E).

Moreover, Schwann cells are not only essential for the development and maintenance of the neuromuscular junction (NMJ) (Wu et al. 2010a), but they also play an important role in muscle spindles.

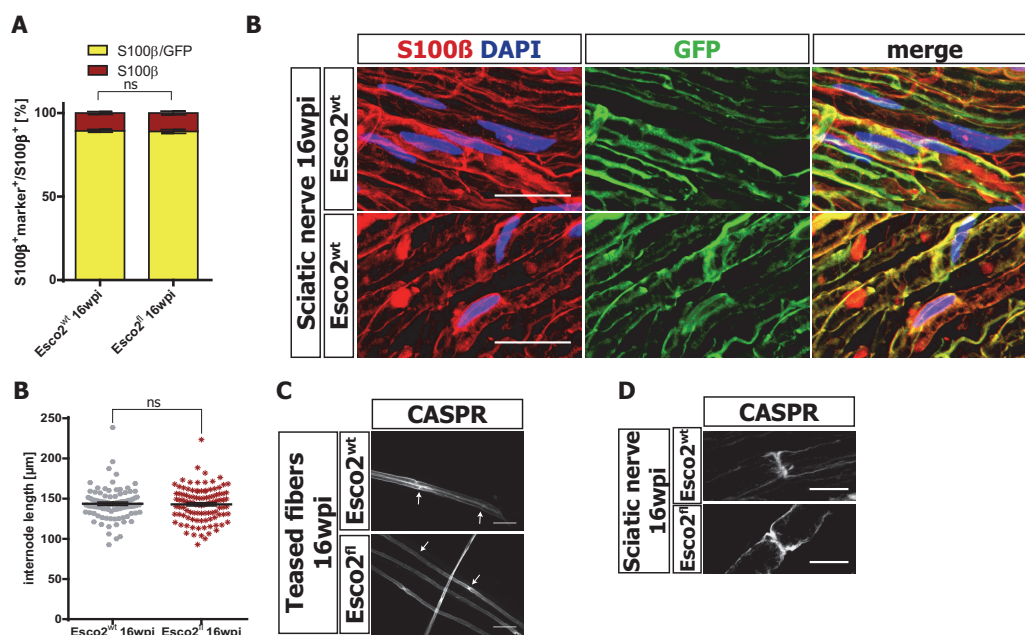


Figure 23: Schwann cells and nodes of Ranvier in the PNS. (A) Quantification of recombined (yellow) and non-recombined (red) Schwann cells (S100β⁺) in Esco2^{wt} and Esco2^{fl} mice at 16wpi. (B) Examples of recombined (yellow) and non-recombined (red) Schwann cells in longitudinal sections of the sciatic nerve. (C) Internode length in teased fibers of peripheral sciatic nerves in Esco2^{wt} and Esco2^{fl} animals at 16wpi. (D) CASPR staining in teased fibers of peripheral sciatic nerves in Esco2^{wt} and Esco2^{fl} animals at 16wpi. Arrows indicate CASPR⁺ nodes of Ranvier, the distance between two nodes was considered as internode length. (E) CASPR⁺ nodes of Ranvier in longitudinal sections of sciatic nerves in Esco2^{wt} and Esco2^{fl} mice at 16wpi. Scale bars represent 20μm (B), 50μm (D), and 10μm (E). Number of animals: n=3 for each bar. Data are presented as mean±sem. Statistical analysis: unpaired student's t-test, ^{ns}p>0.05.

Their death can lead to the fragmentation and disruption of these structures, resulting in severe deficits (Reddy et al. 2003). Therefore we analyzed the neuromuscular junctions by α-Bungarotoxin (αBTX) staining as well as the muscle spindles by neurofilament staining (NFH) in different skeletal muscles at 16wpi in this mouse model (collaboration with Yina Zhang and Stephan Kröger, Institute of Physiology, Ludwig-Maximilians-Universität). In this analysis we neither found an accumulation of fragmented NMJs, nor a disruption of the GFP-associated muscle spindles (data not shown).

Summarizing, tamoxifen induction in the Sox10iCrexGAG-eGFPxEsco2^{fl/fl} mouse line resulted in a high recombination rate of Sox10-expressing cells in the PNS, as well as in muscle-associated Schwann cells. However, as these cells are postmitotic in the adult peripheral nerve, genetic Esco2 ablation did not trigger cell death in this area and thus, did not seem to affect these structures.

3.1.7 NG2-GLIA ABLATED MICE DEVELOP A DECELERATING NERVE CONDUCTION VELOCITY

Experiments and results of this chapter have been performed in collaboration with José Maria Delgado García and Agnès Gruart I Massó from the Universidad Pablo de Olavide in Sevilla. The content was used herein and printed with their permission.

A highly structured and functional organization of the nodes of Ranvier are one of the prerequisites for proper action potential conduction alongside the myelinated axon. Any disturbances in these structures – even to a low degree – were shown to strongly influence electrical properties in the nodal regions and therefore negatively influence the action potential propagation. Thus, as the *Esco2^{fl}* mice showed a high degree of disintegration in their nodes of Ranvier, it was inevitable to determine the nerve conduction velocity of myelinated fibers in the cortical WM. As in our lab we did neither have the expertise nor the equipment to perform these kind of experiments, they were performed by our collaboration partners José Maria Delgado García and Agnès Gruart i Massó (División de Neurociencias, Universidad Pablo de Olavide, Sevilla, Spain).

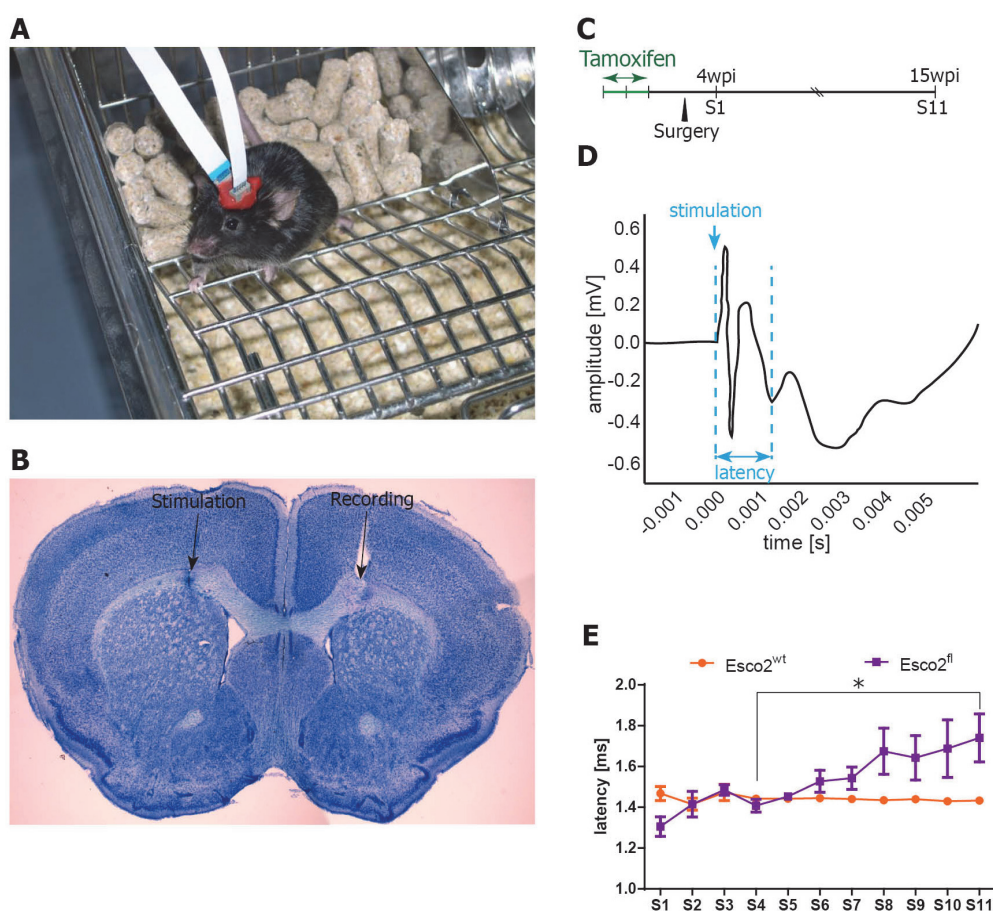


Figure 24: Electrophysiological recordings of the nerve conduction velocity. (A) Example of an awake mouse with implanted electrodes. (B) Exemplary electrode localization in the cortical white matter in a coronal brain section. One electrode was used to evoke a stimulus, the electrode in the other hemisphere recorded the latency of the evoked field potential at this place. (C) Scheme of experimental procedure. (D) Exemplary histogram of the recorded field potentials. Time between the stimulus and the second minimum (blue arrow, latency) indicated the latency of the first component representing the myelinated fibers. (E) Latency recordings of *Esco2^{wt}* and *Esco2^{fl}* mice during different sessions (S1-S11) after the surgery. Number of electrodes: $n=4$ for each timepoint. Data are presented as mean \pm sem. Statistical analysis: One-way ANOVA, $*p<0.05$.

Experiments were performed and data nicely provided by collaboration partners José Maria Delgado García and Agnès Gruart i Massó (División de Neurociencias, Universidad Pablo de Olavide, Sevilla, Spain).

Adult mice at the age of eight to ten weeks were induced with tamoxifen and two weeks later underwent surgery to permanently implant teflon-coated tungsten wire electrodes into the corpus callosum (Figure 24-B, coordinates of stimulating electrode: +1.5mm lateral, 1.34 mm posterior to bregma; coordinates of recording electrode: -1.5mm lateral, 1.34 mm posterior to bregma), as recently reported in (Murcia-Belmonte et al. 2015). After some time of recovery, mice passed eleven recording sessions (S1 – S11) between 4wpi and 15wpi in which the latency of the evoked field potential from the stimulating electrode of the response at the recording electrode was measured. During the first recording sessions (S1 – S5) the latencies of the first component were similar in both the *Esco2*^{wt} and the *Esco2*^{fl} mice (Figure 24-E, Table 18 in supplementary tables). However starting from S6 (corresponding to 8wpi), a slight increase in the latencies could be observed in the latter ones that was further ascending until the end of the experiment, while the wildtype controls retained their starting latencies over the whole time. These results therefore demonstrate a reduction in the nerve conduction velocity in the *Esco2*^{fl} mice starting from around 8wpi, becoming significant at 15wpi. Interestingly, around the same time after induction, a significant increase in the nodal and paranodal lengths in the WM could be observed.

Although the latency does not explicitly represent the nerve conduction velocity, it can directly be correlated to it. Both electrodes were permanently implanted using the same coordinates in all mice, therefore the distance of the recorded signal remains stable and a delay in the latency necessarily describes the slowing down of the nerve conduction velocity in myelinated axons.

Succinctly, these data clearly demonstrate that the maintenance of the oligodendrocyte lineage equilibrium and the structural organization of the node of Ranvier are necessary to keep electrophysiological brain properties, and that the disturbance can lead to long-term perturbation in the nerve conduction velocity.

3.2 NG2-GLIA ABLATION IN THE INJURED BRAIN

As described in the previous chapter, genetic deletion of *Esco2* in NG2-glia cells in the *Sox10iCrexCAG-eGFPxEsco2*^{fl/fl} mouse line is an efficient mechanism to induce apoptotic cell death in recombined cells and to reduce the total number of GFP⁺ cells in the healthy brain over time. However, as the cell cycle of NG2-glia in the healthy GM is rather slow, non-recombined cells have enough time to compensate for this loss, leading to stable numbers of NG2-glia.

On the other hand, NG2-glia are well-known to increase their cell numbers after different kinds of injury. They achieve this increase by shortening their cell cycle length and enhancing their

proliferation rate as well as by actively migrating into the lesion site. The functions behind these active cellular dynamics, however, remain unclear. To analyze the possible functions of NG2-glia after injury, we used the Sox10iCrex^{CAG-eGFPx}Esco2^{fl/fl} mouse line to deplete proliferating cells after injury and thus achieve a reduction of NG2-glia in close proximity to the lesion site.

3.2.1 ESCO2 DELETION CAUSES FAST LOSS OF PROLIFERATIVE RECOMBINED NG2-GLIA IN CLOSE PROXIMITY TO THE LESION SITE

Being eight to ten weeks-old, adult Sox10iCreER^{T2}x^{CAG-eGFPx}Esco2^{fl/fl} mice were induced with tamoxifen according to the protocol described above. After a short five day wash-out period of the tamoxifen, a stab wound lesion of 0.6mm in depth and 1.5mm in length was applied to the somatosensory cortex (Figure 25-A). Coronal sections of the animals' brains were subsequently immunohistochemically analyzed at two, four, seven and 14 days post lesion (dpl).

The GFP⁺ cells in the Esco2^{wt} mice – within a distance of approximately 250µm from both sides of the lesion – showed the normal reaction of NG2-glia after injury with an increase in cell numbers within the first 7dpl and a subsequent stabilization of cell numbers toward control levels until 14dpl. The numbers of GFP⁺ cells in Esco2^{fl} mice on the contrary continuously decreased until 14dpl (Figure 25-C, Table 19 in supplementary tables).

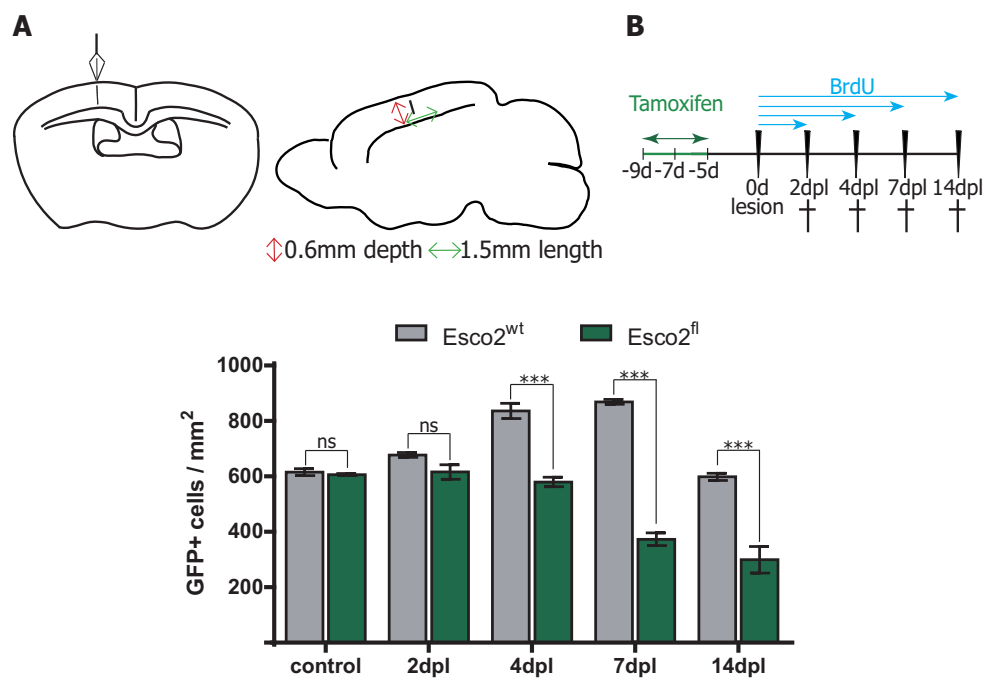


Figure 25: Model of stab wound injury. (A) Schematic drawing of lesion area and lesion size in the cortical GM. (B) Scheme of experimental procedure. (C) Quantification of GFP⁺ cells/mm² at different timepoints after injury surrounding the stab wound lesion in the cortical GM in Esco2^{wt} and Esco2^{fl} mice. Data are presented as mean±sem. Number of animals: n=3 for each bar. Statistical analysis: One-way ANOVA, ^{ns}p>0.05, ***p<0.0001.

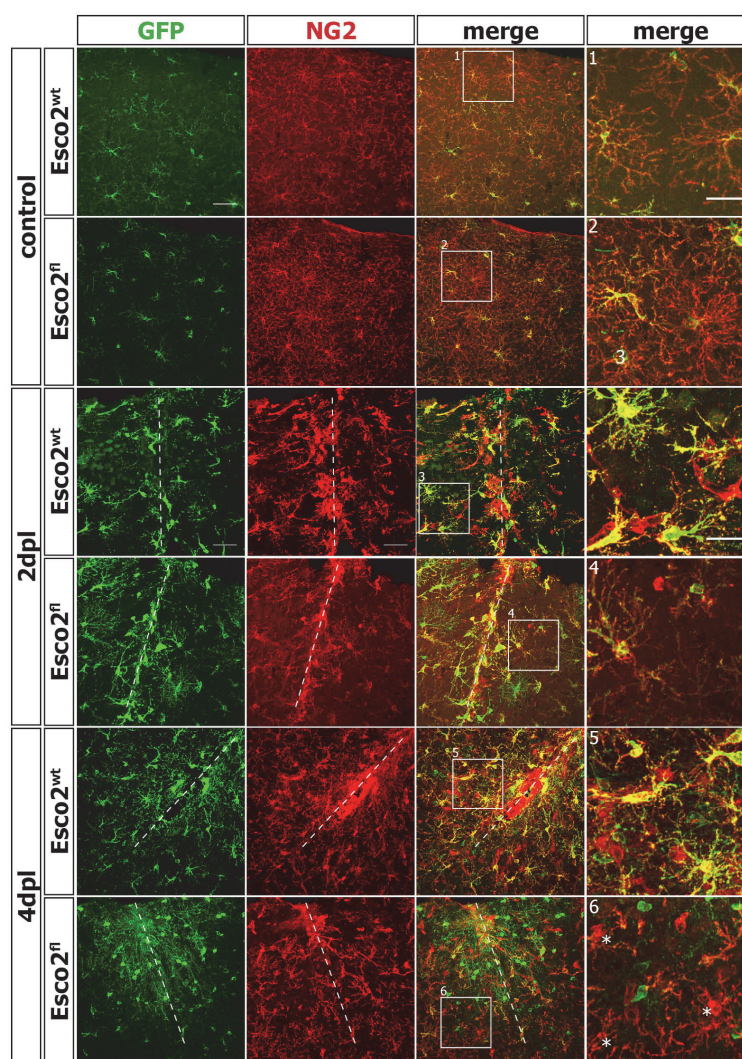


Figure 26: Recombined and non-recombined NG2-glia at early timepoints after lesion. Recombined and non-recombined NG2-glia on the contralateral side and in close proximity to the stab wound lesion (indicated with a dashed line) at the control side and at 2dpl and 4dpl in *Esco2^{wt}* and *Esco2^{fl}* mice. Non-recombined NG2-glia in the blow-up pictures are indicated with an asterisk. Scale bars represent 50µm, and 25µm in the blow-up pictures.

Although the total number of GFP⁺ cells includes all oligodendrocyte lineage cells, it is most likely that the reduction of the GFP⁺ cell pool was a result of the depleted proliferating NG2-glia, as postmitotic oligodendrocytes should not be affected by the lack of *Esco2*. Hence, stimulating the environment by outer insult triggered the proliferative capacity of NG2-glia, and therefore increased the cell death in the NG2-glia population that is lacking the cell cycle protein *Esco2*.

In order to see how specifically recombined NG2-glia react within the total GFP⁺ cell pool after cortical stab wound injury, NG2/GFP double staining was performed in coronal sections and quantified in the same distance around the lesion site (Figure 26, Figure 27 and Figure 28-A). Indeed, comparable to the whole GFP⁺ cell population, the total number of recombined NG2-glia (NG2⁺/GFP⁺) in *Esco2^{fl}* mice was continuously declining, starting at 2dpl, finally at 14dpl most of the GFP⁺NG2-glia have disappeared (Figure 28, Table 20 in supplementary tables).

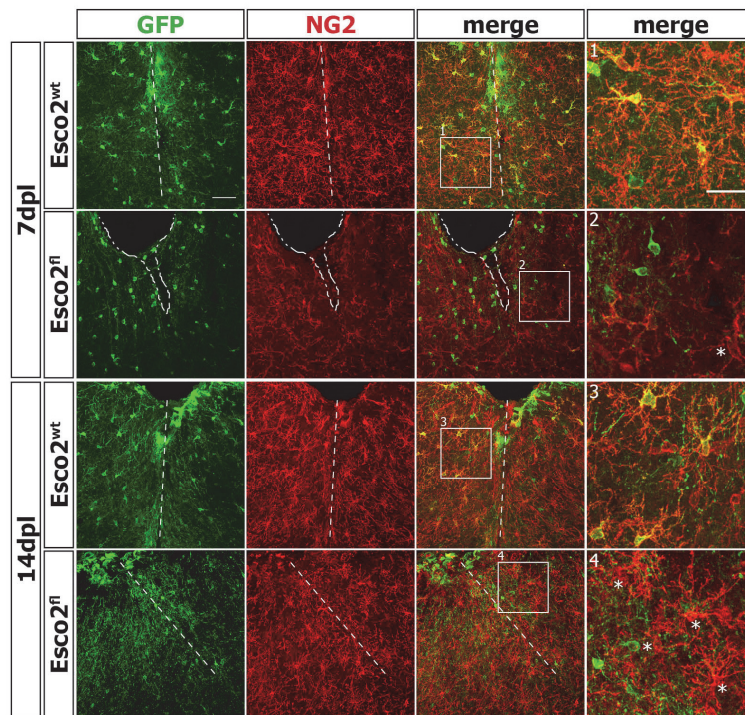


Figure 27: Recombined and non-recombined NG2-glia at late timepoints after lesion. Recombined and non-recombined NG2-glia in close proximity to the stab wound lesion (indicated with a dashed line) at 7dpl and 14dpl in the *Esco2^{wt}* and *Esco2^{fl}* mice. Non-recombined NG2-glia in the blow-up pictures are indicated with an asterisk. Scale bars represent 50μm, and 25μm in the blow-up pictures.

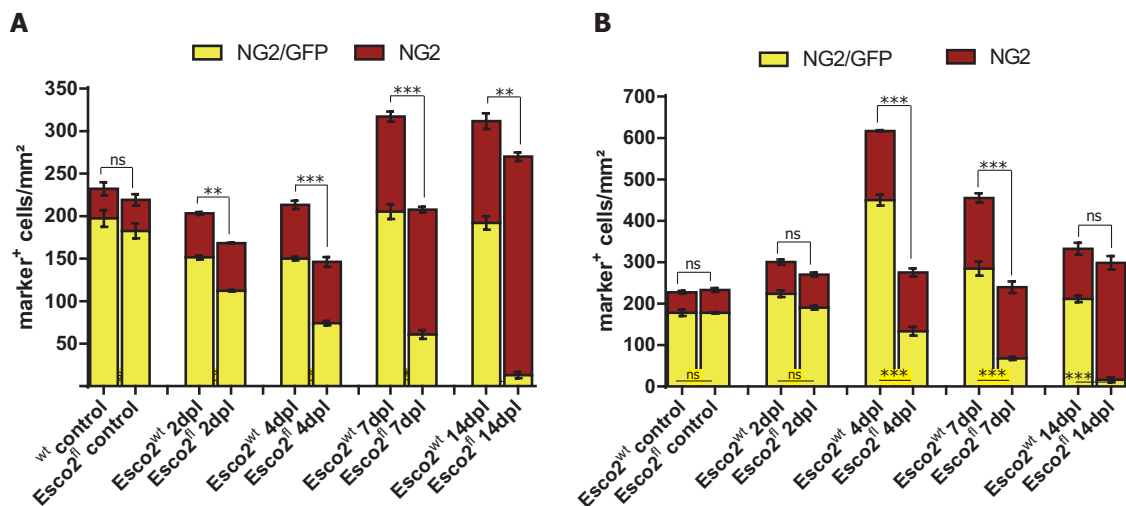


Figure 28: Total numbers of recombined and non-recombined NG2-glia at different timepoints after lesion. (A) Absolute numbers/mm² of recombined (yellow) and non-recombined (red) NG2-glia in the distance of 250μm around the lesion site in the *Esco2^{wt}* and *Esco2^{fl}* mice at different timepoints after the lesion. (B) Absolute numbers/mm² of recombined (yellow) and non-recombined (red) NG2-glia in the lesion core (50μm around the lesion) in the *Esco2^{wt}* and *Esco2^{fl}* mice at different timepoints after the lesion. Data are presented as mean±sem. Number of animals: n=3 for each bar, n=4 for *Esco2^{fl}* at 2dpl and 4dpl in A. Statistical analysis: One-way ANOVA + Tukey post-test, ns>0.05, **p<0.001, ***p<0.0001.

This reduction in the recombined cell fraction resulted in a significantly reduced overall density of NG2-glia compared with *Esco2*^{wt} mice at every timepoint that was analyzed.

Having a close-up look at NG2-glia, it appeared that their cell body as well as their processes occupied a smaller surface and therefore were less hypertrophic as well as less ramified and branched in the *Esco2*^{fl} mice compared with those in the *Esco2*^{wt} controls. Moreover, especially at 4dpl the NG2-glia in the *Esco2*^{fl} mice around the lesion were not homogeneously distributed: NG2-glia-depleted patches of up to 100x100µm² could be found (data not shown). Starting at 4dpl, the non-recombined NG2-glia in the *Esco2*^{fl} mice began to compensate for the loss of recombined cells by increasing their rate of proliferation (data not shown), however, at this stage they were not yet able to fully compensate. In contrast to the contralateral side, the total number of NG2-glia – both NG2⁺/GFP⁻ and NG2⁺/GFP⁺ – significantly decreased in the *Esco2*^{wt} mice within the first four days after the lesion as well (most likely due to direct cell damage). Nevertheless, a significant enrichment in the cell density was measured thereafter that is kept until 14dpl. Notably, the fraction of non-recombined NG2-glia (NG2⁺/GFP⁻) was increasing in proportion to the whole NG2-glia population in *Esco2*^{wt} mice after the lesion (2dpl: 25.4±0.3%, 4dpl: 29.6±1.7%, 7dpl: 35.3±1.9%, 14dpl: 38.4±2.8%), due to higher proliferation rates of this cell fraction compared with its recombined counterpart (data not shown). Looking at the NG2-glia reaction after stab wound injury in the lesion core (around 50µm from each side of the insult), the NG2-glia dynamics in the *Esco2*^{wt} mice were different from the wider surrounding that was analyzed before (Figure 28). The peak of total NG2-glia numbers in the lesion core was already reached at 4dpl in contrast to the 250µm area which peaks only at 7dpl, with more than a two-fold increase compared with the controls. This NG2-glia accumulation was so pronounced that individual NG2-glia in the lesion core were difficult to be identified.

Thereafter, cell numbers were rapidly declining, reaching almost their control level at 14dpl. In the *Esco2*^{fl} mice, recombined NG2-glia (GFP⁺/NG2⁺) were – similar to the bigger surrounding of the lesion – progressively reduced compared with *Esco2*^{wt} littermate controls (Figure 28-B, Table 22 in supplementary tables). Although the non-recombined NG2-glia fraction in the *Esco2*^{fl} mice (NG2⁺/GFP⁻) increased at 7dpl, the whole NG2-glia population (GFP⁺ and GFP⁻) in the lesion core was always kept at control levels and NG2-glia did not increase significantly in the lesion core as it was observed in the *Esco2*^{wt} mice (Figure 28-B, Table 23 in supplementary tables).

Summarizing, we found that following stab wound injury, recombined NG2-glia in the *Esco2*^{fl} mice were – especially inside the lesion core - ablated rapidly. This resulted in a significant reduction in total NG2-glia numbers in close-proximity to the lesion core until 14dpl, as the

remaining non-recombined cells did not have enough time to compensate for the occurred rapid loss.

3.2.2 NG2-GLIA ABLATION DELAYS WOUND CLOSURE

Just recently, NG2-glia were shown to actively migrate into the lesion site and were therefore suggested to play a more important role in the early stages of wound closure after insult in contrast to what has previously been anticipated (von Streitberg and Schneider et al. submitted). To address their role in this context, the size of the lesioned area in both *Esco2*^{wt} and *Esco2*^{fl} mice was analyzed at different timepoints after the lesion (Figure 29), at which the total number of NG2-glia in close-proximity to and inside the lesion core was significantly reduced (Figure 28). At 2dpl, the lesion size in *Esco2*^{wt} ($0.133\pm 0.025\text{mm}^2$) and *Esco2*^{fl} ($0.144\pm 0.014\text{mm}^2$) animals was comparable. While in the control mice the lesion size was significantly reduced within 4dpl ($0.058\pm 0.004\text{mm}^2$) and almost closed within 7dpl ($0.035\pm 0.009\text{mm}^2$), no signs of wound closure could be observed in *Esco2*^{fl} mice at 4dpl, the size of the lesion even slightly increased to $0.153\pm 0.017\text{mm}^2$.

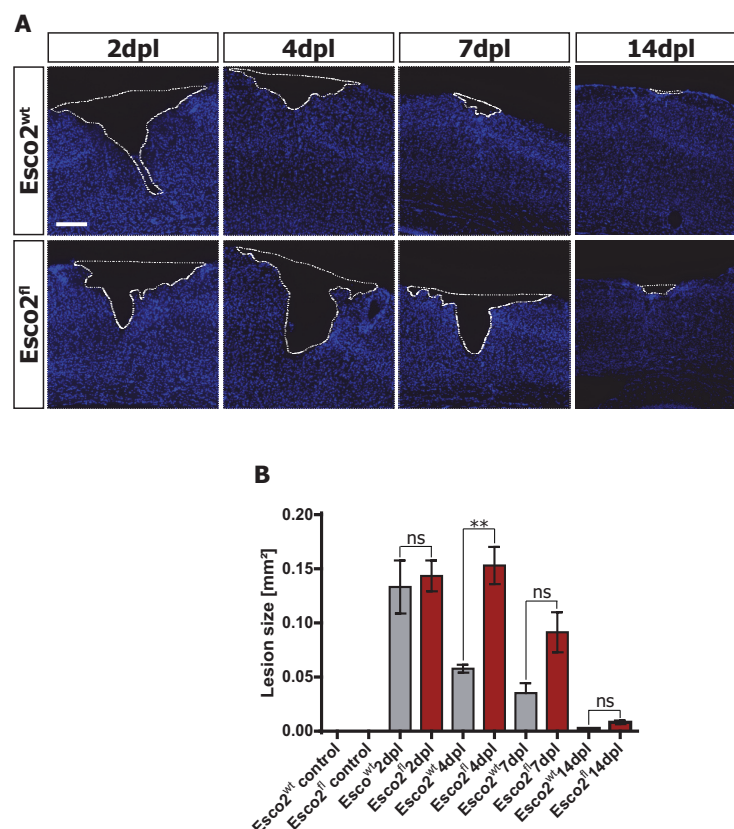


Figure 29: Lesion size at different timepoints after injury. (A) Lesion size (surrounded by dashed line). (B) Quantification of lesion size in mm^2 of *Esco2*^{wt} and *Esco2*^{fl} mice at different timepoints after the lesion. Scale bar represents $200\mu\text{m}$. Data are presented as mean \pm sem. Number of animals: $n=3$ for *Esco2*^{wt} at 2dpl and 7dpl, $n=4$ for *Esco2*^{wt} at 4dpl, $n=5$ for *Esco2*^{fl} at 2dpl and $n=6$ for *Esco2*^{fl} at 4dpl and 7dpl. Statistical analysis: One-way ANOVA + Tukey post-test, $**p<0.001$.

Only between 4dpl and 7dpl, the lesion became smaller ($0.091 \pm 0.018 \text{ mm}^2$). Within 14dpl, the lesion was almost closed both in the Esco2^{wt} ($0.003 \pm 0.0 \text{ mm}^2$) and the Esco2^{fl} animals ($0.008 \pm 0.002 \text{ mm}^2$), indicating that the wound closure capacity has not been completely abolished but only delayed.

Summarizing, the significant reduction of NG2-glia in Esco2^{fl} mice in close proximity to the lesion site and inside the lesion core induced a significant delay in the physiological process of wound closure.

3.2.3 CLOSURE OF THE BLOOD-BRAIN-BARRIER

In brain injuries in which the vasculature was damaged, the fast and efficient closure of the BBB to avoid further cell infiltration and tissue destruction is a normal process of cellular wound healing and repair. As the depletion of proliferating, recombined NG2-glia in the Esco2^{fl} mice after stab wound injury significantly delayed the wound closure (Figure 29), it was reasonable to analyze the blood vessel leakage in our mouse model and to determine if the reduced numbers of NG2-glia induces any delay in the closure of the BBB. To specify whether the closure of the BBB is delayed in Esco2^{fl} mice, we analyzed the leakage of a tail vein-injected green fluorescent dextran into the brain parenchyma at 5dpl in both the Esco2^{wt} and the Esco2^{fl} group. This specific timepoint was chosen because control experiments revealed that the BBB was closed at 5dpl, but still open at 4dpl, as demonstrated in the positive control (Figure 30). However, leakage of the fluorescent dye into the brain parenchyma at 5dpl could neither be detected in Esco2^{wt} , nor in Esco2^{fl} animals. These results indicated that in both groups the BBB was successfully closed within 5dpl and that the loss of NG2-glia in the Esco2^{fl} mice did not significantly influence the astrocyte function in terms of the vasculature repair.

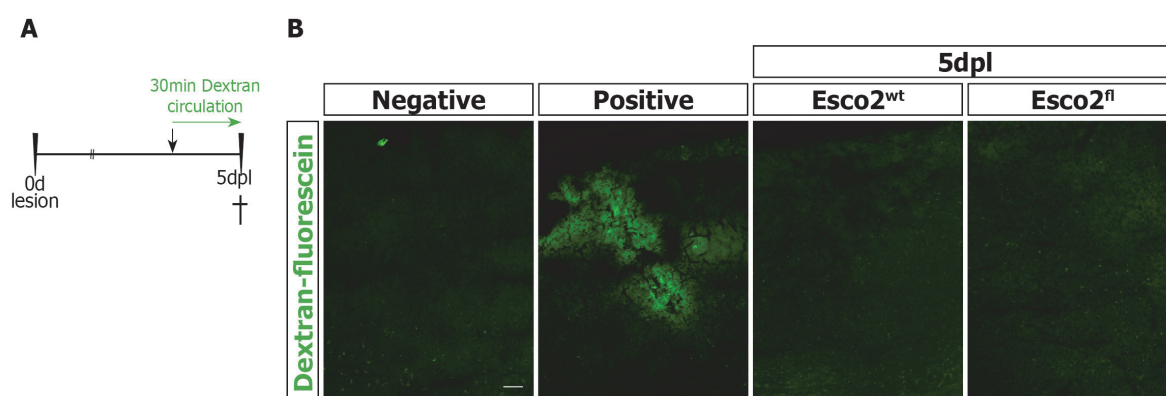


Figure 30: Closure of the blood-brain barrier. (A) Scheme of experimental procedure. (B) Dextran-fluorescein injected into the tail vein of mice is leaking into the brain parenchyma when the BBB is not closed at 4dpl (positive), whereas leakage can neither be detected in Esco2^{wt} nor in the Esco2^{fl} animals at 5dpl, meaning that the BBB was closed equally fast. *These data were obtained in collaboration Axel von Streitberg, Institute of Physiology, LMU Munich.*

3.2.4 REDUCED INJURY RESPONSE OF OTHER GLIAL CELL POPULATIONS

The previous chapters revealed that the loss of recombined NG2-glia after injury causes a reduction in the total NG2-glia population, however as glial cells in the healthy adult brain are highly interactive and dependent on each other, it would not be surprising that glial cells communicate with each other also after TBI.

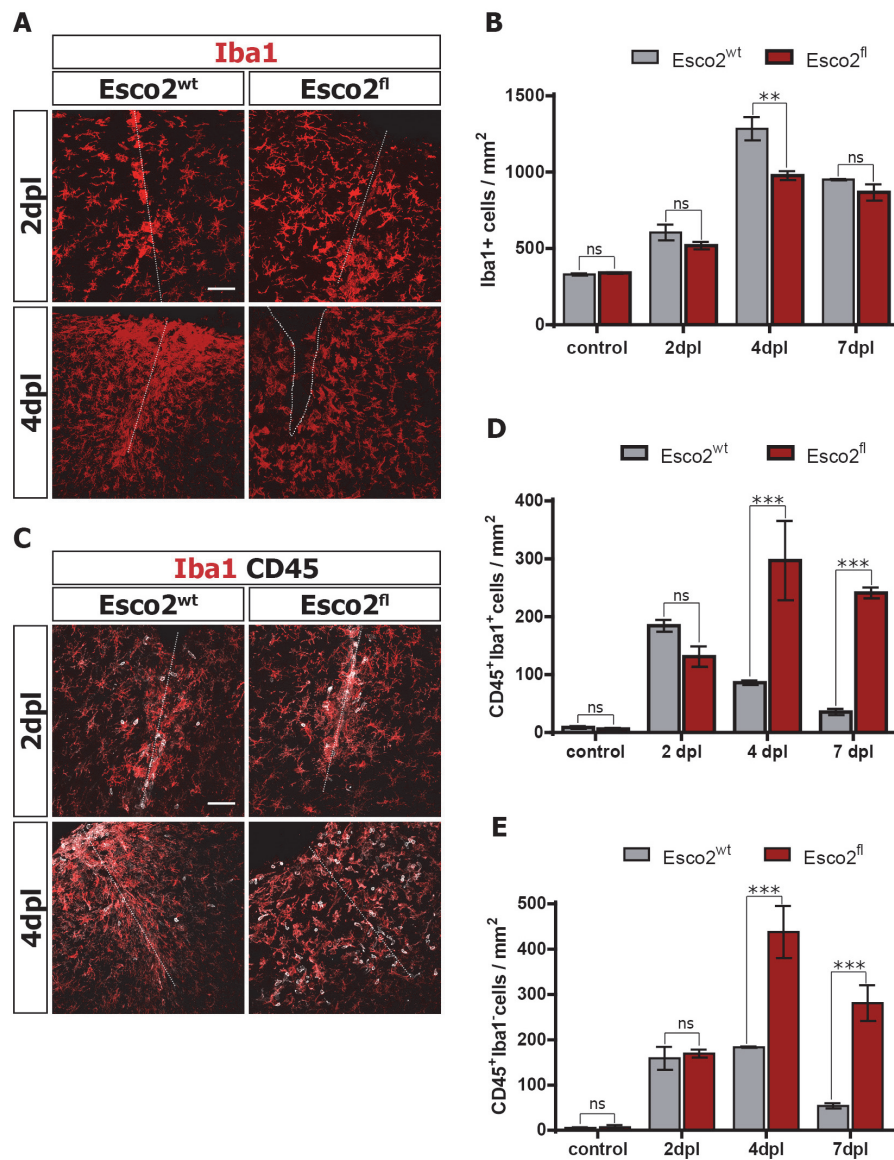


Figure 31: Reaction of resident microglia and invading macrophages. (A) Microglia/macrophages in Esco2^{wt} and Esco2^{fl} mice in the surrounding of around 250µm from the lesion site at 2dpl and 4dpl. (B) Quantification of Iba1⁺ microglia/mm² in Esco2^{wt} and Esco2^{fl} mice at different timepoints after the lesion. (C) Microglia (Iba1⁺), reactive microglia (Iba1⁺/CD45⁺) and invading macrophages (Iba1⁺/CD45⁺) in Esco2^{wt} and Esco2^{fl} mice in close proximity to the lesion site at 2dpl and 4dpl. (D) Quantification of Iba1⁺/CD45⁺ activated microglia/mm² in Esco2^{wt} and Esco2^{fl} mice at different timepoints after the lesion. (E) Quantification of CD45⁺ macrophages/mm² in Esco2^{wt} and Esco2^{fl} mice at different timepoints after the lesion. Scale bars represent 50µm. Data are presented as mean±sem. Number of animals: n=3 for each bar. Statistical analysis: One-way ANOVA + Tukey post-test, ^{ns}p<0.05, ^{**}p<0.001, ^{***}p<0.0001.

Although this research area is just emerging currently, there is already a high body of evidence that glial cells do indeed activate and regulate each other after injury by releasing different factors (Wu et al. 2010b; Kang et al. 2013; Clemente et al. 2013).

In order to determine whether and to which extent NG2-glia affect microglia/macrophages and astrocytes after injury, the two other glial cell types were immunohistochemically analyzed following significant NG2-glia ablation at two, four and seven days after stab wound injury in coronal brain sections within a distance of approximately 250µm around the lesion site.

As mentioned in the introduction, microglia are amongst the first cell types to respond after stab wound injury. Indeed, in the *Esco2*^{wt} control animals, Iba1⁺ microglia rapidly increased in number until 4dpl in response to injury and slowly decreased thereafter to almost normal levels. In the *Esco2*^{fl} mice on the other hand this cellular increase at 4dpl could not be observed, however the analysis for the other timepoints at 2dpl and 7dpl did not reveal any significant differences in cell numbers (Figure 31-A and B, Table 24 in supplementary tables).

Although lower in absolute numbers, significantly more microglia in *Esco2*^{fl} mice at 4dpl turned out to be positive for the marker CD45 (Iba1⁺/CD45⁺) compared with the controls, indicating that more microglia were reactive. This phenomenon could still be observed at 7dpl, demonstrating that microglia/macrophages in the *Esco2*^{fl} mice were also activated for a longer time compared with those in the littermate controls, whose the microglia activation went back to almost physiological levels at this timepoint (Figure 31-C and D, Table 25 in supplementary tables).

Besides the activation of microglia, the infiltration of bone-marrow-derived macrophages that are CD45⁺/Iba1⁻ is a physiological reaction upon injury, going along with a disruption of the BBB. However this population in the *Esco2*^{fl} animals, was significantly higher at 4dpl compared with the controls, where only less than half of these numbers could be identified. At 7dpl, the invading CD45⁺/Iba1⁻ cell fraction in the wildtype was significantly reduced, while they were still present in high numbers in the *Esco2*^{fl} mice (Figure 31-E, Table 26 in supplementary tables).

In order to analyze whether the loss of NG2-glia in the *Sox10iCreER*^{T2}x*CAG-eGFP*x*Esco2*^{fl} mouse model induces similar effects in the reaction of astrocytes as it did in microglia/macrophages, the total numbers (determined as S100β⁺) as well as the reactivity status of astrocytes (determined as GFAP⁺) were immunohistochemically analyzed in coronal brain sections at 4dpl and 7dpl (Figure 32). At 4dpl, the total number of S100β⁺ astrocytes in *Esco2*^{fl} mice was significantly reduced in comparison to the wildtype controls. Between 4dpl and 7dpl, the astrocyte numbers in the *Esco2*^{wt} mice significantly increased as a normal reaction to the injury. This injury-specific increase was also observed in the *Esco2*^{fl} mice, however at this stage the total cell numbers were still significantly lower in the *Esco2*-depleted

animals compared with the *Esco2*^{wt} mice (Table 27 in supplementary tables). Preliminary data suggest that at 14dpl the total numbers of GFAP up-regulated cells again reached the level of the controls (data not shown), indicating that the astrocyte activation is not fully disturbed but only delayed.

Astrocytes in their physiological reaction to injury did not only increase in numbers, they also upregulated the reactivity marker GFAP. Besides the difference in astrocyte numbers between *Esco2*^{wt} and *Esco2*^{fl} mice, also their reactivity status was changed. At 4dpl 81.5±1.2% of the astrocytes were reactive (S100β⁺/GFAP⁺) in the *Esco2*^{wt}, while only 58.1±4.2% of these double-positive cells could be found in the *Esco2*^{fl} mice. Although the proportion of reactive astrocytes in the *Esco2*^{fl} mice increased to 83.4±0.9% until 7dpl and was therefore not different from the *Esco2*^{wt} group (89.5±2.1%), the absolute number of reactive astrocytes remained significantly lower (Figure 32, Table 27 in supplementary tables).

The GFAP-expressing astrocytes in the *Esco2*^{fl} mice first seemed to be less hypertrophic in their morphology and secondly to express lower levels of the GFAP protein compared with the hypertrophic astrocytes that could be observed in the wildtype controls (Figure 32-A blow-up pictures).

In conclusion, the analysis of the other glial cell types in the context of a reduced NG2-glia population revealed that the physiological reaction of both microglia and astrocytes was significantly altered compared to the wildtype condition where sufficient numbers of NG2-glia were present. Moreover, these mice showed an increased number of infiltrated blood cells inside the lesioned tissue even at late stages after injury. These data are giving evidence that NG2-glia play an important role in the communication with and cross-activation of other glial cell populations in the adult brain after injury.

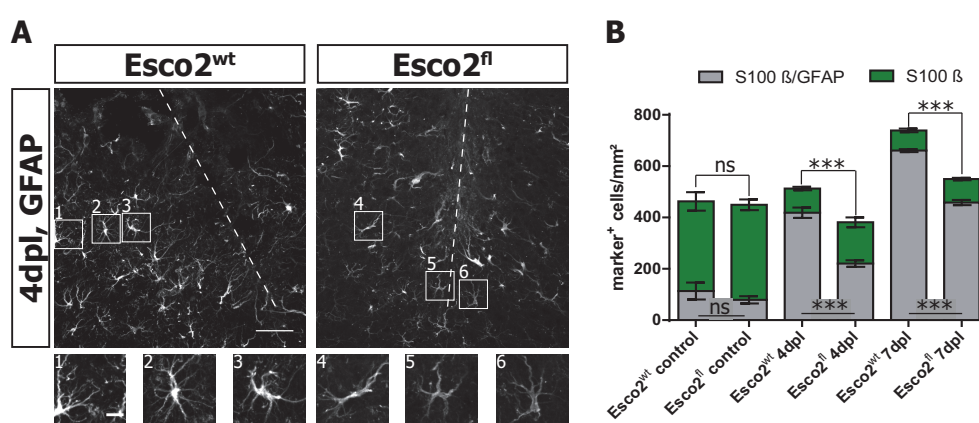


Figure 32: Astrocyte reaction after injury. (A) GFAP-reactive astrocytes in *Esco2*^{wt} and *Esco2*^{fl} mice at 4dpl. Lesion is indicated with a dashed line. Numbered boxes indicate individual GFAP-expressing astrocytes. (B) Quantification of reactive (S100β⁺/GFAP⁺) and non-reactive (S100β⁺) astrocytes at 2dpl and 4dpl in *Esco2*^{wt} and *Esco2*^{fl} animals. Scale bars represent 50μm and 10μm in blow-ups. Data are presented as mean±sem. Number of animals: n=3 for each bar. Statistical analysis: One-way ANOVA + Tukey post-test, ^{ns}p>0.05, ***p<0.0001.

4 DISCUSSION AND FUTURE PERSPECTIVES

4.1 ABLATION OF NG2-GLIA IN THE HEALTHY BRAIN

4.1.1 NG2-GLIA NETWORK IS MAINTAINED AT THE EXPENSE OF OLIGODENDROGENESIS

NG2-glia in the adult cerebral cortex carry the unique feature of being proliferative while at the same time they keep generating mature oligodendrocytes throughout life – two features that turn them into progenitors of their own lineage. Many fate mapping studies of some cortical regions already addressed these cellular properties and described them extensively (Dimou et al. 2008; Simon et al. 2011; Clarke et al. 2012; Young et al. 2013). However, the physiological importance for this lifelong cycling capacity has not been addressed to the same extend so far. In the present study, we aimed to specify the underlying function and the importance of mitotically active NG2-glia by ablating them in the Sox10iCreER^{T2}xCAG-eGFPxEsco2^{fl/fl} mouse line, in which specifically proliferating NG2-glia were targeted to undergo apoptosis.

Although the apoptotic ablation was efficient in Esco2^{fl} mice both in the GM and in the WM of the cerebral cortex (Figure 9 and Figure 10), not all recombined cells could be ablated even within four months, although it was demonstrated that between 80% and 100% of all NG2-glia re-enter their cell cycle within approximately one month in young adult mice (Simon et al. 2011; Young et al. 2013). Moreover, especially in the GM, some of the recombined NG2-glia incorporated BrdU, clearly indicating that these cells could finish their cell cycle even in the apparent absence of Esco2. One reason could be that although Esco2 is ablated in these cells, they are still able to finish their cell cycle properly by using alternative mechanisms to compensate for the lack of the Esco2 protein. The orthologue Esco1 is still present and therefore some of the cycling cells could have overcome the loss of Esco2 due to its partial redundancy and potentially different mechanisms to provide cohesion of sister chromatids (Hou and Zou 2005; Minamino et al. 2015). It seemed that especially cells having an extremely slow cell cycle length could escape the loss of Esco2, while faster cycling cells, e.g. from the WM seemed to be depleted more efficiently. Furthermore, tamoxifen-mediated Cre-recombination was shown to be not equally efficient at different loci in the genome. This could result in the successful recombination of the GFP, but not the Esco2 locus (Nagy 2000), also allowing a normal cell cycle despite a visually apparent recombination, as Esco2 is expressed in normal levels. However, as in this mouse line all cells carry several copies of the BAC encoding the Cre-recombinase (Simon et al. 2012), the probability thereof is rather low. As there are no antibodies working in immunohistochemistry that could be used to stain the very shortly expressed Esco2 protein, the ablation of Esco2 could not be verified with immunohistochemistry in this work. *In situ* hybridization for testing the mRNA-expression

levels of the *Esco2* locus in sections of this mouse line would be a reliable method to address this issue. However, as the timely expression of *Esco2* is very short and no data exist on the number of NG2-glia expressing it at a specific timepoint, this would be difficult to realize.

Besides the death of NG2-glia in the knockout mice, both the number as well as the proportion of recombined NG2-glia was also slightly decreasing over time in *Esco2*^{wt} mice, mainly in the WM but not as prominent in the GM (Figure 11). One explanation hereof would be the existence of a perpetually added pool of non-recombined NG2-glia originating from the SVZ, that only migrate into the WM but not into the GM (Menn et al. 2006; Ortega et al. 2013). Another hypothesis could be the existence of two different subsets of NG2-glia with different proliferation capacities. Low *Sox10* expressing cells (the non-recombined ones) might preferentially proliferate to maintain the NG2-glia population compared with the high *Sox10* expressing (the recombined) ones, which in turn could then be preferentially differentiating. So far, it is supposed that *Sox10* is expressed in all NG2-glia (Kuhlbrodt et al. 1998), however, *Sox10* expression levels in these cells have not been addressed so far. A pilot experiment with the mouse line used in this study strengthened the hypothesis of two subpopulations: Inducing *Esco2*^{fl} mice a second time with tamoxifen after 16wpi when most of the recombined NG2-glia were already ablated did only result in half of the recombination rate compared with the first round of induction. This could mean that these cells did intrinsically not express enough of the *Sox10* transcription factor and subsequently the CreER fusion protein in order to achieve recombination. Moreover, preliminary *Sox10*-stainings in this experiment revealed that only GFP-expressing NG2-glia were also strongly positive for *Sox10*, whereas the non-recombined NG2-glia did not seem to express it at detectable immunohistochemistry levels. However, it cannot be ruled out that the reduced recombination rate after the second recombination at 16wpi was only an effect of the aging brain where the recombination rate is generally less efficient and not due to non-recombinable subsets. To further strengthen the hypothesis of different subpopulations, recent work from our lab demonstrated that GPR17-expressing NG2-glia serve as a reserve pool for the total NG2-glia population. However, the overlap between this GPR17-expressing reserve pool of NG2-glia and the non-recombined (low *Sox10*-expressing) cells remains to be elucidated (Viganò and Schneider et al. in press).

Besides the proliferative capacity and the resulting death of NG2-glia, the closely linked differentiation capacity was also altered in this study. Proliferation and differentiation of NG2-glia are well described for some brain areas (Dimou et al. 2008; Psachoulia et al. 2009; Simon et al. 2011; Young et al. 2013), these two distinct features have however always been addressed simultaneously in one experimental setup by applying BrdU or EdU. So far, no tools allowed the separation of these distinct cellular properties. With the herein described mouse model, we established for the first time a tool to diminish the differentiation of NG2-glia into

mature oligodendrocytes while keeping the cell numbers of the NG2-glia network unaltered. Despite using a novel genetic approach for the ablation of proliferating NG2-glia, the findings in this work are supported by the outcome of previous studies. Ablating proliferating NG2-glia with a high-dose X-irradiation or a continuous infusion of the mitotic blocker cytosine- β -arabino-furanoside (AraC) resulted in a transient ablation of NG2-glia that was restored within a short period of time by the endogenously remaining NG2-glia pool from either the same or adjacent areas (Irvine and Blakemore 2007; Robins et al. 2013). So far no approach ever achieved full ablation of NG2-glia but in all models cells were successfully repopulating. By sensing their environment, these cells were shown to react upon loss of contact inhibition with enhanced proliferation or migration to fill the newly formed gap (Hughes et al. 2013). Accordingly, NG2-glia in this thesis similarly compensated for the loss of neighboring cells (Figure 12), although the compensation mechanism has not been addressed. However, the above mentioned studies did not take the differentiation properties of NG2-glia maturation into new oligodendrocytes into account. This work revealed two major differences compared with the previously reported studies: I) a continuous ablation of single cells over longer times compared with an ablation of the majority of the cells within a short period of time as NG2-glia do have a long cell cycle length and are not synchronized (time effect), and II) a chronic but low ablation effect compared with a complete NG2-glia ablation followed by quick tissue regeneration (cell number effect). These combined effects could only be exploited in this novel mouse model because NG2-glia in the physiological brain are not synchronized in their cell cycles. Hence, the described genetic approach only ablated single cells at different timepoints and in different regions, while not inducing a strong immune reaction to clear the cell debris (Figure 13). The remaining gap of apoptotic cells were closed within a short time window and the absolute number of NG2-glia remained stable, both in the GM and WM at every analyzed timepoint (Figure 11). However, as this cell loss continued over a period of four months, non-recombined NG2-glia were required to keep proliferating at the expense of differentiation (Figure 14). Another hypothesis that would explain the diminished oligodendrogenesis would be an intrinsically distinct differentiation capacity of recombined (GFP⁺) and non-recombined (GFP⁻) NG2-glia in which the first ones are more prone to proliferate and the latter ones to differentiate. As a result of the depletion on the GFP⁺ cells, the cell numbers would remain stable while only the differentiation would be reduced, as it was observed in this mouse model. The proliferative capacity of NG2-glia that were shown to proliferate at least twice (Simon et al. 2011) is still highly debated, and it is unclear whether they have an unlimited number of cell cycles or if they exhaust after a particular yet unknown number of cycles. Some scientists support the idea of NG2-glia passing a certain amount of limited cell cycles before their final differentiation into mature oligodendrocytes (Ffrench-Constant 1994; Raff 2007). Hughes et

al. (2013) demonstrated a direct differentiation from NG2-glia into mature oligodendrocytes without a preceding proliferation *in vivo*, providing some kind of counterevidence for the need of proliferation before differentiation – at least in superficial layers of the cortex. However, as the authors did not follow individual cells over a long time, the possibility remains that these apparently directly differentiating cells have proliferated before and only passed a quiescent state during the time of analysis. Unfortunately, this study could also not dissolve the question about the possible cell cycle numbers of NG2-glia. However, there could still exist a self-renewing subpopulation within the overall population with an unlimited proliferation rate, comparable to neural stem cells. EdU-labeling experiments on the other hand demonstrated a labelling of 100% of NG2-glia in young adult mice within approximately one month, both in the GM and the WM of the cerebral cortex (Clarke et al. 2012; Young et al. 2013), negating this theory. However, the possibility of a NG2-glia stem cell pool could still apply despite all other cells proliferating, as in the SVZ where both the NSC as well as the transient amplifying progenitor cells (TAPs) are able to proliferate, although the latter ones are not stem cells any longer (Doetsch et al. 1997). The mouse model that was used in this work brings forward the debate about the proliferative capacity. The continuous cell death of recombined cells forced the remaining cells into a higher number of cell cycles, but even at late stages after recombination no signs of exhaustion were observed. This could be verified with an experiment in which both the *Esco2^{fl}* and the *Esco2^{wt}* mice received BrdU not directly after the induction, but between 9wpi and 11wpi and were sacrificed directly afterwards. Even at this late stage, non-recombined NG2-glia in the *Esco2^{fl}* mice had incorporated significantly more BrdU compared to the controls, indicating that their proliferative capacity is at least not limited to a few number of cycles, as they were probably proliferating before, in order to compensate. However, the possibility remains that those cells compensating for the loss at the beginning are another subset of cells than those that are proliferating normally at the late stages after induction, when no compensation would be necessary anymore. To address this topic in more detail, the *Esco2^{fl}* mice could be analyzed at even later timepoints after induction to see if their proliferative capacity eventually declines at some point. Challenging this already altered environment with a stab wound or other kinds of injury at 16wpi would be another possibility to address this question. NG2-glia that have already extensively proliferated would be forced to undergo a high number of cell cycles after injury and would eventually exhaust. Moreover, this work disclosed some differences in the proliferative capacity between the GM and the WM of the cerebral cortex. In the WM, most of the NG2-glia were able to proliferate within 16wpi because the majority of the recombined cells died at this timepoint. In contrast to that, it seems that in the GM only a certain pool of NG2-glia was able to proliferate, as even at this long timepoint after induction a high number of recombined NG2-glia that have not

incorporated BrdU and therefore escaped, could be detected. Unfortunately no extensive fate mapping studies at this age of the mice do exist to compare these data with, most of the studies were carried out in young adult mice. However, some of the recombined NG2-glia in the WM of the *Esco2^{fl}* mice could have directly differentiated into mature oligodendrocytes, therefore these cells would not count into the recombined NG2-glia pool any longer (without having proliferated). One possible experiment to approach this question and to verify this hypothesis could be the long-term application of BrdU following EdU in order to see whether all cells carry the same proliferative capacity or if a specific population is more prone to proliferate.

Besides the potentially different proliferative capacity, NG2-glia in WM tracts are known to proliferate more often and faster compared with those in GM tracts (Dimou et al. 2008; Young et al. 2013). For this reason, recombined cells in this mouse model were ablated faster in these tracts (Figure 11). However, the cell cycle length of NG2-glia is also very variable between different WM tracts in the brain. This work revealed that the magnitude of NG2-glia ablation in WM tracts is in line with the cell cycle length: in the corpus callosum, the ablation was faster compared with the optic nerve (data not shown), where the cell cycle was determined to be twice as long (around 20 days in the optic nerve vs. around ten days in the corpus callosum) (Clarke et al. 2012; Young et al. 2013).

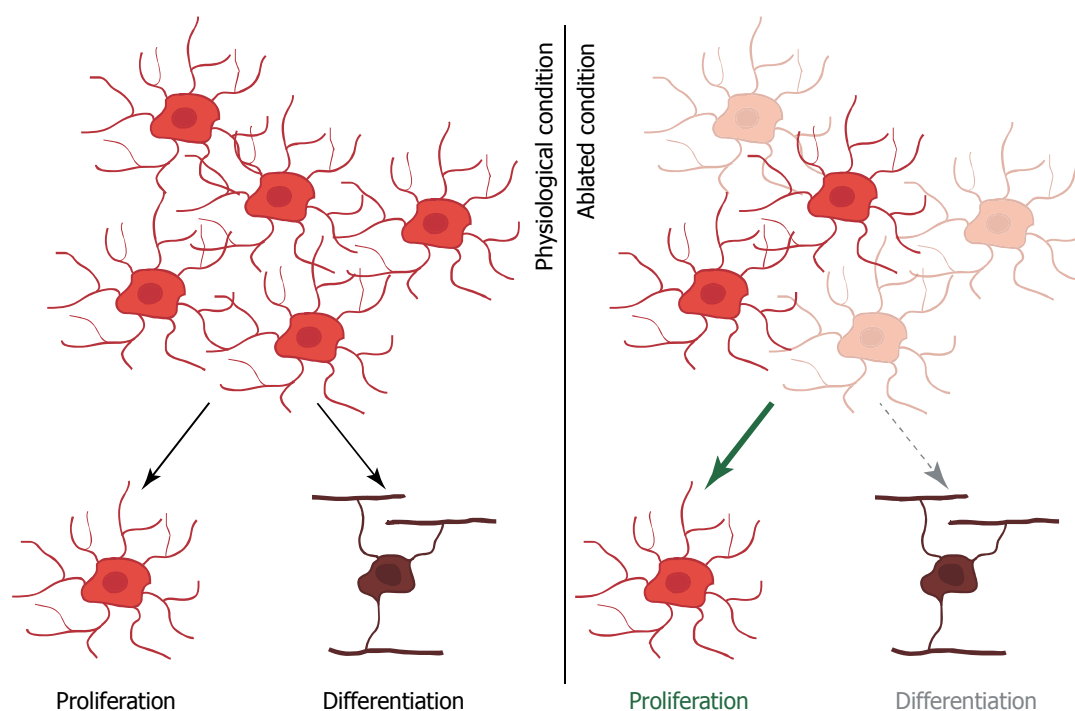


Figure 33: Cellular fate switch of NG2-glia upon long-term cell ablation. Under physiological conditions (left panel), NG2-glia keep a regulated 'steady state' between proliferation and differentiation. However, when many cells are taken out of the network over a long period of time, NG2-glia shift their behaviour and become highly proliferative (green arrow), while at the same time their differentiation capacity is declining (dashed arrow).

Although the cell cycle length was calculated to be around 37 days for the cortical GM in several studies (Simon et al. 2011; Clarke et al. 2012; Young et al. 2013), they did not discriminate between different cortical areas. Figure 10 shows that the death of recombined NG2-glia in this work is not distributed within the GM to the same extent, but is more prominent in the somatosensory and the visual cortex compared with the motor cortex. Thus, it can be assumed that the average cell cycle length of NG2-glia – similar to different WM tracts – is also highly variable between different cortical GM areas. The exact cell cycle lengths of different areas should be determined distinctively in future studies. The reason for these variable cell cycle properties could be the area-intrinsic differences in the activity of neurons, as NG2-glia are known to increase their proliferation rate upon neuronal activity (Gibson et al. 2014). To prove this hypothesis, it would be interesting to artificially increase the endogenous neuronal activity in the Sox10iCreER^{T2}xCAG-eGFPxEsco2^{fl/fl} mouse line either by physiological stimuli (enriched environment or voluntary running on a wheel) or by tetanus toxin induced epilepsy that was shown to permanently hyper-activate neurons in the respective area (Simon et al. 2011; Mainardi et al. 2012).

In conclusion, these data showed that NG2-glia maintain their homeostatic network, even when a long-term apoptotic cell death is induced in the majority of the cells. Moreover, they do so by increasing their proliferation at the expense of differentiation, meaning that the oligodendrocyte lineage loses its physiological 'steady state' between proliferation and differentiation (Figure 33). Given this fact, one could conclude that the homeostatic network and its underlying physiological functions are more important for the overall brain physiology than the de-novo generation of oligodendrocytes. However, whether this switch in the cellular fate is an active regulation, a matter of subpopulation-intrinsic differences in their proliferation and differentiation capacity, or simply a normal evolutionary mechanism that cannot be overcome by an externally applied insult is not known.

4.1.2 OLIGODENDROCYTE LINEAGE EQUILIBRIUM IS REQUIRED TO MAINTAIN NODES OF RANVIER IN THE WHITE MATTER

The signals deciding whether a cell inside this physiological 'steady state' is differentiating into an oligodendrocyte or remains a proliferating progenitor are still unknown, as is the functional importance of this lifelong dynamic process. The recent years of research provided evidence that adult oligodendrogenesis as well as subsequent myelin remodeling is relevant to maintain at least some grade of plasticity in the adult brain. It has been shown that oligodendrogenesis and subsequent myelin remodeling are required to learn a complex motor skill in rodents, while the general physiological brain function remained unchanged in the absence of this remodeling (McKenzie et al. 2014). Moreover, human fMRI studies revealed a high remodeling as well as

an increase in the volume of WM tracts in the late adult brain after learning different motor tasks like juggling, studying a second language or playing the piano (Bengtsson et al. 2005; Scholz et al. 2009; Takeuchi et al. 2010; Lebel et al. 2012). Although these studies provided confirmation for myelin remodeling, they have to be interpreted with precaution. Myelinated fibers can only be identified indirectly with fMRI, by measuring the fractional anisotropy (FA) of the water, and the detected changes are frequently interpreted as changes in myelination. However, changes in FA can also be triggered by solely cellular changes and tissue reactions, without affecting myelination (Pierpaoli and Basser 1996; Yamasaki et al. 2005; Hayashida et al. 2006). As in the adult cortical white matter only 30% of the axons are myelinated (Sturrock 1980), de-novo myelination of previously unmyelinated circuits that could be needed to learn a new task and to strengthen a novel circuit is highly supposable. Hence, adult oligodendrogenesis would be required to provide myelin in sufficient amounts. All of these studies commonly addressed the myelin remodeling process in variable learning paradigms in which the brain function could consequently be improved. However, there was no evidence for the physiological need of oligodendrogenesis where no learning is required to simply maintain the brain's structure and function. The optic nerve on the other hand is giving counterevidence for this suggestion: although fully myelinated (>98% of the axons), adult oligodendrogenesis and myelin remodeling could also be found in comparable amounts as in other WM tracts (Honjin et al. 1977; Young et al. 2013). However, oligodendrocyte differentiation and myelin insertion into already existing sheaths in WM tracts does not only provide plasticity, but it is also a normal process of aging (Lasiene et al. 2009).

Besides the plasticity in the global myelination, the nodes of Ranvier with their highly structured compartments can undergo plastic changes, although the role of this plasticity is far from being understood (Arancibia-Carcamo and Attwell 2014). The elongation of the nodes and paranodes as well as distortions in the distribution pattern of the potassium channel Kv1.2 in the WM of *Esco2^{fl}* mice (Figure 16) is giving evidence for the first time that an adequate amount of both functional NG2-glia as well as newly generated oligodendrocytes is required to maintain the highly structured brain architecture without any functional improvement. Changes in the molecular structure in the nodes of Ranvier were so far only observed after auto-inflammatory conditions, while the knowledge about molecular changes and dynamics of the node of Ranvier under physiological conditions is low. In some MS patients, auto-antibodies against paranodal anchor proteins could be observed. The damage caused by specific antibodies leads to comparable changes in nodal structures in these patients (Mathey et al. 2007; Elliott et al. 2012) as they were observed in this study. Taking this into account, the changes in the structure of the nodes of Ranvier could be a result of: I) the lack of physiological NG2-glia function due to increased proliferation, II) the lack of physiological oligodendrocyte

differentiation and myelin turnover, or III) both together. Regarding the first point, some studies reported already long time ago that some NG2-glia contact and sweep the unmyelinated axolemma in the nodes of Ranvier with their very fine processes (Butt et al. 1999; Huang et al. 2005). NG2-glia were also ascribed the function of clustering and maintaining ion channels at the correct place inside the node of Ranvier – a function that is normally attributed to perinodal astrocytes (Waxman and Ritchie 1993; Butt et al. 1999). Although the full role of node-sensing NG2-glia is not completely understood yet, a model (Figure 34 left column) could be suggested: retractions of the myelin loops and other structural changes in the nodes of Ranvier could occur throughout lifetime also in the wildtype condition. Node-sensing NG2-glia might recognize these changes and subsequently start to differentiate and insert a new myelin sheet into the emerged gap, pushing the old heminodes further apart from each other (Figure 34 mid panel, arrow indicates direction of movement). This would support the hypothesis of aging myelin sheaths with their inherent functions declining over the years. With age, internodes are increasing in number and newly generated internodes in the adult are per se shorter compared with their postnatal counterparts, what would further strengthen the above described hypothesis (Lasiene et al. 2009; Young et al. 2013). As NG2-glia in the herein described mouse model were shown to be much more proliferative compared with their wildtype counterparts (Figure 12), it could be assumed that this was due to their required function of keeping the NG2-glia network stable. Hence it would be possible that during the course of proliferation, they retract their processes from the node of Ranvier. Although this distinct process has not been shown yet, the described nodal retractions could occur, as proliferating NG2-glia – at least in a recent study – were shown to also lose their functional synapses with neurons (Sahel et al. 2015). It is even possible that in the long term, the overall population of NG2-glia undergoes some changes upon ablation in *Esco2^{fl}* mice with those cells that repopulate the WM not being able to form the physiologically required nodal contacts. So far there is no evidence that all NG2-glia have this ability, and it could be the case that only a subpopulation is able to do so. Due to the loss of their nodal connections, either in the short or long term, proliferative NG2-glia could no longer be able to sense eventually occurring nodal and paranodal elongations, and would consequently not be triggered to differentiate and repair the emerging gap. This hypothesis would explain both the nodal phenotype that was observed in *Esco2^{fl}* mice as well as the reduced number of oligodendrocytes in WM tracts of these mice. Summarizing, the structural changes in the nodes could be explained by a combination of abnormal NG2-glia function and reduced oligodendrocyte maturation. The fact that a very high proportion of elongated nodes and paranodes (Figure 16), but only an extremely low number of newly differentiated

oligodendrocytes in relation to the total number of mature oligodendrocytes could be found (Figure 14), reinforces this combined approach.

However, it cannot be completely ruled out at this point that these disturbances are based on the continuous lack of oligodendrogenesis with NG2-glia solely serving as the respective progenitors and not fulfilling any specific function in this context. Oligodendrocyte differentiation and subsequent myelin sheet insertion might be driven by oligodendrocytes themselves in a yet unknown manner (e.g. like neuronal activity). The possibility that the deletion of *Esco2* or arbitrary functions in mature recombined oligodendrocytes lead to the observed nodal phenotype could however be ruled out by fact that these postmitotic cells lack the mRNA expression of the *Esco2* transcript (Zhang et al. 2014). In addition, the NG2CreER^{T2}x*Esco2*^{fl/fl} mouse line that allows the recombination of a pure NG2-glia population was used for a control experiment, resulting in a similar nodal phenotype (Figure 22).

Although node-sensing NG2-glia and adult oligodendrogenesis might play a major role in the functional maintenance of the nodes of Ranvier, perinodal astrocytes, microglia and possibly other yet unknown cell types and factors are also known to contribute to this process (Ffrench-Constant et al. 1986; Hildebrand et al. 1993; Howell et al. 2010). Preliminary analysis of the fibrous astrocytes in the WM of *Esco2*^{fl} mice at long timepoints after tamoxifen induction revealed a decline in the expression level of GFAP in contrast to *Esco2*^{wt} mice, suggesting that these cells encounter some cellular changes derived from the environment. In the long term this could influence their function in the stabilization of the node. Along the same line, astrocytes are involved in the nutritional and energy support to neurons. It was recently reported, that nodes and paranodes in a cell culture system actively react within minutes toward energy deprivation with a significant elongation of these structures (Arancibia-Carcamo et al, unpublished data). In the context of structural or nutritional support malfunctioning, perinodal astrocytes could therefore contribute to the nodal phenotype in *Esco2*^{fl} mice as well. Analyzing the nodes of Ranvier in the cortical GM could further disclose the question about the physiological need of oligodendrocyte lineage plasticity and myelin remodeling, as many GM areas also show a high amount of myelinated fibers (Shafee et al. 2015). Malfunctioning of, or structural changes in these GM fibers is very often associated with mental diseases like schizophrenia (Haroutunian et al. 2014). In case of severe damage, they additionally show a high grade of plasticity, comparable to myelinated fibers in the underlying WM (Hashim et al. 2015). Taking these recent findings into account, there is the chance that at least in highly myelinated GM areas, some structural changes in the nodes of Ranvier could be observed in the *Esco2*^{fl} mice. Performing behavioral tests to address eventual psychological disorders in these mice could give a deeper insight in the physiological implications of myelin plasticity in the GM and other cell types involved.

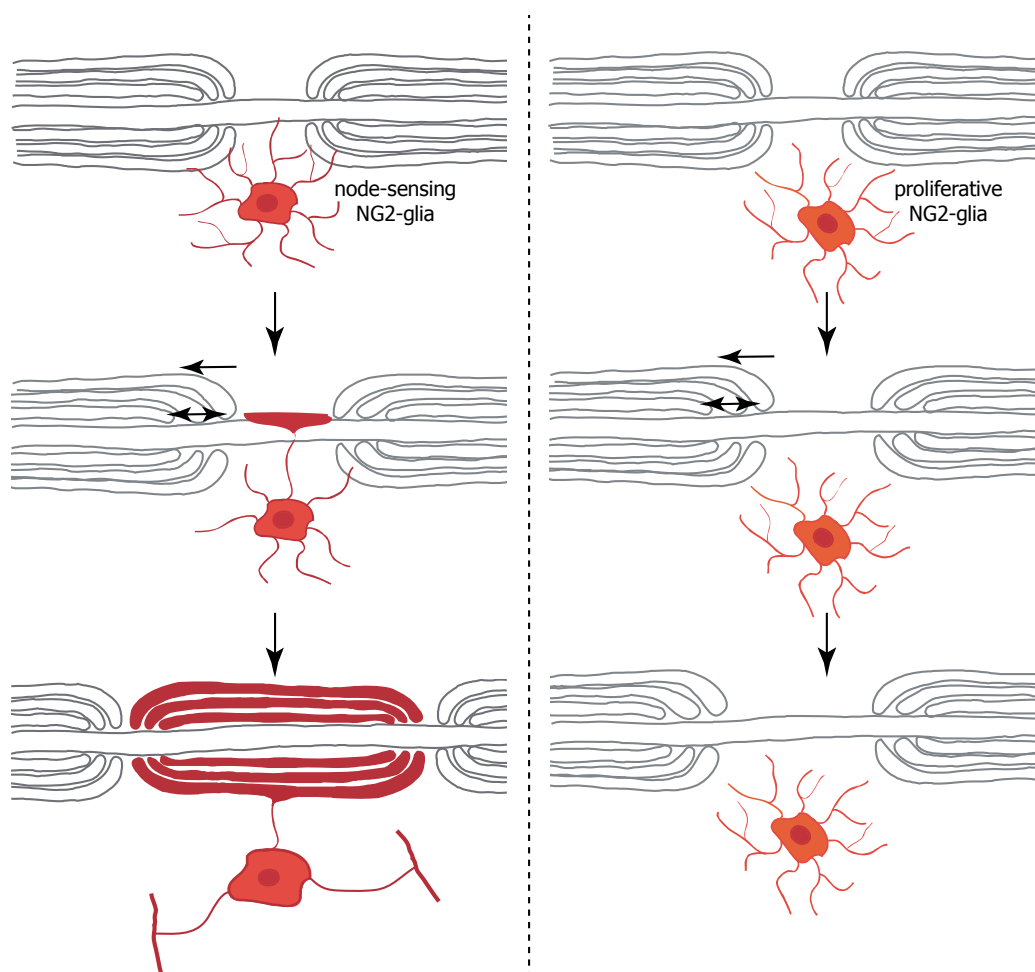


Figure 34: Hypothetical role of NG2-glia at the nodes of Ranvier. Node-sensing NG2-glia (red) that fulfill their normal function, contact the nodes of Ranvier with their processes (left column, top). One possible explanation could be that, as soon as the node and the paranode elongate, the node-sensing NG2-glia perceive these changes and start to differentiate and create a new internode by pushing the old heminodes apart (left column, bottom). Highly proliferative NG2-glia (orange) that can be found in *Esco2^{fl}* mice, lose the nodal contact (right column, top). Therefore nodal changes cannot be sensed anymore by NG2-glia, hence differentiation does not occur resulting in the phenotype of elongated nodes and paranodes (right column, bottom).

Concluding, the herein discussed data demonstrated for the first time that the maintenance of the oligodendrocyte lineage's 'steady state' with regard to the network maintenance and ongoing oligodendrogenesis, is not only important in learning conditions where brain plasticity is required, but also to maintain cellular structures.

4.1.3 NODES OF RANVIER ARE IMPORTANT TO MAINTAIN PHYSIOLOGICAL MOTOR FUNCTIONS

Formerly, myelin-related disorders have mostly been associated with neuronal damage or the direct loss of oligodendrocytes and the subsequent demyelination, while the node of Ranvier was neglected. Only since recently, there is evidence that the entire nodal region with its structural anchor proteins plays an important role in brain physiology (Faivre-Sarrailh and Devaux 2013; Arancibia-Carcamo and Attwell 2014). Disturbances of these structures can be observed in different pathological conditions that comprise myelin breakdown, e.g. multiple

sclerosis, hypoperfusion, as well as during the normal process of aging (Hinman et al. 2006; Howell et al. 2006; Reimer et al. 2011). Vice versa, some kind of disruptions in the nodes of Ranvier without general myelin disorders are thought to cause different neurological and psychiatric diseases (Roussos et al. 2012; Susuki 2013). However, whether nodal disruptions alone are the cause for such pathologies, and to which extent other factors are playing a role in this context, remains to be elucidated.

The findings based on *Esco2^{fl}* mice in this study that show a disarrangement in the nodes of Ranvier while progressively developing motoric dysfunctions (Figure 16 and Figure 17), support the idea that a physical disorder (in this case motor limb dysfunctions) can directly be caused by structural disarrangements in the WM-located nodes of Ranvier. Taking also the conclusions from the previous chapters into account, a conclusive theory can be presented. The lack of functional NG2-glia in the WM leads to structural disturbances in the nodes of Ranvier, what in turn could result in the loss of motor abilities due to the functional loss of the nodes. The control experiments with the *NG2CreER^{T2}xEsco2^{fl/fl}* line strengthened this theory. These mice developed a similar motor phenotype as mice of the *Sox10iCreER^{T2}xEsco2^{fl/fl}* line although it appeared much later, confirming that the motor phenotype is a dose-dependent effect. As the recombination in NG2-glia was much lower, fewer NG2-glia were ablated and to achieve the same effect compared with the other mouse line, a longer time was required. To provide further proof that the cell ablation is directly linked to a behavioral phenotype, different functional behavioral tests specific to distinct WM tracts could be performed. NG2-glia ablation was also prominent in the optic nerve, therefore conducting tests addressing the vision, or electroretinography with *Esco2^{fl}* mice late after induction would be a consequent next step (Tanimoto et al. 2009).

Most interestingly, the grid walk experiment gave the wrong impression that the severity of the motor dysfunctions was higher at the forelimbs opposed to the hindlimbs in the *Esco2^{fl}* mice (Figure 17). However, when stepping with the hindlimbs in this experiment, mice used a bigger surface of the paw than with the forelimb. Therefore, the probability of a hindlimb misstep is much lower compared with the forelimb, although the hindlimbs are still affected to the same extend. This becomes especially evident during the beam crossing performance, where in all of the cases the mice were only clamping their hindlimbs around the beam while the forelimbs seemed to be placed normally. These observations are giving evidence that all parts of the body are evenly affected by the motor malfunctions, but the phenotype is especially highlighted under motor performance.

The distinct mechanisms acting between the structural disturbances of the nodes of Ranvier and the resulting phenotype are currently unknown. The poor performance in beam crossing in the *Esco2^{fl}* group strengthens the assumption that the phenotype is majorly WM-derived,

as this test has just recently been shown to be specific for WM tasks (Scafidi et al. 2013). The main function of cerebral WM is the axonal connection between different cortical areas, therefore changes in the nerve conduction of these WM fibers might be involved. Indeed, in *Esco2^{fl}* mice a late stage delay in the nerve conduction latency in myelinated fibers was observed (Figure 24). Moreover, the onset of this delay could clearly be correlated with the timepoint when nodal and paranodal elongations occurred. Just recently Murcia-Belmonte et al. (2015) reported about elongations of the nodal and paranodal structures together with an increase in myelination in the WM leading to significant changes in the nerve conduction velocity in adult mice, which supports the findings on the correlation between the nodal changes and the changes in the nerve conduction velocity in this work. However, the authors did not address the motor abilities of their mice. Literature yields many examples and explanations why and how changes in the organization of the nodes of Ranvier can influence the conduction velocity of myelinated nerve fibers and therefore result in a disturbed motor output: (I) the right amount of ion channels at the right places and (II) the length of the nodes themselves (Rosenbluth 2009; Arancibia-Carcamo and Attwell 2014; Li 2015).

Regarding the first point, one study reported that the juxtaparanodally located potassium channels Kv1.1 and Kv1.2 are necessary for the fine tuning of action potentials in axons (Wang et al. 1993a). Furthermore, the channels are known to be involved in the fast repolarization of the potential for repetitive stimulation (Devaux et al. 2004). A mislocation of these channels increases the unwanted current flow beneath the myelin sheath, having detrimental effects on action potential propagation (Jensen and Shi 2003; Arancibia-Carcamo and Attwell 2014). These examples are giving further evidence that the misplacement of the Kv1.2 channels in *Esco2^{fl}* mice could lead to changes in the nerve conduction velocity and could be one of the major reasons for the observed motor phenotype. However, other recently discovered subtypes of potassium channels (Kv7.2/3) were shown to be additionally involved in the electrical current flow in juxtaparanodal regions (Battfeld et al. 2014). Along the same line, voltage-gated sodium channels (Nav) that are majorly involved in the action potential propagation could also play a role in this mouse model.

Secondly, elongations of the central nodes alone were shown to negatively influence conduction velocities due to a higher nodal capacitance accompanied by other disturbances (Arancibia-Carcamo and Attwell 2014), while the para- and juxtaparanodal structures remained stable (Rosenbluth 1987; Bhat et al. 2001). Furthermore, already subtle nodal changes can strongly influence the nerve conduction velocity (Babbs and Shi 2013). As in the *Esco2^{fl}* mice, both elongation of the nodal regions and dislocation of the potassium channels were detected, the motor phenotype is most likely derived from a combination of these two effects.

During the analysis after approximately six months, disintegration of the node of Ranvier, the thereof resulting nerve conduction velocity issues, and motor disturbances were non-reversible effects. The respective mice did not regain their motor functions, even after the majority of recombined NG2-glia were ablated and therefore no further impairment from the cellular composition within their brain was expected. The reason could be that once the nodes of Ranvier were destroyed, active repair mechanisms for this structures as found in demyelinating diseases (Rasband et al. 1998) would be required. Indeed, some of the disrupted nodes in the *Esco2^{fl}* group seemed to be actively repaired, noticeable by the patchy paranodal CASPR stainings that are thought to be a sign of recovery (Figure 16, Craner et al. 2003; Howell et al. 2006; Gu and Gu 2011). However, these mechanisms were apparently not able to fully repair the defects. Functional NG2-glia are most likely involved in this restoration mechanism, hence the proliferative changes of the NG2-glia population and the loss of their nodal contacts in the *Esco2^{fl}* mice as discussed in the previous chapter are probably connected to the failure to achieve a full recovery as they are probably not able any more to sense the changes.

Despite that distortions in the WM are the causative reason for the motor phenotype, other possible factors need to be considered. This holds especially for the early onset of the motor phenotype (around 4wpi), happening long before the first nodal/paranodal elongations (around 16wpi) were detected. Preliminary results in this study (data not shown) exhibited some depositions of the amyloid precursor protein (APP) in axons running through the WM, indicating that these neurons are exposed to sub-lethal cellular stress as demonstrated in a previous study (Lappe-Siefke et al. 2003). Moreover, some of the WM projection axons in the *Esco2^{fl}* mice appeared black in the electron microscopy, what is known to be another indicator for the neurons to be stressed (Bignami et al. 1981; Narciso et al. 2001). These findings lead to the assumption that any cellular or even sub-cellular changes in the cortex in *Esco2^{fl}* mice (for details see chapter 4.1.4) could influence the neuronal excitability. Thereof evoked disturbances or malfunctions subsequently would result in the motor phenotype, independent from the structural integrity of the nodes of Ranvier. To prove this hypothesis, it would be interesting to specifically address the neuronal activity at different stages after the induction in our mouse model.

In addition to possible physiological interactions that could be involved in the black box between the immunohistochemical observations and the resulting motor phenotype, this study could at least rule out some factors that might be a reason for the motor dysfunctions. Although this mouse line showed a great intervention into the whole oligodendrocyte lineage progression, and hence, into the physiology of myelin producing cells, global demyelination or other destructions of the already existing myelin sheaths could not be detected (Figure 15). This finding is consistent with a recent study in which the blockage of adult myelin generation

did not affect already existing myelinated tracts (McKenzie et al. 2014). Analysis of the spinal cord in the *Esco2^{fl}* mice did also not reveal any differences compared with *Esco2^{wt}* mice. NG2-glia in the spinal cord are known to be less proliferative under physiological conditions in contrast to their brain-derived counterparts (Huang et al. 2014a). Therefore, apoptotic loss of recombined NG2-glia in the spinal cord was very unlikely to occur or at least to a much lower extent compared with the brain. Motor projection neurons running through the dorsal horn of the spinal cord that are important for peripheral movements, did also not show any signs of damage in the *Esco2^{fl}* mice. In addition to the lack of defects after immunohistochemistry, the horizontal ladder test in which *Esco2^{fl}* mice performed well throughout the experiment, further proved that the spinal cord was not affected by the ablation of proliferating NG2-glia. Moreover, yielded by the analysis of the peripheral nervous system (Figure 23), the muscle spindles as well as the neuromuscular junctions did not reveal any structural changes in *Esco2^{fl}* mice compared with the wildtype littermate controls (data not shown). As Schwann cells in the intact nerve were shown to not proliferate (Cheng and Zochodne 2002), cell death was not expected to occur in our *Esco2*-depleted mice. Consequently, a contribution of the periphery that could explain the motor phenotype can be excluded.

As a concluding remark, the nodal disruptions that subsequently result in a motor phenotype in this work gave further evidence in this novel field of research that the nodes of Ranvier are not only a termination of a myelinated segment, but also comprise important functions for the maintenance of brain and body physiology.

4.1.4 NG2-GLIA FUNCTIONS ARE LOST DESPITE NETWORK MAINTENANCE

Major perpetual cell death of recombined NG2-glia in the *Esco2^{fl}* mice and cellular as well as structural changes could be identified in WM areas in this study, in which the driving force of NG2-glia differentiation was shown to be very high (Clarke et al. 2012; Young et al. 2013). However, outside the areas showing extensive oligodendrogenesis, NG2-glia are also important because of their unique glia-neuron synapses (Bergles et al. 2000; Káradóttir et al. 2005; Mangin and Gallo 2011), as well as due to their just recently discovered role in neuromodulation (Sakry et al. 2014; Sakry et al. 2015) and potentially other yet unknown functions. Although these features have already been described thoroughly, their herein described functional importance to memory consolidation has not yet been assigned.

Although it was long thought that NG2-glia maintain most of their neuron-NG2-glia synapses during proliferation (Fröhlich et al. 2011), a recent study demonstrated that these synapse cannot be functionally maintained (Sahel et al. 2015). Therefore, a change in the NG2-glia network including its NG2-glia-neuron synapses in *Esco2^{fl}* mice could functionally be altered over time, despite the maintenance of the cellular network. Therefore, it might be possible

that the cells compensating for the loss of recombined cells could not fulfill their physiological functions any longer. The finding that *Esco2^{fl}* mice apparently have defects in their short-term memory at 11wpi argues for a progressive decline of the physiological functions of the homeostatic network due to changes in their cellular composition. The short-term working memory is mainly based on fast acting neurotransmitter signaling and processing between different cells including neurons and glial cells (Mongillo et al. 2008), but less on cellular or even myelin rearrangements, as for example complex motor learning skills (McKenzie et al. 2014). Unpublished observations from our lab indicate that NG2-glia are involved in this process, due to the fact that hippocampal learning and training paradigms seem to influence their cell cycle properties (Schneider and Dimou unpublished data). Vice versa, NG2-glia are also able to influence neuronal activity: Sakry et al. (2014, 2015) recently demonstrated that NG2-glia are capable of directly modulating neurons through secretion of the shed proteoglycan NG2 and other factors. Transferring these facts to our mouse model, it can be hypothesized that despite the maintenance of their cellular numbers, the NG2-glia network and their synaptic transmissions to neurons are not properly functioning in *Esco2^{fl}* mice. This hypothesis is strengthened by the learning paradigm that was used in this work: the time window of 30min in which the mice had to establish a working memory was too short to involve the long process of oligodendrogenesis, thus might be the reason of malfunctioning NG2-glia itself (other cell types were also not obviously affected). Hence it can be suggested that in the NG2-glia ablated model, the total NG2-glia network in general could receive less synaptic input compared with the wildtype controls due to a higher proportion of actively cycling cells. This reduced synaptic activity could then be the cause of the failure to establish a short-term memory.

Many studies addressed the neuron-NG2-glia synapse interaction (reviewed in Mangin and Gallo 2011; Sun and Dietrich 2013), however, it is not known whether all NG2-glia are able to form functional synapses in the same way, or if there exist subpopulations preferentially doing that. Although no study specifically addressed this question so far, most of the authors are using terms like 'synapse-bearing' NG2-glia (Sakry et al. 2014), indicating that there are distinctions between different cells from the same cortical regions (Somkuwar et al. 2014). Likewise, it can be hypothesized that in the used mouse model, the highly proliferative non-recombined NG2-glia repopulating the ablated areas receive less synaptic input compared with the recombined NG2-glia that have been resident before the ablation. Consequently, in the long-term the NG2-glia network would be changed progressively and its function would then decline with these occurring changes.

Although NG2-glia seem to play an important role in memory consolidation, they cannot alone be accounted for this process. Certainly neurons, but also astrocytes, microglia and probably

other still unidentified cells are playing an additional role (Gibbs and Bowser 2010; Jiang et al. 2015). The ablation of recombined NG2-glia did not induce any obvious cellular changes in the other cell populations (astrocytes, neurons, or microglia) in the cortical GM in *Esco2^{fl}* mice, being an indication that other cell types might neither be affected. However, in the *Esco2^{fl}* mice nothing specific is known about NG2-glia proliferation or the functionality of other cell types in the perirhinal cortex, where the used NOR paradigm is assigned to (Murray and Richmond 2001).

In conclusion, these data demonstrated that NG2-glia are involved in the consolidation process of a short-term memory. With these findings, for the first time a distinct cellular function can be attributed to NG2-glia that is important in cortical areas where oligodendrogenesis does not seem to play a major role.

4.2 INJURY

4.2.1 ABLATION OF RECOMBINED NG2-GLIA INDUCES A DEFICIT IN CELL NUMBERS IN THE LESION SITE

NG2-glia have been shown to react upon acute traumatic brain injury with a significant increase in their proliferation. Following stab wound injury, a high number of these cells are re-entering their cell cycle and shortening their cell cycle length within a few days (Tan et al. 2005; Buffo et al. 2005; Simon et al. 2011). These proliferative properties could successfully be exploited in the *Sox10iCreER^{T2}xCAG-eGFPxEsco2^{fl/fl}* mouse line that ablated high numbers of recombined NG2-glia in close-proximity to the lesion site (Figure 27). The proliferation and subsequent death of these recombined *Esco2*-ablated NG2-glia occurs relatively fast, starting already at 2dpl. Therefore, in comparison with the healthy situation where non-recombined cells had enough time to compensate, the death of the recombined cells occurred too fast to be fully compensated by the remaining cells. Although the remaining, non-recombined NG2-glia increased their proliferation rate even further compared with the wildtype controls, full compensation for the lost cells could not be reached, even at 14dpl. In the wildtype condition, NG2-glia in close-proximity to the lesion site recede to non-injured levels within one month after injury (von Streitberg and Schneider et al. submitted). However, it is not known whether late-reactive NG2-glia (the non-recombined in this case) are normalizing their numbers equally fast in the *Esco2^{fl}* mice compared with the *Esco2^{wt}* controls.

At 14dpl, only a small number (around 5%) of recombined NG2-glia survived around the lesion site in the *Esco2^{fl}* mice, indicating that the apoptotic loss after injury was more efficient than without an injury. In the non-lesioned situation, only half of the recombined cells underwent apoptosis in the GM within 16wpi (Figure 11). One reason for this divergence could be that less cells are able to escape the *Esco2*-deletion. After injury, NG2-glia re-enter their cell cycle quickly, hence they switch from a slow into a fast mode of proliferation. Being in a fast

proliferation mode, other intracellular signaling mechanisms that regulate the cell cycle could be required (Martinho et al. 2015; Moyon et al. 2015b). Therefore, the loss of the Esco2 protein could be more detrimental during fast proliferation compared with slow proliferation, where more cells escape due to an alternative or compensating mechanism. In this regard, the homolog protein Esco1 that only exists in mammalian cells, could play an important role (Hou and Zou 2005; Whelan et al. 2012b). A second reason for the almost complete ablation of recombined cells could be an intercellular feedback loop between NG2-glia boosting the overall ablation effect. NG2-glia were recently shown to auto-activate themselves during disease via the secreted cytokines IL-1 β and CCL2 (Moyon et al. 2015a). As soon as some recombined NG2-glia in Esco2^{fl} mice proliferate and subsequently die, the following autocrine signaling of their neighboring cells would activate them to proliferate as well, although they would not do so under normal conditions. As those neighboring cells displayed recombined cells with a probability of 80%, they consequently underwent apoptosis as well.

The non-recombined NG2-glia started to re-populate free spots left by ablated cells already between 4dpl and 7dpl in the Esco2^{fl} mice. However, the morphology of these repopulating cells seemed to be less complex and they appeared smaller and therefore occupied a smaller surface area than NG2-glia in the wildtype mice. Thus, in the Esco2^{fl} mice the NG2-glia-free brain surface area was even bigger. In addition, the remaining and re-populating NG2-glia rarely formed contacts with each other, being a further trigger for the remaining cells to proliferate in order to try to compensate, as they were not inhibited by neighboring cells (Hughes et al. 2013). These findings are consistent with a previous study, where the authors reported about less branched re-populating NG2-glia compared to non-proliferating ones after diphtheria toxin (DT)-induced ablation of a major fraction of the population (Birey and Aguirre 2015). The observed lack of cell complexity could be due to the fast proliferation mode, in which these cells do not have enough time to fully regenerate their typical morphology. That applies especially to those cells that cycle more than once in response to the ablation and to injury. Intercellular signaling mechanisms could play an additional role in this regard: in the same study, the blockage of netrin-1 (NTN1) was reported to be involved in the regulation of NG2-glia morphology (Birey and Aguirre 2015). NTN1 is expressed by neurons as well as by OPCs and by astrocytes at least in postnatal stages (Zhang et al. 2014). Further, it is likely that other yet unknown factors could become important as well. Thus, the changed reaction of glial cells that was observed in the Esco2^{fl} mice and the thereof induced lack of signaling molecules could lead to a less complex NG2-glia morphology.

Similar to the non-lesioned condition in the WM, the fraction of non-recombined (NG2⁺/GFP⁻) NG2-glia in the Esco2^{wt} mice proliferated stronger than the recombined fraction (NG2⁺/GFP⁺) at later stages after injury. This resulted in an overall increase in their ratio of the whole NG2-

glia population. Along the same line, Birey and Aguirre et al. (2015) also reported about the existence of two distinct cell populations after injury-like conditions: (I) fast and (II) slowly proliferating NG2-glia with the latter ones being a reserve pool for other cells that were lost. Another recent study used the RNA sequencing technique in the somatosensory cortex where they identified six distinct cell populations within the oligodendrocyte lineage that could potentially react differently to environmental changes (Zeisel et al. 2015). Recent findings from our lab identified an additional GPR17-expressing NG2-glia subpopulation acting as a reserve pool after injury (Viganò and Schneider et al. in press). Although these newly identified subpopulations have been described, only little about their origin and cellular differences is known. However, these studies give further indications that some NG2-glia – in our case the low Sox10-expressing, non-recombined NG2-glia – could display at least one genetically different and slower reacting subpopulation. This subpopulation could be more prone to proliferate at later stages after injury, while the other recombined cells could preferentially proliferate at earlier stages.

The reaction of NG2-glia to injury is known to be quite complex. Besides proliferation, these cells are reacting quite variable to injury, including migration, polarization, and hypertrophy. The majority of cells are even showing a combination of those (Hughes et al. 2013; von Streitberg and Schneider et al. submitted). Whether these different types of reactions originate from genetically different subclasses, or whether they are induced by the extracellular environment remains unclear. In the *Esco2^{fl}* mice on the other hand, the composition of the heterogeneous NG2-glia population might look differently. As those NG2-glia that immediately react to injury have been ablated, the decline in cell numbers could already be detected within the first 2dpl. Induced by yet not fully known mechanisms, remaining NG2-glia are forced to proliferate, although their usual response to injury would be different. As a result, they might not be able to fulfill the full range of their normal reaction to injury (hypertrophy, migration, polarization or proliferation) and one category could appear preferentially. Using repetitive two-photon *in vivo* live imaging of NG2-glia-ablated mice could give a deeper insight in the heterogeneous reaction of the remaining and compensating NG2-glia. One drawback of this experiment, however, would be that the compensating NG2-glia are not intrinsically tagged with GFP – at least in this mouse line – and other labelling mechanisms in order to make them suitable for *in vivo* imaging would be required.

Comparison of the bigger area of the lesion (up to 250µm distance from the lesion site) with the lesion core area (50µm distance from the lesion site) in *Esco2^{fl}* mice gave further evidence of the importance and function of NG2-glia after injury (Figure 27). Within the core, the ablation of recombined NG2-glia was detected later (at 4dpl) compared with its surrounding (at 2dpl). At 14dpl, however, most NG2-glia were depleted in both defined areas of analysis.

These findings suggest that proliferation in the lesion core starts later, but at higher rates once initiated. Although also the non-recombined fraction of NG2-glia in the *Esco2^{fl}* mice started to compensate by increased proliferation in the lesion core, the cell numbers never reached the same level as in the *Esco2^{wt}* mice. However, while no increase could be detected, the cell numbers in the lesion core also did not decrease at any timepoint that was analyzed, indicating that the cells try to compensate for the loss. Deriving from the lesion core analysis in *Esco2^{wt}* mice and from previous two-photon imaging studies, it is known that the stabilization of cell numbers in the *Esco2^{fl}* mice did not only occur due to enhanced proliferation, but also through migration of NG2-glia after injury. Moreover, the peak of migration of NG2-glia directed to the lesion core was shown to appear earlier than the peak of proliferation. The observed decrease of NG2-glia in the bigger surrounding in this study underlines the described migration effect, as cells from the peri-lesion seem to migrate into the lesion core at early stages.

Concluding these findings, the significantly reduced numbers of NG2-glia in the lesion site in *Esco2^{fl}* mice derived from a fast cell death of recombined cells that cannot be compensated by non-recombined cells during the first 7dpl. This effect might even be enhanced by a reduced migration rate, as the respective cells were also ablated there and not enough migrating cells were available.

4.2.2 INCREASE IN NG2-GLIA NUMBERS IN THE LESION CORE IS ESSENTIAL FOR WOUND CLOSURE

So far, many studies addressed the NG2-glia dynamics after injury, both post-mortem and *in vivo* (Buffo et al. 2005; Simon et al. 2011; Hughes et al. 2013; Binamé et al. 2013; Susarla et al. 2014). Although NG2-glia reactivity has also been extensively analyzed in regard to neuronal regeneration failure (Levine et al. 2001; Bradbury et al. 2002; Galtrey and Fawcett 2007; Busch et al. 2010; Xiao et al. 2014), only little is known about the cellular and functional importance in tissue reaction of this cell population. In this work, it was demonstrated for the first time that NG2-glia are fundamental for wound closure after injury. In *Esco2^{fl}* mice lacking NG2-glia in the injury site, repair of the wound tissue is significantly delayed compared with mice that have normal NG2-glia numbers and reactivity (Figure 29). Although the required functionality of NG2-glia for wound closure can clearly be justified by the lack of cells in the lesion core, the underlying mechanisms remain unclear. NG2-glia seem to be important for physically filling the hole in the lesioned tissue and for initiating the formation of a scaffold for other cell types, e.g. fibroblasts, endothelial lineage cells etc., that enter into the injury site to repair the wound (Shechter and Schwartz 2013; Burda and Sofroniew 2014). Concomitantly, NG2-glia might actively secrete extracellular matrix factors as suggested by Garwood et al. (2004) to strengthen the tissue composition for better lesion connectivity and repair.

Besides NG2-glia, microglia/macrophages are known to fundamentally contribute to the early stages of inflammatory reaction and to long-term wound regeneration and closure (Davalos et al. 2005; Hines et al. 2009; Dibaj et al. 2010; David and Kroner 2011). Moreover, hypertrophic astrocytes are beneficial for strengthening the tissue integrity with their cellular processes and for creating a scaffold for other accumulating cells that compact and repair the injured tissue (Sofroniew 2009; Sofroniew and Vinters 2010). The astroglial scar forms an interconnected physical barrier that is important to separate and protect the non-lesioned brain parenchyma from the inflamed lesion core in order to prevent the spreading of tissue damage (Bush et al. 1999; Faulkner et al. 2004; Voskuhl et al. 2009; Sofroniew and Vinters 2010). Hence, both the lack in number as well as the faulty regulated activation of microglia and astrocytes in the lesion of *Esco2^{fl}* mice could hence have contributed in exacerbating the tissue damage and delaying the wound closure. However, as the astrocyte reaction was only reduced but not absent, the here observed effect was not as strong compared with the direct modulation of astrocytes (McGraw et al. 2001). Although a mild astrogliosis occurred in *Esco2^{fl}* mice at 7dpl, only few signs of a physical barrier formation could be observed. This finding additionally explains the longer and more widespread accumulation of invasive immune cells in the lesion site. Reduced numbers of resident microglia could result in less phagocytic activity in the lesion, inducing a longer-lasting, stronger and further spreading tissue inflammation. This hypothesis is consistent with previous studies showing that excess debris inside a lesion as well as a reduced number of microglia after injury is blocking tissue repair and even exacerbating the lesion (Hines et al. 2009; Lalancette-Hébert et al. 2007; Ruckh et al. 2012).

Besides the cellular components discussed so far, the extracellular matrix in the lesion site of *Esco2^{fl}* mice should be additionally scrutinized. It is known that not only astrocytes, but also NG2-glia and other cell types in the lesioned brain express a variety of ECM proteins (mainly CSPGs) that negatively modulate the regenerative potential (McKeon et al. 1999; Yamaguchi 2000; Garwood et al. 2004; Castro et al. 2005; Kwok et al. 2011; Ji and Tsirka 2012; Brown et al. 2012). A reduction of the growth-inhibitory EMC deposition could have effects on the long-term neuronal regenerative capacity in *Esco2^{fl}* mice. Underlining this hypothesis, Rodriguez et al. (2014) recently reported about an improved regenerative neuronal potential in the spinal cord of mice with a reduced CSPG deposition following an inhibited activation of glial cell types after injury by reducing the NG2-glia reactivity. Although these factors have been reported to be detrimental to the neuronal regeneration in most cases, they are essential to strengthen and agglutinate the cavernous tissue after immune reaction. As the cellular reactivity and most probably also the intercellular signaling was disturbed in the injury site in *Esco2^{fl}* mice, the secretion of ECM proteins could also be reduced. Consequently, the whole glial scar in the respective injured tissue would be less sticky, additionally contributing to the

delay in wound closure. At 14dpl, the tissue reaction in terms of cellular components normalized in the *Esco2^{fl}* mice. However, it is not known if the disturbance of cellular reactivity during the early stages influences the general composition of the ECM also later on.

In summary, this work clearly demonstrated the important role of increasing NG2-glia numbers inside the lesion core for wound closure that might, besides the physical appearance of cells include the scaffold formation for other components, as well as secretion of stabilizing factors.

4.2.3 WOUND HEALING IS THE RESULT OF A NG2-GLIA ORCHESTRATED CELL-TO-CELL SIGNALING CASCADE

Although NG2-glia were shown to be important, they cannot be accounted for the lesion repair alone. All the numerous cell types that are present in the lesion site are individually contributing to a proper tissue reaction and the following repair (Shechter and Schwartz 2013; Burda and Sofroniew 2014). In addition to the lack of NG2-glia in close proximity to and inside the lesion core of the *Esco2^{fl}* mice, the reaction of both microglia/macrophages and astrocyte dynamics were significantly altered in the first days after the lesion when the strongest ablation effects were observed (Figure 31 and Figure 32). As the partial ablation of one single cell type already induced such a strong reactive disturbance of other cell types, a complex cell-to-cell signaling model is suggested for the concerted tissue reaction after TBI (Figure 35). The obtained data in this work furthermore strongly propose an orchestrating role of NG2-glia in this cell-to-cell signaling network regulating the role of both microglia and astrocytes. Microglia ablation after injury for example did not show such a deleterious effect on other cell populations (Gowing et al. 2006). As illustrated in the model, single cells and other tissue components are individually reacting to injury and some of their responses and released factors are vice versa strongly regulating the behavior of neighboring cells that also carry important roles in the whole process. So far, some studies addressed and discussed the signaling mechanisms of astrocytes and microglia, and their effect on tissue reaction and wound repair (John et al. 2003; Farina et al. 2007). The mechanisms that might influence NG2-glia reactions are also at the beginning to be explored (Arnett et al. 2001; Rhodes et al. 2006; Filipovic and Zecevic 2008; Su et al. 2011; Clemente et al. 2013; Moyon et al. 2015a), while the role and the secreted factors of NG2-glia in this cell-to-cell signaling network are still unknown on the other hand. However, this model only includes the major cell types while many other factors, e.g. damaged neurons, fibroblasts, leukocytes, miRNAs etc., that play an additional role in cell-to-cell interactions have not been considered in the further discussion (John et al. 2003; Su et al. 2015).

At 2dpl, the microglia/macrophage reaction in the *Esco2^{fl}* mice was comparable to the wildtype controls (Figure 31). At this timepoint the microglial reaction was not expected to be highly altered, as the NG2-glia ablation was only mild, and the cellular brain function as well as cell-to-cell signaling mechanisms should consequently not be disturbed. Moreover, resident

microglia and bone marrow-derived macrophages (BMDMs) are the first cells reacting immediately to injury, activated by factors directly derived from the blood (Shechter and Schwartz 2013). These immediate reaction was probably not altered in the NG2-depleted model. The astrocyte reaction in the NG2-glia-ablated mouse model was not analyzed at 2dpl, as astrocytes were shown to only react at later stages upon injury compared with other glial cell types (Buffo et al. 2005; Robel et al. 2011b; Bardehle et al. 2013). Therefore, no obvious differences in *Esco2*^{wt} and *Esco2*^{fl} mice were expected. Between 2dpl and 4dpl when the decrease of NG2-glia in the ablation model became more prominent, the Iba1⁺ microglia population could not be fully augmented in comparison with the *Esco2*^{wt} mice. Hence, an accumulation of microglia/macrophages in the lesion core was missing. Preliminary analysis revealed that the proliferation rate in microglia was unaltered, therefore it can be assumed that migration deficits were resulting in a failure of microglia accumulation due to missing signals from the depleted NG2-glia. Similar to what could be observed in the microglia population at 4dpl, astrocytes in the *Esco2*^{fl} mice failed to increase in numbers compared with *Esco2*^{wt} mice (Figure 32), and with data from literature (Hampton et al. 2004; Sofroniew and Vinters 2010). This deficiency in cell density became more obvious at 7dpl, when the NG2-glia deficiency peaked. Microglia/macrophage numbers in the *Esco2*^{fl} mice were on the other hand again similar to the wildtype controls at 7dpl, although at this timepoint, the NG2-glia deficit was still very distinct. One explanation could be that in order to achieve a proper microglia reaction, only a certain threshold of tissue reaction is required, and that this threshold was achieved at this timepoint despite the lacking NG2-glia numbers. Microglia might as well release factors that function in an autocrine feedback loop, therefore the population could have supported itself to recover. Additionally, NG2-glia-to-microglia signaling could only be required to elicit a special reaction e.g. migration, or reaction during a special time window. The mechanisms inducing the late-phase microglia reactions might be derived from somewhere else. Moreover there is the possibility that infiltrating BMDMs at this late reaction stage take over the function of resident microglia and unlike microglia, are not dependent on NG2-glia signaling.

These findings of the altered glial response conforms to a previous study, where the authors blocked the NG2-glia reactivity after SCI and found a reduced microglial and astrocyte reactivity, while the proliferative capacity of these cells remained unaltered (Rodriguez et al. 2014). However, the authors did not address the mechanism that could be relevant for the disturbed activation. Taking the suggested cell-to-cell signaling model into account, one could hypothesize that the lack of NG2-glia and a consequent lack of their released signaling factors leads to the failure in activating both microglia and astrocytes.

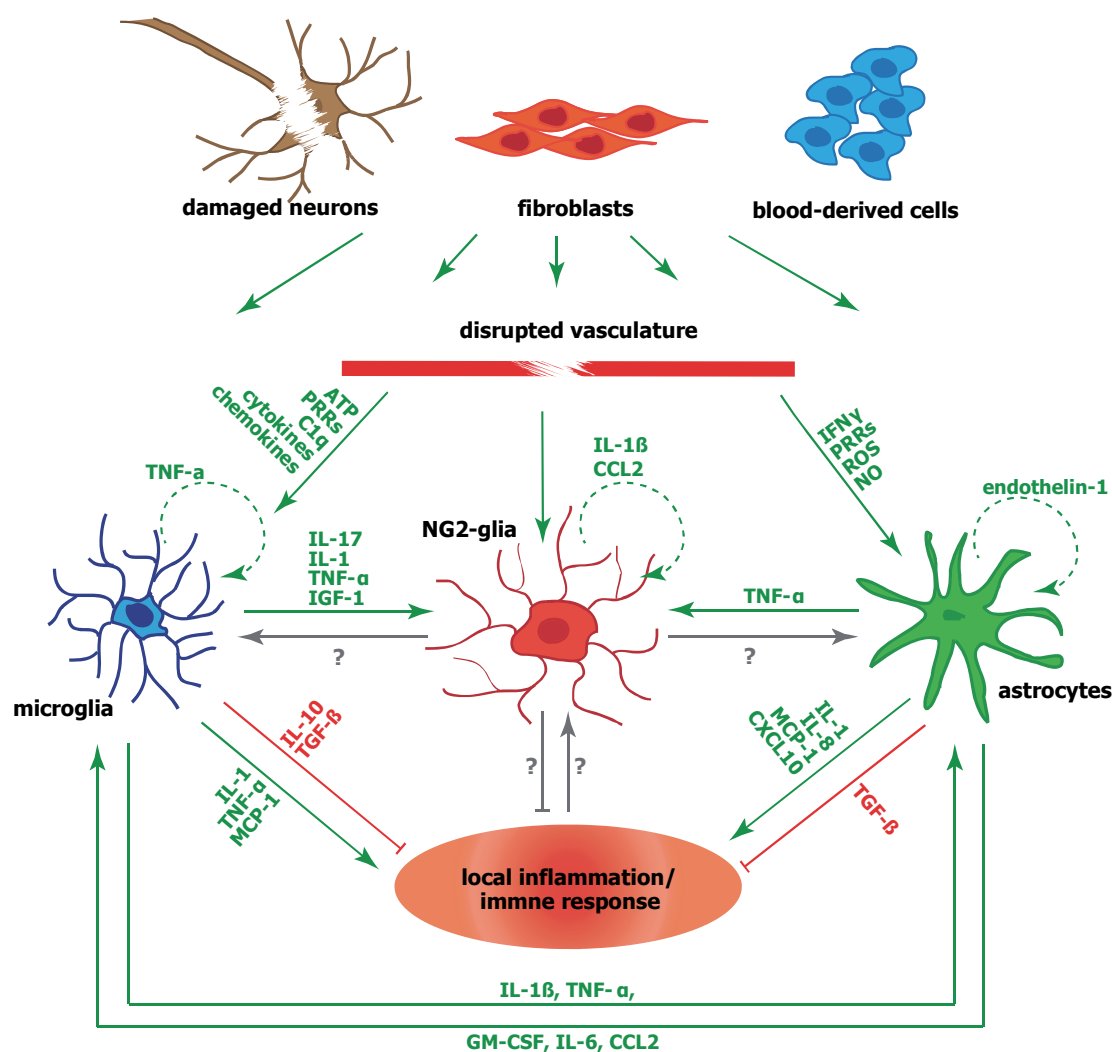


Figure 35: Cell-to-cell signaling mechanisms after acute brain injury. Cellular tissue reaction and subsequent wound healing following TBI displays a complicated cell-to-cell signaling network, including all kinds of resident brain cells, as well as invading cells from the periphery. Microglia are mainly activated by blood-derived signals and are known to regulate NG2-glia by secreted factors, astrocytes as well as the local tissue inflammation by a series of different factors. Astrocytes, that also carry receptors to be activated upon tissue damage, are additionally able to modify the local cellular tissue reaction via the secretion of cytokines and chemokines. Although NG2-glia are known to react to stimuli derived from different sources, their role in this signaling network still needs to be further explored. NG2-glia are suggested to play an orchestrating role in the regulation of tissue inflammation. Abbreviations: ATP: adenosine triphosphate; PRR: pattern-recognition receptor; TNF- α : tumor necrosis factor α ; IL: interleukine; CCL2: chemokine (C-C motif) ligand 2; IGF-1: insulin-like growth factor 1; IFN γ : interferon γ ; ROS: reactive oxygen species; NO: nitric oxide; MCP-1: monocyte chemoattractant protein 1; TGF- β : transforming growth factor β ; CXCL10: chemokine (C-X-C motif) ligand 10; GM-CSF: granulocyte-macrophage colony-stimulating factor.

This hypothesis is strengthened by different studies showing that microglia/macrophages and NG2-glia are able to influence each other by secretory mechanisms (Du Wu et al. 2002; Rhodes et al. 2006; Kang et al. 2013) (Figure 35). Late-stage responding astrocytes are also known to secrete a series of factors, e.g. granulocyte-macrophage colony stimulating factor (GM-CSF), interleukine-6 (IL-6), and a number of chemokines from the CCL-family that elicit a reaction in microglia/macrophages (Farina et al. 2007). The obtained data furthermore suggest that astrocytes – in contrast to the microglia/macrophages – are more sensitive to, or

dependent on NG2-glia-derived signals in order to increase their cellular tissue reactivity, as their reactivity did not recover during the absence of NG2-glia. Although this work clearly demonstrated the dependency of astrocyte reactions on NG2-glia, several other studies already reported about important signaling mechanisms derived from other tissue-derived factors, including an autocrine astrocyte pathway via endothelin-1 (Figure 35, Gadea et al. 2008; Sofroniew 2009; Wang et al. 2015; Gyoneva and Ransohoff 2015).

Despite the finding of reduced microglia numbers, the reason why especially at later timepoints a higher immune cell infiltration and a higher number of reactive microglia was observed could have several reasons: (I) BMDMs under wildtype conditions infiltrate the lesion site and subsequently undergo a fate-switch into M1 or M2 macrophages, making them indistinguishable from resident microglia. As this fate switch is highly dependent on the environment (Miron et al. 2013; Kumar et al. 2013), changes in the signaling cascade in the *Esco2^{fl}* mice could disturb this fate switch, resulting in an accumulation of BMDMs in the lesion site. Such changes could either derive from the direct lack of NG2-glia or from the secondary decrease in the general cellular reactivity. (II) Moreover, tissue reaction after injury is a highly balanced interaction between pro- and anti-inflammatory signals, with the latter ones being especially important to late-stage reactions that reduce inflammation and initiate wound healing (Sofroniew 2015; Corps et al. 2015). Especially M2-polarized microglia were shown to regulate the anti-inflammatory injury reaction. However, NG2-glia certainly play an additional role in this context, as microarray analysis of reactive NG2-glia identified many signaling pathways involved in cell-to-cell signaling (Simon and Dimou unpublished data). (III) The apoptotic loss of numerous NG2-glia in the *Esco2^{fl}* mice at already early stages further increased the tissue damage and accumulated debris. Therefore, the recruitment of blood-derived immune cells is being augmented, as microglia/macrophages were shown to respond to outer stimuli (e.g. ATP) in a dose-dependent manner (Davalos et al. 2005; Koizumi et al. 2007).

In conclusion, the reduction of cell numbers in the lesion site in *Esco2^{fl}* mice suggests that NG2-glia play a crucial role in the orchestration of cell-to-cell signaling and cellular reaction of other resident cell types following TBI.

4.3 TRANSLATIONAL APPROACHES AND CLINICAL IMPLICATIONS

Most of the studies deepening the general understanding of NG2-glia either in health or in disease were carried out using rodents, while the access to human tissue and therefore the knowledge of the human counterparts remains vague. Although these cells have already been discovered and used for tissue culture a long time ago (Armstrong et al. 1992; Gogate et al.

1994; Chang et al. 2000), it took several years to identify that adult human NG2-glia also carry the uniqueness of being proliferative in cortical regions outside the neurogenic niches (Geha et al. 2010; Rhee et al. 2009). Along the same line, Yeung et al. (2014) just recently reported that in adult human cortices there is a certain amount (although very low) of oligodendrocyte as well as myelin turnover. Considering these findings, there is evidence that some more well described rodent NG2-glia characteristics can be translated, and potentially used for repair mechanisms in humans. As multiple sclerosis is a major disease burden in young adults (Murray 2015), remyelination out of an either brain resident or transplanted NG2-glia pool is one of the main translational goals to be achieved in medical research; already more or less successful (Gupta et al. 2012). However, this work emphasized for the first time, that the deep mechanistic understanding of NG2-glia is also in many other aspects indispensable for future clinical purposes.

NG2-glia proliferation, differentiation and subsequent myelin production are rapidly declining during the process of aging (Lasiene et al. 2009; Psachoulia et al. 2009; Clarke et al. 2012; Young et al. 2013), and so is the white matter volume and the therewith associated cognitive abilities in humans (Bartzokis et al. 2001; Hasan et al. 2008; Zahr et al. 2009). There are speculations that the decline in NG2-glia proliferation and differentiation is the reason for the progressive loss of cognitive functions. Furthermore the work presented in this study demonstrated that a disturbance of the oligodendrocyte lineage equilibrium even during the young adulthood has a high impact on the maintenance of both spatial cognitive and motor abilities. Understanding the fundamental mechanisms driving both proliferation as well as differentiation of NG2-glia and circumventing the age-related decline of these characteristics in humans, would be one step forward in providing a cure for our aging society.

After injury, the situation of gaining benefits from understanding NG2-glia is similarly promising. Addressing neuronal loss after TBI or SCI and the causative lack of functional recovery is a main focus of clinical research. Several approaches promoting recovery for neuronal repair were already extensively used, including transplantation of stem cells (Lu et al. 2014), as well as *in vivo* reprogramming of glial cells into functional neurons (Grande et al. 2013; Heinrich et al. 2014). However, this work clearly demonstrated the valuable impact on NG2-glia in the repair mechanisms after injury. Triggering them towards a specific reaction in early stages after injury by externally applying stimulating cues could be exploited for the progress in the recovery of TBI in humans.

5 MATERIALS

5.1 CHEMICALS

| | |
|-------------------------------------------------|------------------|
| 0,9% NaCl solution (Saline) | Braun |
| 2-Propanol (Isopropanol) | Roth |
| 4',6-diamidino-2-phenylindole dilactate (DAPI) | Invitrogen |
| 5-Bromo-2'-Deoxy-Uridine (BrdU) | Sigma |
| Acetone | Roth |
| Agarose | Serva |
| Araldit Kit | Fluka |
| Bovine serum albumin | Sigma |
| Bromphenol blue | Sigma |
| Calcium chloride dihydrate | Sigma |
| Citric acid monohydrate | Roth |
| Corn oil | Sigma |
| Dextran-fluorescein | LifeTechnologies |
| Dimethylarsinic acid sodium salt trihydrate | Merck |
| di-Sodium hydrogen phosphate dihydrate | Merck |
| dNTPs | PeqLab |
| Ethanol 70 % | Roth |
| Ethanol p.a. | Roth |
| Ethidiumbromide | Roth |
| Ethylene glycol | Sigma |
| Ethylenediamine-tetraacetic acid (EDTA) | Sigma |
| Formaldehyde (Formol) | Roth |
| Formamide | Roth |
| Glacial acetic acid | Roth |
| Glutaraldehyde (electron microscopy grade) 25 % | Serva |
| Glycerine | Sigma |
| Glycerole | Sigma |
| Glycine | Sigma |
| Goat Serum | Gibco |
| In-situ cell death detection kit | Roche |
| Lead citrate | Sigma |
| Mounting solution (AquaPolymount) | Polysciences |
| Osmium tetroxide solution 4 % | Sigma |

| | |
|---------------------------|----------------|
| Paraformaldehyd | Sigma |
| Potassium chloride | Sigma |
| Potassium hydroxide | Sigma |
| Proteinkinase K | Roth |
| Q-solution | Qiagen |
| Sodium acetate trihydrate | Sigma |
| Sodium bicarbonate | Sigma |
| Sodium carbonate | Fluka |
| Sodium chloride | Sigma |
| Sodium dodecyl sulfate | Roth |
| Sodium hydroxide | Fluka |
| Sodium hydroxide pellets | Sigma |
| Sodium nitrite | Fluka |
| Sodium phosphate | Sigma |
| Sucrose | Merck |
| Sudan Black B | Sigma |
| Tamoxifen | Sigma |
| Taq Polymerase | NEB/ self-made |
| TRISbase | Sigma |
| TRISHCL | Sigma |
| Triton X-100 | Sigma |
| Tween20 | Sigma |

5.2 DRUGS

| | |
|---------------------------------|-------------|
| Atipamezol | Vetoquinol |
| Carprofen (Rimadyl) | Pfizer |
| Fentanyl | Sandoz |
| Flumazenil | Hexal |
| Ketamin | Pfizer |
| Medetomidin | Vetoquinol |
| Naloxon | Chemos |
| Xylazinhydrochlorid (Rompun) 2% | Bayer |
| Xylocain Pumpspray | AstraZeneca |

5.3 CONSUMABLES

| | |
|----------------|----------|
| 24-well plates | Sarstedt |
| 48-well plates | Sarstedt |

| | |
|-------------------------------------------|-----------------------------|
| Coverslips | Roth |
| Driller | Foredom |
| Eye cream | Bebanthen |
| Falcon tubes (15ml, 50ml) | Greiner |
| Filter tips | Sarstedt |
| Insulin syringes U-100 | BD Micro Fine (PZN: 324870) |
| Microscope slides Superfrost | Thermo Scientific |
| Microscope slides | Roth |
| Needles | Braun |
| Nescofilm | Nescofilm |
| Parafilm | Parafilm |
| Operation instruments | FST |
| Pipet tips | Sarstedt |
| Pipets | Gilson |
| Reaction tubes (0.5ml, 1.5ml, 2ml, 5ml) | Eppendorf |
| Reaction tubes for PCR | Eppendorf |
| Rotilabo® cotton buds | Roth |
| Serological pipets (5ml, 10ml, 15ml) | Sarstedt |
| Sugi sponge strips rectangular/triangular | Kettenbach |
| Surgical blades | Schreiber Instrumente |
| Suture | Ethicon |
| Syringe (1ml) | Braun |
| Transfer pipets | Sarstedt |
| V-Lance™ Knife, 19 Gauge | Alco © Surgical |

5.4 SOFTWARE

| | |
|----------------------------------|---------------------------------------------|
| Any-maze | Stoelting |
| Fiji/ImageJ | Wayne Rasband National Institutes of Health |
| GraphPad Prism 5 | GraphPad Software, Inc. |
| VLC Media Player 2.1.3 Rincewind | Free Software Foundation Inc. |
| Zen 2008 | Zeiss |
| Zen 2011 | Zeiss |

5.5 TECHNICAL EQUIPMENT

| | |
|-----------------------------------|---------|
| Cryostate | Leica |
| Digital video camera Camileo X200 | Toshiba |

| | |
|------------------------|--------------------|
| Geldoc™ XR | BIO-RAD |
| Microscope Imager.M2 | Zeiss |
| Microscope LSM700 | Zeiss |
| Microscope Observer.Z1 | Zeiss |
| Microscope Leica MZ6 | Leica |
| Perfusion pump | Gilson |
| pH meter WTW | inoLab |
| Stereotactic apparatus | Stoelting |
| Thermocycler 3000 | Biometra |
| Thermomixer comfort | Eppendorf |
| Thermoshaker | Gerhardt |
| Vortex-Genie | Bender & Hobein AG |
| Water bath | Haake |

5.6 BUFFERS AND SOLUTIONS

5.6.1 BUFFERS FOR DNA EXTRACTION AND GENOTYPING

10mM Tris-HCL

1.211g TRISbase

Ad 1l H₂O, adjust to pH8.5

Lysis Buffer

1mM NaCl

5mM EDTA

0.2% SDS

0.2M NaCl

10mg/ml Proteinase K (freshly added)

Ad 1l H₂O

10x PCR buffer

500mM Potassium chloride

100mM TRISHCl

In H₂O, adjust to pH8.7

50x TAE buffer

242g TRISBase

37.2g Disodium EDTA

57.1ml Glacial acetic acid

Ad 1l H₂O

6x Loading buffer

| | |
|---------------------|-----------------|
| 10mM | TRISHCl (pH7.6) |
| 0.03% | Bromphenol blue |
| 0.03% | Xylencyanol |
| 60% | Glycerin |
| 60mM | EDTA |
| In H ₂ O | |

5.6.2 BUFFERS FOR ANIMAL TISSUE PREPARATION

20% Paraformaldehyde (stock solution)

| | |
|------------------------------------------------------------------------|----------------------------|
| 134g | Di-sodium-hydrogenphosphat |
| 400g | PFA powder |
| 10ml | Sodium hydroxide |
| Ad 1600ml H ₂ O, pass through filter paper, adjust to pH7.4 | |

4% PFA

| | |
|-------|------------------|
| 100ml | 20% PFA |
| 400ml | H ₂ O |

10x Phosphate buffered saline (PBS)

| | |
|-----------------------------------------|-------------------------------|
| 73.66g | Di-sodium-hydrogenphosphat |
| 10g | Potassium-dihydrogenphosphate |
| 400g | Sodium chloride |
| 10g | Potassium chloride |
| Ad 5l H ₂ O, adjust to pH7.4 | |

1x PBS

| | |
|----------------|------------------|
| 100ml | 10x PBS |
| 800ml | H ₂ O |
| Readjust pH7.4 | |

Cryoprotection solution

| | |
|-----------|---------|
| 30% | Sucrose |
| In 1x PBS | |

5.6.3 BUFFERS FOR IMMUNOHISTOCHEMISTRY

Blocking solution

| | |
|-----------|------------|
| 10% | Goat serum |
| 0.5% | TritonX |
| In 1x PBS | |

Citrate buffer

10mM Citrate
0.05% Tween20
In H₂Odd, adjust to pH6.0

10x Phosphate buffer

65g Sodiumdihydrogenphosphate
15g Sodium hydroxide
Ad 400ml H₂Odd, adjust to pH7.2-7.4

Storing solution

150ml Glycerol
150ml Ethylen glycol
50ml 10x Phosphate buffer
Ad 500ml H₂Odd

5.6.4 BUFFERS FOR IN SITU CELL DEATH DETECTION

Permeabilisation solution

0.1% TritonX
0.1% Sodium citrate
In 1x PBS, always prepare freshly

DNaseI solution

50mM TRISHCl
1mg/ml BSA
300U DNaseI
In H₂Odd, adjust to pH7.5

5.6.5 BUFFERS FOR CRESYL VIOLET STAINING

0.1% Cresylviolet staining solution

300mg Cresylviolet
1.63g Sodium acetate
2.9ml Glacial acetic acid
Ad 300ml H₂Odd, stir for 30min at 60°C and filter

5.6.6 BUFFERS FOR SUDAN BLACK STAINING

Sudan Black staining solution

5 spatula tips Sudan Black B

In 70% EtOH, stir properly and filter

5.6.7 BUFFERS FOR ELECTRON MICROSCOPY

0.2M Cacodylat buffer

21.4g Dimethylarsinic acid sodium salt trihydrate

0.22g Calcium chloride dehydrate

Ad 500ml H₂O, adjust to pH7.2

Karnovski fixative

2.5% Glutaraldehyde

2% Paraformaldehyde (PFA)

0.1M Cacodylat buffer

Storing solution

4% PFA

2.5% Sucrose

In 0.1M Cacodylat buffer

Washing buffer

2% Sucrose

In 0.1M Cacodylat buffer

Osmication solution

2% Osmium tetroxide solution

0.002% Calcium chloride

2% Sucrose

In 0.2M Cacodylat buffer

Lead citrate buffer

1.33g Lead citrate

1.76g Sodium citrate

Ad 30ml H₂O (EM purity), dissolve with 8ml NaOH and fill up to 50ml with H₂O (EM purity)

Uranyl acetate

Spatula tip Uranyl acetate

Ad 1ml 70% MeOH, stir under light exclusion and centrifuge 10min at 6000rpm

5.6.8 SOLUTIONS FOR DRUG AND DYE APPLICATIONS

Rimadyl stock solution

50mg/ml Carprofen (Rimadyl)
In NaCl (0.9%)

Ketamin/Rompun anesthesia solution

2.5ml NaCl (0.9mg/ml)
1ml Ketamin
0.25ml Rivapoun

MMF (Sleep) mix

0.25ml Fentanylcitrat
0.5ml Midazolam
0.25ml Medetomidin
4ml NaCl (0.9%)

Awake mix

1.5ml Naloxon
2.5ml Flumazenil
0.25ml Atipamezol
0.75ml NaCl (0.9%)

BrdU drinking water

1mg BrdU
10g Sucrose

Ad 1l H₂O (tap water) and stir 30min under light protection

Tamoxifen solution

40mg Tamoxifen
100µl EtOH p.a.

Ad 1ml corn oil and shake for 3hrs at 37°C

Dextran-fluorescein solution

5mg Dextran-fluorescein
1ml NaCl (0.9%)

6 METHODS

6.1 ANIMALS

6.1.1 MOUSE LINES

6.1.1.1 Sox10iCreER^{T2}xCAG-eGFPxEsco2^{FL/FL}

This mouse line was a crossing product of three different mouse lines. The Sox10iCreER^{T2} line is an inducible BAC (Bacterial artificial chromosome) transgenic mouse-line. The BAC with the improved Cre-recombinase (iCre) fused to the modified human estrogen receptor (ER^{T2}) under the Sox10 promoter was randomly inserted into the mouse genome, with 2.2 copies per cell (Simon et al. 2012). The line was crossed with a green fluorescent protein (GFP) reporter line, to visualize the recombination rate (Nakamura 2006).

The Esco2^{fl/fl} line is an inducible conditional knockout mouse working with the Cre-LoxP system (elaborately described in chapter 1.6). Parts of the coding sequence including the start codon of the cell cycle protein Esco2 was flanked with LoxP sites and are therefore cut when the iCre is active. The mouse line had a pure C57BL/6J background. The Sox10 and the eGFP allele were bred homozygous whereas the Esco2 locus was bred heterozygous in order to receive both heterozygous wildtype and knockout mice in the same litter.

In this work, the term Esco2^{wt} refers to the pure Esco2^{wt/wt} genotype, whereas the term Esco2^{fl} refers to both the mixed Esco2^{wt/fl} as well as the pure Esco2^{fl/fl} alleles. This two genotypes were mixed, because both the homozygous and the heterozygous animals showed the same cellular behavior, and were therefore pooled.

6.1.1.2 NG2CreER^{T2}xCAG-eGFPxEsco2^{FL/FL}

This mouse line is also a crossing product of three different mouse lines. The NG2CreER^{T2} is an inducible knockin mouse, where the open reading frame of the CreER^{T2} was inserted into the endogenous NG2 locus (Huang et al. 2014b). This mouse line was crossed with the CAG-eGFP and the Esco2^{fl/fl} as described in 6.1.1.1. To avoid the loss of the NG2 proteoglycan, the NG2 locus was bred heterozygous, the Esco2 locus was bred heterozygous in order to receive both heterozygous wildtype and knockout mice in the same litter. The mouse line had a pure C57BL/6J background.

6.1.2 GENOTYPING

6.1.2.1 DNA ISOLATION

Genomic DNA was isolated using small tail or ear biopsies that were lysed in 500µl lysis buffer at 55°C over night (o.n.) in the shaker and afterwards centrifuged for 5 minutes (min) at 10000 rounds per minute (rpm) at room temperature (RT). The supernatant was transferred

into a new eppendorf tube, the DNA was precipitated with 500µl isopropanol for 5min and pelleted by 10min centrifugation at 10000rpm. The supernatant was removed and the DNA pellet dried at RT. Afterwards the DNA was dissolved in 200µl 10mM Tris-HCL pH8 at 55°C for 2hrs in the shaker and kept at 4°C until further usage.

6.1.2.2 PCR

In order to define the genotype of the mice for a specific locus, a gene specific polymerase chain reaction (PCR) was performed, using the mastermix reactions displayed in Table 3. Primer sequences of the according genes are shown in Table 4. For the NG2CreER^{T2} PCR, two preparations were needed: one mastermix containing the forward and a reverse mutant primer, another one containing the forward and the reverse wildtype primer. After running the gene specific PCR program (cf. Table 5), samples were enriched with 10x loading buffer, separated on a 2% agarose gel and visualized.

Table 3: Mastermix for genotyping PCR.

| Substance | Volume [µl] |
|------------------------|-------------|
| H ₂ O | 11µl |
| Buffer A | 2.5µl |
| MgCl ₂ | 2.5µl |
| Betaine solution | 5µl |
| dNTPs | 0.5µl |
| Forward primer (100mM) | 0.5µl |
| Reverse primer (100mM) | 0.5µl |
| Taq polymerase | 0.5µl |
| DNA | 2µl |
| Total volume | 25µl |

Table 4: Primer sequences for genotyping PCR.

| Gene locus | Direction | Primer sequence | Band size |
|---------------------------------|---------------|-----------------------------------|------------|
| Sox10iCreER^{T2} | forward | 5'-AAACACCCACACCTAGAGAC-3' | 452bp |
| | reverse | 5'-ACCATTTCTGTTGTTTCAGC-3' | |
| NG2CreER^{T2} | forward | 5'-GGCAAACCCAGAGCCCTGCC-3' | WT: 557bp |
| | reverse (WT) | 5'-GCTGGAGCTGACAGCGGGTG-3' | Cre: 829bp |
| | reverse (Cre) | 5'-GCCCCGACCGACGATGAAGC-3' | |
| CAG-eGFP | forward | 5'-CTG CTA ACC ATG TTC ATG CC-3' | 350bp |
| | reverse | 5'-GGT ACA TTG AGC AAC TGA CTG-3' | |
| Esco2 | forward | 5'-ATCTGGGTCCTCATTCTGCACAGC-3' | WT: 279bp |
| | reverse | 5'-GTGCACATACTTATTGACAGGTGG-3' | FL: 347bp |

Table 5: PCR cycle programs for genotyping.

| Sox10iCreER ^{T2} | | NG2CreER ^{T2} | | GFPII-reporter | | Esco2 | |
|---------------------------|-------|------------------------|-------|----------------|-------|---------------|-------|
| Temp. [°C] | Time | Temp. [°C] | Time | Temp. [°C] | Time | Temp. [°C] | Time |
| 94 | 3min | 94 | 3min | 94 | 5min | 94 | 3min |
| 94 | 30sec | 94 | 30sec | 94 | 30sec | 94 | 30sec |
| 52 | 30sec | 64 | 30sec | 55 | 30sec | 60 | 30sec |
| 72 | 1min | 72 | 45sec | 72 | 1min | 72 | 1min |
| 72 | 10min | 72 | 2min | 72 | 10min | 72 | 10min |

6.1.3 TAMOXIFEN ADMINISTRATION

Tamoxifen was diluted in corn oil and 10% EtOH p.a. with a final concentration of 40mg/ml and dissolved by shaking at 37°C for a minimum of 3hrs. 250µl of the tamoxifen solution was applied orally to adult mice (8-10 weeks, ~25g bodyweight) with a gavage needle every second day for a total of three times (10mg or 400mg/kg bodyweight, total of 30mg). For mice with less body weight accordingly less of the tamoxifen solution was applied.

6.1.4 BRDU ADMINISTRATION

In order to achieve long-term labelling of dividing cells, the DNA base analogue 5-Bromo-2'-Deoxy-Uridine (BrdU) was administered via the drinking water. BrdU was dissolved at a concentration of 1mg/ml with addition of 1% sucrose under light protected stirring for 30min at RT. The BrdU solution could be kept in the fridge for 1 week and was refreshed in the drinking bottles every 3rd day.

6.1.5 BEHAVIORAL ASSESSMENT

Standardized behavioral tests were performed to assess the motor phenotype of adult mice. Prior to the data analysis, adult mice (8-12 weeks) were trained for 2 weeks every second day to perform the behavioral tests. During the first week of training, mice received tamoxifen according to the normal protocol described above. After the training period motor behavior was assessed on a weekly basis until the mice were sacrificed at the end of the experiment. Tests were monitored by a digital video camera and afterwards analyzed in slow motion mode in a blinded manner. Statistical analysis of the behavioral experiments was done with the GraphPad Prism 5 software. As the same mice were analyzed multiple times, the repeated-measures ANOVA was used to determine significance. Significant differences were indicated with * for $p < 0.05$, ** for $p < 0.01$ or *** for $p < 0.001$.

6.1.5.1 GRID WALK

Mice were placed in an arena (60x40x18cm) with a grid ground (1cm mash size) elevated 50cm from the ground and could move freely for 2.5min. Total step and misstep numbers

were counted and analyzed. A misstep was counted when the stepping foot slipped through the grid.

6.1.5.2 BEAM CROSSING

Mice had to cross a round wooden beam of 1cm diameter and 70cm in length elevated 20cm from the ground. Mice had to fully cross the beam three times for a successful score (100%). When the mouse fell down, it was rated with 0%.

6.1.5.3 HORIZONTAL LADDER

Mice had to cross a 1m horizontal ladder with different step intervals (1-2cm spacing) elevated 50cm from the ground. In order to prevent the mice from learning, the step pattern was changed weekly. Total step and misstep numbers were counted and analyzed.

6.1.5.4 OPEN FIELD

Mice could run free in a rectangular open field arena (59.5x37x19cm) that was subdivided into 12 equal rectangles (15x15cm) for 4min. The number of crossed fields over the whole period was counted.

6.1.5.5 NOVEL OBJECT RECOGNITION TEST

For the Novel Object Recognition (NOR) test, mice were habituated to the open field arena and the environment for two consecutive days for 5min each. The following day, two similar objects were placed in the arena and during the 5min habituation period, the interaction time of the mice with each object was analyzed. After a 30min interval, one object was replaced by an object that was similar in size but different in shape and colour. During the 5min acquisition period, the interaction time of mice with the object as well as the total distance of travelling was analyzed. The interaction index was calculated by:

$$\text{interaction index} = \frac{\text{interaction new object}}{\text{total interaction time}} \times 100.$$

6.1.6 ANESTHESIA

Prior to perfusion or surgery, mice were anesthetized with either Ketamin/Rompune or Medetomidin/Midazolam/Fentanyl (MMF). Before any further processes, mice were tested for the complete lack of reflexes at the hind-paws or the upper tail.

6.1.6.1 KETAMINE/ROMPUNE

Ketamine/Rompune anesthesia was used for perfusion of the mice (see section 6.1.8). Therefore 1ml ketamin (10%) and 0.25ml xylazine hydrochloride (2%) and was mixed with 2.5ml saline (0.9%). Adult mice with an average weight of 25g received an intraperitoneal (i.p.) injection of 350µl of the anesthetic what was considered to be a lethal overdose.

6.1.6.2 MMF

Medetomidin/Midazolam/Fentanyl (MMF) anesthesia was used to anesthetize mice for surgeries, as previously reported in Sirko et al. 2013. The solution that was i.p. injected contained 0.5mg/kg body weight Medetomidin, 5mg/kg body weight Midazolam and 0.05mg/kg body weight Fentanyl. The injection volume (in μ l) was calculated by the body weight (in g) \times 10 + 20 μ l excess. As the anesthesia needs to be antagonized, the same volume of an antisedate was i.p. injected to wake the animals up containing 2.5mg/kg body weight Atipamezol, 0.5mg/kg body weight Flumazenil and 1.2mg/kg body weight Naloxone.

6.1.7 MODEL OF STAB WOUND INJURY

Surgeries were performed in accordance to the policies of the state of Bavaria under the license numbers 55.2-1-54-2531-144-07 (old) and 55.2-1-54-2532-171-11 (new).

The stab wound injury is a mouse model for an acute traumatic brain injury. To perform a stab wound adult mice (2-3 months old) were deeply anesthetized with MMF (see chapter 6.1.6.2) and the fur was removed from the skull. During the anesthesia the eyes of the mice were protected with a special eye crème. For the operation, mice were placed and fixed in a stereotactic apparatus, the skin was cut open longitudinally and completely detached from the skull. A unilateral small craniotomy (around 2mm in diameter) was performed in the skull at the somatosensory cortex (rostral to the bregma) with a dental driller, without damaging the meninges. The cortical GM was longitudinally cut with a 19 gauge V-Lance™ knife. The cut was about 1.5mm in length and 0.6mm in depth to exclude an injury of the WM. After the surgery the skin lesion was stitched and the animals were woken up from the anesthesia with the antisedate. For pain prevention, the mice received Carprofen (Rimadyl) (4mg/kg body weight) 30min prior to and 24hrs after the surgery.

6.1.8 TRANSCARDIAL PERFUSION

Mice received a lethal dose of ketamine/rompune intraperitoneal (i.p) (see section 6.1.6). Before the clinical death, the thorax of the mice was opened and a needle was inserted into the right ventricle. To open the blood circulation, the left atrium was opened. After a 5min washout of the blood with PBS, mice were perfused for 23min with 4% PFA. After careful preparation of the brains they were postfixed for around 20min in 4% PFA and afterwards cryoprotected in 30% sucrose (in PBS).

6.2 IMMUNOHISTOCHEMISTRY

6.2.1 TISSUE COLLECTION AND SECTIONING

6.2.1.1 BRAINS

After the transcardial perfusion (see chapter 6.1.8) brains were dissected, postfixed for 20min in 4% PFA and cryoprotected in 30% sucrose. For immunohistochemistry whole brains were sectioned (either coronal or sagittal) as 30µm free floating sections at the cryostat. Sections were either directly stained or kept until further usage in storing solution at -20°C.

6.2.1.2 SCIATIC NERVES

After the transcardial perfusion (see chapter 6.1.8) sciatic nerves from both legs were dissected, postfixed for 10min in 4% PFA and cryoprotected in 30% sucrose. Sciatic nerves were cut longitudinally in sections of 20µm thickness and directly mounted on superfrost glass slides. For teased fiber preparation, 0.5cm sciatic nerve samples were teased with forceps and directly mounted on superfrost glass slides. Sections and fibers were stored at -20°C until further processing.

6.2.1.3 SKELETAL MUSCLES

After the transcardial perfusion (see chapter 6.1.8) different skeletal muscles were dissected, directly cryoprotected in 30% sucrose. Muscles pairs from both body sides were cut together longitudinally in sections of 40µm thickness at the cryostat and directly mounted on superfrost glass slides. Sections were stored at -20°C until further processing.

6.2.2 IMMUNOHISTOCHEMICAL STAININGS

Prior to antibody incubation, sections were blocked for 30min in blocking solution. Primary antibodies (for details and final concentrations see Table 6) were incubated over night at 4°C in blocking solution on a shaker. Afterwards sections were washed 3 times in 1x PBS. Secondary antibodies (see Table 7) directed against the host of the primary antibody were all diluted 1:500 in blocking solution and incubated for 2hrs at RT on the shaker. 5min before the end of the incubation time, sections were counterstained with DAPI (1:1000). Sections were properly washed in 1x PBS, mounted on glass slides, dried at RT and embedded with Aqua-Polymount.

In order to allow the antibody directed against BrdU to enter the nucleus, a special treatment prior to the staining was necessary. Sections were incubated for 20min in 0.01M citrate buffer (pH6, 0.05% Tween20) at 96°C, washed with 1x PBS and 10min fixed in 4%PFA. Secondary antibody staining was performed according to the protocol described above.

Table 6: List of primary antibodies.

| Recognized antigen | Host | Dilution | Company |
|---------------------------------------------------------|-----------------------|----------|-----------------------------------------|
| AN2 | Rat | 1:50 | Prof. Trotter (University of Mainz) |
| BrdU | Rat IgG2a | 1:100 | Biozol (OBT0030) |
| CASPR clone K65/35 | Mouse IgG1 | 1:100 | UC Davis/NIH NeuroMab Facility (75-001) |
| CC1 (APC) | Mouse IgG2b | 1:100 | Calbiochem (OP80) |
| CD45 | Rat IgG2b | 1:500 | BD Pharmingen (550539) |
| GFAP | Mouse IgG1 | 1:400 | Sigma-Aldrich (G3893) |
| GFAP | Rabbit | 1:400 | Sigma-Aldrich (G9269) |
| GFP | Chicken | 1:1000 | Aves Lab (GFP-1020) |
| Iba1 | Rabbit | 1:500 | Wako (019-19741) |
| Ki67 | Rabbit | 1:100 | Thermo Fischer (14-5698-82) |
| Ki67 | Rat | 1:250 | eBioscience (RM-9106-S) |
| Kv1.2 clone K14/16 | Mouse IgG2b | 1:100 | UC Davis/NIH NeuroMab Facility 75-008 |
| NeuN | Mouse IgG1 | 1:100 | Millipore (MAB337) |
| NFH | Rabbit | 1:500 | Sigma-Aldrich (N4142) |
| NG2 | Rabbit | 1:500 | Millipore (AB5320) |
| S100β | Mouse | 1:300 | Sigma-Aldrich (S2532) |
| S100 | Rabbit | 1:300 | Sigma-Aldrich (S2644) |
| α-Bungarotoxin A594 conjugated | Bungarus multicinctus | 1:1000 | Invitrogen (B13423) |

Table 7: List of secondary antibodies.

| Antibody | Host | Label | Dilution | Company |
|-------------------------|--------|----------|----------|-----------------------|
| Anti-chicken | Goat | Alexa488 | 1:500 | Invitrogen (A11039) |
| Anti-rat | Goat | Cy3 | 1:500 | Dianova (112-165-167) |
| | Goat | Alexa647 | 1:500 | Invitrogen (A21247) |
| Anti-rabbit | Goat | Alexa647 | 1:500 | Dianova (111-605-144) |
| | Goat | Alexa649 | 1:500 | Dianova (111-495-144) |
| | Donkey | Cy5 | 1:500 | Dianova (711-175-152) |
| | Donkey | Cy3 | 1:500 | Dianova (711-165-152) |
| Anti-mouse | Goat | Alexa647 | 1:500 | Dianova (115-605-006) |
| | Goat | Cy3 | 1:500 | Dianova (115-165-166) |
| Anti-mouse IgG2b | Goat | Alexa647 | 1:500 | Invitrogen (A21241) |

6.2.3 QUANTIFICATIONS AND STATISTICAL ANALYSIS

For the immunohistochemical analysis, Z-stack images of 12-10 μ m were collected with a Zeiss confocal microscope system (LSM710) with the 40x objective. The quantitative analysis was done afterwards using the Fiji or ImageJ cell counter plugin on collapsed stacks. Total cell numbers of single stacks were counted and afterwards calculated in cells/mm². Double-labeling of cells was verified by switching between different channels in the software. For the

quantification, a total of 9 Z-stacks (3 stacks from 3 different sections each) were analyzed per mouse. Group sizes of $n \geq 3$ were used, reflecting the standard of other work published in this field. All data (if not explicitly stated) were displayed as mean \pm standard error of the mean (sem). Statistical analysis was performed with the GraphPad Prism 5 software. As all the cell numbers and other types of quantifications showed a Gaussian distribution, significant differences were determined using the unpaired Student's t-test for two or the One-way ANOVA for more than two groups. Significant differences were indicated with * for $p < 0.05$, ** for $p < 0.01$ or *** for $p < 0.001$.

6.3 TUNEL STAINING

To visualize apoptotic cells in brain section a terminal deoxynucleotidyl transferase dUTP nick end labeling (TUNEL) staining was performed, using an in situ cell death detection kit (Roche). Therefore cells were fixed in 4% PFA, washed properly in 1x PBS and incubated for 2min on ice in permeabilisation solution. After a brief wash a positive control was incubated for 10min at RT in DNaseI solution and properly washed in 1x PBS. Sections were then incubated for 60min at 37°C in label and enzyme solution according to the manufacturer's protocol (solutions provided with the kit). A negative control was incubated without the enzyme solution. After washing the sections immunostainings for co-labeling of TUNEL⁺ cells was performed as described in chapter 6.2.2.

6.4 CRESYL VIOLET STAINING

Free floating sections were mounted on superfrost slides and dried properly at RT. Slides were then hydrated in a decreasing ethanol row (100%, 70%, 50%, 3min each) and then washed for 3min in H₂O. The staining was performed for 20min in cresylviolet staining solution at RT and afterwards washed for 3min in H₂O. After the staining, sections were dehydrated in an increasing alcohol row (50%, 70%, 100%, 3min each), for 3min in 2-propanol and finally for 3min in xylol. After the sections were dried, they were embedded in DCX mounting medium. The staining was visualized under a brightfield microscope.

6.5 MYELIN VISUALIZATION

6.5.1 SUDAN BLACK STAINING

Free floating sections were mounted on superfrost slides and properly dried. Slides were incubated for 10min in Sudan Black staining solution and washed briefly in H₂O. The staining was then differentiated in 70% EtOH, washed in H₂O again and mounted in Aqua-Polymount. The myelin staining was then visualized with the 25x objective of a Zeiss bright field

microscope. The intensity of the gray value was calculated using a Fiji plugin. For each animal 12 fields from six different sections with the same area were analyzed and the average displayed.

6.5.2 ELECTRON MICROSCOPY

6.5.2.1 TISSUE PREPARATION

Animals were deeply anesthetized for perfusion (see chapter 6.1.6.1) and perfused with the Karnovsky fixative. Compared to the normal perfusion, these mice were perfused with higher pressure, using around 50ml of the fixative. Brains were dissected and postfixed for 3hrs at 4°C and then transferred into storing solution, where they were incubated o.n. or kept at 4°C until further processing. Prior to cutting, the brains were washed in washing solution for 4-5hrs, and the somatosensory cortex was cut into 500µm sections at the vibratome. Small pieces of the WM were cut out of the area of interest with a razor blade and underwent osmication. This was done by incubating the tissue for 2hrs on a precooled metal plate (-20°C) under light exclusion in the osmication solution. This step was needed to stabilize lipids that are the main components of myelin. Afterwards the sections were carefully washed in washing solution o.n. at 4°C followed by a dehydration in a graded alcohol row for 20min each (70%, 80%, 90%, 96%, 100% and 100%) and a 30min incubation in propylenoxide in a glass vial. Finally, the sections were incubated o.n. at 4°C in a 1:1 propylenoxide:araldite mixture. Sections were embedded in molds using an araldite epoxy embedding kit (according to the manufacturing protocol) and polymerization was achieved by incubation for 2d at 60°C. In the first 12hrs, the orientation of the embedded tissue was checked and re-oriented if necessary.

6.5.2.2 ULTRATOME SECTIONING

The embedded tissue blocks were first trimmed with a razor blade, and afterwards semi-thin cross-sections of the WM were cut and stained for 1min with toluidine blue to analyze the cutting plane under the light microscope. Ultrathin sections were cut between 80-90nm thickness and as many as possible were placed on a grid and properly dried on a filter paper.

6.5.2.3 CONTRASTING

Ultrathin sections on the grid were incubated on a drop of 4% uranyl acetate for 30min and washed first in 70% MeOH, then in 35% MeOH and afterwards twice in H₂O. After drying the sections they were incubated for 5min on a drop of a lead citrate solution and finally washed in H₂O.

6.5.2.4 PICTURE ACQUISITION AND ANALYSIS OF MYELIN ABBERATIONS

Pictures of different magnifications were randomly taken using a transmission electron microscope (TEM) Libra 120 system from Zeiss. Pictures were analyzed in a blinded manner

by two independent persons (Dr. Leda Dimou and myself) for myelin aberrations. Myelin aberrations included: Myelin outfoldings, vacuolization/degeneration of myelinated axons, myelination of multiple axons and other myelin aberrations.

6.6 BBB CLOSURE ANALYSIS

At the day of analysis, mice were deeply anesthetized and around 100µl of a 3000Da dextran-fluorescein (5mg/ml) was injected into the tail vein. After 30min brains were collected and immediately frozen on dry ice. Brains were cut in sections of 20µm and thoroughly dried. Afterwards the sections were briefly washed in 1x PBS and fixed for 20min in 4% PFA. After washing them properly in 1x PBS, sections were dried and mounted with Aqua Polymount. Leakage of the fluorescent dye into the brain parenchyma was analyzed with the 20x objective of a Zeiss epifluorescent microscope. Contralateral non-lesioned hemispheres served as a negative control.

6.7 DETERMINATION OF THE LESION SIZE

Pictures of the lesioned area were acquired with the 10x objective of a Zeiss epifluorescent microscope using the DAPI channel. The lesion size was determined by measuring the DAPI-free area with a plugin in the Fiji software. For each animal >7 sections were analyzed and the biggest lesion that could be found was used for the quantification.

7 REFERENCES

- Almeida RG, Czopka T, Ffrench-Constant C, Lyons DA (2011) Individual axons regulate the myelinating potential of single oligodendrocytes in vivo. *Development* 138(20):4443–4450
- Alonso G (2005) NG2 proteoglycan-expressing cells of the adult rat brain: possible involvement in the formation of glial scar astrocytes following stab wound. *GLIA* 49(3):318–338. doi: 10.1002/glia.20121
- Arancibia-Carcamo IL, Attwell D (2014) The node of Ranvier in CNS pathology. *Acta Neuropathol* 128(2):161–175. doi: 10.1007/s00401-014-1305-z
- Armstrong RC, Dorn HH, Kufta CV, Friedman E, Dubois-Dalcq ME (1992) Pre-oligodendrocytes from adult human CNS. *J. Neurosci.* 12(4):1538–1547
- Arnett HA, Mason J, Marino M, Suzuki K, Matsushima GK, Ting JP (2001) TNF alpha promotes proliferation of oligodendrocyte progenitors and remyelination. *Nat. Neurosci.* 4(11):1116–1122. doi: 10.1038/nn738
- Azevedo FA, Carvalho LR, Grindberg LT, Farfel JM, Ferretti, Renata, E.L, Leite RE, Filho WJ, Lent R, Herculano-Houzel S (2009) Equal Numbers of Neuronal and Nonneuronal Cells Make the Human Brain an Isometrically Scaled-Up Primate Brain. *The Journal of Comparative* 10(513):532–541. doi: 10.1002/cne.21974
- Babbs CF, Shi R (2013) Subtle paranodal injury slows impulse conduction in a mathematical model of myelinated axons. *PLoS ONE* 8(7):e67767. doi: 10.1371/journal.pone.0067767
- Balderas I, Rodriguez-Ortiz CJ, Bermudez-Rattoni F (2015) Consolidation and reconsolidation of object recognition memory. *Behavioural Brain Research*(285):213–222
- Banerjee S, Bhat MA (2008) Glial ensheathment of peripheral axons in *Drosophila*. *J Neurosci Res* 86(6):1189–1198
- Banerjee S, Pillai AM, Paik R, Li J, Bhat MA (2006) Axonal ensheathment and septate junction formation in the peripheral nervous system of *Drosophila*. *The Journal of Neuroscience* 26(12):3319–3329
- Bardehle S, Krüger M, Buggenthin F, Schwausch J, Ninkovic J, Clevers H, Snippert HJ, Theis FJ, Meyer-Luehmann M, Bechmann I, Dimou L, Götz M (2013) Live imaging of astrocyte responses to acute injury reveals selective juxtavascular proliferation. *Nat Neurosci* 16(5):580–586
- Barres BA (2008) The mystery and magic of glia: a perspective on their roles in health and disease. *Neuron* 60(3):430–440. doi: 10.1016/j.neuron.2008.10.013

- Bartzokis G, Beckson M, Lu PH, Nuechterlein KH, Edwards N, Mintz J (2001) Age-related changes in frontal and temporal lobe volumes in men: a magnetic resonance imaging study. *Arch Gen Psychiatry* 58(5):461–465
- Battefeld A, Tran BT, Gavrilis J, Cooper EC, Kole, Maarten H P (2014) Heteromeric Kv7.2/7.3 channels differentially regulate action potential initiation and conduction in neocortical myelinated axons. *J. Neurosci.* 34(10):3719–3732. doi: 10.1523/JNEUROSCI.4206-13.2014
- Bauer NG, Richter-Landsberg C, Ffrench-Constant C (2009) Role of the oligodendroglial cytoskeleton in differentiation and myelination. *GLIA* 57(16):1691–1705. doi: 10.1002/glia.20885
- Baulmann DC, Ohlmann A, Flügel-Koch C, Goswami S, Cvekl A, Tamm ER (2002) Pax6 heterozygous eyes show defects in chamber angle differentiation that are associated with a wide spectrum of other anterior eye segment abnormalities. *Mechanisms of Development* 118(1-2):3–17
- Baumann N, Pham-Dinh D (2001) Biology of oligodendrocyte and myelin in the mammalian central nervous system. *Physiol Rev* 81(2):871–927
- Bechler ME, Byrne L, Ffrench-Constant C (2015) CNS Myelin Sheath Lengths Are an Intrinsic Property of Oligodendrocytes. *Curr Biol.* doi: 10.1016/j.cub.2015.07.056
- Bengtsson SL, Nagy Z, Skare S, Forsman L, Forssberg H, Ullén F (2005) Extensive piano practicing has regionally specific effects on white matter development. *Nat Neurosci* 8(9):1148–1150. doi: 10.1038/nn1516
- Bercury KK, Macklin WB (2015) Dynamics and mechanisms of CNS myelination. *Dev. Cell* 32(4):447–458. doi: 10.1016/j.devcel.2015.01.016
- Bergles DE, Roberts JD, Somogyi P, Jahr CE (2000) Glutamatergic synapses on oligodendrocyte precursor cells in the hippocampus. *Nature* 405(6783):187–191. doi: 10.1038/35012083
- Bhat MA, Rios JC, Lu Y, Garcia-Fresco GP, Ching W, St. Martin M, Li J, Einheber S, Chesler M, Rosenbluth J, Salzer JL, Bellen HJ (2001) Axon-Glia Interactions and the Domain Organization of Myelinated Axons Requires Neurexin IV/Caspr/Paranodin. *Neuron* 30(2):369–383. doi: 10.1016/S0896-6273(01)00294-X
- Bignami A, Dahl D, Nguyen BT, Crosby CJ (1981) The fate of axonal debris in Wallerian degeneration of rat optic and sciatic nerves: Electron microscopy and immunofluorescence studies with neurofilament antisera. *Journal of Neuropathology & Experimental Neurology* 40(5):537–550
- Binamé F, Sakry D, Dimou L, Jolivel V, Trotter J (2013) NG2 regulates directional migration of oligodendrocyte precursor cells via Rho GTPases and polarity complex proteins. *The Journal of Neuroscience* 33(26):10858–10874

- Birey F, Aguirre A (2015) Age-Dependent Netrin-1 Signaling Regulates NG2+ Glial Cell Spatial Homeostasis in Normal Adult Gray Matter. *J. Neurosci.* 35(17):6946–6951. doi: 10.1523/JNEUROSCI.0356-15.2015
- Bockamp E, Maringer M, Spangenberg C, Fees S, Fraser S, Eshkind L, Oesch F, Zabel B (2002) Of mice and models: improved animal models for biomedical research. *Physiological Genomics* 11(3):115–132
- Boda E, Viganò F, Rosa P, Fumagalli M, Labat-Gest V, Tempia F, Abbracchio MP, Dimou L, Buffo A (2011) The GPR17 receptor in NG2 expressing cells: focus on in vivo cell maturation and participation in acute trauma and chronic damage. *GLIA* 59(12):1958–1973. doi: 10.1002/glia.21237
- Boscia F, D'Avanzo C, Pannaccione A, Secondo A, Casamassa A, Formisano L, Guida N, Sokolow S, Herchuelz A, Annunziato L (2012) Silencing or knocking out the Na(+)/Ca(2+) exchanger-3 (NCX3) impairs oligodendrocyte differentiation. *Cell Death Differ.* 19(4):562–572. doi: 10.1038/cdd.2011.125
- Bradbury EJ, Moon LD, Popat RJ, King R von, Bennett GS, Patel PN, Fawcett JW, McMahon SB (2002) Chondroitinase ABC promotes functional recovery after spinal cord injury. *Nature* 416(6881):636–640
- Brady ST, Witt AS, Kirkpatrick LL, de Waegh, Sylvie M., Readhead C, Tu P, Lee, Virginia M. - Y. (1999) Formation of Compact Myelin Is Required for Maturation of the Axonal Cytoskeleton. *The Journal of Neuroscience* 19(17):7278–7288
- Brill MS, Ninkovic J, Winpenny E, Hodge RD, Ozen I, Yang R, Lepier A, Gascón S, Erdelyi F, Szabo G, Parras C, Guillemot F, Frotscher M, Berninger B, Hevner RF, Raineteau O, Götz M (2009) Adult generation of glutamatergic olfactory bulb interneurons. *Nat Neurosci*(12):1524–1533. doi: 10.1038/nn.2416
- Brinkmann BG, Agarwal A, Sereda MW, Garratt AN, Müller T, Wende H, Stassart RM, Nawaz S, Humml C, Velanac V, Radyushkin K, Goebbels S, Fischer TM, Franklin RJ, Lai C, Ehrenreich H, Birchmeier C, Schwab MH, Nave K (2008) Neuregulin-1/ErbB signaling serves distinct functions in myelination of peripheral and central nervous system. *Neuron* 59(4):581–595
- Brown JM, Xia J, Zhuang B, Cho K, Rogers CJ, Gama CI, Rawat M, Tully SE, Uetani N, Mason DE, Tremblay ML, Peters EC, Habuchi O, Chen DF, Hsieh-Wilson LC (2012) A sulfated carbohydrate epitope inhibits axon regeneration after injury. *Proc. Natl. Acad. Sci. U.S.A.* 109(13):4768–4773. doi: 10.1073/pnas.1121318109
- Buffo A, Vosko MR, Ertürk D, Hamann GF, Jucker M, Rowitch DH, Götz M (2005) Expression pattern of the transcription factor Olig2 in response to brain injuries: Implications for neuronal repair. *PNAS* 120(50):18183–18188

- Burda JE, Sofroniew MV (2014) Reactive Gliosis and the Multicellular Response to CNS Damage and Disease. *Neuron* 81(2):229–248. doi: 10.1016/j.neuron.2013.12.034
- Busch SA, Horn KP, Cuascut FX, Hawthorne AL, Bai L, Miller RH, Silver J (2010) Adult NG2+ cells are permissive to neurite outgrowth and stabilize sensory axons during macrophage-induced axonal dieback after spinal cord injury. *Journal of Neuroscience* 30(1):1–18
- Bush TG, Puvanachandra N, Horner CH, Polito A, Ostenfeld T, Svendsen CN, Mucke L, Johnson MH, Sofroniew MV (1999) Leukocyte infiltration, neuronal degeneration, and neurite outgrowth after ablation of scar forming, reactive astrocytes in adult transgenic mice. *Neuron* 23(2):297–308. doi: 10.1016/S0896-6273(00)80781-3
- Bushong EA, Martone ME, Jones YZ, Ellisman MH (2002) Protoplasmic astrocytes in CA1 radiatum occupy separate anatomical domains. *The Journal of Neuroscience* 22(2):183–192
- Butt AM, Duncan Alan, Hornby MF, Kirvell SL, Hunter A, Levine JM, Berry M (1999) Cells Expressing the NG2 Antigen Contact Nodes of Ranvier in Adult CNS White Matter. *GLIA*:84–91
- Butt AM, Fern RF, Matute C (2014) Neurotransmitter signaling in white matter. *GLIA* 62(11):1762–1779. doi: 10.1002/glia.22674
- Butt AM, Kiff J, Hubbard P, Berry M (2002) Synantocytes: new functions for novel NG2 expressing glia. *Journal of Neurocytology* 31(6/7):551–565. doi: 10.1023/A:1025751900356
- Cai J, Qi Y, Hu X, Tan M, Liu Z, Zhang J, Li Q, Sander M, Qiu M (2005) Generation of oligodendrocyte precursor cells from mouse dorsal spinal cord independent of Nkx6 regulation and Shh signaling. *Neuron* 45(1):41–53. doi: 10.1016/j.neuron.2004.12.028
- Calver AR, Hall AC, Yu W, Walsh FS, Heath JK, Betsholtz C, Richardson WD (1998) Oligodendrocyte Population Dynamics and the Role of PDGF In Vivo. *Neuron* 20(5):869–882. doi: 10.1016/S0896-6273(00)80469-9
- Cassiani-Ingoni R, Coksaygan T, Xue H, Reichert-Scriver SA, Wiendl H, Rao MS, Magnus T (2006) Cytoplasmic translocation of Olig2 in adult glial progenitors marks the generation of reactive astrocytes following autoimmune inflammation. *Exp. Neurol.* 201(2):349–358. doi: 10.1016/j.expneurol.2006.04.030
- Castro R de, Tajrishi R, Claros J, Stallcup WB (2005) Differential responses of spinal axons to transection: influence of the NG2 proteoglycan. *Exp. Neurol.* 192(2):299–309
- Chandler KJ, Chandler RL, Broeckelmann EM, Hou Y, Southard-Smith EM, Mortlock DP (2007) Relevance of BAC transgene copy number in mice: transgene copy number variation across multiple transgenic lines and correlations with transgene integrity and expression. *Mamm Genome* 18(10):693–708. doi: 10.1007/s00335-007-9056-y

- Chang A, Nishiyama A, Peterson J, Prineas J, Trapp BD (2000) NG2-positive oligodendrocyte progenitor cells in adult human brain and multiple sclerosis lesions. *J. Neurosci.* 20(17):6404–6412
- Chari DM, Blakemore WF (2002) Efficient recolonisation of progenitor-depleted areas of the CNS by adult oligodendrocyte progenitor cells. *GLIA* 37(4):307–313
- Chari DM, Crang A, Blakemore WF (2003) Decline in rate of colonization of oligodendrocyte progenitor cell (OPC)-depleted tissue by adult OPCs with age. *Journal of Neuropathology & Experimental Neurology* 62(9):908–916
- Chen J, Magavi, Sanjay S P, Macklis JD (2004) Neurogenesis of corticospinal motor neurons extending spinal projections in adult mice. *Proc. Natl. Acad. Sci. U.S.A.* 101(46):16357–16362. doi: 10.1073/pnas.0406795101
- Cheng C, Zochodne D (2002) In vivo proliferation, migration and phenotypic changes of Schwann cells in the presence of myelinated fibers. *Neuroscience* 115(1):321–329. doi: 10.1016/S0306-4522(02)00291-9
- Chittajallu R, Aguirre A, Gallo V (2004) NG2-positive cells in the mouse white and grey matter display distinct physiological properties. *J Physiol.*(561.1):109–122
- Clark R, Kochanek P (2001) *Brain Injury*. Springer US
- Clarke LE, Young KM, Hamilton NB, Li H, Richardson WD, Attwell D (2012) Properties and fate of oligodendrocyte progenitor cells in the corpus callosum, motor cortex, and piriform cortex of the mouse. *J. Neurosci.* 32(24):8173–8185. doi: 10.1523/JNEUROSCI.0928-12.2012
- Clemente D, Ortega MC, Melero-Jerez C, Castro F de (2013) The effect of glia-glia interactions on oligodendrocyte precursor cell biology during development and in demyelinating diseases. *Front Cell Neurosci* 7:268. doi: 10.3389/fncel.2013.00268
- Corps KN, Roth TL, McGavern DB (2015) Inflammation and neuroprotection in traumatic brain injury. *JAMA Neurol* 72(3):355–362. doi: 10.1001/jamaneurol.2014.3558
- Craner MJ, Lo AC, Black JA, Waxman SG (2003) Abnormal sodium channel distribution in optic nerve axons in a model of inflammatory demyelination. *Brain* 126(Pt 7):1552–1561. doi: 10.1093/brain/awg153
- Cregg JM, DePaul MA, Filous AR, Lang BT, Tran A, Silver J (2014) Functional regeneration beyond the glial scar. *Exp. Neurol.* 253:197–207. doi: 10.1016/j.expneurol.2013.12.024
- Czopka T, Ffrench-Constant C, Lyons DA (2013) Individual oligodendrocytes have only a few hours in which to generate new myelin sheaths in vivo. *Dev. Cell* 25(6):599–609. doi: 10.1016/j.devcel.2013.05.013

- Davalos D, Grutzendler J, Yang G, Kim JV, Zuo Y, Jung S, Littman DR, Dustin ML, Gan W (2005) ATP mediates rapid microglial response to local brain injury in vivo. *Nat Neurosci* 8(6):752–758
- David S, Kroner A (2011) Repertoire of microglial and macrophage responses after spinal cord injury. *Nature Reviews Neuroscience* 12(7). doi: 10.1038/nrn3053
- Dawson M (2003) NG2-expressing glial progenitor cells: an abundant and widespread population of cycling cells in the adult rat CNS. *Molecular and Cellular Neuroscience* 24(2):476–488. doi: 10.1016/S1044-7431(03)00210-0
- De Biase, Lindsay M, Nishiyama A, Bergles DE (2010) Excitability and synaptic communication within the oligodendrocyte lineage. *J. Neurosci.* 30(10):3600–3611. doi: 10.1523/JNEUROSCI.6000-09.2010
- Devaux JJ, Kleopa KA, Cooper EC, Scherer SS (2004) KCNQ2 is a nodal K⁺ channel. *J. Neurosci.* 24(5):1236–1244. doi: 10.1523/JNEUROSCI.4512-03.2004
- Dibaj P, Nadrigny F, Steffens H, Scheller A, Hirrlinger J, Schomburg ED, Neusch C, Kirchhoff F (2010) NO mediates microglial response to acute spinal cord injury under ATP control in vivo. *GLIA* 58(9):1133–1144. doi: 10.1002/glia.20993
- Dimou L, Gallo V (2015) NG2-glia and their functions in the central nervous system. *GLIA*. doi: 10.1002/glia.22859
- Dimou L, Götz M (2014) Glial cells as progenitors and stem cells: new roles in the healthy and diseased brain. *Physiol. Rev.* 94(3):709–737. doi: 10.1152/physrev.00036.2013
- Dimou L, Simon C, Kirchhoff F, Takebayashi H, Götz M (2008) Progeny of Olig2-expressing progenitors in the gray and white matter of the adult mouse cerebral cortex. *J. Neurosci.* 28(41):10434–10442. doi: 10.1523/JNEUROSCI.2831-08.2008
- Doerflinger NH, Macklin WB, Popko B (2003) Inducible site-specific recombination in myelinating cells. *Genesis* 35(1):63–72
- Doetsch F, Garcia-Verdugo JM, Alvarez-Buylla A (1997) Cellular composition and three-dimensional organization of the subventricular germinal zone in the adult mammalian brain. *J. Neurosci.* 17(13):5046–5061
- Du Wu C, Jackson-Lewis V, Vila M, Tieu K, Teismann P, Vadseth C, Choi D, Ischiropoulos H, Przedborski S (2002) Blockade of Microglial Activation Is Neuroprotective in the 1-Methyl-4-Phenyl-1,2,3,6-Tetrahydropyridine Mouse Model of Parkinson Disease. *The Journal of Neuroscience* 22(5):1763–1771
- Edgar JM, McLaughlin M, Werner HB, McCulloch MC, Barrie JA, Brown A, Faichney AB, Snaidero N, Nave K, Griffiths IR (2009) Early ultrastructural defects of axons and axon-glia junctions in mice lacking expression of *Cnp1*. *GLIA* 57(16):1815–1824. doi: 10.1002/glia.20893

- Elliott C, Lindner M, Arthur A, Brennan K, Jarius S, Hussey J, Chan A, Stroet A, Olsson T, Willison H, Barnett SC, Meinl E, Linington C (2012) Functional identification of pathogenic autoantibody responses in patients with multiple sclerosis. *Brain* 135(Pt 6):1819–1833. doi: 10.1093/brain/aws105
- Evans TA, Barkauskas DS, Myers JT, Hare EG, You JQ, Ransohoff RM, Huang AY, Silver J (2014) High-resolution intravital imaging reveals that blood-derived macrophages but not resident microglia facilitate secondary axonal dieback in traumatic spinal cord injury. *Exp. Neurol.* 254:109–120. doi: 10.1016/j.expneurol.2014.01.013
- Faivre-Sarrailh C, Devaux JJ (2013) Neuro-glial interactions at the nodes of Ranvier: implication in health and diseases. *Front. Cell. Neurosci.* 7. doi: 10.3389/fncel.2013.00196
- Farina C, Aloisi F, Meinl E (2007) Astrocytes are active players in cerebral innate immunity. *Trends Immunol* 28(3):138–145. doi: 10.1016/j.it.2007.01.005
- Faulkner JR, Herrmann JE, Woo MJ, Tansey KE, Doan NB, Sofroniew MV (2004) Reactive astrocytes protect tissue and preserve function after spinal cord injury. *J. Neurosci.* 24(9):2143–2155. doi: 10.1523/JNEUROSCI.3547-03.2004
- Ffrench-Constant C, Miller RH, Kruse J, Schachner M, Raff MC (1986) Molecular specialization of astrocyte processes at nodes of Ranvier in rat optic nerve. *J. Cell Biol.* 102(3):844–852
- Ffrench-Constant C, Raff MC (1986) Proliferating bipotential glial progenitor cells in adult rat optic nerve. *Nature* 319(6053):499–502. doi: 10.1038/319499a0
- Ffrench-Constant C (1994) Developmental Timers: How do embryonic cells measure time? *Current Biology* 4(5):415–419. doi: 10.1016/S0960-9822(00)00090-7
- Filipovic R, Zecevic N (2008) The effect of CXCL1 on human fetal oligodendrocyte progenitor cells. *GLIA* 56(1):1–15. doi: 10.1002/glia.20582
- Fröhlich N, Nagy B, Hovhannisyan A, Kukley M (2011) Fate of neuron-glia synapses during proliferation and differentiation of NG2 cells. *J. Anat.* 219(1):18–32. doi: 10.1111/j.1469-7580.2011.01392.x
- Frühbeis C, Fröhlich D, Kuo WP, Amphornrat J, Thilemann S, Saab AS, Kirchhoff F, Möbius W, Goebbels S, Nave K, Schneider A, Simons M, Klugmann M, Trotter J, Krämer-Albers E (2013) Neurotransmitter-triggered transfer of exosomes mediates oligodendrocyte-neuron communication. *PLoS Biol* 11(7):e1001604
- Fulton D, Paez PM, Campagnoni AT (2010) The multiple roles of myelin protein genes during the development of the oligodendrocyte. *ASN NEURO* 2(1):25–37. doi: 10.1042/AN20090051
- Fünfschilling U, Supplie LM, Mahad D, Boretius S, Saab AS, Brinkmann BG, Kassmann CM, Tzvetanova ID, Möbius W, Diaz F, Meijer D, Suter U, Hamprecht B, Sereda MW, Moraes

- CT, Frahm J, Goebbels S, Nave K (2012) Glycolytic oligodendrocytes maintain myelin and long-term axonal integrity. *Nature* 485(7399):517–521
- Gadea A, Schinelli S, Gallo V (2008) Endothelin-1 regulates astrocyte proliferation and reactive gliosis via a JNK/c-Jun signaling pathway. *J. Neurosci.* 28(10):2394–2408. doi: 10.1523/JNEUROSCI.5652-07.2008
- Galtrey CM, Fawcett JW (2007) The role of chondroitin sulfate proteoglycans in regeneration and plasticity in the central nervous system. *Brain Res Rev* 54(1):1–18
- García-Marqués J, Núñez-Llaves R, López-Mascaraque L (2014) NG2-glia from pallial progenitors produce the largest clonal clusters of the brain: time frame of clonal generation in cortex and olfactory bulb. *J. Neurosci.* 34(6):2305–2313. doi: 10.1523/JNEUROSCI.3060-13.2014
- Garwood J, Garcion E, Dobbertin A, Heck, Nicolas, Calco, Valerie, Ffrench-Constant C, Faissner A (2004) The extracellular matrix glycoprotein Tenascin-C is expressed by oligodendrocyte precursor cells and required for the regulation of maturation rate, survival and responsiveness to platelet-derived growth factor. *Eur J Neurosci* 20(10):2524–2540
- Ge W, Yang X, Zhang Z, Wang H, Shen W, Deng Q, Duan S (2006) Long-term potentiation of neuron-glia synapses mediated by Ca^{2+} -permeable AMPA receptors. *Science* 312(5779):1533–1537. doi: 10.1126/science.1124669
- Ge W, Zhou W, Luo Q, Jan LY, Jan YN (2009) Dividing glial cells maintain differentiated properties including complex morphology and functional synapses. *Proc. Natl. Acad. Sci. U.S.A.* 106(1):328–333. doi: 10.1073/pnas.0811353106
- Geha S, Pallud J, Junier M, Devaux B, Leonard N, Chassoux F, Chneiweiss H, Daumas-Duport C, Varlet P (2010) NG2+/Olig2+ cells are the major cycle-related cell population of the adult human normal brain. *Brain Pathol* 20(2):399–411. doi: 10.1111/j.1750-3639.2009.00295.x
- Gensert JM, Greenwood K (1997) Endogenous Progenitors Remyelinate Demyelinated Axons in the Adult CNS. *Neuron*(19):197–203
- Geren BB, Raskind J (1953) Development of the Fine Structure of the Myelin Sheath in Sciatic Nerves of Chick Embryos. *Proc Natl Acad Sci U S A* 39(8):880–884
- Geren BB, Schmitt FO (1954) The structure of the Schwann cell and its relation to the axon in certain invertebrate nerve fibers. *Proc. Natl. Acad. Sci. U.S.A.* 40(9):863
- Gibbs ME, Bowser DN (2010) Astrocytic adrenoceptors and learning: $\alpha 1$ -Adrenoceptors. *Neurochemistry International* 57(4):404–410
- Gibson EM, Purger D, Mount CW, Goldstein AK, Lin GL, Wood LS, Inema I, Miller SE, Bieri G, Zuchero JB, Barres BA, Woo PJ, Vogel H, Monje M (2014) Neuronal Activity Promotes

- Oligodendrogenesis and Adaptive Myelination in the Mammalian Brain. *Science* 344(6183):1252304. doi: 10.1126/science.1252304
- Gliem M, Krammes K, Liaw L, van Rooijen N, Hartung H, Jander S (2015) Macrophage-derived osteopontin induces reactive astrocyte polarization and promotes re-establishment of the blood brain barrier after ischemic stroke. *GLIA*. doi: 10.1002/glia.22885
- Gogate N, Verma L, Zhou JM, Milward E, Rusten R, O'Connor M, Kufta C, Kim J, Hudson L, Dubois-Dalcq M (1994) Plasticity in the adult human oligodendrocyte lineage. *The Journal of Neuroscience* 14(8):4571–4587
- Gowing G, Vallieres L, Julien J (2006) Mouse model for ablation of proliferating microglia in acute CNS injuries. *GLIA* 53(3):331–337. doi: 10.1002/glia.20288
- Grande A, Sumiyoshi K, Lopez-Juarez, Alejandro, Howard J, Sakthivel B, Aronow B, Campbell K, Nakafuku M (2013) Environmental impact on direct neuronal reprogramming in vivo in the adult brain. *Nature Communications*:4:2373
- Greenhalgh AD, David S (2014) Differences in the phagocytic response of microglia and peripheral monocytes after spinal cord injury and its effects on cell death. *Journal of Neuroscience* 34(18):6316–6322
- Greenwood K (2003) Evidence that perinatal and adult NG2-glia are not conventional oligodendrocyte progenitors and do not depend on axons for their survival. *Molecular and Cellular Neuroscience* 23(4):544–558. doi: 10.1016/S1044-7431(03)00176-3
- Griffiths I, Klugmann M, Anderson T, Yool D, Schwab MH, Schneider A, Zimmermann F, McCulloch M, Nadon N, Nave K (1998) Axonal Swellings and Degeneration in Mice Lacking the Major Proteolipid of Myelin. *Science* 280(5369):1610–1613. doi: 10.1126/science.280.5369.1610
- Gu C, Gu Y (2011) Clustering and activity tuning of Kv1 channels in myelinated hippocampal axons. *J Biol Chem*. 286(29):25835–25847
- Guo F, Ma J, McCauley E, Bannerman P, Pleasure D (2009) Early postnatal proteolipid promoter-expressing progenitors produce multilineage cells in vivo. *J. Neurosci*. 29(22):7256–7270. doi: 10.1523/JNEUROSCI.5653-08.2009
- Gupta N, Henry RG, Strober J, Kang S, Lim DA, Bucci M, Caverzasi E, Gaetano L, Mandelli ML, Ryan T, Perry R, Farrell J, Jeremy RJ, Ulman M, Huhn SL, Barkovich AJ, Rowitch DH (2012) Neural stem cell engraftment and myelination in the human brain. *Sci Transl Med* 4(155):155ra137. doi: 10.1126/scitranslmed.3004373
- Gyoneva S, Ransohoff RM (2015) Inflammatory reaction after traumatic brain injury: therapeutic potential of targeting cell-cell communication by chemokines. *Trends Pharmacol Sci* 36(7):471–480. doi: 10.1016/j.tips.2015.04.003

- Haberlandt C, Derouiche A, Wyczynski A, Haseleu J, Pohle J, Karram K, Trotter J, Seifert G, Frotscher M, Steinhäuser C, Jabs R (2011) Gray matter NG2 cells display multiple Ca²⁺-signaling pathways and highly motile processes. *PLoS ONE* 6(3):e17575. doi: 10.1371/journal.pone.0017575
- Halassa MM, Fellin T, Haydon PG (2009) Tripartite synapses: roles for astrocytic purines in the control of synaptic physiology and behavior. *Neuropharmacology* 57(4):343–346. doi: 10.1016/j.neuropharm.2009.06.031
- Hamilton N, Vayro S, Wigley R, Butt AM (2010) Axons and astrocytes release ATP and glutamate to evoke calcium signals in NG2-glia. *GLIA* 58(1):66–79. doi: 10.1002/glia.20902
- Hammerschmidt K, Whelan G, Eichele G, Fischer J (2015) Mice lacking the cerebral cortex develop normal song: insights into the foundations of vocal learning. *Scientific Reports*(5):8808. doi: 10.1038/srep08808
- Hampton DW, Rhodes KE, Zhao C, Franklin R J M, Fawcett JW (2004) The responses of oligodendrocyte precursor cells, astrocytes and microglia to a cortical stab injury, in the brain. *Neuroscience* 127(4):813–820. doi: 10.1016/j.neuroscience.2004.05.028
- Haroutunian V, Katsel P, Roussos P, Davis K, Altshuler L, Bartzokis G (2014) Myelination, Oligodendrocytes, and Serious Mental Illness 62(11):1856–1877
- Hasan KM, Kamali A, Kramer LA, Papnicolaou AC, Fletcher JM, Ewing-Cobbs L (2008) Diffusion tensor quantification of the human midsagittal corpus callosum subdivisions across the lifespan. *Brain Res.* 1227:52–67. doi: 10.1016/j.brainres.2008.06.030
- Hashim E, Rowley CD, Grad S, Bock NA (2015) Patterns of myeloarchitecture in lower limb amputees: an MRI study. *Front Neurosci* 9:15. doi: 10.3389/fnins.2015.00015
- Hayashida Y, Hirai T, Morishita S, Kitajima M, Murakami R, Korogi Y, Makino K, Nakamura H, Ikushima I, Yamura M, Kochi M, Kuratsu J, Yamashita Y (2006) Diffusion-weighted Imaging of Metastatic Brain Tumors: Comparison with Histologic Type and Tumor Cellularity. *American Journal of Neuroradiology* 27(7):1419–1425
- He F, Sun YE (2007) Glial cells more than support cells? *Int. J. Biochem. Cell Biol.* 39(4):661–665. doi: 10.1016/j.biocel.2006.10.022
- Heinrich C, Bergami M, Gascón S, Lepier A, Viganò F, Dimou L, Sutor B, Berninger B, Götz M (2014) Sox2-mediated conversion of NG2 glia into induced neurons in the injured adult cerebral cortex. *Stem Cell Reports* 3(6):1000–1014
- Herculano-Houzel S (2014) The Glia/Neuron Ratio: How it Varies Uniformly Across Brain Structures and Species and What that Means for Brain Physiology and Evolution. *GLIA* 62(9):1377–1391. doi: 10.1002/glia.22683

- HILDEBRAND C, REMAHL S, PERSSON H, BJARTMAR C (1993) Myelinated nerve fibres in the CNS. *Progress in Neurobiology* 40(3):319–384. doi: 10.1016/0301-0082(93)90015-K
- Hill RA, Nishiyama A (2014) NG2 cells (polydendrocytes): listeners to the neural network with diverse properties. *GLIA* 62(8):1195–1210. doi: 10.1002/glia.22664
- Hill RA, Patel KD, Medev J, Reiss AM, Nishiyama A (2013) NG2 Cells in White Matter But Not Gray Matter Proliferate in Response to PDGF. *Journal of Neuroscience* 33(36):14558–14566
- Hines DJ, Hines RM, Mulligan SJ, Macvicar BA (2009) Microglial processes block the spread of damage in the brain and require functional chloride channels. *GLIA* 57(15):1610–1618. doi: 10.1002/glia.20874
- Hinman JD, Peters A, Cabral H, Rosene DL, Hollander W, Rasband MN, Abraham CR (2006) Age-related molecular reorganization at the node of Ranvier. *J Comp Neurol*. 495(4):351–362
- Hohlfeld R, Kerschensteiner M, Meinl E (2007) Dual role of inflammation in CNS disease. *Neurology* 68(22 Suppl 3):S58-63. doi: 10.1212/01.wnl.0000275234.43506.9b
- Honjin R, Sakato S, Yamashita T (1977) Electron microscopy of the mouse optic nerve: a quantitative study of the total optic nerve fibers. *Archivum histologicum Japonicum = Nihon soshikigaku kiroku* 40(4):321–332
- Hou F, Zou H (2005) Two human orthologues of Eco1/Ctf7 acetyltransferases are both required for proper sister-chromatid cohesion. *Molecular Biology of the Cell* 16(8):3908–3918
- Howell OW, Palser A, Polito A, Melrose S, Zonta B, Scheiermann C, Vora AJ, Brophy PJ, Reynolds R (2006) Disruption of neurofascin localization reveals early changes preceding demyelination and remyelination in multiple sclerosis. *Brain* 129(12):3173–3185. doi: 10.1093/brain/awl290
- Howell OW, Rundle JL, Garg A, Komada M, Brophy PJ, Reynolds R (2010) Activated microglia mediate axoglial disruption that contributes to axonal injury in multiple sclerosis. *J Neuropathol Exp Neurol* 69(10):1017–1033. doi: 10.1097/NEN.0b013e3181f3a5b1
- Huang JK, Phillips GR, Roth AD, Pedraza L, Shan W, Belkaid W, Mi S, Fex-Svenningsen A, Florens L, Yates, John R 3rd, Colman DR (2005) Glial membranes at the node of Ranvier prevent neurite outgrowth. *Science* 310(5755):1813–1817. doi: 10.1126/science.1118313
- Huang S, Tang C, Sun S, Cao W, Qi W, Xu J, Huang J, Lu W, Liu Q, Gong B, Zhang Y, Jiang J (2014a) Protective Effect of Electroacupuncture on Neural Myelin Sheaths is Mediated via Promotion of Oligodendrocyte Proliferation and Inhibition of Oligodendrocyte Death After Compressed Spinal Cord Injury. *Mol. Neurobiol.* doi: 10.1007/s12035-014-9022-0

- Huang W, Zhao N, Bai X, Karram K, Trotter J, Goebbels S, Scheller A, Kirchhoff F (2014b) Novel NG2-CreERT2 knock-in mice demonstrate heterogeneous differentiation potential of NG2 glia during development. *GLIA* 62(6):896–913. doi: 10.1002/glia.22648
- Hughes EG, Kang SH, Fukaya M, Bergles DE (2013) Oligodendrocyte progenitors balance growth with self-repulsion to achieve homeostasis in the adult brain. *Nat Neurosci* 16(6):668–676
- Indra AK, Warot X, Brocard J, Bornert JM, Xiao JH, Chambon P, Metzger D (1999) Temporally-controlled site-specific mutagenesis in the basal layer of the epidermis: comparison of the recombinase activity of the tamoxifen-inducible Cre-ER(T) and Cre-ER(T2) recombinases. *Nucleic Acids Res* 27(22):4324–4327
- Irvine K, Blakemore WF (2007) A different regional response by mouse oligodendrocyte progenitor cells (OPCs) to high-dose X-irradiation has consequences for repopulating OPC-depleted normal tissue. *Eur J Neurosci* 25(2):417–424. doi: 10.1111/j.1460-9568.2007.05313.x
- Jahn O, Tenzer S, Werner HB (2009) Myelin proteomics: molecular anatomy of an insulating sheath. *Mol. Neurobiol.* 40(1):55–72. doi: 10.1007/s12035-009-8071-2
- JAISSER F (2000) Inducible Gene Expression and Gene Modification in Transgenic Mice. *Journal of the American Society of Nephrology* 11(suppl 2):S95
- Jensen JM, Shi R (2003) Effects of 4-aminopyridine on stretched mammalian spinal cord: the role of potassium channels in axonal conduction. *J Neurophysiol* 90(4):2334–2340. doi: 10.1152/jn.00868.2002
- Ji K, Tsirka SE (2012) Inflammation modulates expression of laminin in the central nervous system following ischemic injury. *J Neuroinflammation* 9:159. doi: 10.1186/1742-2094-9-159
- Jiang Y, Liu Y, Zhu C, Ma X, Ma L, Zhou L, Huang Q, Cen L, Pi R, Chen X (2015) Minocycline enhances hippocampal memory, neuroplasticity and synapse-associated proteins in aged C57 BL/6 mice. *Neurobiol Learn Mem* 121:20–29. doi: 10.1016/j.nlm.2015.03.003
- John GR, Lee SC, Brosnan CF (2003) Cytokines: powerful regulators of glial cell activation. *Neuroscientist* 9(1):10–22
- Kang SH, Fukaya M, Yang JK, Rothstein JD, Bergles DE (2010) NG2+ CNS Glial Progenitors Remain Committed to the Oligodendrocyte Lineage in Postnatal Life and following Neurodegeneration. *Neuron* 68(4):668–681. doi: 10.1016/j.neuron.2010.09.009
- Kang Z, Wang C, Zepp J, Wu L, Sun K, Zhao J, Chandrasekharan U, DiCorleto PE, Trapp BD, Ransohoff RM, Li X (2013) Act1 mediates IL-17-induced EAE pathogenesis selectively in NG2+ glial cells. *Nat Neurosci* 16(10):1401–1408

- Káradóttir R, Cavelier P, Bergersen LH, Attwell D (2005) NMDA receptors are expressed in oligodendrocytes and activated in ischaemia. *Nature* 438(7071):1162–1166. doi: 10.1038/nature04302
- Káradóttir R, Hamilton NB, Bakiri Y, Attwell D (2008) Spiking and nonspiking classes of oligodendrocyte precursor glia in CNS white matter. *Nat Neurosci* 11(4):450–456. doi: 10.1038/nn2060
- Karram K, Chatterjee N, Trotter J (2005) NG2-expressing cells in the nervous system: role of the proteoglycan in migration and glial-neuron interaction. *J. Anat.* 207(6):735–744
- Kassmann CM, Lappe-Siefke C, Baes M, Brügger B, Mildner A, Werner HB, Natt O, Michaelis T, Prinz M, Frahm J, Nave K (2007) Axonal loss and neuroinflammation caused by peroxisome-deficient oligodendrocytes. *Nature Genetics* 39(8):969–976
- Kerman BE, Kim HJ, Padmanabhan K, Mei A, Georges S, Joens MS, Fitzpatrick, James A J, Jappelli R, Chandross KJ, August P, Gage FH (2015) In vitro myelin formation using embryonic stem cells. *Development* 142(12):2213–2225. doi: 10.1242/dev.116517
- Kerschensteiner M, Meinl E, Hohlfeld Reinhard (2009) Neuro-immune crosstalk in CNS diseases. *Neuroscience* 158(3):1122–1132. doi: 10.1016/j.neuroscience.2008.09.009
- Kessaris N, Fogarty M, Iannarelli P, Grist M, Wegner M, Richardson WD (2006) Competing waves of oligodendrocytes in the forebrain and postnatal elimination of an embryonic lineage. *Nat Neurosci* 9(2):173–179. doi: 10.1038/nn1620
- Kettenmann H, Hanisch U, Noda M, Verkhratsky A (2011) Physiology of microglia. *Physiol. Rev.* 91(2):461–553. doi: 10.1152/physrev.00011.2010
- Kigerl KA, Gensel JC, Ankeny DP, Alexander JK, Donnelly DJ, Popovich PG (2009) Identification of two distinct macrophage subsets with divergent effects causing either neurotoxicity or regeneration in the injured mouse spinal cord. *The Journal of Neuroscience* 29(43):13435–13444. doi: 10.1523/JNEUROSCI.3257-09.2009
- Kim SU, Vellis J de (2005) Microglia in health and disease. *J. Neurosci. Res.* 81(3):302–313. doi: 10.1002/jnr.20562
- Kimelberg HK, Nedergaard M (2010) Functions of astrocytes and their potential as therapeutic targets. *Neurotherapeutics* 7(4):338–353. doi: 10.1016/j.nurt.2010.07.006
- Kimelberg HK (2010) Functions of mature mammalian astrocytes: a current view. *Neuroscientist* 16(1):79–106. doi: 10.1177/1073858409342593
- Koizumi S, Shigemoto-Mogami Y, Nasu-Tada K, Shinozaki Y, Ohsawa K, Tsuda M, Joshi BV, Jacobson KA, Kohsaka S, Inoue K (2007) UDP acting at P2Y₆ receptors is a mediator of microglial phagocytosis. *Nature* 446(7139):1091–1095. doi: 10.1038/nature05704

- Komitova M, Serwanski DR, Lu QR, Nishiyama A (2011) NG2 cells are not a major source of reactive astrocytes after neocortical stab wound injury. *GLIA* 59(5):800–809. doi: 10.1002/glia.21152
- Kondo T, Raff M (2000) Oligodendrocyte Precursor Cells Reprogrammed to Become Multipotential CNS Stem Cells. *Science* 289(5485):1754–1757. doi: 10.1126/science.289.5485.1754
- Kuhlbrodt K, Herbarth B, Sock E, Hermans-Borgmeyer I, Wegner M (1998) Sox10, a novel transcriptional modulator in glial cells. *Journal of Neuroscience* 18(1):237–250
- Kukley M, Capetillo-Zarate E, Dietrich D (2007) Vesicular glutamate release from axons in white matter. *Nat. Neurosci.* 10(3):311–320. doi: 10.1038/nn1850
- Kukley M, Kiladze M, Tognatta R, Hans M, Swandulla D, Schramm J, Dietrich D (2008) Glial cells are born with synapses. *FASEB J.* 22(8):2957–2969. doi: 10.1096/fj.07-090985
- Kukley M, Nishiyama A, Dietrich D (2010) The fate of synaptic input to NG2 glial cells: neurons specifically downregulate transmitter release onto differentiating oligodendroglial cells. *J. Neurosci.* 30(24):8320–8331. doi: 10.1523/JNEUROSCI.0854-10.2010
- Kumar A, Stoica BA, Sabirzhanov B, Bums MP, Faden AI, Loane DJ (2013) Traumatic brain injury in aged animals increases lesion size and chronically alters microglial/macrophage classical and alternative activation states. *Neurobiology of Aging* 34(5):1397–1411. doi: 10.1016/j.neurobiolaging.2012.11.013
- Kwok, Jessica C. F., Dick G, Wang D, Fawcett JW (2011) Extracellular matrix and perineuronal nets in CNS repair. *Dev Neurobiol* 71(11):1073–1089. doi: 10.1002/dneu.20974
- Lalancette-Hébert M, Gowing G, Simard A, Weng YC, Kriz J (2007) Selective ablation of proliferating microglial cells exacerbates ischemic injury in the brain. *J. Neurosci.* 27(10):2596–2605. doi: 10.1523/JNEUROSCI.5360-06.2007
- Lammertse DP, Jones L, Charlifue SB, Kirshblum SC, Apple DF, Ragnarsson KT, Falci SP, Heary RF, Choudhri TF, Jenkins AL, Betz RR, Poonian D, Chthbert JP, Jha A, Snyder DA, Knoller N (2012) Autologous incubated macrophage therapy in acute, complete spinal cord injury: results of the phase 2 randomized controlled multicenter trial. *Spinal Cord* 50(9):661–671
- Lang B, Liu HL, Liu R, Feng GD, Jiao XY, Ju G (2004) Astrocytes in injured adult rat spinal cord may acquire the potential of neural stem cells. *Neuroscience* 128(4):775–783
- Lappe-Siefke C, Goebbels S, Gravel M, Nicksch E, Lee J, Braun PE, Griffiths IR, Nave K (2003) Disruption of *Cnp1* uncouples oligodendroglial functions in axonal support and myelination. *Nature Genetics* 33(3):366–374. doi: 10.1038/ng1095
- Lasiene J, Matsui A, Sawa Y, Wong F, Horner PJ (2009) Age-related myelin dynamics revealed by increased oligodendrogenesis and short internodes. *Aging Cell* 8(2):201–213. doi: 10.1111/j.1474-9726.2009.00462.x

- Lebel C, Gee M, Camicioli R, Wieler M, Martin W, Beaulieu C (2012) Diffusion tensor imaging of white matter tract evolution over the lifespan. *NeuroImage* 60(1):340–352. doi: 10.1016/j.neuroimage.2011.11.094
- Lee S, Leach MK, Redmond SA, Chong SC, Mellon SH, Tuck SJ, Feng Z, Corey JM, Chan JR (2012a) A culture system to study oligodendrocyte myelination processes using engineered nanofibers. *Nat Methods* 9(9):917–922
- Lee Y, Morrison BM, Li Y, Lengacher S, Farah MH, Hoffman PN, Liu Y, Tsingalia A, Jin L, Zhang P, Pellerin L, Magistretti PJ, Rothstein JD (2012b) Oligodendroglia metabolically support axons and contribute to neurodegeneration. *Nature* 487(7408):443–448
- Leong SY, Rao VT, Bin JM, Gris P, Sangaralingam M, Kennedy TE, Antel JP (2014) Heterogeneity of oligodendrocyte progenitor cells in adult human brain. *Annals of Clinical and Translational Neurology* 1(4):272–283
- Leoni G, Rattray M, Fulton D, Rivera A, Butt AM (2014) Immunoablation of cells expressing the NG2 chondroitin sulphate proteoglycan. *J. Anat.* 224(2):216–227. doi: 10.1111/joa.12141
- Levine JM (1994) Increased expression of the NG2 chondroitin-sulfate proteoglycan after brain injury. *Journal of Neuroscience* 14:4716–4730
- Levine JM, Enquist LW, Card P (1998) Reactions of oligodendrocyte precursor cells to alpha herpesvirus infection of the central nervous system. *GLIA* 23(4):316–328
- Levine JM, Reynolds R, Fawcett JW (2001) The oligodendrocyte precursor cell in health and disease. *TRENDS in Neurosciences* 24(1):39–47
- Li J (2015) Molecular regulators of nerve conduction - Lessons from inherited neuropathies and rodent genetic models. *Exp. Neurol.* 267:209–218. doi: 10.1016/j.expneurol.2015.03.009
- Lin S, Bergles DE (2002) Physiological characteristics of NG2-expressing glial cells. *Journal of Neurocytology* 31(6/7):537–549. doi: 10.1023/A:1025799816285
- Lin S, Bergles DE (2004) Synaptic signaling between GABAergic interneurons and oligodendrocyte precursor cells in the hippocampus. *Nat. Neurosci.* 7(1):24–32. doi: 10.1038/nn1162
- Lu P, Woodruff G, Wang Y, Graham L, Hunt M, Di Wu, Boehle E, Ahman R, Poplawski G, Brock J, Goldstein, Lawrence, S.B., Tuszynski MH (2014) Long-distance axonal growth from human induced pluripotent stem cells after spinal cord injury. *Neuron* 83(4):789–796
- Lu Q, Sun T, Zhu Z, Ma N, Garcia M, Stiles CD, Rowitch DH (2002) Common Developmental Requirement for Olig Function Indicates a Motor Neuron/Oligodendrocyte Connection. *Cell* 109(1):75–86. doi: 10.1016/S0092-8674(02)00678-5

- Lundgaard, Iben, Luzhynskaya A, Stockley JH, Wang, Zhen, Evans KA, Swire M, Volbracht K, Gautier HO, Franklin RJ, Ffrench-Constant C, Attwell D, Káradóttir R (2013) Neuregulin and BDNF induce a switch to NMDA receptor-dependent myelination by oligodendrocytes. *PLoS Biol* 11(12):e1001743
- Maas AI, Stocchetti N, Bullock R (2008) Moderate and severe traumatic brain injury in adults. *Lancet Neurology* 7(8):728–741
- Magavi SS, Leavitt BR, Macklis JD (2000) Induction of neurogenesis in the neocortex of adult mice. *Nature* 405(6789):951–955
- Magnus T, Coksaygan T, Korn T, Xue H, Arumugam TV, Mughal MR, Eckley DM, Tang S, Detolla L, Rao MS, Cassiani-Ingoni R, Mattson MP (2007) Evidence that nucleocytoplasmic Olig2 translocation mediates brain-injury-induced differentiation of glial precursors to astrocytes. *J. Neurosci. Res.* 85(10):2126–2137. doi: 10.1002/jnr.21368
- Mainardi M, Pietrasanta M, Vannini E, Rossetto O, Caleo M (2012) Tetanus neurotoxin-induced epilepsy in mouse visual cortex. *Epilepsia* 53(7):e132-6. doi: 10.1111/j.1528-1167.2012.03510.x
- Maldonado PP, Vélez-Fort M, Angulo MC (2011) Is neuronal communication with NG2 cells synaptic or extrasynaptic? *J. Anat.* 219(1):8–17. doi: 10.1111/j.1469-7580.2011.01350.x
- Mangin J, Gallo V (2011) The curious case of NG2 cells: transient trend or game changer? *ASN NEURO* 3(1):e00052. doi: 10.1042/AN20110001
- Mangin J, Li P, Scafidi J, Gallo V (2012) Experience-dependent regulation of NG2 progenitors in the developing barrel cortex. *Nat. Neurosci.* 15(9):1192–1194. doi: 10.1038/nn.3190
- Martinho RG, Guilgur LG, Prudêncio P (2015) How gene expression in fast-proliferating cells keeps pace. *Bioessays* 37(5):514–524. doi: 10.1002/bies.201400195
- Mathey EK, Derfuss T, Storch MK, Williams KR, Hales K, Woolley DR, Al-Hayani A, Davies SN, Rasband MN, Olsson T, Moldenhauer A, Velhin S, Hohlfeld R, Meinl E, Linington C (2007) Neurofascin as a novel target for autoantibody-mediated axonal injury. *J Exp Med* 204(10):2363–2372. doi: 10.1084/jem.20071053
- May D, tress O, Seifert G, Willecke K (2013) Connexin47 protein phosphorylation and stability in oligodendrocytes depend on expression of connexin43 protein in astrocytes. *The Journal of Neuroscience* 33(18):7985–7996
- McCarthy GF, Leblond CP (1988) Radioautographic evidence for slow astrocyte turnover and modest oligodendrocyte production in the corpus callosum of adult mice infused with 3H-thymidine. *J. Comp. Neurol.* 271(4):589–603. doi: 10.1002/cne.902710409
- McGraw J, Hiebert GW, Steeves JD (2001) Modulating astrogliosis after neurotrauma. *J. Neurosci. Res.* 63(2):109–115

- McKenzie IA, Ohayon D, Li H, Paes de Faria, J., Emery B, Tohyama K, Richardson WD (2014) Motor skill learning requires active central myelination. *Science* 346(6207):318–322. doi: 10.1126/science.1254960
- McKeon RJ, Jurynek MJ, Buck CR (1999) The chondroitin sulfate proteoglycans neurocan and phosphacan are expressed by reactive astrocytes in the chronic CNS glial scar. *J. Neurosci.* 19(24):10778–10788
- Menn B, Garcia-Verdugo JM, Yaschine C, Gonzales-Perez O, Rowitch DH, Alvarez-Buylla A (2006) Origin of oligodendrocytes in the subventricular zone of the adult brain. *The Journal of Neuroscience* 26(30):7907–7918
- Mensch S, Baraban M, Alonso G, Czopka T, Ausborn J, El Manira A, Lyons DA (2015) Synaptic vesicle release regulates myelin sheath number of individual oligodendrocytes in vivo. *Nat Neurosci* 18(5):628–632
- Metzger D, Clifford J, Chiba H, Chambon P (1995) Conditional site-specific recombination in mammalian cells using a ligand-dependent chimeric Cre recombinase. *Proc Natl Acad Sci U S A* 92(15):6991–6995
- Minamino M, Ishibashi M, Nakato R, Akiyama K, Tanaka H, Negishi L, Hirota T, Sutani T, Bando, Masashige, Shirahige, Katsuhiko (2015) Esco1 acetylates cohesin via a mechanism different from that of Esco2. *Current Biology*. doi: 10.1016/j.cub.2015.05.017
- Miron VE, Boyd A, Zhao J, Yuen TJ, Ruckh JM, Shadrach JL, van Wijngaarden P, Wagers AJ, Williams A, Franklin, Robin J M, Ffrench-Constant C (2013) M2 microglia and macrophages drive oligodendrocyte differentiation during CNS remyelination. *Nat. Neurosci.* 16(9):1211–1218. doi: 10.1038/nn.3469
- Mitew S, Hay CM, Peckham H, Xiao J, Koenig M, Emery B (2014) MECHANISMS REGULATING THE DEVELOPMENT OF OLIGODENDROCYTES AND CENTRAL NERVOUS SYSTEM MYELIN. *Neuroscience*(276):29–47
- Mongillo G, Barak O, Tsodyks M (2008) Synaptic Theory of Working Memory. *Science* 319(5869):1543–1546. doi: 10.1126/science.1150769
- Moyon S, Dubessy AL, Aigrot MS, Trotter M, Huang JK, Dauphinot L, Potier MC, Kerninon C, Parsadaniantz SM, Franklin RJ, Lubetzki C (2015a) Demyelination causes adult CNS progenitors to revert to an immature state and express immune cues that support their migration. *The Journal of Neuroscience* 35(1):4–20
- Moyon S, Liang J, Casaccia P (2015b) Epigenetics in NG2 glia cells. *Brain Res.* doi: 10.1016/j.brainres.2015.06.009
- Murcia-Belmonte V, Esteban PF, Martinez-Hernandez J, Gruart A, Lujan R, Delgado-Garcia JM, Castro F de (2015) Anosmin-1 over-expression regulates oligodendrocyte precursor cell

- proliferation, migration and myelin sheath thickness. *Brain Struct Funct.* doi: 10.1007/s00429-014-0977-4
- Murray CJ (2015) Global, regional, and national age–sex specific all-cause and cause-specific mortality for 240 causes of death, 1990–2013: a systematic analysis for the Global Burden of Disease Study 2013. *The Lancet* 385(9963):117–171. doi: 10.1016/S0140-6736(14)61682-2
- Murray EA, Richmond BJ (2001) Role of perirhinal cortex in object perception, memory, and associations. *Current Opinion in Neurobiology*(11):188–193
- Nagy A (2000) Cre Recombinase: The Universal Reagent for Genome Tailoring. *Genesis*(26):99–109
- Nakamura T (2006) Neural Crest Cells Retain Multipotential Characteristics in the Developing Valves and Label the Cardiac Conduction System. *Circulation Research* 98(12):1547–1554. doi: 10.1161/01.RES.0000227505.19472.69
- Narciso MS, Hokoc JN, Martinez AM (2001) Watery and dark axons in Wallerian degeneration of the opossum's optic nerve: different patterns of cytoskeletal breakdown? *An Acad Bras Cienc.* 73(2):231–243
- Nave K, Salzer JL (2006) Axonal regulation of myelination by neuregulin 1. *Current Opinion in Neurobiology* 16(5):492–500
- Nave K (2010) Myelination and support of axonal integrity by glia. *Nature* 468(7321):244–252. doi: 10.1038/nature09614
- Nimmerjahn A, Kirchhoff F, Helmchen F (2005) Resting microglial cells are highly dynamic surveillants of brain parenchyma in vivo. *Science* 308(5726):1314–1318. doi: 10.1126/science.1110647
- Nishiyama A, Chang A, Trapp BD (1999) NG2+ glial cells: a novel glial cell population in the adult brain. *J Neuropathol Exp Neurol.* 58(11):1113–1124
- Nishiyama A, Komitova M, Suzuki R, Zhu X (2009) Polydendrocytes (NG2 cells): multifunctional cells with lineage plasticity. *Nat. Rev. Neurosci.* 10(1):9–22. doi: 10.1038/nrn2495
- Nishiyama A, Lin X, Giese N, Heldin C, Stallcup WB (1996) Co-localization of NG2 proteoglycan and PDGF α -receptor on O2A progenitor cells in the developing rat brain. *J. Neurosci. Res.* 43(3):299–314
- Nishiyama A, Watanabe M, Yang Z, Bu J (2002) Identity, distribution, and development of polydendrocytes: NG2-expressing glial cells. *Journal of Neurocytology* 31(6/7):437–455. doi: 10.1023/A:1025783412651
- Nishiyama A, Yu M, Drazba JA, Tuohy VK (1997) Normal and reactive NG2+ glial cells are distinct from resting and activated microglia. *J. Neurosci. Res.* 48(4):299–312

- O'Connor WT, Smyth A, Gilchrist MD (2011) Animal models of traumatic brain injury: A critical evaluation. *Pharmacology and Therapeutics* 130(2):106–113
- Onn I, Heidinger-Pauli JM, Guacci V, Unal E, Koshland D (2008) Sister chromatid cohesion: a simple concept with complex reality. *Annual Reviews in Cell Developmental Biology* 24:105–129
- Ortega F, Gascón S, Masserdotti G, Desphande A, Simon C, Fischer J, Dimou L, Lie DC, Schroeder T, Berninger B (2013) Oligodendroglial and neurogenic adult subependymal zone neural stem cells constitute distinct lineages and exhibit differential responsiveness to Wnt signalling. *Nature Cell Biology* 15(6):602–613
- Parenti R, Cicirata F, Zappalà A, Catania A, La Delia F, Cicirata V, Tress O, Willecke K (2010) Dynamic expression of Cx47 in mouse brain development and in the cuprizone model of myelin plasticity. *GLIA* 58(13):1594–1609
- Park E, Bell JD, Baker AJ (2008) Traumatic brain injury: Can the consequences be stopped? *Canadian Medical Association Journal* 178(9):1163–1170
- Parras C, Hunt C, Sugimori M, Nakafuku M, Rowitch DH, Guillemot F (2007) The proneural gene *Mash1* specifies an early population of telencephalic oligodendrocytes. *The Journal of Neuroscience* 27(16):4233–4242
- Passlick S, Grauer M, Schäfer C, Jabs R, Seifert G, Steinhäuser C (2013) Expression of the $\alpha 2$ -Subunit Distinguishes Synaptic and Extrasynaptic GABA_A Receptors in NG2 Cells of the Hippocampus. *Journal of Neuroscience* 33(29):12030–12040
- Paukert M, Bergles DE (2006) Synaptic communication between neurons and NG2+ cells. *Current Opinion in Neurobiology* 16(5):515–521. doi: 10.1016/j.conb.2006.08.009
- Pekny M, Pekna M (2014) Astrocyte reactivity and reactive astrogliosis: costs and benefits. *Physiol Rev* 94(4):1077–1098. doi: 10.1152/physrev.00041.2013
- PFEIFFER S, WARRINGTON A, BANSAL R (1993) The oligodendrocyte and its many cellular processes. *Trends in Cell Biology* 3(6):191–197. doi: 10.1016/0962-8924(93)90213-K
- Pierpaoli C, Basser PJ (1996) Toward a quantitative assessment of diffusion anisotropy. *Magn. Reson. Med.* 36(6):893–906. doi: 10.1002/mrm.1910360612
- Pineau I, Lacroix S (2009) Endogenous Signals Initiating Inflammation in the Injured Nervous System. *GLIA* 57(4):351–361
- Pineau I, Sun L, Bastien D, Lacroix S (2010) Astrocytes initiate inflammation in the injured mouse spinal cord by promoting the entry of neutrophils and inflammatory monocytes in an IL-1 receptor/MyD88-dependent fashion. *Brain, Behavior, and Immunity* 24(4):540–553. doi: 10.1016/j.bbi.2009.11.007

- Pringle NP, Mudhar HS, Collarini EJ, Richardson WD (1992a) PDGF receptors in the rat CNS: during late neurogenesis, PDGF alphareceptor expression appears to be restricted to glial cells of the oligodendrocyte lineage. *Development* 115:535–551
- Psachoulia K, Jamen F, Young KM, Richardson WD (2009) Cell cycle dynamics of NG2 cells in the postnatal and ageing brain. *Neuron Glia Biol.* 5(3-4):57. doi: 10.1017/S1740925X09990354
- Raff M (2007) Intracellular developmental timers. *Cold Spring Harb Symp Quant Biol* 72:431–435. doi: 10.1101/sqb.2007.72.007
- Raff MC, Miller RH, Noble M (1983) A glial progenitor cell that develops in vitro into an astrocyte or an oligodendrocyte depending on culture medium. *Nature* 303(5916):390–396
- Rahman S, Jones MJ, Jallepalli PV (2015) Cohesin recruits the *esco1* acetyltransferase genome wide to repress transcription and promote cohesion in somatic cells. *PNAS*. doi: 10.1073/pnas.1505323112
- Ramón y Cajal, Santiago (1928) Degeneration and regeneration of the nervous system. Oxford University Press, London
- Rasband MN, Trimmer JS, Schwarz TL, Levinson SR, Ellisman MH, Schachner M, Shrager P (1998) Potassium channel distribution, clustering, and function in remyelinating rat axons. *J. Neurosci.* 18(1):36–47
- Reddy LV, Koirala S, Sugiura Y, Herrera AA, Ko C (2003) Glial Cells Maintain Synaptic Structure and Function and Promote Development of the Neuromuscular Junction In Vivo. *Neuron* 40(3):563–580. doi: 10.1016/S0896-6273(03)00682-2
- Reimer MM, McQueen J, Searcy L, Scullion G, Zonta B, Desmazieres A, Holland PR, Smith J, Gliddon, Catherine, Wood ER, Herzyk P, Brophy PJ, McCulloch J, Horsburgh K (2011) Rapid disruption of axon-glia integrity in response to mild cerebral hypoperfusion. *Journal of Neuroscience* 31(49):18185–18194
- Rhee W, Ray S, Yokoo H, Hoane ME, Lee CC, Mikheev AM, Horner PJ, Rostomily RC (2009) Quantitative analysis of mitotic Olig2 cells in adult human brain and gliomas: implications for glioma histogenesis and biology. *GLIA* 57(5):510–523. doi: 10.1002/glia.20780
- Rhodes KE, Raivich G, Fawcett JW (2006) The injury response of oligodendrocyte precursor cells is induced by platelets, macrophages and inflammation-associated cytokines. *Neuroscience* 140(1):87–100
- Richardson WD, Kessaris N, Pringle N (2006) Oligodendrocyte wars. *Nat. Rev. Neurosci.* 7(1):11–18. doi: 10.1038/nrn1826
- Richardson WD, Young KM, Tripathi RB, McKenzie I (2011) NG2-glia as Multipotent Neural Stem Cells: Fact or Fantasy? *Neuron* 70(4):661–673. doi: 10.1016/j.neuron.2011.05.013

- Rivers LE, Young KM, Rizzi M, Jamen F, Psachoulia K, Wade A, Kessaris N, Richardson WD (2008) PDGFRA/NG2 glia generate myelinating oligodendrocytes and piriform projection neurons in adult mice. *Nat Neurosci* 11(12):1392–1401. doi: 10.1038/nn.2220
- Robel S, Bardehle S, Lepier A, Brakebusch C, Götz M (2011a) Genetic deletion of CDC42 reveals a crucial role for astrocyte recruitment to the injury site in vitro and in vivo. *The Journal of Neuroscience* 31(35):12471–12482. doi: 10.1523/JNEUROSCI.2696-11.2011
- Robel S, Berninger B, Götz M (2011b) The stem cell potential of glia: lessons from reactive gliosis. *Nature Reviews Neuroscience* 12(2):88–104. doi: 10.1038/nrn2978
- Robertis Ed, Gerschenfeld HM, Wald F (1958) Cellular Mechanism of Myelination in the Central Nervous System. *J. Cell Biol.* 4(5):651–658
- Robins SC, Villemain A, Liu X, Djogo T, Kryzskaya D, Storch K, Kokoeva MV (2013) Extensive regenerative plasticity among adult NG2-glia populations is exclusively based on self-renewal. *GLIA* 61(10):1735–1747. doi: 10.1002/glia.22554
- Rodriguez JP, Coulter M, Miotke J, Meyer RL, Takemaru K, Levine JM (2014) Abrogation of β -catenin signaling in oligodendrocyte precursor cells reduces glial scarring and promotes axon regeneration after CNS injury. *J. Neurosci.* 34(31):10285–10297. doi: 10.1523/JNEUROSCI.4915-13.2014
- Rosenbluth J (1987) Abnormal axoglial junctions in the myelin-deficient rat mutant. *Journal of Neurocytology* 16(4):497–509
- Rosenbluth J (1999) A brief history of myelinated nerve fibers: one hundred and fifty years of controversy. *Journal of Neurocytology* 28(4-5):251–262
- Rosenbluth J (2009) Multiple functions of the paranodal junction of myelinated nerve fibers. *J. Neurosci. Res.* 87(15):3250–3258. doi: 10.1002/jnr.22013
- Rothstein JD, Dykes-Hoberg M, Pardo CA, Bristol LA, Jin L, Kuncl RW, Kanai Y, Hediger MA, Wang Y, Schielke JP, Welty DF (1996) Knockout of glutamate transporters reveals a major role for astroglial transport in excitotoxicity and clearance of glutamate. *Neuron* 16(3):675–686. doi: 10.1016/S0896-6273(00)80086-0
- Roussos P, Katsel P, Davis KL, Bitsios P, Giakoumaki SG, Jogia J, Rozsnyai K, Collier D, Frangou S, Siever LJ, Haroutunian V (2012) Molecular and genetic evidence for abnormalities in the nodes of Ranvier in schizophrenia. *JAMA Psychiatry* 69(1):7–15
- Ruckh JM, Zhao J, Shadrach JL, van Wijngaarden P, Rao TN, Wagers AJ, Franklin, Robin J M (2012) Rejuvenation of regeneration in the aging central nervous system. *Cell Stem Cell* 10(1):96–103. doi: 10.1016/j.stem.2011.11.019
- Sahel A, Ortiz FC, Kerninon C, Maldonado PP, Angulo MC, Nait-Oumesmar B (2015) Alteration of synaptic connectivity of oligodendrocyte precursor cells following demyelination. *Front Cell Neurosci* 9:77. doi: 10.3389/fncel.2015.00077

- Sakry D, Neitz A, Singh J, Frischknecht R, Marongiu D, Binamé F, Perera SS, Endres K, Lutz B, Radyushkin K, Trotter J, Mittmann T, Barres BA (2014) Oligodendrocyte Precursor Cells Modulate the Neuronal Network by Activity-Dependent Ectodomain Cleavage of Glial NG2. *PLoS Biol* 12(11):e1001993. doi: 10.1371/journal.pbio.1001993
- Sakry D, Yigit H, Dimou L, Trotter J (2015) Oligodendrocyte Precursor Cells Synthesize Neuromodulatory Factors. *PLoS ONE* 10(5):e0127222. doi: 10.1371/journal.pone.0127222
- Sala S, Agosta F, Pagani E, Copetti M, Comi G, Filippi M (2012) Microstructural changes and atrophy in brain white matter tracts with aging. *Neurobiology of Aging*(33):488–498
- Salzer JL, Brophy PJ, Peles E (2008) Molecular domains of myelinated axons in the peripheral nervous system. *GLIA* 56(14):1532–1540. doi: 10.1002/glia.20750
- Sampaio-Baptista C, Khrapitchev AA, Foxley S, Schlagheck T, Scholz J, Jbabdi S, DeLuca GC, Miller KL, Taylor A, Thomas N, Kleim J, Sibson NR, Bannerman D, Johansen-Berg H (2013) Motor Skill Learning Induces Changes in White Matter Microstructure and Myelination. *Journal of Neuroscience* 33(50):19499–19503. doi: 10.1523/JNEUROSCI.3048-13.2013
- Santambrogio L, Belyanskaya SL, Fischer FR, Cipriani B, Brosnan CF, Ricciardi-Castagnoli P, Stern LJ, Strominger JL, Riese R (2001) Developmental plasticity of CNS microglia. *Proc. Natl. Acad. Sci. U.S.A.* 98(11):6295–6300. doi: 10.1073/pnas.111152498
- Sauer B (2002) Cre7lox: one more step in the timing of the genome. *Endocrine* 19(3):221–227
- Scafidi J, Hammond TR, Scafidi S, Ritter J, Jablonska B, Roncal M, Szigeti-Buck K, Coman D, Huang Y, McCarter RJ, Hyder F, Horvath TL, Gallo V (2013) Intranasal epidermal growth factor treatment rescues neonatal brain injury. *Nature* 506(7487):230–234. doi: 10.1038/nature12880
- Schlegel AA, Rudelson JJ, Tse PU (2012) White matter structure changes as adults learn a second language. *J Cogn Neurosci* 24(8):1664–1670. doi: 10.1162/jocn_a_00240
- Scholz J, Klein MC, Behrens, Timothy E J, Johansen-Berg H (2009) Training induces changes in white-matter architecture. *Nat Neurosci* 12(11):1370–1371. doi: 10.1038/nn.2412
- Shafee R, Buckner RL, Fischl B (2015) Gray matter myelination of 1555 human brains using partial volume corrected MRI images. *NeuroImage* 105:473–485. doi: 10.1016/j.neuroimage.2014.10.054
- Shechter R, Schwartz M (2013) CNS sterile injury: just another wound healing? *Trends in Molecular Medicine* 19(3):135–143
- Shimshek DR, Kim J, Hübner MR, Spergel DJ, Buchholz F, Casanova E, Stewart AF, Seeburg PH, Sprengel R (2002) Codon-improved Cre recombinase (iCre) expression in the mouse. *Genesis* 32(1):19–26

- Silver J, Miller JH (2004) Regeneration beyond the glial scar. *Nature Reviews Neuroscience* 5(2):146–156
- Silver J, Schwab ME, Popovich PG (2014) Central nervous system regenerative failure: Role of oligodendrocytes, astrocytes and microglia. *Cold Spring Harbour Perspectives in Biology* 7(3):a020602
- Simon C, Götz M, Dimou L (2011) Progenitors in the adult cerebral cortex: cell cycle properties and regulation by physiological stimuli and injury. *GLIA* 59(6):869–881. doi: 10.1002/glia.21156
- Simon C, Lickert H, Götz M, Dimou L (2012) Sox10-iCreERT2: A mouse line to inducibly trace the neural crest and oligodendrocyte lineage. *Genesis* 50(6):506–515. doi: 10.1002/dvg.22003
- Sirko S, Behrendt G, Johansson PA, Tripathi P, Costa M, Bek S, Heinrich C, Tiedt S, Colak D, Dichgans M, Fischer IR, Plesnila N, Staufienbiel M, Haass C, Snapyan M, Saghatelian A, Tsai L, Fischer A, Grobe K, Dimou L, Götz M (2013) Reactive glia in the injured brain acquire stem cell properties in response to sonic hedgehog. [corrected]. *Cell Stem Cell* 12(4):426–439. doi: 10.1016/j.stem.2013.01.019
- Snaidero N, Möbius W, Czopka T, Hekking, Liesbeth H P, Mathisen C, Verkleij D, Goebbels S, Edgar J, Merkler D, Lyons DA, Nave K, Simons M (2014) Myelin membrane wrapping of CNS axons by PI(3,4,5)P3-dependent polarized growth at the inner tongue. *Cell* 156(1–2):277–290. doi: 10.1016/j.cell.2013.11.044
- Snaidero N, Simons M (2014) Myelination at a glance. *Journal of Cell Science* 127(Pt 14):2999–3004
- Sobottka B, Ziegler U, Kaech A, Becher B, Goebels N (2011) CNS live imaging reveals a new mechanism of myelination: the liquid croissant model. *GLIA* 59(12):1841–1849. doi: 10.1002/glia.21228
- Sofroniew MV (2009) Molecular dissection of reactive astrogliosis and glial scar formation. *TRENDS in Neurosciences* 32(12):638–647. doi: 10.1016/j.tins.2009.08.002
- Sofroniew MV, Vinters HV (2010) Astrocytes: biology and pathology. *Acta Neuropathol.* 119(1):7–35. doi: 10.1007/s00401-009-0619-8
- Sofroniew MV (2015) Astrocyte barriers to neurotoxic inflammation. *Nat. Rev. Neurosci.* 16(5):249–263. doi: 10.1038/nrn3898
- Somjen GG (1988) Nervenkitz: Notes on the History of the Concept of Neuroglia. *GLIA* 1(1):2–9
- Somkuwar SS, Staples MC, Galinato MH, Fannon MJ, Mandyam CD (2014) Role of NG2 expressing cells in addiction: a new approach for an old problem. *Front Pharmacol* 5:279. doi: 10.3389/fphar.2014.00279

- Stallcup WB, Beasley L (1987) Bipotential glial precursor cells of the optic nerve express the NG2 proteoglycan. *Journal of Neuroscience* 7(9):2737–2744
- Steinhauser C, Kressin K, Kuprijanova E, Weber M, Seifert G (1994) Properties of voltage-activated Na⁺ and K⁺ currents in mouse hippocampal glial cells in situ and after acute isolation from tissue slices. *Pflügers Arch.* 428(5-6):610–620. doi: 10.1007/BF00374585
- STURROCK RR (1980) Myelination of the corpus callosum. *Neuropathol Appl Neurobiol* 6(6):415–420. doi: 10.1111/j.1365-2990.1980.tb00219.x
- Su W, Aloï MS, Garden GA (2015) MicroRNAs mediating CNS inflammation: Small regulators with powerful potential. *Brain, Behavior, and Immunity.* doi: 10.1016/j.bbi.2015.07.003
- Su Z, Yuan Y, Chen J, Zhu Y, Qiu Y, Zhu F, Huang A, He C (2011) Reactive astrocytes inhibit the survival and differentiation of oligodendrocyte precursor cells by secreted TNF- α . *J Neurotrauma* 28(6):1089–1100. doi: 10.1089/neu.2010.1597
- Sun D, Tani M, Newman TA, Krivacic K, Phillips, M., Chernowsky, A., Gill P, Wei T, Griswold KJ, Ransohoff RM, Weller RO (2000) Role of chemokines, neuronal projections, and the blood-brain barrier in the enhancement of cerebral EAE following focal brain damage. *J Neuropathol Exp Neurol.*(59):1031–1043
- Sun W, Dietrich D (2013) Synaptic integration by NG2 cells. *Front Cell Neurosci* 7:255. doi: 10.3389/fncel.2013.00255
- Susarla BT, Villapol S, Yi J, Geller HM, Symes AJ (2014) Temporal patterns of cortical proliferation of glial cell populations after traumatic brain injury in mice. *ASN NEURO* 6(3):e00143
- Susuki K (2013) Node of ranvier disruption as a cause of neurological diseases. *ASN NEURO* 5(3):e00118
- Takebayashi H, Nabeshima Y, Yoshida S, Chisaka O, Ikenaka K, Nabeshima Y (2002) The Basic Helix-Loop-Helix Factor Olig2 Is Essential for the Development of Motoneuron and Oligodendrocyte Lineages. *Current Biology* 12(13):1157–1163. doi: 10.1016/S0960-9822(02)00926-0
- Takeuchi H, Sekiguchi A, Taki Y, Yokoyama S, Yomogida Y, Komuro N, Yamanouchi T, Suzuki S, Kawashima R (2010) Training of Working Memory Impacts Structural Connectivity. *Journal of Neuroscience* 30(9):3297–3303. doi: 10.1523/JNEUROSCI.4611-09.2010
- Tan AM, Zhang W, Levine JM (2005) NG2: a component of the glial scar that inhibits axon growth. *J. Anat.* 207(6):717–725
- Tanaka Y, Tozuka Y, Takata T, Shimazu N, Matsumura N, Ohta A, Hisatsune T (2009) Excitatory GABAergic activation of cortical dividing glial cells. *Cereb. Cortex* 19(9):2181–2195. doi: 10.1093/cercor/bhn238

- Tanimoto N, Muehlfriedel RL, Fischer MD, Fahl E, Humphries P, Biel M, Seelinger M (2009) Vision tests in the mouse: Functional phenotyping with electroretinography. *Frontiers in Bioscience*(14):2730–2737
- Tomassy GS, Berger DR, Chen H, Kasthuri N, Hayworth KJ, Vercelli A, Seung HS, Lichtman JW, Arlotta P (2014) Distinct profiles of myelin distribution along single axons of pyramidal neurons in the neocortex. *Science* 344(6181):319–324. doi: 10.1126/science.1249766
- Tripathi RB, Clarke LE, Burzomato V, Kessar N, Anderson PN, Attwell D, Richardson WD (2011) Dorsally and Ventrally Derived Oligodendrocytes Have Similar Electrical Properties but Myelinate Preferred Tracts. *Journal of Neuroscience* 31(18):6809–6819
- Tripathi RB, Rivers LE, Young KM, Jamen F, Richardson WD (2010) NG2 glia generate new oligodendrocytes but few astrocytes in a murine experimental autoimmune encephalomyelitis model of demyelinating disease. *J. Neurosci.* 30(48):16383–16390. doi: 10.1523/JNEUROSCI.3411-10.2010
- Trotter J, Karram K, Nishiyama A (2010) NG2 cells: properties, progeny and origin. *Brain Res Rev* 63(1-2):72–82
- Uhlmann F, Nasmyth K (1998) Cohesion between sister chromatids must be established during DNA replication. *Current Biology* 8(20):1095–1102. doi: 10.1016/S0960-9822(98)70463-4
- Unal E, Heidinger-Pauli JM, Koshland D (2007) DNA double-strand breaks trigger genome-wide sister-chromatid cohesion through Eco1 (Ctf7). *Science* 317(5835):245–248. doi: 10.1126/science.1140637
- Vallstedt A, Klos JM, Ericson J (2005) Multiple dorsoventral origins of oligodendrocyte generation in the spinal cord and hindbrain. *Neuron* 45(1):55–67. doi: 10.1016/j.neuron.2004.12.026
- Varnum MM, Ikezu T (2012) The classification of microglial activation phenotypes on neurodegeneration and regeneration in Alzheimer's disease brain. *Arch. Immunol. Ther. Exp. (Warsz.)* 60(4):251–266. doi: 10.1007/s00005-012-0181-2
- Vasioukhin V, Degenstein L, Wise B, Fuchs E (1999) The magical touch: Genome targeting in epidermal stem cells induced by tamoxifen application to mouse skin. *Proceedings of the National Academy of Sciences* 96(15):8551–8556. doi: 10.1073/pnas.96.15.8551
- Vega H, Waisfisz Q, Gordillo M, Sakai N, Yanagihara I, Yamada M, van Goslia D, Kayserili H, Xu C, Ozono K, Jabs EW, Inui K, Joenje H (2005) Roberts syndrome is caused by mutations in ESCO3, a human homolog of yeast eco1 that is essential for the establishment of sister chromatid cohesion. *Nature Genetics* 37(5):468–470. doi: 10.1038/ng1548
- Ventura RE, Goldman JE (2006) Telencephalic oligodendrocytes battle it out. *Nat. Neurosci.* 9(2):153–154. doi: 10.1038/nn0206-153

- Viganò F, Schneider S, Cimino M, Bonfanti E, Gelosa P, Sironi L, Abbracchio MP, Dimou L (in press) GPR17 expressing NG2-glia: oligodendrocyte progenitors serving as reserve pool after injury. *GLIA*
- Virchow R (1854) Ueber das ausgebreitete Vorkommen einer dem Nervenmark analogen Substanz in den thierischen Geweben. *Archiv f. pathol. Anat.* 6(4):562–572. doi: 10.1007/BF02116709
- von Streitberg A, Schneider S, Straube C, Buggenthin F, Eichele G, Marr C, Götz M, Dimou L (submitted) Brain injury leads to transient loss of NG2-glia homeostasis
- Voskuhl RR, Peterson RS, Song B, Ao Y, Morales, Laurie Beth J, Tiwari-Woodruff S, Sofroniew MV (2009) Reactive astrocytes form scar-like perivascular barriers to leukocytes during adaptive immune inflammation of the CNS. *J. Neurosci.* 29(37):11511–11522. doi: 10.1523/JNEUROSCI.1514-09.2009
- Wake H, Lee PR, Fields RD (2011) Control of local protein synthesis and initial events in myelination by action potentials. *Science* 333(6049):1647–1651. doi: 10.1126/science.1206998
- Wang A, He BP (2009) Characteristics and functions of NG2 cells in normal brain and neuropathology. *Neurological Research* 31(2):144–150
- Wang H, Kunkel DD, Martin TM, Schwartzkroin PA, Tempel BL (1993a) Heteromeric K⁺ Channels in terminal and juxtaparanodal regions of neurons. *Nature*(365):75–79
- Wang H, Kunkel DD, Martin TM, Schwartzkroin PA, Tempel BL (1993b) Heteromultimeric K⁺ channels in terminal and juxtaparanodal regions of neurons. *Nature* 365(6441):75–79. doi: 10.1038/365075a0
- Wang Y, Gao Z, Zhang Y, Feng S, Liu Y, Shields, Lisa B E, Zhao Y, Zhu Q, Gozal D, Shields CB, Cai J (2015) Attenuated Reactive Gliosis and Enhanced Functional Recovery Following Spinal Cord Injury in Null Mutant Mice of Platelet-Activating Factor Receptor. *Mol. Neurobiol.* doi: 10.1007/s12035-015-9263-6
- Wanner IB, Anderson MA, Song B, Levine J, Fernandez A, Gray-Thompson Z, Ao Y, Sofroniew MV (2013) Glial Scar Borders Are Formed by Newly Proliferated, Elongated Astrocytes That Interact to Corral Inflammatory and Fibrotic Cells via STAT3-Dependent Mechanisms after Spinal Cord Injury. *Journal of Neuroscience* 33(31):12870–12886
- Waxman SG, Ritchie JM (1993) Molecular dissection of the myelinated axon. *Ann Neurol* 33(2):121–136. doi: 10.1002/ana.410330202
- Weisser SB, McLarren KW, Kuroda E, Sly LM (2013) Generation and characterization of murine alternatively activated macrophages. *Methods Mol. Biol.* 946:225–239. doi: 10.1007/978-1-62703-128-8_14

- Welser-Alves JV, Crocker SJ, Milner R (2011) A dual role for microglia in promoting tissue inhibitor of metalloproteinase (TIMP) expression in glial cells in response to neuroinflammatory stimuli. *J Neuroinflammation* 8:61
- Whelan G, Kreidl E, Peters J, Eichele G (2012a) The non-redundant function of cohesin acetyltransferase Esco2. *Nucleus* 3(4):330–334. doi: 10.4161/nucl.20440
- Whelan G, Kreidl E, Wutz G, Egner A, Peters J, Eichele G (2012b) Cohesin acetyltransferase Esco2 is a cell viability factor and is required for cohesion in pericentric heterochromatin. *EMBO J.* 31(1):71–82. doi: 10.1038/emboj.2011.381
- Wigley R, Butt AM (2009) Integration of NG2-glia (synantocytes) into the neuroglial network. *Neuron Glia Biol.* 5(1-2):21–28. doi: 10.1017/S1740925X09990329
- Wigley R, Hamilton N, Nishiyama A, Kirchhoff F, Butt AM (2007) Morphological and physiological interactions of NG2-glia with astrocytes and neurons. *J. Anat.* 210(6):661–670. doi: 10.1111/j.1469-7580.2007.00729.x
- Wilhelmsson U, Bushong EA, Price DL, Smarr BL, van Phung, Terada M, Ellisman MH, Pekny M (2006) Redefining the concept of reactive astrocytes as cells that remain within their unique domains upon reaction to injury. *Proc. Natl. Acad. Sci. U.S.A.* 103(46):17513–17518. doi: 10.1073/pnas.0602841103
- Wilhelmsson U, Li L, Pekna M, Berthold C, Blom S, Eliasson C, Renner O, Bushong EA, Ellisman MH, Morgan TE, Pekny M (2004) Absence of Glial Fibrillary acidic protein and vimentin prevents hypertrophy of astrocytic processes and improves post-traumatic regeneration. *The Journal of Neuroscience* 24(21):5016–5021. doi: 10.1523/JNEUROSCI.0820-04.2004
- Wu H, Xiong WC, Mei L (2010a) To build a synapse: signaling pathways in neuromuscular junction assembly. *Development* 137(7):1017–1033. doi: 10.1242/dev.038711
- Wu J, Yoo S, Wilcock D, Lytle JM, Leung PY, Colton CA, Wrathall JR (2010b) Interaction of NG2+ glial progenitors and microglia/macrophages from the injured spinal cord. *GLIA* 58(4):410–422. doi: 10.1002/glia.20932
- Xiao L, Saiki C, Ide R (2014) Stem cell therapy for central nervous system injuries. glial cells hold the key. *Neural Regen Res* 9(13):1253–1260
- Yamaguchi Y (2000) Lecticans: organizers of the brain extracellular matrix. *Cell Mol Life Sci* 57(2):276–289
- Yamasaki F, Kurisu K, Satoh K, Arita K, Sugiyama K, Ohtaki M, Takaba J, Tominaga A, Hanaya R, Yoshioka H, Hama S, Ito Y, Kajiwara Y, Yahara K, Saito T, Thohar MA (2005) Apparent diffusion coefficient of human brain tumors at MR imaging. *Radiology* 235(3):985–991. doi: 10.1148/radiol.2353031338

- Yates MA, Juraska JM (2007) Increases in size and myelination of the rat corpus callosum during adulthood are maintained into old age. *Brain Res.* 1142:13–18. doi: 10.1016/j.brainres.2007.01.043
- Yeung, Maggie S Y, Zdunek S, Bergmann O, Bernard S, Salehpour M, Alkass K, Perl S, Tisdale J, Possnert G, Brundin L, Druid H, Frisén J (2014) Dynamics of oligodendrocyte generation and myelination in the human brain. *Cell* 159(4):766–774. doi: 10.1016/j.cell.2014.10.011
- Yin X, Crawford TO, Griffin JW, Tu P, Lee, Virginia M. -Y., Li C, Roder J, Trapp BD (1998) Myelin-associated glycoprotein is a myelin signal that modulates the caliber of myelinated axons. *Journal of Neuroscience* 18(6):1953–1962
- Young KM, Psachoulia K, Tripathi RB, Dunn S, Cossell L, Attwell D, Tohyama K, Richardson WD (2013) Oligodendrocyte Dynamics in the Healthy Adult CNS: Evidence for Myelin Remodeling. *Neuron* 77(5):873–885. doi: 10.1016/j.neuron.2013.01.006
- Zahr NM, Rohlfing T, Pfefferbaum A, Sullivan EV (2009) Problem solving, working memory, and motor correlates of association and commissural fiber bundles in normal aging: a quantitative fiber tracking study. *NeuroImage* 44(3):1050–1062. doi: 10.1016/j.neuroimage.2008.09.046
- Zatorre RJ, Fields RD, Johansen-Berg H (2012) Plasticity in gray and white: neuroimaging changes in brain structure during learning. *Nat. Neurosci.* 15(4):528–536. doi: 10.1038/nn.3045
- Zawadzka M, Rivers LE, Fancy SP, Zhao C, Tripathi R, Jamen F, Young K, Goncharevich A, Pohl H, Rizzi M, Rowitch DH, Kessaris N, Suter U, Richardson WD, Franklin RJ (2010) CNS-Resident Glial Progenitor/Stem Cells Produce Schwann Cells as well as Oligodendrocytes during Repair of CNS Demyelination. *Cell Stem Cell* 6(6):578–590. doi: 10.1016/j.stem.2010.04.002
- Zeisel A, Muñoz-Manchado AB, Codeluppi S, Lönnerberg P, La Manno G, Juréus A, Marques S, Munguba H, He L, Betsholtz C, Rolny C, Castelo-Branco G, Hjerling-Leffler J, Linnarsson S (2015) Brain structure. Cell types in the mouse cortex and hippocampus revealed by single-cell RNA-seq. *Science* 347(6226):1138–1142. doi: 10.1126/science.aaa1934
- Zhang Y, Chen K, Sloan SA, Bennett ML, Scholze AR, O’Keefe S, Phatnani Hp, Guarnieri P, Caneda C, Ruderisch N, Deng S, Liddelow sA, Zhang C, Daneman R, Maniatis T, Barres BA, Wu JQ (2014) An RNA-sequencing transcriptome and splicing database of glia, neurons, and vascular cells of the cerebral cortex. *The Journal of Neuroscience* 34(36):11929–11947. doi: 10.1523/JNEUROSCI.1860-14.2014
- Zhao J, Raha-Chowdhury R, Fawcett JW, Watts C (2009) Astrocytes and oligodendrocytes can be generated from NG2+ progenitors after acute brain injury: intracellular localization of

- oligodendrocyte transcription factor 2 is associated with their fate choice. *Eur. J. Neurosci.* 29(9):1853–1869. doi: 10.1111/j.1460-9568.2009.06736.x
- Zhou X, He X, Ren Y (2014) Function of microglia and macrophages in secondary damage after spinal cord injury. *Neural Regen Res* 9(20):1787–1795
- Zhu X, Bergles DE, Nishiyama A (2008) NG2 cells generate both oligodendrocytes and gray matter astrocytes. *Development* 135(1):145–157. doi: 10.1242/dev.004895
- Zhu X, Hill RA, Dietrich D, Komitova M, Suzuki R, Nishiyama A (2011) Age-dependent fate and lineage restriction of single NG2 cells. *Development* 138(4):745–753. doi: 10.1242/dev.047951
- Zukor K, Belin S, Wang C, Keelan N, Wang X, He Z (2013) Short hairpin RNA against PTEN enhances regenerative growth of corticospinal tract axons after spinal cord injury. *Journal of Neuroscience* 33(39):1530–15361

8 ACKNOWLEDGEMENTS

In the end I would like to thank...

Leda Dimou for the opportunity to perform my PhD in her just emerging lab and for the direct supervision of my projects. She guided me through my whole PhD and helped me both technically and conceptually whenever it was necessary. She was not only a good supervisor, but also mentor for personal advice.

Magdalena Götz for giving me the opportunity to be a part of her big group. She provided me with a scientific environment that offered many scientific disciplines and broadened my general knowledge. With her unlimited energy and capacious scientific understanding she is a role model for every emerging scientist. As a member of my TAC she also helped me guiding my project with great scientific discussions and new ideas.

Michael Wegner for being a member of my TAC. He missed no chance to travel to Munich, to support me with useful comments and inspirations that clearly guided and improved my projects.

Konstanze Winklhofer for being an initial member of my TAC. With her different background she gave important input to my projects from another point of view.

The GSN with all the members that helped me through the bureaucratic tangle until the end of my PhD. They gave me a great number of opportunities to attend great courses, provided me with financial support, but also ensured free-time entertainment.

Martin Kerschensteiner for being the 2nd reviewer of my written thesis.

Patrick Küry for being the 3rd reviewer of my written thesis.

Francesca Viganò and Axel von Streitberg for the great discussions about my project including proofreading of manuscripts and the great collaborations with many interesting experiments. But they were additionally the best office colleagues one can imagine, giving mental support whenever it was necessary as well as a lot of chocolate and other sweets in any situation.

Corinna Haupt and Sophia Bardehle for always having an open ear. They always helped me in difficult situations, no matter if scientific or personal.

Detlef Franzen, Gabi Jäger, Carmen Meyer, Ines Mülhahn, Tatiana Simon-Ebert and Manja Thorwirth for the technical assistance. They supported me with their technical experience whenever I needed it.

Michaela for doing so many genotypings for me.

Animal caretakers for taking care all this time of the huge amount of mice I had.

The 'NG2-group' for the scientific discussions and a lot of fun together.

All other people from the institute of physiology for being great colleagues. They were always available for scientific discussions and open to share their expertise. They all participated in making these past years a personally unforgettable time for me.

Steffen Jäkel for mentally supporting me in every moment and being able to stand me during this time. He helped me surviving any difficult situation and in the end helped me in improving this written thesis. Without him I could not have done this.

9 APPENDIX

9.1 SUPPLEMENTARY TABLES

9.1.1 SUPPLEMENTARY TABLES FOR NG2-GLIA ABLATION IN THE HEALTHY BRAIN

Table 8: Absolute numbers of GFP⁺ cells in Esco^{wt} and Esco^{fl} mice in the cerebral GM and WM at different timepoints after induction.

| | GM [cells/mm ²] | | WM [cells/mm ²] | |
|---------------------|-----------------------------|-------|-----------------------------|-------|
| | 1wpi | 16wpi | 1wpi | 16wpi |
| Esco2 ^{wt} | 615.3 | 698.7 | 1985 | 2219 |
| | ± | ± | ± | ± |
| | 12.7 | 15.1 | 18 | 17 |
| Esco2 ^{fl} | 606.5 | 511.9 | 2005 | 1686 |
| | ± | ± | ± | ± |
| | 3.7 | 141.6 | 21 | 114 |

Table 9: Absolute numbers of recombined (GFP⁺) NG2-glia in Esco^{wt} and Esco^{fl} mice in the cerebral GM and WM at different timepoints after induction.

| | GM [cells/mm ²] | | | | WM [cells/mm ²] | | | |
|---------------------|-----------------------------|-------|-------|-------|-----------------------------|-------|-------|-------|
| | 1wpi | 6wpi | 11wpi | 16wpi | 1wpi | 6wpi | 11wpi | 16wpi |
| Esco2 ^{wt} | 174.0 | 180.7 | 140.6 | 151.3 | 197.3 | 140.1 | 114.4 | 113.4 |
| | ± | ± | ± | ± | ± | ± | ± | ± |
| | 3.0 | 1.4 | 2.1 | 6.2 | 14.6 | 13.2 | 17.6 | 7.9 |
| Esco2 ^{fl} | 165.3 | 142.4 | 81.6 | 88.5 | 182.6 | 93.2 | 42.4 | 26.1 |
| | ± | ± | ± | ± | ± | ± | ± | ± |
| | 5.4 | 2.3 | 2.6 | 7.1 | 8.7 | 3.0 | 3.6 | 13.0 |

Table 10: Absolute numbers of total (GFP⁺ and GFP⁻) NG2-glia in Esco^{wt} and Esco^{fl} mice in the cerebral GM and WM at different timepoints after induction.

| | GM [cells/mm ²] | | | | WM [cells/mm ²] | | | |
|---------------------|-----------------------------|-------|-------|-------|-----------------------------|-------|-------|-------|
| | 1wpi | 6wpi | 11wpi | 16wpi | 1wpi | 6wpi | 11wpi | 16wpi |
| Esco2 ^{wt} | 228.8 | 246.6 | 225.9 | 248.5 | 232.2 | 254.8 | 243.5 | 206.4 |
| | ± | ± | ± | ± | ± | ± | ± | ± |
| | 3.1 | 1.2 | 2.0 | 1.1 | 16.1 | 7.8 | 6.4 | 2.9 |
| Esco2 ^{fl} | 221.4 | 241.6 | 232.8 | 244.2 | 219.1 | 251.9 | 239.8 | 232.9 |
| | ± | ± | ± | ± | ± | ± | ± | ± |
| | 6.0 | 0.7 | 4.5 | 3.2 | 5.8 | 17.0 | 10.3 | 18.6 |

Table 11: Forelimb missteps of Esco2^{wt} and Esco2^{fl} mice in the grid walk experiment at different timepoints after induction.

| | 3wpi | 6wpi | 11wpi | 15wpi | 29wpi |
|---------------------|------|------|-------|-------|-------|
| | [%] | [%] | [%] | [%] | [%] |
| Esco2 ^{wt} | 1.8 | 2.3 | 2.4 | 2.6 | 3.6 |
| | ± | ± | ± | ± | ± |
| | 0.1 | 0.1 | 0.3 | 0.2 | 0.4 |
| Esco2 ^{fl} | 1.7 | 5.6 | 8.8 | 9.5 | 13.6 |
| | ± | ± | ± | ± | ± |
| | 0.2 | 0.6 | 0.3 | 0.9 | 0.6 |

Table 12: Hindlimb missteps of *Esco2*^{wt} and *Esco2*^{fl} mice in the grid walk experiment at different timepoints after induction.

| | 3wpi | 6wpi | 11wpi | 15wpi | 29wpi |
|----------------------------|------|------|-------|-------|-------|
| | [%] | [%] | [%] | [%] | [%] |
| <i>Esco2</i> ^{wt} | 0.2 | 0.9 | 3.4 | 3.8 | 6.1 |
| | ± | ± | ± | ± | ± |
| | 0.1 | 0.2 | 0.4 | 0.5 | 0.5 |
| <i>Esco2</i> ^{fl} | 0.4 | 0.5 | 0.9 | 0.6 | 1.8 |
| | ± | ± | ± | ± | ± |
| | 0.2 | 0.2 | 0.2 | 0.3 | 0.1 |

Table 13: Time of *Esco2*^{wt} and *Esco2*^{fl} mice spent on an accelerating rotarod. Time is displayed in seconds [s]. Data are presented as mean±sem.

| | 5wpi | 6wpi | 7wpi | 8wpi | 9wpi | 11wpi | 12wpi |
|----------------------------|-------|-------|-------|-------|-------|-------|-------|
| | [ms] | [ms] | [ms] | [ms] | [ms] | [ms] | [ms] |
| <i>Esco2</i> ^{wt} | 214.3 | 209.0 | 187.7 | 249.7 | 263.0 | 279.7 | 261.0 |
| | ± | ± | ± | ± | ± | ± | ± |
| | 26.6 | 8.2 | 19.7 | 21.8 | 14.6 | 24.2 | 18.0 |
| <i>Esco2</i> ^{fl} | 130.3 | 136.3 | 151.3 | 171.7 | 179.7 | 185.7 | 176.0 |
| | ± | ± | ± | ± | ± | ± | ± |
| | 13.1 | 24.9 | 53.2 | 37.6 | 24.2 | 11.5 | 21.1 |

Table 14: Absolute numbers of recombined (GFP⁺) NG2-glia in NG2-*Esco2*^{wt} and NG2-*Esco2*^{fl} mice in the cerebral GM and WM at different timepoints after induction.

| | GM [cells/mm ²] | | WM [cells/mm ²] | |
|---------------------------------|-----------------------------|------|-----------------------------|------|
| | 1wpi | 1ypi | 1wpi | 6wpi |
| NG2- <i>Esco2</i> ^{wt} | 100.8 | | 113.6 | |
| | ± | - | ± | - |
| | 2.4 | - | 5.0 | - |
| NG2- <i>Esco2</i> ^{fl} | 94.7 | 46.7 | 109.9 | 21.0 |
| | ± | ± | ± | ± |
| | 6.3 | 5.9 | 6.7 | 6.1 |

Table 15: Absolute numbers of total (GFP⁺ and GFP⁻) NG2-glia in NG2-*Esco2*^{wt} and NG2-*Esco2*^{fl} mice in the cerebral GM and WM at different timepoints after induction.

| | GM [cells/mm ²] | | WM [cells/mm ²] | |
|---------------------------------|-----------------------------|-------|-----------------------------|-------|
| | 1wpi | 1ypi | 1wpi | 6wpi |
| NG2- <i>Esco2</i> ^{wt} | 215.4 | | 231.0 | |
| | ± | - | ± | - |
| | 2.9 | - | 6.7 | - |
| NG2- <i>Esco2</i> ^{fl} | 233.2 | 220.0 | 242.2 | 206.8 |
| | ± | ± | ± | ± |
| | 3.4 | 1.2 | 9.3 | 5.1 |

Table 16: Forelimb missteps of NG2-Esco2^{fl} mice in the grid walk experiment at different timepoints after induction.

| | 3wpi | 15wpi | 32wpi | 40wpi | 50wpi |
|-------------------------|-----------------|-----------------|-----------------|-----------------|-----------------|
| | [%] | [%] | [%] | [%] | [%] |
| NG2-Esco2 ^{fl} | 2.2 ± 0.2 | 3.2 ± 0.1 | 5.5 ± 0.6 | 7.7 ± 0.7 | 8.4 ± 0.6 |

Table 17: Forelimb missteps of NG2-control mice in the grid walk experiment at different timepoints after induction.

| | 3wpi | 8wpi | 15wpi |
|-------------|-----------------|-----------------|-----------------|
| | [%] | [%] | [%] |
| NG2-control | 2.5 ± 0.3 | 2.4 ± 0.2 | 2.6 ± 0.5 |

Table 18: Latencies of conduction velocities in Esco^{wt} and Esco^{fl} mice. Latencies from the stimulating to the recording electrodes are displayed in milliseconds [ms]. Data are presented as mean±sem.

| | S1 | S2 | S3 | S4 | S5 | S6 | S7 | S8 | S9 | S10 | S11 |
|--------------------|--------------------|--------------------|--------------------|--------------------|---------------------|--------------------|--------------------|--------------------|-------------------|---------------------|-------------------|
| | [ms] | [ms] | [ms] | [ms] | [ms] | [ms] | [ms] | [ms] | [ms] | [ms] | [ms] |
| Esco ^{wt} | 1.468 ± 0.03 | 1.415 ± 0.03 | 1.473 ± 0.04 | 1.443 ± 0.01 | 1.443 ± 0.006 | 1.445 ± 0.01 | 1.44 ± 0.01 | 1.435 ± 0.01 | 1.44 ± 0.01 | 1.430 ± 0.005 | 1.433 ± 0.1 |
| Esco ^{fl} | 1.305 ± 0.05 | 1.415 ± 0.06 | 1.485 ± 0.03 | 1.408 ± 0.03 | 1.453 ± 0.01 | 1.528 ± 0.05 | 1.543 ± 0.05 | 1.675 ± 0.1 | 1.643 ± 0.1 | 1.688 ± 0.1 | 1.740 ± 0.1 |

9.1.2 SUPPLEMENTARY TABLES FOR NG2-GLIA ABLATION IN THE INJURED BRAIN

Table 19: Absolute numbers of GFP⁺ cells in Esco^{wt} and Esco^{fl} mice in close proximity to the lesion site at different timepoints after the lesion.

| | control | 2dpi | 4dpi | 7dpi | 14dpi |
|---------------------|--------------------------|--------------------------|--------------------------|--------------------------|--------------------------|
| | [cells/mm ²] | [cells/mm ²] | [cells/mm ²] | [cells/mm ²] | [cells/mm ²] |
| Esco2 ^{wt} | 615.3 ± 12.7 | 677.4 ± 8.9 | 836.1 ± 27.3 | 869.1 ± 9.1 | 598.5 ± 13.1 |
| Esco2 ^{fl} | 606.5 ± 3.7 | 616.2 ± 26.3 | 597.9 ± 17.1 | 373.1 ± 23.0 | 299.5 ± 47.9 |

Table 20: Absolute numbers of recombined (GFP⁺) NG2-glia in Esco^{wt} and Esco^{fl} mice in close proximity to the lesion site at different timepoints after the lesion.

| | control | 2dpl | 4dpl | 7dpl | 14dpl |
|--------------------|--------------------------|--------------------------|--------------------------|--------------------------|--------------------------|
| | [cells/mm ²] | [cells/mm ²] | [cells/mm ²] | [cells/mm ²] | [cells/mm ²] |
| Esco ^{wt} | 197.3 | 151.5 | 150.0 | 205.4 | 192.0 |
| | ± | ± | ± | ± | ± |
| | 9.9 | 2.4 | 2.0 | 8.7 | 8.0 |
| Esco ^{fl} | 182.6 | 112.2 | 74.1 | 60.73 | 12.9 |
| | ± | ± | ± | ± | ± |
| | 8.8 | 1.1 | 2.6 | 5.0 | 3.6 |

Table 21: Absolute numbers total (GFP⁺ and GFP⁻) NG2-glia in Esco^{wt} and Esco^{fl} mice in the bigger surrounding of the lesion site at different timepoints after the lesion.

| | control | 2dpl | 4dpl | 7dpl | 14dpl |
|--------------------|--------------------------|--------------------------|--------------------------|--------------------------|--------------------------|
| | [cells/mm ²] | [cells/mm ²] | [cells/mm ²] | [cells/mm ²] | [cells/mm ²] |
| Esco ^{wt} | 232.2 | 203.2 | 213.2 | 317.1 | 311.4 |
| | ± | ± | ± | ± | ± |
| | 16.1 | 4.0 | 4.2 | 7.3 | 2.4 |
| Esco ^{fl} | 219.1 | 168.3 | 146.1 | 207.7 | 270.0 |
| | ± | ± | ± | ± | ± |
| | 5.8 | 1.1 | 3.1 | 2.3 | 1.3 |

Table 22: Absolute numbers of recombined (GFP⁺) NG2-glia in Esco^{wt} and Esco^{fl} mice in the lesion core at different timepoints after the lesion.

| | control | 2dpl | 4dpl | 7dpl | 14dpl |
|--------------------|--------------------------|--------------------------|--------------------------|--------------------------|--------------------------|
| | [cells/mm ²] | [cells/mm ²] | [cells/mm ²] | [cells/mm ²] | [cells/mm ²] |
| Esco ^{wt} | 177.8 | 224.0 | 449.8 | 284.4 | 211.6 |
| | ± | ± | ± | ± | ± |
| | 7.8 | 8.2 | 12.8 | 17.0 | 4.8 |
| Esco ^{fl} | 177.0 | 190.2 | 133.3 | 67.6 | 16.0 |
| | ± | ± | ± | ± | ± |
| | 1.8 | 4.7 | 10.7 | 3.6 | 6.2 |

Table 23: Absolute numbers total (GFP⁺ and GFP⁻) NG2-glia in Esco^{wt} and Esco^{fl} mice in the lesion core at different timepoints after the lesion.

| | control | 2dpl | 4dpl | 7dpl | 14dpl |
|--------------------|--------------------------|--------------------------|--------------------------|--------------------------|--------------------------|
| | [cells/mm ²] | [cells/mm ²] | [cells/mm ²] | [cells/mm ²] | [cells/mm ²] |
| Esco ^{wt} | 227.6 | 300.4 | 616.9 | 455.1 | 332.4 |
| | ± | ± | ± | ± | ± |
| | 4.7 | 4.7 | 12.4 | 26.6 | 7.8 |
| Esco ^{fl} | 232.9 | 270.2 | 275.6 | 240.0 | 298.7 |
| | ± | ± | ± | ± | ± |
| | 6.4 | 7.8 | 19.8 | 11.1 | 12.3 |

Table 24: Absolute numbers of Iba1⁺ microglia in Esco^{wt} and Esco^{fl} mice in the bigger surrounding of the lesion site at different timepoints after the lesion.

| | control | 2dpl | 4dpl | 7dpl |
|---------------------|--------------------------|--------------------------|--------------------------|--------------------------|
| | [cells/mm ²] | [cells/mm ²] | [cells/mm ²] | [cells/mm ²] |
| Esco2 ^{wt} | 329.8 | 604.7 | 1285 | 951.4 |
| | ± | ± | ± | ± |
| | 2.1 | 51.9 | 75.8 | 4.5 |
| Esco2 ^{fl} | 339.6 | 518.9 | 977.1 | 876.7 |
| | ± | ± | ± | ± |
| | 4.7 | 24.5 | 29.6 | 53.3 |

Table 25: Absolute numbers of Iba1⁺CD45⁺ activated microglia in Esco^{wt} and Esco^{fl} mice in the bigger surrounding of the lesion site at different timepoints after the lesion.

| | control | 2dpl | 4dpl | 7dpl |
|---------------------|--------------------------|--------------------------|--------------------------|--------------------------|
| | [cells/mm ²] | [cells/mm ²] | [cells/mm ²] | [cells/mm ²] |
| Esco2 ^{wt} | 8.9 | 184.4 | 86.0 | 35.5 |
| | ± | ± | ± | ± |
| | 2.3 | 10.2 | 39 | 5.4 |
| Esco2 ^{fl} | 6.2 | 131.2 | 297.0 | 241.2 |
| | ± | ± | ± | ± |
| | 1.8 | 17.3 | 68.5 | 9.4 |

Table 26: Absolute numbers of CD45⁺ invading macrophages in Esco^{wt} and Esco^{fl} mice in the bigger surrounding of the lesion site at different timepoints after the lesion.

| | control | 2dpl | 4dpl | 7dpl |
|---------------------|--------------------------|--------------------------|--------------------------|--------------------------|
| | [cells/mm ²] | [cells/mm ²] | [cells/mm ²] | [cells/mm ²] |
| Esco2 ^{wt} | 5.3 | 159.2 | 183.5 | 54.1 |
| | ± | ± | ± | ± |
| | 1.5 | 25.2 | 1.5 | 5.8 |
| Esco2 ^{fl} | 7.1 | 169.3 | 438.0 | 281.1 |
| | ± | ± | ± | ± |
| | 4.4 | 8.9 | 57.7 | 39.5 |

Table 27: Absolute numbers of the total astrocyte (S100β⁺) and the reactive astrocyte (S100β⁺GFAP⁺) population in Esco^{wt} and Esco^{fl} mice in the bigger surrounding of the lesion site at different timepoints after the lesion.

| | Esco2 ^{wt} | | Esco2 ^{fl} | |
|---------|--------------------------|--------------------------------------|--------------------------|--------------------------------------|
| | S100β ⁺ | S100β ⁺ GFAP ⁺ | S100β ⁺ | S100β ⁺ GFAP ⁺ |
| | [cells/mm ²] | [cells/mm ²] | [cells/mm ²] | [cells/mm ²] |
| control | 462.8 | 113.5 | 449.5 | 78.9 |
| | ± | ± | ± | ± |
| | 3.1 | 33.1 | 16.2 | 14.2 |
| 4dpl | 512.7 | 418.5 | 381. | 220.8 |
| | ± | ± | ± | ± |
| | 17.1 | 20.5 | 7.0 | 12.8 |
| 7dpl | 739.2 | 660.7 | 594.6 | 458.1 |
| | ± | ± | ± | ± |
| | 11.8 | 5.9 | 7.9 | 10.2 |

9.2 ABBREVIATIONS

| | |
|----------------------|-----------------------------------------------------------------|
| AEP | Anterior entopeduncular region |
| AMPA | α -amino-3-hydroxy-5-methyl-4-isoxazolepropionic acid |
| APC (CC1) | Adenomatosis polyposis coli |
| APP | Amyloid precursor protein |
| AraC | Cytosine-D-arabinofuranoside |
| ATP | Adenosine triphosphate |
| BAC | Bacterial artificial chromosome |
| BBB | Blood brain barrier |
| BMDM | Bone marrow-derived macrophage |
| BMP | Bone morphogenic protein |
| BrdU | 5'-bromo-desoxyuridine |
| CASPR | Contactin-associated protein |
| Kv1.2 | Potassium voltage-gated channel subfamily A member 2 |
| CC1 | See APC |
| CCI | Controlled cortical impact |
| CCL2 | Chemokine (C-C motif) ligand 2 |
| CD45 | Cluster of differentiation 45 |
| CD68 | Cluster of differentiation 45, microsialin |
| CGE | Caudal ganglionic eminence |
| CNPase | 2',3'-cyclic nucleotide 3'-phosphodiesterase |
| CNS | Central nervous system |
| CSPG | Chondroitin sulfate proteoglycan |
| d | Day |
| DAPI | 4',6'-diamidino-2-phenylindole |
| dpi | Days post induction |
| dpl | Days post lesion |
| DNA | Desoxyribonucleic acid |
| DT | Diphtheria toxin |
| E | Embryonic day |
| EAE | Experimental autoimmune encephalitis |
| ECM | Extracellular matrix |
| EdU | 5'-ethynyl-desoxyuridine |
| e.g. | Exempli gratia |
| EM | Electron microscopy |
| ER | Estrogen receptor |
| Esco2 | Establishment of cohesion 1 homolog 2 |
| FA | Fractional anisotropy |
| fMRI | Functional magnetic resonance imaging |
| g | Gram |
| GABA | Gamma-aminobutyric acid |
| GFAP | Glial fibrillary acidic protein |
| GFP | Green fluorescent protein |
| GM | Gray matter |
| Gp | Guinea pig |
| GPR17 | G-protein coupled receptor 17 |
| GSTn | Glutathione-S-transferase n |
| hrs | Hours |
| Iba1 | Induction of brown adipocytes 1 |
| iCreER ^{T2} | Improved Cre recombinase fused to a truncated estrogen receptor |
| IL | Interleukine |
| INF γ | Interferone gamma |
| iNOS | Inducible nitric oxide synthase |

| | |
|----------------|------------------------------------------------------------------------|
| i.p. | intraperitoneal |
| kg | Kilogram |
| LCA | Leucocyte common antigen |
| LGE | Lateral ganglionic eminence |
| LoxP | Locus of crossover phage |
| LTP | Long-term potentiation |
| M | Molar |
| m | Mouse |
| MAG | Myelin-associated glycoprotein |
| Mash1 | Mammalian achaete scute homolog-1 |
| MBP | Myelin basic protein |
| mg | Milligram |
| MGE | Medial ganglionic eminence |
| min | Minute |
| mm | Millimeter |
| MMF | Medetomidin/Midazolam/Fentanyl |
| MS | Multiple sclerosis |
| NeuN | Neuronal nuclear antigen |
| NG2 | Neuron-glia antigen 2 |
| NMDA | N-methyl-D-aspartate |
| NMJ | Neuromuscular junction |
| NOR | Novel object recognition |
| NSC | Neural stem cell |
| NTN1 | Netrin 1 |
| OHT | 4'-hydroxy-tamoxifen |
| o.n. | Over night |
| OLIG2 | Oligodendrocyte transcription factor 2 |
| OPC | Oligodendrocyte progenitor cell |
| Pax6 | Paired box 6 |
| PCR | Polymerase chain reaction |
| PDGFR α | Platelet-derived growth factor α receptor |
| PFA | Paraformaldehyde |
| Plp | Proteolipid protein |
| pMN | Precursor motoneuron |
| PNS | Peripheral nervous system |
| PTEN | Phosphatase and tensin homolog |
| PTGDS | Prostaglandin D2 Synthase |
| Rb | Rabbit |
| rpm | Rounds per minute |
| Rt | Rat |
| RT | Room temperature |
| s.c. | Subcutan |
| S100 β | S100 calcium binding protein β |
| SEM | Standard error of the mean |
| SCI | Spinal cord injury |
| SHH | Sonic Hedgehog |
| Sox | SRY (sex determining region Y)-related high mobility group box protein |
| SVZ | Subventricular zone |
| SWI | Stab wound injury |
| TAM | Tamoxifen |
| TAP | Transient amplifying progenitor |
| TBI | Traumatic brain injury |
| TIMP 1 | Tissue inhibitor of metalloproteinase 1 |

| | |
|--------------|-------------------------------------|
| TGF α | Transforming growth factor α |
| TNF α | Tumor necrosis factor α |
| VEGF | Vascular endothelial growth factor |
| WM | White matter |
| Wt | Wildtype |
| wpi | Weeks post induction |
| wpl | Weeks post lesion |
| μ m | Micrometer |

9.3 LIST OF FIGURES

| | |
|---------------------------------------------------------------------------------------------------------------------|----|
| Figure 1: Cell types in the adult central nervous system (CNS) | 1 |
| Figure 2: Waves of oligodendrocyte progenitor cells (OPCs) in the developing brain | 3 |
| Figure 3: Oligodendrocyte lineage during differentiation | 4 |
| Figure 4: Lineage specificity of NG2-glia in health and disease | 6 |
| Figure 5: Heterogeneity of NG2-glia between gray and white matter | 11 |
| Figure 6: Neuronal activity and motor learning influences myelin plasticity | 17 |
| Figure 7: Stages and time line of different cellular responses after acute brain injury | 20 |
| Figure 8: Heterogeneous reaction of NG2-glia after cortical stab wound injury | 23 |
| Figure 9: Genetic ablation of proliferating NG2-glia in the adult brain | 31 |
| Figure 10: NG2-glia ablation in different cerebral areas | 32 |
| Figure 11: Long term analysis of recombined NG2-glia | 34 |
| Figure 12: Proliferating NG2-glia in the cortical GM and WM | 35 |
| Figure 13: Reaction of other cell types in the cortical gray matter at 16wpi | 36 |
| Figure 14: Newly generated oligodendrocytes in the cortical GM and WM | 38 |
| Figure 15: Myelin analysis in the white matter | 39 |
| Figure 16: Nodes of Ranvier at 16wpi in the cortical white matter | 41 |
| Figure 17: Beam crossing, grid walk and rotarod behavioral experiment | 43 |
| Figure 18: Open field and horizontal ladder behavioral experiment | 44 |
| Figure 19: Novel object recognition (NOR) experiment at 11wpi | 45 |
| Figure 20: Long-term analysis of recombined NG2-glia in NG2CreER ^{T2} mice | 47 |
| Figure 21: Motor behavior assessment of NG2CreER ^{T2} xCAG-eGFPxEsc ^{o2} ^{fl} mice | 48 |
| Figure 22: Nodes of Ranvier in the NG2CreER ^{T2} xCAG-eGFPxEsc ^{o2} ^{fl} mice | 49 |
| Figure 23: Schwann cells and nodes of Ranvier in the PNS | 51 |
| Figure 24: Electrophysiological recordings of the nerve conduction velocity | 52 |
| Figure 25: Model of stab wound injury | 54 |
| Figure 26: Recombined and non-recombined NG2-glia at early timepoints after lesion | 55 |
| Figure 27: Recombined and non-recombined NG2-glia at late timepoints after lesion | 56 |

| | |
|--------------------------------------------------------------------------------------------------------------|----|
| Figure 28: Total numbers of recombined and non-recombined NG2-glia at different timepoints after lesion..... | 56 |
| Figure 29: Lesion size at different timepoints after injury | 58 |
| Figure 30: Closure of the blood-brain barrier..... | 59 |
| Figure 31: Reaction of resident microglia and invading macrophages..... | 60 |
| Figure 32: Astrocyte reaction after injury | 62 |
| Figure 33: Cellular fate switch of NG2-glia upon long-term cell ablation | 67 |
| Figure 34: Hypothetical role of NG2-glia at the nodes of Ranvier | 72 |
| Figure 35: Cell-to-cell signaling mechanisms after acute brain injury..... | 85 |

9.4 LIST OF TABLES

| | |
|------------------------------------------------------------------------------------------------------------------------------------------------------------------------------------------------------------------------|-----|
| Table 1: Positive and negative effects of reactive astrogliosis | 25 |
| Table 2: Tamoxifen-inducible mouse lines to target NG2-glia. | 27 |
| Table 3: Mastermix for genotyping PCR. | 97 |
| Table 4: Primer sequences for genotyping PCR..... | 97 |
| Table 5: PCR cycle programs for genotyping. | 98 |
| Table 6: List of primary antibodies..... | 102 |
| Table 7: List of secondary antibodies..... | 102 |
| Table 8: Absolute numbers of GFP ⁺ cells in Esco ^{wt} and Esco ^{fl} mice in the cerebral GM and WM at different timepoints after induction. | 137 |
| Table 9: Absolute numbers of recombined (GFP ⁺) NG2-glia in Esco ^{wt} and Esco ^{fl} mice in the cerebral GM and WM at different timepoints after induction. | 137 |
| Table 10: Absolute numbers of total (GFP ⁺ and GFP ⁻) NG2-glia in Esco ^{wt} and Esco ^{fl} mice in the cerebral GM and WM at different timepoints after induction. | 137 |
| Table 11: Forelimb missteps of Esco2 ^{wt} and Esco2 ^{fl} mice in the grid walk experiment at different timepoints after induction. | 137 |
| Table 12: Hindlimb missteps of Esco2 ^{wt} and Esco2 ^{fl} mice in the grid walk experiment at different timepoints after induction. | 138 |
| Table 13: Time of Esco2 ^{wt} and Esco2 ^{fl} mice spent on an accelerating rotarod. Time is displayed in seconds [s]. Data are presented as mean±sem. | 138 |
| Table 14: Absolute numbers of recombined (GFP ⁺) NG2-glia in NG2-Esco ^{wt} and NG2-Esco ^{fl} mice in the cerebral GM and WM at different timepoints after induction..... | 138 |
| Table 15: Absolute numbers of total (GFP ⁺ and GFP ⁻) NG2-glia in NG2-Esco ^{wt} and NG2-Esco ^{fl} mice in the cerebral GM and WM at different timepoints after induction..... | 138 |
| Table 16: Forelimb missteps of NG2-Esco2 ^{fl} mice in the grid walk experiment at different timepoints after induction. | 139 |

| | |
|-----------------------------------------------------------------------------------------------------------------------------------------------------------------------------------------------------------------------------------------------------------------------------------------------------------------|-----|
| Table 17: Forelimb missteps of NG2-control mice in the grid walk experiment at different timepoints after induction. | 139 |
| Table 18: Latencies of conduction velocities in <i>Esco^{wt}</i> and <i>Esco^{fl}</i> mice. Latencies from the stimulating to the recording electrodes are displayed in milliseconds [ms]. Data are presented as mean±sem. | 139 |
| Table 19: Absolute numbers of GFP ⁺ cells in <i>Esco^{wt}</i> and <i>Esco^{fl}</i> mice in close proximity to the lesion site at different timepoints after the lesion..... | 139 |
| Table 20: Absolute numbers of recombined (GFP ⁺) NG2-glia in <i>Esco^{wt}</i> and <i>Esco^{fl}</i> mice in close proximity to the lesion site at different timepoints after the lesion. | 140 |
| Table 21: Absolute numbers total (GFP ⁺ and GFP ⁻) NG2-glia in <i>Esco^{wt}</i> and <i>Esco^{fl}</i> mice in the bigger surrounding of the lesion site at different timepoints after the lesion. | 140 |
| Table 22: Absolute numbers of recombined (GFP ⁺) NG2-glia in <i>Esco^{wt}</i> and <i>Esco^{fl}</i> mice in the lesion core at different timepoints after the lesion. | 140 |
| Table 23: Absolute numbers total (GFP ⁺ and GFP ⁻) NG2-glia in <i>Esco^{wt}</i> and <i>Esco^{fl}</i> mice in the lesion core at different timepoints after the lesion. | 140 |
| Table 24: Absolute numbers of Iba1 ⁺ microglia in <i>Esco^{wt}</i> and <i>Esco^{fl}</i> mice in the bigger surrounding of the lesion site at different timepoints after the lesion. | 141 |
| Table 25: Absolute numbers of Iba1 ⁺ CD45 ⁺ activated microglia in <i>Esco^{wt}</i> and <i>Esco^{fl}</i> mice in the bigger surrounding of the lesion site at different timepoints after the lesion. | 141 |
| Table 26: Absolute numbers of CD45 ⁺ invading macrophages in <i>Esco^{wt}</i> and <i>Esco^{fl}</i> mice in the bigger surrounding of the lesion site at different timepoints after the lesion. | 141 |
| Table 27: Absolute numbers of the total astrocyte (S100β ⁺) and the reactive astrocyte (S100β ⁺ GFAP ⁺) population in <i>Esco^{wt}</i> and <i>Esco^{fl}</i> mice in the bigger surrounding of the lesion site at different timepoints after the lesion. | 141 |

9.5 CURRICULUM VITAE

Personal Details

Name Sarah Schneider

Date of birth April 27th, 1987 in Riedlingen, Germany

Career Summary

Since 01.2012 PhD thesis, Ludwig-Maximilians University, Munich, Germany

- Planned and promoted projects in an English speaking international environment, including international collaboration projects on the functional role of NG2-glia in the adult rodent brain
- Acquired leadership skills with the supervision of internship students and technical assistants
- Skills applied: mouse models (postnatal and adult), behavioral animal experiments, animal operations, cell isolation, fluorescent and electron microscopy, immunohistochemistry, *in situ* hybridization, statistical analysis

03-09.2011 Master thesis, Technical University Munich, Germany

- Engineered and functionally characterized potential therapeutic proteins of the leptin satiety hormone for prolonged plasma half-life that are effective in animal experiments in a collaboration project (Grade A)
- Skills applied: Molecular cloning, bacterial protein overexpression, protein purification, protein spectroscopy, biochemical protein characterization, *in vitro* assays of protein functionality

03-10.2010 Various Student internships, Technical University Munich, Germany

- Generated mutated improved aminotransferases for technical application in collaboration with a company (Grade A)
- Analyzed the impact of mastitis pathogens on cattle primary cells (Grade A)
- Skills applied: Isolation and maintenance of primary cell cultures, RT-PCR, Site specific mutagenesis, protein purification, functionality screening

03-06.2009 Bachelor thesis, University Clinics, Ulm, Germany

- Developed an *in vitro* model mimicking human cytomegalovirus infections in a clinical environment (Grade A)
- Skills applied: Cell culture, isolation and maintenance of human blood cells, handling of viral suspensions, western blots, immunocytochemistry, fluorescent microscopy, cell migration assays

08-12.2008 Student research assistant, Ulm University, Germany

- Screened polymorphisms in gene expression of different ecotypes of *Arabidopsis thaliana*
- Skills applied: PCR, transgenic plant models, RNA isolation, northern blots

03-04.2008 Research internship, Friedrich-Löffler-Institut, Tübingen, Germany

- Analyzed infection mechanisms of avian influenza virus and prion proteins in a federal research center for animal health
- Skills applied: Western blot, cell culture, prion protein isolation and infection

Education

M.Sc. Molecular Biotechnology, Technical University Munich, Germany (Grade A)

B.Sc. Biotechnology, Ulm University, Germany (Grade A)

Exchange Student, Queens University, Belfast, Northern Ireland (Grade A)

Abitur (A-levels), Riedlingen, Germany (Grade A)

Additional skills and activities

| | |
|------------------------|-------------------------------------------------------------------------------------------|
| Professional trainings | Paper writing, presentation skills, conflict management, teaching skills, time management |
| Language skills | German (native), English (fluent), Spanish (conversational), French (advanced) |
| Computer skills | MS Office, AdobeCreativeSuite, GraphPad, VectorNTI |
| Side jobs | Private teacher for students in Sciences and English, waitress |

Scientific Contributions

| | |
|------------|------------------------------------------------------------------------------------|
| July 2015 | XII European Meeting on Glial Cells in Health and Disease, Bilbao, Spain (poster) |
| Feb. 2015 | Current topics in myelin research, Kassel, Germany (invited talk) |
| March 2014 | Gordon Research Conference and Seminar Myelin, Ventura, USA (poster) |
| Feb. 2014 | <interact>2014, München, Germany (poster) |
| July 2013 | XI European Meeting on Glial Cells in Health and Disease, Berlin, Germany (poster) |
| July 2013 | LMU-Harvard Young Scientists Forum, Munich, Germany (selected talk) |
| Feb. 2013 | Current topics in myelin research, Kassel, Germany (poster) |

9.6 LIST OF PUBLICATIONS

Morath, Volker; Bolze, Florian; Schlapschy, Martin; **Schneider, Sarah**; Sedlmayer, Ferdinand; Seyfarth, Katrin et al. (2015): PASylation of Murine Leptin Leads to Extended Plasma Half-Life and Enhanced in Vivo Efficacy. In: *Molecular pharmaceuticals* 12 (5), S. 1431–1442. DOI: 10.1021/mp5007147.

Sirko, Svetlana; Irmeler, Martin; Gascón, Sergio; Bek, Sarah; **Schneider, Sarah**; Dimou, Leda et al. (2015): Astrocyte reactivity after brain injury: The role of galectins 1 and 3. In: *GLIA*. DOI: 10.1002/glia.22898.

Viganò, Francesca; **Schneider, Sarah**; Cimino, Mauro; Bonfanti, Elisabetta; Gelosa, Paolo; Sironi, Luigi; Abbrachio, Maria Pia; Dimou, Leda (2015): GPR17 expressing NG2-glia: oligodendrocyte progenitors serving as reserve pool after injury. In: *GLIA* (64), S. 287–299. DOI: 10.1002/glia.22929.

Parts of this thesis will be published in:

von Streitberg, Axel; **Schneider, Sarah**; Straube, Christoph; Buggenthin, Felix; Eichele, Gregor; Marr, Carsten, Götz, Magdalena; Dimou, Leda: NG2-glia transiently overcome their homeostatic network and contribute to wound closure after brain injury. *Submitted*.

Schneider, Sarah; Delgado García, José Maria; Gruart i Massó, Agnès; Zhang, Yina; Kröger, Stephan, Eichele, Gregor; Götz, Magdalena; Dimou, Leda. Decrease in newly generated oligodendrocytes results in disrupted myelin structures and motor dysfunctions. (XXX)

Eidesstattliche Versicherung/Affidativ

Hiermit erkläre ich an Eides statt, dass ich die vorliegende Dissertation selbstständig angefertigt habe, mich außer der angegebenen keiner weiteren Hilfsmittel bedient und alle Erkenntnisse, die aus dem Schrifttum ganz oder annähernd übernommen sind, als solche kenntlich gemacht und nach ihrer Herkunft unter Bezeichnung der Fundstelle einzeln nachgewiesen habe.

I hereby confirm that the dissertation is the result of my own work and that I have only used sources or materials listed and specified in the dissertation.

München, den

Munich, date

Unterschrift

Signature

Declaration of contributions:

Electrophysiological experiments and its data analysis to determine the nerve conduction velocity, as described in chapter 3.1.7, were carried out by the collaboration partners José Maria Delgado García and Agnès Gruart i Massó. The content of Figure 24 was also provided by them and printed in this thesis with their permission.

München, den

Munich, date

Unterschrift Laborleiter

Signature head of lab

Unterschrift

Signature